CHARACTERIZATION OF BIOSURFACTANT FROM HYDROCARBONOCLASTIC BACTERIUM AND ITS PROSPECT IN REMEDIATION OF ENVIRONMENTAL POLLUTANTS

THESIS SUBMITTED IN PARTIAL FULFILLMENT OF THE REQUIREMENTS FOR THE DEGREE OF DOCTOR OF PHILOSOPHY

By

ALEMTOSHI

Regd. No. Ph.D./EVS/00353

DEPARTMENT OF ENVIRONMENTAL SCIENCE

SCHOOL OF SCIENCES

AUGUST 2025

CHARACTERIZATION OF BIOSURFACTANT FROM HYDROCARBONOCLASTIC BACTERIUM AND ITS PROSPECT IN REMEDIATION OF ENVIRONMENTAL POLLUTANTS

BY

Alemtoshi and

Dr. Pranjal Bharali

Submitted

In partial fulfilment of the requirements for the Degree of Doctor of Philosophy in Environmental Science of Nagaland University

नागालैण्डविश्वविद्यालय

NAGALAND UNIVERSITY

(संसदद्वारापारितअधिनियम1989, क्रमांक35केअंतर्गतस्थापितकेंद्रीयविश्वविद्यालय)

(A Central University established by an Act of Parliament No.35 of 1989)

मुख्यालय : लुमामी, जिला : जुन्हेबोटो (नागालैण्ड), पिनकोड – 798627

Hqrs: Lumami, Dist. Zunheboto (Nagaland), Pin Code – 798627

वेबसाइट / Website : www.nagalanduniversity.ac.in

Dr. Pranjal Bharali
Assistant Professor
Department of Environmental Science Email: bharalip@nagalanduniversity.ac.in

CERTIFICATE

This is to certify that the thesis entitled, **"Characterization of Biosurfactant from Hydrocarbonoclastic Bacterium and its Prospect in Remediation of Environmental Pollutants"** submitted to Nagaland University in partial fulfilment of the requirements for the Degree of Doctor of Philosophy in Environmental Science is an original research work carried out by Mr. **Alemtoshi**, registration no. **Ph.D./EVS/00353**, Dated: **30/08/2019**, under my supervision.

Further, certified that no part of this thesis has been submitted anywhere for any other research degree.

Dr. Pranjal Bharali

(Supervisor)

नागालैण्डविश्वविद्यालय

NAGALAND UNIVERSITY

(संसदद्वारापारितअधिनियम1989, क्रमांक35केअंतर्गतस्थापितकेंद्रीयविश्वविद्यालय)

(A Central University established by an Act of Parliament No.35 of 1989)

मुख्यालय : लुमामी, जिला : जुन्हेबोटो (नागालैण्ड), पिनकोड – 798627

Hqrs: Lumami, Dist. Zunheboto (Nagaland), Pin Code – 798627

वेबसाइट / Website : www.nagalanduniversity.ac.in

DECLARATION

I, Mr. **Alemtoshi**, hereby declare that the subject matter of this thesis entitled, **"Characterization of Biosurfactant from Hydrocarbonoclastic Bacterium and its Prospect in Remediation of Environmental Pollutants"** is the record of work done by me, that the contents of this thesis did not form basis of the award of any previous degree to me or to the best of my knowledge to anybody else, and that the thesis has not been submitted by me for any research degree in any other University/Institute.

This is being submitted to the Nagaland University for the degree of Doctor of Philosophy in Environmental Science.

Alemtoshi
(Scholar)

Dr. Pranjal Bharali
(Supervisor)

Head
Department of Environmental Science
Nagaland University

नागालैण्डविश्वविद्यालय

NAGALAND UNIVERSITY

(संसदद्वारापारितअधिनियम1989, क्रमांक35केअंतर्गतस्थापितकेंद्रीयविश्वविद्यालय)

(A Central University established by an Act of Parliament No.35 of 1989)

मुख्यालय : लुमामी, जिला : जुन्हेबोटो (नागालैण्ड), पिनकोड – 798627

Hqrs: Lumami, Dist. Zunheboto (Nagaland), Pin Code – 798627

वेबसाइट / Website : www.nagalanduniversity.ac.in

CERTIFICATE

This is to Certify that Mr. **Alemtoshi**, a registered Research Scholar for Ph.D. degree in Environmental Science under Nagaland University, bearing Ph.D. Registration No.**Ph.D./EVS/00353**, has satisfactorily completed all the courses offered in the Pre-Ph.D.Course Work Programme in the Department of Environmental Science, Nagaland University, *Hqrs*. Lumami.

The Course Includes:

ESP01 Research Methodology

ESP02 Literature Review and Report Writing

ESP04 Environmental Monitoring

Head
Department of Environmental Science
Nagaland University

Sl. No. : 20- 9702

NAGALAND UNIVERSITY

STATEMENT OF MARKS

Ph. D COURSE WORK EXAMINATION 2021

DEPARTMENT OF ENVIRONMENTAL SCIENCE

The following are the marks secured by Ms. ***Alemtoshi***
Roll No . **01** *of Ph.D Course Work Examination held in* **2021**

Subject(s)/Paper(s)	Max. Marks	Minimum Qualifying Marks	Marks Secured
Paper No. ESP01	100	35	**58**
Paper No. ESP02	100	35	**70**
Paper No. ESP03	100	35	**69**
Total Aggregate Marks			**197**
Average Pass Mark – 55 %			

Result	Division	Percentage
Passed	**I Division**	**65.66%**

Marks compared by

NAGALAND UNIVERSITY HQRS : LUMAMI

COE/Dy. Registrar (Exams)/AR (Exams)

Asstt. Registrar (Exams)
Nagaland University
Hqrs. Lumami

NAGALAND UNIVERSITY

HEAD QUARTERS : LUMAMI

Ph. D COURSE WORK EXAMINATION

This is to certify that Mr/Ms ALEMTOSHI

of Nagaland University bearing Roll No. 01 *is qualified in the Ph.D Course Work Examination*

in the Department of ENVIRONMENTAL SCIENCE *Nagaland University held in the Year 20.21*

दिभागाध्यक्ष / Head
पर्यावरण विज्ञान विभाग
Department of Environmental science
नागालैण्ड विश्वविद्यालय / Nagaland University
लुमामी / Lumami- 798 627

Head of Department

Dean
School of Sciences
Nagaland University
Hqrs. Lumami Nagaland

School of Sciences

Sl.no. 00353

NAGALAND UNIVERSITY
नागालैण्ड विश्वविद्यालय

(A Central University Established by the Act of Parliament of India 1989)
(भारत के संसद द्वारा पारित अधिनियम 1989 के अन्तर्गत स्थापित केंद्रीय विश्वविद्यालय)
Headquarters: Lumami मुख्यालय: लुमामी

Ph.D. Admission cum Registration Certificate

This is to certify that

Mr. / Mrs. / Ms. Alemtoshi *has been registered for research works leading to the Degree of Doctorate of Philosophy in Nagaland University*

Under the Supervision of Prof. / Dr. Pranjal Bharali

Co- Supervisor Prof. / Dr. _____

Department of Environmental Science

His / Her Registration number is PhD/EVS/00353

With effect from 30/8/2019

Date 19/5/2022

NAGALAND UNIVERSITY H.Q. LUMAMI

19/5/22

Dy. / Asst. Registrar (Acad)
Deputy Registrar (Acad)
Nagaland University
Headquarters : Lumami

नागालैण्डविश्वविद्यालय

NAGALAND UNIVERSITY

(संसदद्वारापारितअधिनियम1989, क्रमांक35केअंतर्गतस्थापितकेंद्रीयविश्वविद्यालय)

(A Central University established by an Act of Parliament No.35 of 1989)

मुख्यालय : लुमामी, जिला : जुन्हेबोटो (नागालैण्ड), पिनकोड – 798627

Hqrs: Lumami, Dist. Zunheboto (Nagaland), Pin Code – 798627

वेबसाइट / Website : www.nagalanduniversity.ac.in

Plagiarism Self Declaration Certificate

Name of Research Scholar	Alemtoshi
Registration Number	Ph.D./EVS/00353
Title of Ph.D. thesis	*Characterization of Biosurfactant from Hydrocarbonoclastic Bacterium and its Prospect in Remediation of Environmental Pollutants*
Name & Institutional Address of the Supervisor	Dr. Pranjal Bharali Nagaland University, Lumami-798627
Name of the Department and School	Department of Environmental Science, School of Sciences
Date of submission	29/08/2025
Date of plagiarism check	27/08/2025
Percentage of similarity detected by the DrillBit software	5%

I hereby declare/certify that the Ph.D. Thesis submitted by me is complete in all respect, as per the guidelines of the UGC/NU for this purpose. I also certify that the thesis has been checked for plagiarism using **DrillBit** similarity check software. It is also certified that the contents of the electronic version of the thesis are the same as the final hardcopy of the thesis. Copy of the Report generated by the software is also enclosed.

Place: **Alemtoshi**

Date: Name & Signature of the Scholar

DrillBit

The Report is Generated by DrillBit Plagiarism Detection Software

Submission Information

Author Name	Alemtoshi
Title	CHARACTERIZATION OF BIOSURFACTANT FROM HYDROCARBONOCLASTIC BACTERIUM AND ITS PROSPECT IN REMEDIATION OF ENVIRONMENTAL POLLUTANTS
Paper/Submission ID	4283225
Submitted by	bharalip@nagalanduniversity.ac.in
Submission Date	2025-08-27 02:01:18
Total Pages, Total Words	119, 32215
Document type	Thesis

Result Information

Similarity 5 %

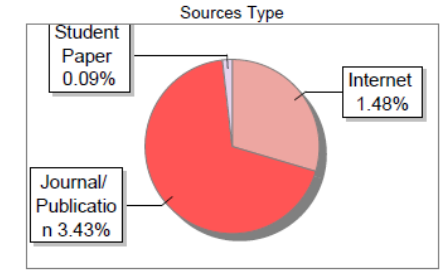

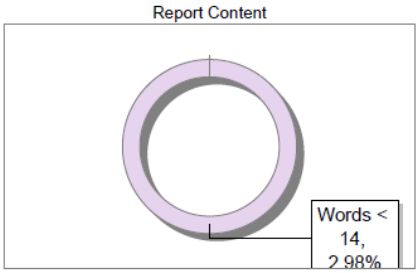

Exclude Information

Quotes	Excluded
References/Bibliography	Excluded
Source: Excluded < 14 Words	Excluded
Excluded Source	0 %
Excluded Phrases	Not Excluded

Database Selection

Language	English
Student Papers	No
Journals & publishers	Yes
Internet or Web	Yes
Institution Repository	Yes

A Unique QR Code use to View/Download/Share Pdf File

DrillBit

DrillBit Similarity Report

5	53	A
SIMILARITY %	MATCHED SOURCES	GRADE

A-Satisfactory (0-10%)
B-Upgrade (11-40%)
C-Poor (41-60%)
D-Unacceptable (61-100%)

LOCATION	MATCHED DOMAIN	%	SOURCE TYPE
1	www.science.gov	<1	Internet Data
2	coek.info	<1	Internet Data
3	idr.l2.nitk.ac.in	<1	Publication
4	Thesis Submitted to Shodhganga Repository	<1	Publication
5	Biodiesel derived waste glycerol as an economic substrate for biosurfactant prod by Bharali-2014	<1	Publication
6	www.ncbi.nlm.nih.gov	<1	Internet Data
7	journals.athmsi.org	<1	Publication
8	spandidos-publications.com	<1	Internet Data
9	Optimization and characterization of a glycolipid produced by, by Haloi, Saurav Medh- 2019	<1	Publication
10	worldwidescience.org	<1	Internet Data
11	academicjournals.org	<1	Publication
12	A critical review of the reactivity of manganese oxides with organic contaminant by Remucal-2014	<1	Publication
13	Thesis submitted to shodhganga - shodhganga.inflibnet.ac.in	<1	Publication

Acknowledgement

First and foremost, I want to thank the Almighty God for His abundant blessings and grace upon me throughout the course of my research journey. Secondly, I extend sincere gratitude to my supervisor Dr. Pranjal Bharali, Department of Environmental Science, Nagaland University for his valuable guidance, optimistic encouragements, constructive feedbacks and sincere undertaking and commitment in the successful completion of this thesis work.

I extend my sincere appreciation to the Head of the Department for the opportunity and necessary facilities provided during my research. I would also like to thank all the respected faculty members and non-teaching staff for their constant support, advice and encouragement. My sincere thanks to all my lab mates and fellow research scholars for their support and companionship.

I would like to express my sincere gratitude to the Department of Chemistry, Department of Botany and Department of zoology, Nagaland University for the invaluable support and assistance throughout the course of my research work. I would also like to extend my gratitude to:

- CSIR North East Institute of Science and Technology, Jorhat, Assam
- Department of Environmental Science, Bharathiar University, Coimbatore
- Department of MBBT, Tezpur university, Assam
- Department of Applied biology, USTM, Meghalaya
- Assam Agricultural University, Jorhat, Assam and
- Sathyabama Institute of Science and technology, Chennai

for their support and cooperation in carrying out the sample analysis required for this research work. Their technical assistance and facilities were instrumental in the successful completion of my study.

I am thankful to the Ministry of tribal Affairs, Govt. of India for the financial support provided through NFST fellowship for my research work. I wish to express my heartfelt gratitude to my family members, friends, relatives and all well-wishers for their unwavering support, constant prayers and encouragement.

With sincere appreciation I acknowledge all who have directly or indirectly contributed to the successful completion of this work.

Date……..

(Alemtoshi)

Department of Environmental Science
Nagaland University

Dedication

I heartily dedicate this thesis in honour of my Late grandmother, Mrs. Nungshilemla who had been an immense source of inspiration and guidance in my life. She was someone who truly believed in the enlightenment by virtue of education. Her calm strength, tenacity and unwavering encouragement to continuously aspire for profound knowledge had been my motivation throughout my Ph. D research work.

CONTENTS

Chapter 4

List of Figures

List of Tables

Chapter 1. Introduction and Review of Literature

There is a mounting global concern over the degradation of environment by various anthropogenic activities resulting in the continuous release of numerous hazardous pollutants into our surroundings causing severe environmental degradation. Exposure to these broad spectra of environmental contaminants can elicit a wide array of pathophysiological responses in human body (Sokan-Adeaga et al., 2023). Chronic or acute exposure may initiate or exacerbate the onset and progression of numerous disease states, encompassing respiratory dysfunction, cardiovascular disorders, neurodegenerative conditions, endocrine disruption and various forms of carcinogenesis (Xu et al., 2022). These toxicants exert their effects through various mechanisms, including oxidative stress induction (Samet and Wages, 2018), disruption of cellular redox homeostasis (Andreau et al., 2012), interference with enzymatic activity (Shetty et al., 2023) and genotoxic interactions (Lavorgna et al., 2020). The bioaccumulation of such pollutants, along with their potential to interact synergistically or antagonistically within biological systems underscores the complexity and severity of their impact on humans. An estimated 24 % of the global morbidity burden and 23 % of total mortality are linked to environmental determinants, including exposure to hazardous biological pathogens, physicochemical agents and toxic environmental contaminants (Xu et al., 2022). Environmental pollution exerts detrimental effects not only on human health but also on a wide range of aquatic terrestrial flora and fauna, including microbial communities (Anetor et al., 2022; Sazykina et al., 2022) thereby jeopardizing the entire biotic component of the environment.

One of the most common contaminants that largely affects different components of the environment is Petrochemicals/petroleum hydrocarbons. Petrochemicals comprise a complex mixture of paraffinic, cycloalkane, aromatic, polyaromatic (PAH) and complex nitrogen, sulphur and oxygen containing (NSO) hydrocarbon compounds (Phulpoto et al., 2022). Within crude oil, low molecular weight alkanes (C_{10}–C_{20}) are identified as particularly toxic and may constitute approximately 50–95 % of total hydrocarbon content, contingent upon the geological origin of the oil (Phulpoto et al., 2022). In contrast, high molecular weight hydrocarbons are predominantly solid under ambient conditions and exhibit recalcitrance to microbial degradation due to their complex structure and low

bioavailability (Phulpoto et al., 2022). Primary anthropogenic sources of such contamination include petroleum extraction and refining operations, hydrocarbon transport infrastructure, fuel distribution networks, storage facilities and related industrial equipment. Release of these hydrophobic pollutants into the environment poses significant ecological and environmental hazards due to their persistence, toxicity and potential for bioaccumulation (Phulpoto et al., 2022). Even at trace concentrations, the presence of petrochemical contaminants in soil matrices can significantly impair microbial proliferation and disrupt key biochemical and metabolic pathways thus greatly reducing the microbial diversity (Gao et al., 2022; Shi et al., 2022). These compounds possess the potential to infiltrate trophic networks, where their inherent toxicity, carcinogenicity and mutagenicity impart serious threats to biological systems across multiple taxa (Alaidaroos, 2023; Mohanty et al., 2025). Hence, extended exposure to petrochemicals contaminants, raising serious issues for the environment, ecological systems and public health leading to both short-term and long-term environmental damage (Channdankere et al., 2014).

Apart from Petro-based hydrophobic pollutants, anthropogenically generated kitchen waste such as waste residual cooking oil (WRCO) is another significant environmental challenge in contemporary society especially in urban areas, where dense populations and a high concentration of food and beverage businesses amplifies its impact. Large amounts of WRCO are generated during food preparation in both households and industrial settings. In India, this problem is especially prominent due to the country's diverse culinary traditions, which commonly involve frying vegetables, grains and legumes with various spices in vegetable oil. The deep frying process causes the oil to undergo hydrolysis, oxidation and polymerization resulting in the rise of free fatty acids, glycerol, monoacylglycerols and diacylglycerols levels (Kumar et al., 2025). A significant proportion of volatile compounds generated in the cooking oil are released into the atmosphere as vapor phase emissions, while the remainder either undergo secondary chemical transformations or are assimilated into the matrix of the fried food products (Choe and Min, 2007). The indiscriminate disposal of such untreated WRCO into sewage systems or open environments can induce a range of adverse environmental impacts, affecting both biotic and abiotic components. Due to its high fluidity, WRCO spreads rapidly and even minimal quantities can cause extensive ecological damage. It not only obstructs and clogs municipal sewer infrastructures but also impairs the operational efficiency of

wastewater treatment facilities (Thushari and Babel, 2022). When released into natural aquatic systems, WRCO exerts deleterious effects on marine and freshwater biota. Empirical evidence indicates that the formation of hydrophobic films on the surfaces of fish, birds, aquatic flora and other organisms impedes gas exchange, resulting in hypoxia and eventual mortality (Olu-Arotiowa et al., 2022). Although oil undergoes natural degradation in aquatic environments, the oxidative breakdown processes significantly deplete dissolved oxygen (DO) levels, which are critical for sustaining aquatic life. Moreover, the high oxygen demand during biodegradation elevates the biochemical oxygen demand (BOD), further accelerating water quality deterioration (Foo et al., 2021). Consequently, the accumulation of WRCO in the environment is classified as hazardous due to its ecological toxicity. Effective management strategies, including the recycling and valorisation of WRCO, are imperative to mitigate its negative environmental impacts. WRCO, despite being classified as hazardous, retains considerable resource potential and should not be indiscriminately discarded. Its biotransformation represents a promising and sustainable strategy for mitigating associated environmental risks. Given the inherently endergonic nature of its degradation, the direct utilization of WRCO as a carbon rich feedstock in microbial bioprocesses offers a viable and efficient approach. Employing WRCO in microbial fermentation or bioconversion systems not only facilitates the synthesis of value added bioproducts but also contributes to waste valorisation and cost effective production processes. This dual benefit enhances the economic viability of industrial biotechnology applications while reducing the environmental burden associated with WRCO disposal (Bialy et al., 2011).

Heavy metals are another concerning toxic pollutant that has detrimental effect on all lifeforms, including human beings. Heavy metal contamination is a major threat to the environment due to their toxic, persistent and bio-accumulative nature (Das et al., 2017; Ali et al., 2019; Gogoi et. al., 2024). The source of these heavy metal contaminations can be natural such as volcanic eruptions, soil erosion and geological weathering of rocks containing metals or can be due to anthropogenic activities such as industrialization, mining, smelting or agriculture (Ali et al., 2019; Briffa et al., 2020). In the environment, these heavy metal pollutants are found in association with the sub-surface soil sediments that often results its release into the ground water leading to contamination (Yang et al., 2020). Contamination of the soil by heavy metal disrupts the activity of soil microorganisms by exerting toxic effects leading to the

change in the population size, diversity and overall activity of the soil microbes (Singh and Kalamdhad, 2011). They inhibit the microbial activity and reduces microbial biomass and activity of the soil enzyme thereby affecting the process of organic matter decomposition and nutrient cycling (Su et al., 2014). Sensitive microorganisms such as actinomycetes can be affected by the presence of heavy metal contaminants even at very low concentrations (Hiroki, 1992). Heavy metals exert phytotoxicity in plants by inducing reduced nutrient uptake, slow plant growth, chlorosis, reduced yield, disruption in plant metabolism and reduced molecular nitrogen fixation in leguminous plants (Singh and Kalamdhad, 2011). In humans, heavy metals are known to cause decreased immunity, gastrointestinal cancer, intrauterine growth retardation and physical disabilities (Singh and Kalamdhad, 2011). Heavy metals are carcinogenic and affects the functioning of organs such as lungs, liver, kidney, urinary system, immune system, reproductive system, nervous system and even the basic physiological processes of cells and gene expression (Jaishankar et al., 2014; Su et al., 2014; Akün, 2020). They can affect also the calcium metabolism in our body leading to cartilage and bone fracture (Su et al., 2014) and can cause skin lesions including hyperkeratosis and hyperpigmentation (Hughes et al., 2002; Jomova et al., 2011). Heavy metal such as mercury (Hg) undergoes biotransformation into methylmercury, a neurotoxic compound inside the body that can cause various health complications such as birth defects and mental retardation and can also lead to dysfunctioning of organs such as nerves, muscles and kidneys (Morais et al., 2012).

The remediation of hydrocarbon contaminants from the environment is carried out through conventional *in-situ* and *ex-situ* techniques such as containment booms, skimmers, hydraulic containment, soil vapor extraction, immobilization, chemical oxidation-reduction, photocatalytic oxidation, phytoextraction, phytoaccumulation, phytoabsorption, phytosequestration etc (Ossai et al., 2019). Some of the existing conventional remediation technologies that are commonly employed for the management of heavy metal pollution include physical methods such as heat treatment (Sharma et al., 2018), soil replacement (Khalid et al., 2017), vitrification (Khalid et al., 2017) and electrokinetic remediation (Sharma et al., 2018). Chemical methods include chemical precipitation (Pohl, 2020), soil amendment (Sharma et al., 2018), soil washing (Dermont et al., 2008) and chemical oxidation and extraction (Yoo et al., 2017). Phytoremediation is another existing bio-based remediation techniques in which green plants are used for removal of heavy metals from soil (Das et al., 2017).

However, existing conventional physical, chemical and biological technologies used for remediation of these environmental pollutants are often associated with several drawbacks such as high maintenance cost, labour intensive, high energy input, low efficiency, production of secondary pollutants, site specific, season/time specific, alteration of soil properties and microflora structure, influenced by environment variables, biosafety issues etc (Juwarkar et al., 2007; Sharma et al., 2018; Li et al., 2019; Gomaa and El-Meihy, 2019). Therefore, there is a need for cleaner, ecofriendly, cost effective and efficient technology such as biobased green treatment strategy to tackle these hazardous pollutants (Usman et al., 2016). One such environmentally benign approach is the use of biological surfactant (Surface Active agent), that could be derived from a wide range of organisms *viz*., microbes, plants and animals and used extensively for bioremediation applications (Rodrigues et al., 2006). The presence of biosurfactants can potentially enhance the mineralization and biodegradation of hydrocarbon pollutants by solubilization and emulsification of the contaminants and serving as an important mediator by increasing the bioavailability of hydrophobic substrates for microorganisms (Parthasarathi and Sivakumaar, 2011; Lawniczak et al., 2013; Santos et al., 2016). Biosurfactants are also known to form complexes with heavy metal in the soil thereby reducing the interfacial tension between the soil and the metal ions resulting in the removal of the heavy metal from the contaminated environment (Santos et al., 2016). They are exclusively used in various bioremediation applications such as oil spills remediation (Karlapudi et al., 2018), microbial enhanced oil recovery (MEOR) (Karlapudi et al., 2018), soil remediation (Datta et al., 2024), heavy metal remediation (Sarubbo et al., 2018), organic pollutant remediation (Patel et al., 2020), waste water treatment (Patel et al., 2020) etc. The pivotal functions of biosurfactants in key biomedical applications includes their roles in drug delivery systems, induction of tumor cell differentiation and apoptosis, antimicrobial and antiviral therapies, wound healing processes and modulation of immune responses (Wang et al., 2024). In the agricultural sector, biosurfactants serve as biopesticides for the management of pests, pathogens, phytopathogenic fungi and nematodes (Sorhie et al., 2022). Additionally, they enhance plant immune responses and are employed in soil hydrophilization to optimize moisture retention and promote uniform distribution of fertilizers (Silva et al., 2024) and can also acts as plant growth promoter by aiding in the bioavailability and uniform distribution of complex nutrients in the soil for its uptake by plants (Sorhie et al., 2022).

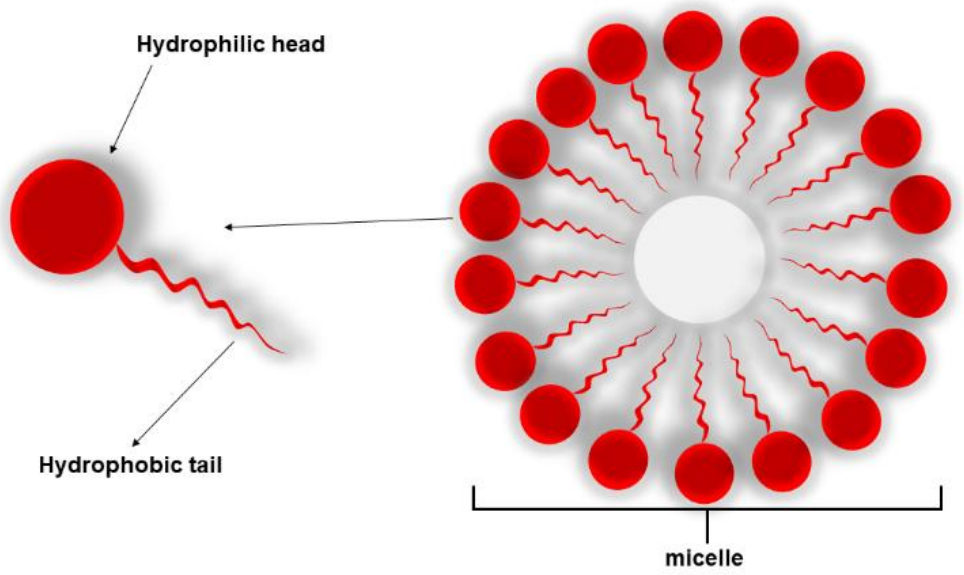

Figure 1. Schematic representation of a typical biosurfactant

Biosurfactants (BS) are natural amphiphilic biomolecules with both hydrophilic and hydrophobic moieties that has the property to accumulate between liquid phases, air-liquid and solid-liquid phases, possess the ability to reduce surface tension (ST) and interfacial tension (IFT) (Md, 2012; Santos et al., 2016). Biosurfactants possess several desirable biochemical properties *viz*. biodegradability, non-toxicity, biocompatibility, superior stability etc. (Banat et al., 2010; Chandankere et al., 2014; Sanjivkumar et al., 2021). Among the known biosurfactants, microbial biosurfactants are produced by a wide array of microorganisms that are adhere to cell surfaces or secreted extracellularly in the surrounding medium (Chioma et al., 2013). The basic chemical structure of a microbial biosurfactants is identical with that of other biosurfactants i.e. consisting of a hydrophilic polar head which may be either charged (cationic/anionic) or neutral and a hydrophobic non-polar tail (Figure 1) (Santos et al., 2016). The hydrophobic (non-polar) end section is insoluble in water and can contain a long chain of fatty acids, hydroxyl fatty acids, or α-alkyl-β-hydroxy fatty acids while the hydrophilic (polar) end might contain a phosphate, carboxylic acid, cyclic peptide, carbohydrate, amino acid or alcohol (Chioma et al., 2013). In aqueous solution, biosurfactants orients itself with the hydrophobic tail pointing towards the air and hydrophilic head pointing towards water in the air-water interface due to their amphiphilic nature. With the increase in the concentration of biosurfactants, the

surface tension (ST) reduces to a critical level and no further reduction is observed as the solution becomes saturated with biosurfactant. At this concentration, the biosurfactant molecules aggregate themselves to form a structure known as micelles where the hydrophilic heads face towards the water phase and the hydrophobic tail hides inside (Figure 1). This concentration at which the micelle starts to form is known as critical micelle concentration (CMC) (Figure 2) (Esposito et al., 2023). Micelles are known to attain several structures and sizes (Figure 3) which are mostly influenced by the polarity and pH of the surrounding aqueous medium and may affect its functioning such as complexation with heavy metals during bioremediation process (Champion et al., 1995; Zhang et al., 2022). Another factor associated with the efficiency of biosurfactants is the Hydrophile-Lipophile Balance (HLB) value. The HLB can be is defined as the ratio of hydrophile group to lipophile group, which fundamentally designate whether a biosurfactant will promote water-in-oil (WO) or oil-in-water (OW) emulsion. Water-in-oil emulsification is stabilised by lipophilic biosurfactants with HLB values less than 6. In contrast, HLB values between 10 and 18 refers to hydrophilic biosurfactants that may facilitate the emulsification of oil in water (Arathi et al., 2021).

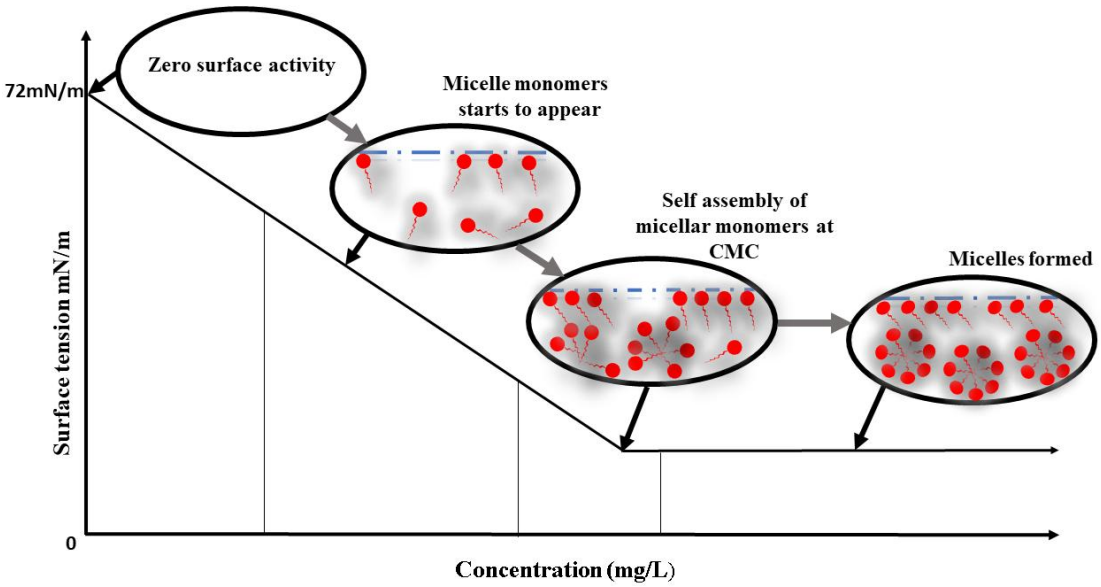

Figure 2. Critical Micelle Concentration (CMC) of biosurfactant

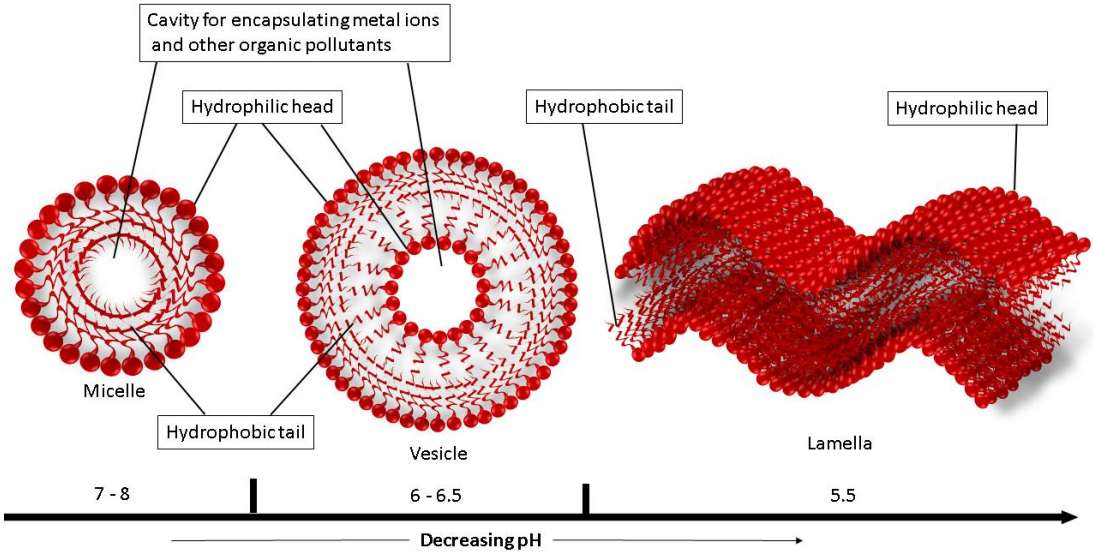

Figure 3. Effect of pH on micellar structure

Microorganisms produces a diverse range of biosurfactants with different structural profiles which are generally categorized based on their chemical structure and microbial origin, *viz*; glycolipids, polymeric type, lipopeptides, fatty acid, particulate type and phospholipids (Santos et al., 2016). Based on molecular weight, biosurfactant can also be classified into low molecular and high molecular weight surface active agents. Low molecular weight surface active agents include glycolipids, lipopeptides, lipoproteins, fatty acids, neutral lipids and phospholipids, while high molecular weight surface active agents consist of polymeric and particulate type biosurfactants (Santos et al., 2016). Biosurfactants with different molecular masses exhibits different mechanisms in the removal of hydrophobic pollutants. Lower molecular mass biosurfactants shows mobilization below their CMC and solubilization mechanisms above their CMC whereas higher molecular mass biosurfactants exhibits emulsification in the removal of hydrophobic pollutants (Plociniczal et al., 2011). Biosurfactant has the ability to reduce the ST and IFT of different interphases, reduces the free energy of the systems and thereby assist in pseudo solubilization of hydrophobic substrates in aqueous systems (Kumar et al., 2017). In contrast to chemical surfactants, biosurfactants offer remarkable advantages such as superior biodegradability, low toxicity, high sensitivity, selectivity and stability (Md, 2012; Chandankere et al., 2014). They feature a low CMC, excellent foaming properties and

greater efficiency and stability across a wide range of salinity, pH and temperature, making them more effective and eco-friendlier (Bharali and Konwar, 2011).

Rhamnolipid (RL) belongs to the class of glycolipid biosurfactant, mainly produced by *Pseudomonas* sp., and have drawn interest in recent decades due to its low toxicity, ecological acceptability, biodegradability and capacity to be produced from less expensive and renewable resources (Makkar, 2002; Banat et al., 2010; Md, 2012; Chandankere et al., 2014). Such environmentally compatible traits of RLs makes it a potential green alternative to synthetic surfactant for application in various sectors and industries such as petroleum recovery, bioremediation of oil spills, heavy metal removal, removal of organic pollutants, food industries, therapeutics and synthesis of nanoparticles (Md, 2012; Santos et al., 2016). Moreover, RL molecules have been reported to be associated with the alteration of cell surface hydrophobicity and thereby enhance the interaction of hydrophobic substrate with the bacteria cell surface. Al-Tahhan et al. (2000) reported that RL are responsible for increase in the cell surface hydrophobicity of *Pseudomonas* sp. through the release of cell wall's lipopolysaccharide (LPS). It has been found that when organisms need to find new habitat, RL molecules play an important role in cell desorption, and are also involved in cell adhesion under adverse environmental conditions to provide the greatest stability (Md, 2012). RLs are known to show antimicrobial activities against many fungal and bacterial species and might show antibiofilm activity as a defensive mechanism to prevent other microorganisms from forming colonies (Chrzanowski et al., 2012). Moreover, RL inhibits certain organisms by inserting themselves into different cell fragments, proteins, DNA, cell membranes and other peptides (Cserhati et al., 2002). RLs are also known to show insecticidal activity against *Myzus persicae* by affecting the cuticle membrane of the insect, thus eventually killing it (Kim et al., 2011). Table 1 shows the applications of RLs in various sectors reported by a number of researchers.

Table 1. Applications of rhamnolipid in various sectors

Application	Industries/ Sectors	Year	Reference
Antiviral agents	Pharmaceuticals	2025	Touabi et al. (2025)
Removal of waste lubricant oil from soil	Bioremediation	2024	Lopes et al. (2024)

Antiviral, antitumor and antimicrobial agent	Pharmaceuticals	2024	Cerqueira dos Santos et al. (2024)
Phytoextraction of Cd, Cu, Fe, Pb and Zn from copper smelter-affected soil	Bioremediation	2024	Parus et al. (2024)
Personal and skin care products	Cosmetic	2023	Karnwal et al. (2023)
Plant growth enhancers	Agriculture	2023	Hu et al. (2023)
Stabilization of Pb, Cd, and As in soil	Bioremediation	2023	Song et al. (2023)
Removal of PAH	Bioremediation	2023	Kumari et al. (2023)
Recovery of heavy oil	Petroleum	2022	Biktasheva et al. (2022)
Removal of Pb and Hg from marine intertidal sediment	Bioremediation	2021	Chen et al. (2021)
Removal of Vanadium from contaminated sediment	Bioremediation	2021	San Martín et al. (2021)
Bioremediation of petroleum-contaminated soils	Bioremediation	2020	Xue et al. (2020)
Pesticide bioremediation	Agriculture	2018	Hassen et al. (2018)
Dermal drug delivery	Pharmaceuticals	2017	Müller et al. (2017)
Bioremediation of ground water	Bioremediation	2017	Chang et al. (2017)
Remediation of marine oil spills	Bioremediation	2014	Chen et al. (2013)
Food additives	Food industries	2013	Campos et al. (2013)
Removal of oil from waste wate	Bioremediation	2009	Zhang et al. (2009)
Antitumor agent	Pharmaceuticals	2006	Andrä et al. (2006)

The RLs are produced by the microorganisms in two major forms i.e. mono-RLs and di-RLs. The molecular structure of mono-RLs and di-RLs is characterized by the presence of either one or two L-rhamnose sugar molecules respectively. These sugar units are chemically recognized as 6-deoxy-L-mannose and are covalently linked to one or two β-hydroxy (3-hydroxy) fatty acid chains. These linkage between the rhamnose sugars and the fatty acid components occurs through an O-glycosidic linkage resulting in a glycolipid molecule (El-Housseiny et al., 2020; Thakur et al., 2021). Based on the number of rhamnose unit (Rha) and hydrophobic tail, mono and di-rhamnolipid can be further classified into Mono-Rhamnose Mono-Lipidic, Mono-

Rhamnose Di-Lipidic, Di- Rhamnose Mono-Lipidi, and Di- Rhamnose Di-Lipidic as shown in (Figure 4) (Esposito et al., 2023).

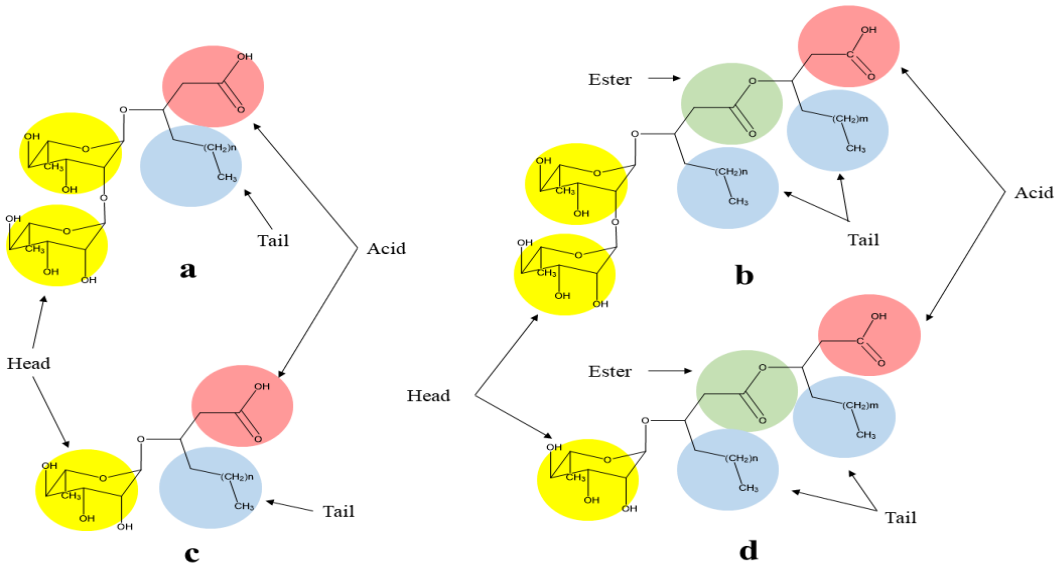

Figure 4. Structure of (a) Di- Rhamnose Mono-Lipidic, (b) Di- Rhamnose Di-Lipidic, (c) Mono-Rhamnose Mono-Lipidic and (d) Mono- Rhamnose Di-Lipidic

The physicochemical properties of RLs are influenced by the congener composition, which varies depending on carbon source, growth conditions and the media composition (Costa et al., 2010). Different *Pseudomonas* strains produce diverse types of RL congeners ~~as~~ because the precursors for the biosynthesis of RL is greatly influenced by the type of carbon source used (Thakur et al., 2021). Table 2 shows the types, molecular formula (Mol. form), molecular weight (Mol. wt.), pseudo molecular ion i.e. mass/charge (m/z) value, and ion fragment (m/z) pattern RL congeners produced by *Pseudomonas* strains previously reported by various researchers.

Table 2. Chemical composition of rhamnolipid congeners produced by *Pseudomonas* strains

Rhamnolipid (HAA)	**Mol. form.**	**Mol. wt.**	**Pseudo-molecular ion *(m/z)***	**Ion Fragments *(m/z)***	**Reference**
Rha-C_8-C_{10}	$C_{22}H_{44}O_9$	452	451	103, 141, 169, 305	
Rha-C_{10}-C_8	$C_{22}H_{44}O_9$	452	451	103, 141, 169, 333	

Rha-C_{10}-C_{10}	$C_{32}H_{38}O_{13}$	630	629	103, 119, 163, 169, 187, 333	
Rha-C_{10}-$C_{12:1}$	$C_{32}H_{60}O_{13}$	652	651	103, 119, 169, 333	
Rha-C_{10}-C_{12}	$C_{28}H_{52}O_9$	532	531	103, 163, 169, 197, 333	Déziel et al. (1999),
Rha-C_{12}-C_{10}	$C_{28}H_{52}O_9$	532	531	103, 163, 169, 197, 361	Haba et al. (2003a), Haba et al. (2003b),
Rha-Rha-C_8-C_{10}	$C_{22}H_{44}O_9$	452	451	103, 141, 169, 205, 451	Rooney et al. (2009), Behrens et al. (2016),
Rha-Rha-C_{12}-C_{10}	$C_{32}H_{62}O_{13}$	654	653	529.34, 381.15, 339.09, 154.81, 112.82	Loiseau et al. (2018), Zhao et al. (2019), Pourfadakari et al. (2020)
Rha-Rha-C_{10}- C_{10}	$C_{32}H_{58}O_{13}$	650	649	479.22, 421.161, 54.81, 112.82	
Rha-Rha-C_{10}-C_8	$C_{30}H_{54}O_{13}$	622	621	479, 248.82, 154.81, 112.82	
Rha-Rha-C_{10}-$C_{12:1}$	$C_{32}H_{60}O_{13}$	652	651	103, 169, 205, 247, 478.89	
Rha-Rha-C_{10}-C_{12}	$C_{32}H_{62}O_{13}$	654	653	103, 143, 145, 163, 169, 197, 205, 247, 479	
Rha-Rha-C_{10}-C_{14}	$C_{36}H_{66}O_{13}$	706	705	478.89, 339.09, 248.82, 154.81, 112.82	
Rha-Rha C_{10}-$C_{14:1}$	$C_{36}H_{64}O_{13}$	704	703	478.89, 339.09, 248.82, 154.81, 112.82	
Rha-Rha-$C_{10:1}$-C_{10}	$C_{32}H_{56}O_{13}$	648	647	475.26, 353.10, 311.05, 154.81, 112.82	
Rha-Rha-C_{10}-C_{14}	$C_{36}H_{66}O_{13}$	706	705	478.89, 339.09, 248.82, 154.81, 112.82	

Rha-Rha-C_8-$C_{12:1}$	$C_{32}H_{56}O_{13}$	648	647	452, 339.09, 248.82, 154.81, 112.82
Rha-$C_{12:2}$		357	356	187, 333
Rha-$C_{8:2}$		301	300	131, 169, 187
Rha-Rha-$C_{8:1}$-$C_{8:1}$		590	589	449, 309, 279, 140
Rha-Rha-$C_{12:1}$-C_{12}		704	703	505, 311
Rha-Rha-C_{12}-$C_{12:1}$		704	703	507, 311

The potential uses of RLs in the fields of environmental protection (Pacwa-Płociniczak et al., 2011), petroleum extraction (Makkar and Cameotra, 2002), synthesis of specific compounds (Das et al., 2013; Sorhie et al., 2022), manufacturing of pharmaceuticals (Md, 2012) and food industries (Cameotra and Makkar, 1998) have sparked interest in them. When RLs are released into the environment during various environmental remediation processes, they inevitably come into direct contact with a wide range of biotic components that inhabits the polluted ecosystem. These biotic components span across a vast spectrum, ranging from microorganisms such as bacteria and fungi to higher organisms, including plants, insects and even mammals including humans. Understanding how RLs interact with these many organisms is essential due to the extensive exposure caused by the incorporation of high dosages of RLs, either manually administered or from the imported RL generating strains during the remediation process. To evaluate the possible hazards and advantages of RL application in bioremediation and environmental management, a comprehensive grasp of these interactions is necessary. Therefore, it is of utmost importance to study the concentration dependent effects of RLs on the environment to accurately determine their level of eco-compatibility.

Although biosurfactants such as RLs, possess numerous advantages over conventional synthetic surfactants including superior biodegradability, lower ecotoxicity and functional stability under a wide range of environmental conditions, their large scale industrial commercialization remains significantly constrained. This is primarily attributable to several interrelated technical and economic limitations. Currently, there is growing interest in the market for RLs but they cannot effectively compete with their chemical counterpart due to various factors, specifically their higher cost of production (Chrzanowski et al., 2011; Md, 2012; Thakur et al., 2021).

It has been reported that the culture conditions have a great influence on the type and amount of biosurfactant produced (Md, 2012). The high cost of fermentation substrates, particularly carbon sources required for microbial growth and metabolite synthesis, constitutes a major economic barrier. Furthermore, downstream processing and purification of RLs are complex, energy intensive and cost prohibitive, often involving multiple unit operations to achieve the required purity levels for industrial applications. Additionally, the inherent low volumetric productivity and yield of RLs under conventional fermentation conditions further compromise process scalability and economic feasibility. These cumulative constraints present a substantial bottleneck to the widespread industrial deployment and commercialization of RL biosurfactants despite their environmental compatibility and functional efficacy. In this regard, screening for more efficient biosurfactants producing native microbial strains can be an effective strategy to increase the biosurfactant yield and their prospects (Chandankere et al., 2014). Native biosurfactants producing strains could readily be isolated from the natural environment, which might prove more efficient and cost effective when compared to mass culturing, maintaining and effectiveness of an exotic microbial species in a foreign environment. Moreover, through the use of native bacterial strains issues related to legitimate and biosafety concerns can be addressed. Still, there is a critical research gap persists in the development of economically feasible bioprocesses for RL production. Specifically, there is a need for the identification and utilization of low cost renewable feedstocks to reduce upstream production costs. In addition, constructing genetically engineered microbial strains with enhanced metabolic flux toward RL biosynthesis, improved tolerance to end-product inhibition and minimized by-product formation is essential. Furthermore, implementing intensified and scalable downstream processing strategies is crucial to achieve high recovery efficiency and product purity at a reduced cost. Addressing these gaps will be pivotal in advancing RL biosurfactants from laboratory scale research to commercial scale implementation. Therefore, it requires a multidisciplinary approach encompassing synthetic biology, bioprocess engineering and life cycle assessment to create economically viable and environmentally sustainable production platforms for RLs.

1.2. Objectives

In view of the aforementioned limitations and the clearly identified research gaps within the current body of knowledge, the present research work has been systematically undertaken with the following objectives with the aim to address the key challenges in the field and to contribute to the development of a more cost-effective, scalable and sustainable approach for RL biosurfactant production for possible bioremediation applications.

i. Screening and isolation of efficient biosurfactant producing bacteria from the environment.
ii. Morpho-physiochemical characterization of the selected bacterial isolate.
iii. Physicochemical and biological characterization of the biosurfactant produced by the selected bacterial strain
iv. Determining the efficiency of the selected biosurfactant in bioremediation application

Chapter 2. Materials and Method

2.1. Collection of environmental samples

A total of thirty different numbers of soil samples were collected from ten hydrocarbons contaminated sampling sites in Mokokchung Town municipal area, Nagaland, India (Figure 5). The sampling locations included sites like, automobile workshops, car wash and fuel pumps. Three soil samples were collected from each sampling sites in a sterile sample container with the help of a sterile stainless-steel spatula, transferred to the laboratory and stored at 4 °C for further analysis.

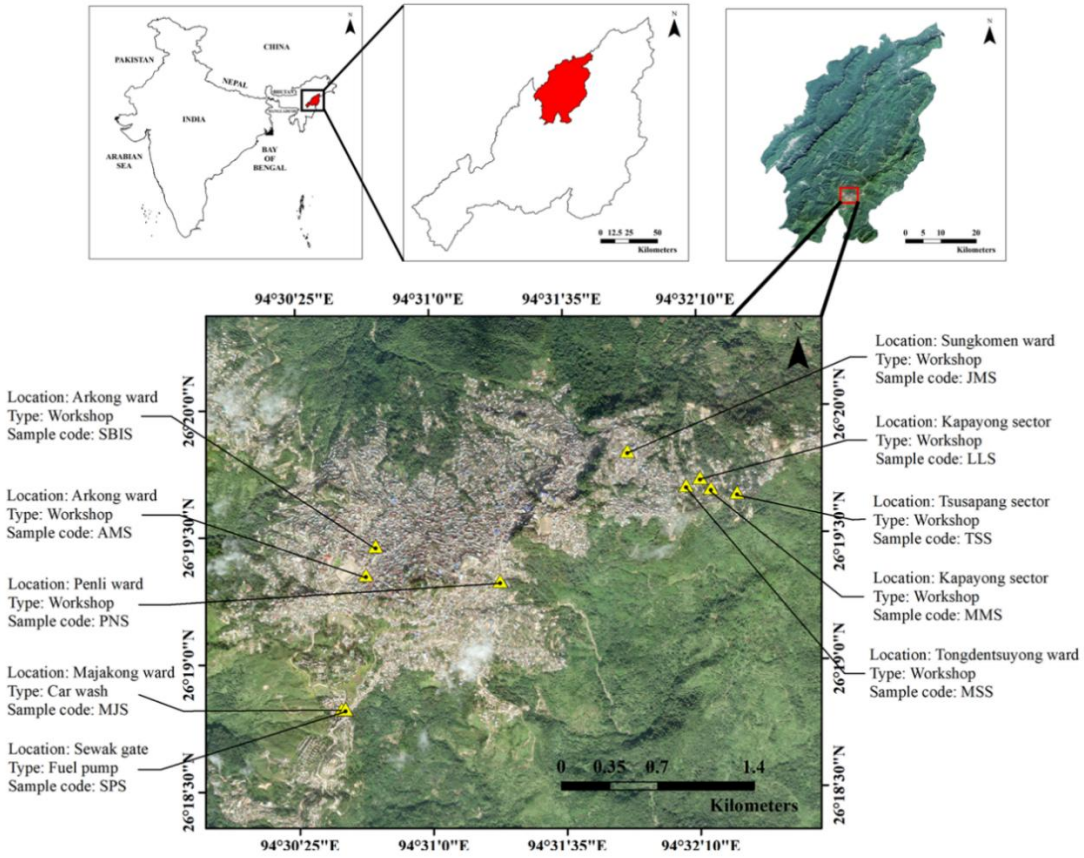

Figure 5. Sampling map

2.2. Isolation of hydrocarbonoclastic oleophilic bacteria from collected environmental samples

Isolation of hydrocarbonoclastic oleophilic bacteria was initiated via enrichment culture technique, where 5 g of each soil samples were inoculated into a 250 mL Erlenmeyer flask containing 100 mL of sterile Bushnell Haas media (Hi-media, India) with 2 % (v/v) n-hexadecane (Merck, India) as the sole carbon source. The cultures were shaken in an orbital shaker (Optics Technology, India) for 14 days at 140 rpm for the first cycle at 30˚ C ± 1. An aliquot of 1 mL from each of the original

culture was transferred to 250 mL flasks containing fresh Bushnell Haas media with n-hexadecane and incubated for another 14 days for the second cycle. The process was repeated up to the fifth cycle. After the fifth cycle, the viable bacterial populations were isolated from the liquid culture using serial dilution technique in Bushnell Haas agar plates, which were supplemented with n-hexadecane (2% v/v).

2.3. Culturing of bacterial isolates

The bacterial isolates obtained after five cycle of enrichment culture were later grown in mineral salt medium (MSM) which constituted 2.0 g urea, 2.0 g $(NH_4)_2SO_4$, 3.61 g Na_2HPO_4, 1.75 g KH_2PO_4, 0.2 g $MgSO_4$ $7H_2O$, 50 mg $CaCl_2$ $2H_2O$, 1.0 mg $FeSO_4$ $7H_2O$, 50 µg $CuSO_4$ $7H_2O$, 10 µg $MnSO_4$ $5H_2O$, 10 µg H_3BO_3, 70 µg $ZnSO_4$ $7H_2O$, and 10 µg MnO_3 in 1 litre of distilled water and the pH of MSM was adjusted to 6.8 using 6 N HCl (Bharali et al., 2011). The culture was supplemented with 2 % (v/v) n-hexadecane as the sole carbon source and the temperature and pH was adjusted and maintained at 6.8 and 30 ˚C respectively in an orbital shaker with an agitation rate of 140 rpm for 14 days (Bharali et al., 2022).

2.4. Screening of BS production by selected oleophilic bacteria

After the incubation, the liquid culture media were centrifuged at 10000 rpm for 10 minutes to separate the bacterial cell mass from the broth culture medium and the resultant cell free culture supernatants (CFCS) was used for the screening of biosurfactant (BS) production through various screening methods such as surface tension measurement, oil displacement assay, drop collapse test, penetration assay, CTAB agar test, and haemolysis test. The isolate that demonstrated the best results in the screening assays was selected for further characterization.

2.4.1. Surface tension measurement

Reduction in surface tension of the CFCS of each bacterial isolate was measured by *du Nouy* ring method using a surface tensiometer (Jencon, India) at 25 ˚C. In this technique, a platinum ring suspended from a balancing hook which is immersed in the liquid. The ring is steadily raised by lowering the sample plate and the tensiometer measures the force applied to the ring as it pulls through the surface (Varjani et al., 2014). Measurements were done in triplicates and the instrument was calibrated using distilled water (72 mN/m) before every reading (Bodour et al., 1998).

2.4.2. Oil displacement assay

About 10 µL of crude oil obtained from the abandoned Changpang oil field, Wokha, Nagaland was added on to the surface of 40 mL of distilled water in a glass petri dish (100 × 15 mm, Qualigens, Thermo Fisher Scientific) allowing it to form a thin oil layer. Then, 10 µL of CFCS of individual bacterial isolate was added on to the centre of the crude oil layer to test the presence of BS. The presence of BS in the solution causes the oil to displace around the edges of the petri dish within a minute (Cheng et al., 2017).

2.4.3. Drop collapse test

A few microlitres of distilled water were placed on a hydrophobic surface (Transparent polypropylene sheet uniformly coated with n-hexadecane) at room temperature to form bead shaped water droplet. To the droplets few microlitres (50 µL) of CFCS was added and after 5 minutes, the shape of the water droplets was observed (Bodour et al., 1998; Ghasemi et. al., 2019).

2.4.4. Penetration assay

150 µL of hydrophobic paste containing n-hexadecane and silica gel (60-120 mesh) were added into the wells of 96 well microtiter plate. 10 µL of n-hexadecane was applied on top of the paste to form a thin oil layer. Then, 100 µL of CFCS containing 10 µL of 0.5 % (w/v) safranin stain (Hi-media, India) were added and BS activity was observed (Kumar et al., 2017).

2.4.5. CTAB agar test

The fresh bacterial culture was serially diluted and inoculated onto Cetyltrimethylammonium Bromide (CTAB) Methylene Blue (MB) agar medium containing 0.15 g CTAB (Merk, India), 0.005 methylene blue (Merk, India) and 16 g of bacteriological grade agar (Hi- media, India) in 1000 mL distilled water, in order to screen the production of BS. After 48 hours of incubation at 30 °C, the plates were examined to see if the bacterial colonies had dark blue halos surrounding them (Aparna et al., 2012).

2.4.6. Hemolysis test

Blood agar plates were prepared with 5 % (v/v) of sterile mammalian blood. Sterile tubes containing anti-coagulants sodium citrate (3.2 % w/v) were used to collect fresh mammalian blood. Nutrient agar media was prepared by dissolving 28 g of

dehydrated nutrient agar powder (Hi- media, India) in 1000 mL of distilled water, which was then sterilized through autoclaving at 121˚C for 15 minutes. Following sterilization, the media at a temperature around 40 ˚C was enriched with 2 % (v/v) mammalian blood and poured into sterile petri dishes for solidification. Under aseptic conditions, discs measuring 5 mm in diameter were prepared by soaking it in the CFCS for about 30 minutes and carefully placed on the blood agar media. Subsequently, the plates were incubated at 30 °C for 24 hours. Distilled water served as the negative control (Mulligan et al., 1984; Youssef et al., 2004; Ghasemi, 2019).

2.5. Determination of oleophilic nature of the selected bacterial isolate

The bacterial isolate was cultivated in MSM supplemented with 2 % (v/v) of various hydrocarbon oils such as diesel, kerosene, waste lubricating oil, mustard oil and soybean as the sole carbon source. Incubation was carried out at 30 °C for 14 days under a constant agitation rate of 140 rpm using an orbital shaker incubator. After incubation, the culture media were centrifuged at 10000 rpm for 10 minutes. To determine the oleophilic property through BS production by the bacterial isolate, surface tension measurements of the CFCS were performed using a surface tensiometer as described in the section 2.4.1

2.6. Identification of selected bacterial isolate

2.6.1. Morphological Characterization

Colony features of the selected bacterial isolate were analysed according to the Bergey's Manual of Determinative Bacteriology (Bergey 1994) for morphological identification. Furthermore, field-emission scanning electron microscopy (FE-SEM) (JEOL, JSM7610F) was employed to analyse the external morphology of bacterial cells. Briefly, the bacteria cells were washed with 0.1 M PBS was fixed on sterile coverslip by gently immersing it in 2.5 % (v/v) glutaraldehyde solution at room temperature ~~in~~ for 60 minutes. The coverslip was then washed first with 0.1 M PBS (*Appendix-I*) for 2 minutes followed by distilled water for another 2 minutes. Dehydration was done by treating with different dilution of ethanol (25, 50, 75, and 95 %) for 5 minutes each and less than a minute in 100 % ethanol. The sample was then coated with gold and observed under electron microscope (Fischer et al., 2024). Grams reaction method was used to analyse the cell wall of the bacterial cells, following the methodology as described by Hussey and Zayaitz (2007). Spore staining was done to

ascertain the endospore forming capacity of the selected bacterial isolate (Oktari et al., 2017)

2.6.2. Biochemical Characterization

As described by Cappuccino and Sherman (2013), standard biochemical tests that includes, catalase test, oxidase test, motility test, urea test, indole test, methyl red (MR) test, Voges-Proskauer (VP) test, citrate test, triple sugar iron (TSI) test, hydrogen sulphide test and nitrate test (*Appendix-I*) were carried out. Carbohydrates fermentation test was performed for glucose, sucrose, lactose and mannitol.

2.6.3. Molecular Characterization

The selected bacterial isolate was identified at molecular level through 16S rRNA gene sequencing.

2.6.3.1. Isolation of genomic DNA

Genomic DNA was isolated from bacterial cells using the NucleoSpin® Microbial DNA Mini Kit (Macherey-Nagel, Germany), following the manufacturer's instructions.

2.6.3.2. PCR amplification of 16S rRNA gene

The bacterial 16S rRNA gene region was amplified using a standard polymerase chain reaction (PCR) protocol (Suchman, 2011). Taq DNA polymerase (Thermo Fisher Scientific, USA) was employed for the amplification. A total of 50 ng of genomic DNA was utilized as the template. The amplicon size was 80 bp and the primers used were 27F and 806R, with the sequences, AGAGTTTGATCMTGGCTCAG and GGACTACHVGGGTWTCTAAT respectively. PCR was conducted with an annealing temperature of 54 °C in a Veriti Thermal Cycler (Thermo Fisher Scientific, USA).

2.6.3.3. Agarose gel electrophoresis

A 2 % (w/v) agarose gel, spiked with LabSafe™ nucleic acid stain (G-Biosciences, USA), was prepared using SeaKem® LE Agarose (Lonza, Switzerland) in 0.5 X Tris-Borate-EDTA (TBE) buffer. PCR products (5.0 µL) were mixed with 1 µL of 6 X gel loading dye and loaded onto the gel. A 100 bp+3k DNA ladder (ExcelBand, SMOBIO, Taiwan) was used as a reference for size confirmation. Electrophoresis was conducted at 5 V/cm until the tracking dye migrated two-thirds of

the gel length. Bands were visualized using a ultra violet (UV) transilluminator and documented with the GelDoc-XR system (BIO-RAD, USA).

2.6.3.4. PCR product cleanup

The ExoSAP-IT™ PCR Product Cleanup Reagent (Thermo Fisher Scientific, USA) was used for enzymatic clean-up of the amplified PCR products, hydrolyzing excess primers and nucleotides in a single step. The purified PCR products were then ready for downstream applications such as DNA sequencing.

2.6.3.5. DNA sequencing

Post amplification, the PCR products were purified using the EXOSAP-IT kit (Invitrogen, USA) and sequenced directly using the ABI PRISM® BigDye™ Terminator v3.1 Cycle Sequencing Kit (Applied Biosystems, USA), according to the manufacturer's protocols. Sequencing was performed on a 3130 Genetic Analyzer (Applied Biosystems, USA). The resulting sequences were analysed with Sequencing Analysis Software v5.2 and ChromasPro v3.1.

2.6.3.6. Phylogenetic tree

Using NCBI BLAST, the 16S rRNA gene sequence was compared to the database of bacterial sequences. Based on the BLAST result, the evolutionary distance of the selected bacterial isolate with its most closely related strains was computed and the sequence obtained was deposited in NCBI Genebank database. Evolutionary analyses were conducted in MEGA 11 software using the maximum likelihood approach with 1000 bootstrap (Tamura et al., 2021). The Kimura 2-parameter model and the Maximum Likelihood technique were used to infer the evolutionary history (Kimura, 1980). The proportion of trees that exhibit a clustering of related taxa is displayed adjacent to the branches. A matrix of pairwise distances determined using the Maximum Composite Likelihood (MCL) technique was used to automatically generate the initial tree(s) for the heuristic search.

2.7. Growth kinetics of hydrocarbonoclastic oleophilic bacterium

The seed culture of selected bacterial strain was inoculated in MSM (pH 6.8) with 2% (v/v) n-hexadecane as the sole carbon source and incubated in an orbital shaker at 30 ˚C with an agitation rate of 140 rpm for 22 days to determine the growth behaviour and biomass quantification. Using a UV-Vis spectrometer (PerkinElmer LAMBDA® 365+double-beam UV/Vis), optical density (OD) values of the culture

was checked at 600 nm wavelength after every 24 hours of incubation, continuously for 22 days. The growth curve was obtained by plotting the absorbance value of the culture at 600 nm against the incubation time period (Singh et al. 2013).

2.8. Isolation of BS

After 14 days of incubation, bacterial cells of selected bacterial strain were removed from the culture medium by centrifugation at 10000 rpm for 10 minutes. The CFCS was precipitated by acidifying it to pH 2 using 6 N HCl and stored overnight at 4 °C. The precipitate was collected by centrifuging at 10000 rpm for 15 minutes and washed twice with phosphate buffer saline (PBS, pH 7.4) solution to remove the excess acid present with the precipitate. After washing the recovered pellets were dried in a hot air oven to remove the total moisture. The dried crude BS was then measured gravimetrically.

For partial purification of BS, the acidified CFCS precipitate was extracted thrice-using ethyl acetate at room temperature. The solvent was extracted from the organic phase and concentrated in a rotary evaporator (EV11, EVATOR) using a round-bottom flask. A sticky, honey-coloured BS was obtained at the end of the process (Bharali et al., 2011).

2.9. Purification of BS

2.9.1. Thin Layer chromatography (TLC)

The BS extracted from culture supernatant the selected bacterial strain was partly purified by solvent extraction using ethyl acetate, as describe in the section 2.8., before further purification using chromatographic methods. Thin layer chromatographic technique using TLC plates coated with silica gel 60F-254 (0.2 mm thickness, Merck) were used to identify and for the further purification of BS (Lotfabad et al. 2010). Chloroform: methanol: water (65:15:2) (v/v/v), respectively was used as the mobile phase system (Bharali et al., 2011). Developing agents such as anthrone reagent (*Appendix-I*), iodine vapour, and ninhydrin reagent (*Appendix-I*) were used to detect the presence of carbohydrate, lipid and amino acid moieties in the separated BS, respectively (Silva et al., 2010; Bharali et al., 2014).

2.9.2. *Column Chromatography*

Liquid column chromatography technique was used to separate various fractions of glycolipid type BS. A 26 cm × 3.3 cm glass column (Qualigens, Thermo

Fisher Scientific) packed with 50 g of column-grade silica gel 70-230 mesh size Merck was employed for purifying BS. A 5 g sample of partially purified BS was loaded onto the column dissolved in 10 mL of chloroform, followed by cleaning the column with chloroform to remove neutral lipids. Subsequently, fractions were collected at a flow rate of 1 mL/min, with 20 mL portions obtained using chloroform: methanol mobile phases in a sequence of 50:3 v/v (1000 mL), 50:5 v/v (200 mL), and 50:50 v/v (100 mL). A final rinse with a 1:1 (v/v) mixture of chloroform and methanol removed the residual BS from the column. The collected fractions were then evaporated to dryness under vacuum using a rotary evaporator (Mishra, 2019).

2.10. Quantification of glycolipid type BS

The direct quantification of the glycolipid type BS contained in the sample was conducted using the orcinol assay. 0.19 % (w/v) orcinol (3,5-dihydroxytoluene) reagent was prepared in 53 % sulfuric acid (v/v) (H_2SO_4) (*Appendix-I*). Sample containing BS was mixed with orcinol reagent in the ratio of 1:9 (v/v) (Sobri et al., 2018; Rahman et al., 2010). 1mL of distilled water (blank) was also subjected to treatment with orcinol reagent. Standard solutions of rhamnose ranging from 0 to 50 µg/mL were prepared in distilled water. Following preparation, all sample tubes, including blanks and standards, were immersed in a water bath at 80 °C for 30 minutes. Afterward, the tubes were allowed to cool to room temperature in a dark cupboard for 30 minutes. Prior to measuring the BS concentration in the sample, a baseline was established using blanks with an absorbance reading at 421 nm (Sobri et al., 2018). The concentrations of glycolipid were subsequently computed and expressed as rhamnose equivalents (RE) in grams per liter (g/L) by multiplying the rhamnose (Rh) values by a coefficient factor of 3.0 specifically for glycolipid (Rahman et al., 2010). The experiment was conducted in triplicate to obtain the standard deviation (SD).

2.11. Determination of surface activity

2.11.1. Determination of critical micelle concentration (CMC)

From the stock solution of BS, various concentrations of the BS solutions were prepared in water. The surface tension of the dilutions was measured at room temperature in order to calculate the critical micelle concentration (CMC). CMC was determined by plotting the surface tension as a function of BS concentration. Three

iterations of these studies were conducted in order to obtain the standard error and standard deviation (SD) (Chandankere et al., 2014).

2.11.2. *Emulsification Index* (E_{24} %)

E_{24} % was determined by adding 2 mL of CFCS and an equal amount of different hydrocarbon oil viz, diesel, kerosene, petrol, vegetable oil, waste vegetable oil and crude oil in different test tubes and vortexed for 2 minutes. The mixture was allowed to incubate for 24 hours at room temperature (Sarubbo et al., 2006; Câmara et al., 2019). The percentage of emulsification after 24 hours, E_{24} (%) was calculated using the following equation 2.1,

$$E_{24}(\%) = \frac{\text{Height of emulsion layer}}{\text{Total height of the solution}} \times 100 \qquad \textit{Equation 2.1}$$

All experiments were performed in triplicate to determine standard deviation.

2.11.3. Determination of cell surface hydrophobicity

The bacterial adhesion to hydrocarbons (BATH) assay was used to determine the cell surface hydrophobicity of selected bacterial strain. In summary, the bacterial strain was cultured in 100 mL of MSM containing 2% (v/v) n-hexadecane for two weeks at 30 °C and 140 rpm in an orbital shaker. After being separated for 15 minutes at 5000 rpm by centrifugation, and the cells were resuspended in sterile MSM. Then, after adding an aliquot of 500 µL of n-hexadecane to the 5 mL bacterial cell suspension, it was vortexed for two minutes. Optical density (OD) measurement was done at 600 nm and the bacterial cell adherence (%) to n-hexadecane was calculated using the following equation 2.2 (Chandankere et al., 2014)

$$\text{BATH} = 1 - \left(\frac{\text{A600 of the aqueous phase}}{\text{A600 of the initial cell suspension}}\right) \times 100 \qquad \textit{Equation 2.2}$$

where, A_{600} is the absorbance at 600 nm

The experiment was performed in triplicate to determine standard deviation.

2.12. Physicochemical characterization

2.12.1. Fourier-transform Infrared Spectroscopy (FTIR)

Infrared spectroscopy (IR) analysis was performed on a FTIR system (Perkin Elmer-Spectrum Two). The functional groups of the partially purified BS were analysed from the IR spectrum at wavelength range of 400–4000 cm^{-1} (Zhu et al., 2020). A translucent disc was prepared using a mixture of 10 mg of extracted BS and

100 mg of spectral purity potassium bromide (KBr) at 25 Mpa for 30s (Zhao et al., 2019). The resultant KBr disc was analysed in a FTIR spectrophotometer.

2.12.2. Thermogravimetric Analysis (TGA)

The thermal characteristics of the BS were investigated using a thermal gravimetric (TG) device (Netzsch STA 2500 Regulus). Around 8.6 mg of the BS sample was placed in an aluminium crucible and heated at a rate of 10 °C per minute in an inert environment. The flow rate of N_2 gas was maintained at 40 mL/min. The TG thermogram was generated by plotting the weight percentage (%) and heat flow against a temperature range from 0 °C to 500 °C (Abbasi et al., 2012; Khan and Sasmal, 2022).

2.12.3. Differential Scanning Colorimetry (DSC)

Differential Scanning Calorimetry instrument (Shimadzu, DSC-60, Serial no. C30724300032SA) was used to evaluate the thermal properties of BS. Prior to analysis, 10 mg of dry BS was weighed into the aluminium pans and hermetically sealed. The sample was then heated at a rate of 10 °C per minute from 30 °C to 400 °C. The onset peak, melting temperature, and enthalpy were obtained by analysing the data using the universal V3.5B TA instruments software (Lotfabada et al., 2009; Abbasi et al., 2012; Lan et al. 2015).

2.12.4. X-ray Diffraction (XRD)

The crystallinity of the extracted BS was analysed using a Miniflex Benchtop X-ray diffractometer system (RIGAKU). XRD patterns were obtained using CuKα radiation with a wavelength of 1.54 Å, employing maximum voltage and current settings of 40 kV and 30 mA, respectively. Data collection occurred over a range of 3.382º - 116.373º. Crystallinity index (CI %) was calculated using the given equation 2.3 (Acharjee et al., 2024)

$$\text{CI}\ (\%) = \frac{\Sigma \text{Ac}}{\Sigma(\text{Ac}+\text{Aa})} \times 100 \qquad \textit{Equation 2.3}$$

where, Ac is the total area of crystalline peaks, and Aa is the total area of the amorphous halo.

2.12.5. Field Emission Scanning Electron Microscopy coupled With Energy Dispersive X-Ray Spectroscopy (FE-SEM EDX)

The elemental composition of the isolated BS was analysed using field emission scanning electron microscopy (FE-SEM) in combination with energy dispersive X-ray spectroscopy (EDX). This technique enabled simultaneous morphological visualization and elemental characterization thereby providing comprehensive information about the surface features as well as the elemental composition of the sample. Imaging and analysis were carried out using a FE-SEM instrument (JEOL, JSM7610F) operated at an accelerating voltage of 15 kV as previously described by Maity et al. (2020).

2.12.6. Zeta Potential

The Zeta potential of the extracted BS was assessed via laser Doppler anemometry, while electrophoretic mobility was measured at 25 °C using a Zetasizer cuvette DTS1060 (Zetasizer Nano series, Malvern Instruments Nano Zs, 2000) (Kaszuba et al., 2010). The BS sample was prepared by uniformly dissolving it in deionised water and was filtered through Whatman filter paper (Merck, India) before loading the sample into the zeta cell

2.12.7. Liquid Chromatography and Mass Spectroscopy (LCMS)

The characterization of BS was conducted on an MS Q-TOF Mass Spectrometer model G6550B, manufactures by Agilent Technologies. The separation was based on reversed-phase chromatography using a Zorbax Eclipse XDB-C18 column, 3.0 × 150 mm, 3.5 µm, at a temperature of 40 °C. The flow rate was 0.2 mL/min. The mobile phase gradient consisted of 10 mM aqueous ammonium formate buffer with 0.05 % formic (A) and acetonitrile (B). The gradient started at 20 % B from 0 to 2 minutes, increased to 50 % from 2 to 10 minutes and reached 100 % from 10 to 15 minutes. It remained constant at 100 % for 5 minutes and was then decreased to 20 % over 8.10 minutes and kept constant until equilibration was achieved. Total run time was 30 minutes and the injection volume of sample was 2 µL (Behrens et al., 2016)

2.12.8. Nuclear Magnetic resonance (NMR)

The molecular structure of extracted BS was characterised using carbon (^{13}C NMR) and proton nuclear magnetic resonance (^{1}H NMR). The samples were prepared

by dissolving about 3 mg of BS in 1 mL of 100 % chloroform-d ($CDCl_3$) (Merk) and analysed using a NMR spectrometer (Advance DPX 500 & 300 MHz FT NMR Spectrometer, Bruker). Chemical shifts were measured in parts per million (ppm) with respect to the solvent shift, which served as the chemical standard. Using previously published data, peaks were predicted and compared (Sharma et al., 2015).

2.13. Stability studies

2.13.1. Effect of different variables on Emulsification activity (E_{24} %)

2.13.1.1. Effect of temperature on E_{24} %

CFCS was exposed to 121˚C, 100˚C, 80˚C, 40˚C, 25˚C, and 4 ˚C for 60 minutes and allowed to emulsify with diesel to determine the effect of temperature on the emulsification capacity of the BS. The percentage of emulsification (E_{24} %) was calculated using the formulae as describe in equation 2.1. All experiments were performed in triplicate to determine standard deviation.

2.13.1.2. Effect of salinity on E_{24} %

Different concentration of sodium chloride (NaCl) (Merck, India) concentration, 2 %, 5 %, 8 %, and 10 % (w/v) were added to CFCS. The supernatant with varying salt concentration were allowed to emulsify with diesel to check the variation in the emulsification indices. The mixture was allowed to incubate for 24 hours at room temperature. The percentage of emulsification (E_{24} %) was calculated using the formulae as describe in equation 2.1. All experiments were performed in triplicate to determine standard deviation.

2.13.1.3. Effect of pH on E_{24} %

The pH of the CFCS was adjusted in the range of 3, 5, 7, and 10 and allowed to emulsify with diesel. The mixture was allowed to incubate for 24 hours at room temperature. The percentage of emulsification (E_{24} %) was calculated using the formulae as describe in equation 2.1. All experiments were performed in triplicate to determine standard deviation.

2.13.1.4. Effect of heavy metal ions on E_{24} %

Different heavy metallic salt viz; $NaAsO_2$, $CdCl_2$ and K_2CrO_4 were added to CFCS. The supernatant with varying heavy metallic salt concentration were allowed to emulsify with diesel to check the variation in the E_{24} % emulsification values. The

mixture was allowed to incubate for 24 hours at room temperature. The percentage of emulsification (E_{24} %) was calculated using the formulae as describe in equation 2.1. All experiments were performed in triplicate to determine standard deviation.

2.13.1.5. Effect of time on E_{24} %

E_{24} % of the CFCS with diesel was calculated after 24 hours, 15 days, and 30 days to determine the stability of the emulsification layer with time. A graph was plotted to depict the variation in the E_{24} % within the aforesaid time span. The percentage of emulsification (E_{24} %) was calculated using the formulae as describe in equation 2.1. All experiments were performed in triplicate to determine standard deviation.

2.13.2. Effect of different variables on surface activity

2.13.2.1. Effect of temperature on surface activity

Reduction in surface tension of the CFCS was checked after exposing it exposed to a wide range of temperature viz; 121˚C, 100˚C, 80˚C, 40˚C, 25˚C, and 4 ˚C for 60 minutes to determine the effect of temperature on surface activity using *du Noüy* ring method as described in the section 2.4.1. All experiments were performed in triplicate to determine standard deviation.

2.13.2.2. Effect of salinity on surface activity

The effect of salinity on the surface activity was evaluated by adding different concentration of NaCl concentration, 2%, 5%, 8%, and 10% (w/v) to CFCS and the reduction in surface tension of the resultant salt-CFCS mixture solution was measured using a surface tensiometer using *du Noüy* ring method as described in the section 2.4.1. All experiments were performed in triplicate to determine standard deviation

2.13.2.3. Effect of pH on surface activity

In order to determine the effect of pH on the surface activity, the pH of the CFCS was adjusted in the range of 3, 5, 7, and 10 pH and the reduction in surface tension of the resultant CFCS solution was measured using a surface tensiometer using *du Noüy* ring method as described in the section 2.4.1. All experiments were performed in triplicate to determine standard deviation.

2.13.2.4. Effect of heavy metal ion on surface activity

The surface tension measurements of the CFCS containing different metallic salts ($NaAsO_2$, K_2CrO_4, and $CdCl_2$) of different concentrations (100 ppm, 300 ppm, and 500 ppm) were checked to determine the effect of metal ion on the surface tension activity using *du Noüy* ring method as described in the section 2.4.1. All experiments were performed in triplicate to determine standard deviation.

2.14. Biological activity

2.14.1. Antibacterial activity

The antibacterial activity was determined against three Gram positive and four Gram negative test bacterial strains using the disc diffusion assay (Hudzicki, 2009). *Staphylococcus aureus, Bacillus subtilis* and *Listeria monocytogenes* were the Gram-positive strains and *Escherichia coli, Klebsiella pneumonia*, *Ralstonia eutropha* and *Salmonella enteric* were used as Gram negative test bacterial strains. The disc diffusion assay was carried out to screen the antibacterial activity of the isolated BS using Muller Hinton agar (MHA) media (Hi-media, India). Sterile agar media were poured onto sterilized petri dishes (100 × 15 mm, Qualigens Thermo Fisher) and allowed to cool down inside laminar air flow chamber (Optics, India). The test microorganisms were evenly spread onto the Petri dishes containing agar medium using spread plate technique. Using sterile filter paper, discs measuring 5 mm in diameter were prepared by soaking it for about 10 minutes in a solution of BS prepared in DMSO (10 % v/v) (Merck, India) at a concentration of 40 mg/mL. The discs were gently placed over the culture media and incubated at 37 ˚C for 24 hours. The diameter of the clear zones around the filter paper discs containing the BS solution was measured using an antibiotic zone scale to determine its antibacterial activity (Das and Mukherjee, 2005; Christova et al., 2011). DMSO (10 % v/v) was used as the negative control while Streptomycin (10 mcg/disc) (Hi-media, India) was used as the positive antibacterial agent. All experiments were conducted on triplicates to obtain the stand deviation.

Half maximal inhibitory concentration (IC_{50}) values denote the concentration of a compound or agent required to inhibit 50 % of the pathogen population and was performed through micro dilution method (Zhao et al., 2022). Briefly, the test bacterial strains with positive results in the disc diffusion assay were serially diluted in 96 well microtiter plate. About 10 µL of 3 -(4,5-dimethylthiazol-2-yl)-2,5-diphenyltetrazolium bromide (MTT) solution (0.45 mg/mL) (ThermoFisher scientific) was added to each

well and about to incubate in a dark place for about 60 minutes which led to the coloration of the wells containing the samples. Blue colour wells indicated the live bacteria and yellow colour indicated the dead bacteria and the MIC values were determined by measuring the OD at 600 nm with a microplate reader (Multiskan SkyHigh Microplate Spectrophotometer, ThermoFisher Scientific) (Costa et al., 2010; Zhao et al., 2022). All experiments were performed in triplicate to determine standard deviation.

2.14.2. Larvicidal activity

Larvicidal assay was carried out using shrimp larvae. For the assay, brine shrimp (*Artemia salina*) eggs (Red Ring Artemia Cyst, MAF) were hatched in brine water (20 g/L) and kept in an aerated container to allow it to attain a similar developmental stage of the larval lifecycle. Different concentrations (200−1400 µg/mL) of BS were prepared in distilled water in test tubes. To them, an equal number of larvae (i.e. seven larvae) of same stage were transferred and incubated for 24 hours at room temperature. The number and the time taken for the larval death in each tube were noted. SDS (0.1 % w/v) (Merck, India) was used as positive control and brine solution (2 %) was kept as negative control. The lethal concentration (LC_{50}) for the sample were calculated through linear regression analysis of concentration response data in Microsoft Excel (Ghribi et al., 2012; Jayasree et al., 2018; Diab et al., 2020). All experiments were performed in triplicate to determine standard deviation.

2.14.3. Phytotoxicity

The biological activity of the BS was tested using a phytotoxicity assay by measuring the root development and seed germination. In this assay, 5.0 mL of BS solution with concentration at CMC, below CMC and above CMC were added to a sterilised Petri dish (100 × 15 mm, Qualigens Thermo Fisher) lined with Whatman No. 1 filter paper (Merck, India). 15 healthy seeds of *Vigna radiata*, were pre-treated with 2% (v/v) sodium hypochlorite (Merck, India) and cultured in a Petri plate at 20 °C in the dark for 5 days. The germination index (GI) was computed using the equation 2.4.1, 2.4.2, and 2.4.3 as described by Gidudu and Chirwa (2022). Distilled water was used as negative control and 0.1% (w/v) SDS positive as control. All experiments were performed in triplicate to determine standard deviation.

$$\text{Relative seed germination (\%)} = \frac{\text{Number of seeds germinated in the sample}}{\text{Number of seeds germinated in the control}} \times 100$$

Equation 2.4.1

$$\text{Relative root length (\%)} = \frac{\text{Mean root length in the sample}}{\text{Mean root length in the control}} \times 100$$

Equation 2.4.2

$$\text{Germination index (\%)} = \frac{\text{Relative root length}}{\text{Relative seed germination}} \times 100$$

Equation 2.4.3

2.14.4. Antibiofilm activity

The influence of varying BS concentrations (1000–3.9 µg/mL) on biofilm activity was evaluated using a 96-well microtiter plate assay. For the assay *Lysinibacillus* sp. was used as the test bacterial strain known to produce biofilm. Tryptic soy broth (TSB) (Hi-media, India) supplemented with 1 % (w/v) glucose (Merck, India) was used as the culture medium. A 200 µL aliquot of the BS solution was added to the first well, and 100 µL of TSB was dispensed into each subsequent well. A serial dilution was performed by transferring 100 µL from the first well to subsequent wells. Following the preparation of dilutions, 100 µL of the bacterial test culture was added to all wells. The microtiter plate was incubated at 37 °C ± 2 for 24 hours. After incubation, the contents of the wells were aspirated, and each well was washed with 200 µL of phosphate-buffered saline (PBS). To fix the biofilm, 200 µL of 100 % methanol (Merck, India) was added to each well and incubated for 15 minutes. The wells were then stained with 200 µL of 1 % (w/v) crystal violet (Hi-media, India) for 20 minutes. Excess stain was aspirated, and the wells were rinsed with distilled water. Subsequently, 200 µL of 33 % (v/v) acetic acid (Merck, India) was added to solubilize the stain, and the OD was measured at 630 nm using a microplate reader (Al-Razn et al., 2021). TSB without BS was used as a control, and all experiments were performed in triplicate to determine standard deviation.

2.14.5. Cytotoxicity Assessment

2.14.5.1. Cell viability – MTT assay

Primary rat liver cells (hepatocytes) provided by Dr. J. Manivannan of Bharathiar University, Coimbatore, Tamil Nadu, India were grown in Dulbecco's Modified Eagle's Medium (DMEM) (*Appendix-I*) containing penicillin (100 units/mL), 10% (v/v) Fetal Bovine Serum (FBS) and streptomycin (100 g/mL). The

culture medium was replenished every 48 hours and the cells were maintained under controlled conditions at 37 °C in a humidified atmosphere containing 5 % CO_2. As determined by the trypan blue exclusion assay, cell populations exhibiting >90 % viability were selected for microplate-based assays. Subsequently, proliferated cells were seeded into fluorescence-compatible 96-well plates at a density of 2×10^3 cells per well for BS exposure analysis. MTT assay (3-[4,5-dimethylthiazol-2-yl]-2,5-diphenyltetrazolium bromide) was employed to evaluate cell viability as described by Li et al. (2015). The assay is grounded on mitochondrial dehydrogenases that transform MTT into formazan crystals. The cells were exposed to a series of BS concentration of 25, 50, 75 and 100 µg/mL for 24 hours at 37 °C with 5 % CO_2 in a cell culture incubator. MTT was then administered to the cells at the concentration of 0.45 mg/mL. After 4 hours of treatment at 37 °C, the supernatant was removed and developed formazan crystals were dissolved in 100 µL of DMSO (10 % v/v). Absorption was read at 570 nm on a multimode microplate reader (Synergy H1MFG, Biotek, USA). The cell viability was determined by the absorbance data when compared with the control cells which were 100 % viable.

2.14.5.2. Cellular oxidative stress – DCFDA assay

The level of intracellular reactive oxygen species (ROS) was assessed using the general ROS indicator CM-H2DCFDA [5-(and-6)-chloromethyl-2′,7′-dichlorodihydrofluorescein diacetate] from Invitrogen, USA. Free radicals change H2DCF (2',7'-dichlorodihydrofluorescein) into DCF (2'-7'dichlorofluorescein), a green luminous molecule, when intracellular esterases deacetylate it (Ng and Ooi, 2021). In summary, the rat liver cells were treated with different concentrations of BS (25, 50, 75 and 100 µg/mL) and then incubated with 10 µM CM-H2DCFDA at 37 °C for 45 minutes in a CO_2 incubator. The cells were then washed twice with PBS to remove DCF and the fluorescence intensity of DCF was measured (Exitation/Emission: 485/530 nm) using a multimode microplate reader (Synergy H1MFG, Biotek, USA). The findings were expressed in arbitrary units (a.u.) (Maadurshni et al., 2022).

2.14.5.3. Cellular superoxide generation – DHE assay

This study utilized the Dihydroethidium (DHE, Sigma Aldrich) fluorescence method to evaluate the generation of cellular superoxide in rat liver cells after exposure to various concentration of BS (25, 50, 75 and 100 µg/mL) as stated by Nagarajan et

al. (2024). Briefly, the rat liver cells were treated with different concentration of BS and were incubated at 37 °C in the dark for 30 minutes with 5 μM DHE in a cell culture incubator. The cells were then washed twice by PBS to remove any leftover staining solution. Through the use of a multimode microplate reader (Synergy H1MFG, Biotek, USA) the fluorescence intensity of DHE was measured (Exitation/Emission: 510/590 nm) and expressed in arbitrary units (a.u.). To evaluate the cytotoxicity of BS, a one-way analysis of variance (ANOVA) was performed followed by Duncan's Multiple Range Test (DMRT) for comparison of cellular parameter means. A threshold of $P < 0.05$ was considered indicative of statistical significance throughout the analysis (Walling et al., 2023).

2.14.6. In silico antiviral activity of BS through Molecular docking approach

For the study, cell surface-binding protein OPG105 (Uniprot ID: Q8V4Y0) was retrieved from Uniprot server. The homology model was prepared and the structure assessment was done for the E8L protein of Monkeypox virus (MPXV) using Swiss-Model online tool (https://swissmodel.expasy.org/). Ramachandran plot of the protein structure was also prepared to analyse the geometric stability of the protein. The structure of chondroitin sulphate, aztreonam, tecovirimat and lidocaine were retrieved from pubchem database (https://pubchem.ncbi.nlm.nih.gov/) in SDF (Structure Data File) format and imported to Chemdraw 3D and the energies were optimized using MM2 (Molecular Mechanics 2) force field method. While, structure of the rhamnolipid (RL) BS were sketched using Chemdraw software and energy optimization were done using MM2 force field (Chemoffice 2021). Once optimized, the structures were exported in mol2 format and used for the *in silico* and molecular docking studies. The ADME (Absorption, Distribution, Metabolism and Excretion) predictions for the RL congeners under study were computed using Swiss ADME web-based services (http://www.swissadme.ch/) for determining their pharmacophore and drug likeness properties. Docking simulations were performed using Molegro Virtual Docker (MVD) software version 6.0 which uses MolDock scoring function as a measure for binding affinity. This scoring function is based on the differential evolution and is computed using the scoring function

$$E_{score} = E_{inter} + E_{intra,}$$

where E_{inter} is the ligand–protein interaction energy and E_{intra} is the internal energy of the ligand.

In order to run docking simulations, water molecules from receptor protein were removed, polar hydrogens were added and charges were assigned. Active pockets within the receptor protein were detected by MVD and docking simulations were performed for 30 runs each, out of which the top poses were selected for studying the molecular interaction. The visualization of the molecular interactions and their energies were done using BIOVIA Discovery Studios (Design 2014).

2.15. Bioremediation application

2.15.1. Crude oil Removal

Sand samples artificially contaminated with crude petroleum were washed in the aqueous BS solution. Dried acid washed sand was mixed with crude oil (10 % w/w) and kept at room temperature for 15 days. 100 mL of BS solution at different concentrations (at CMC, above CMC and below CMC) were mixed with 5 g of sand samples and stored at room temperature with 200 rpm in an orbital incubator shaker for 24 h. A hot air oven was used to dry the sand for the following 24 h at 50 °C after the aqueous BS solution was decanted. The flask with only crude oil contaminated sand and water was kept as control. Gravimetric analysis method was used to determine the amount of residual oil using the following equation 2.5.

$$\text{Crude oil removed (\%)} = \frac{(Oi - Or)}{Oi} \times 100 \qquad \text{Equation 2.5}$$

where O_i = initial weight of the contaminated sand sample before washing and, O_r = weight of the contaminated sand sample after washing (Costa et al., 2010). The experiment was performed in triplicate to determine standard deviation.

2.15.2. Crude oil degradation

1.0 mL of the freshly grown culture of the bacterial strain was inoculated in 250 mL volume Erlenmeyer flasks each containing 2 % (v/v) of crude oil, and MSM. The cultures were allowed to incubate at 30 ± 2 °C in an orbital shaker for 15, 30, 45 and 60 days at 140 rpm. Distilled water was used as control and was subjected to the same culture conditions. After each incubation period, the cultures were centrifuged at 4500 rpm for 10 minutes to separate the bacterial biomass and the residual hydrocarbon oil fractions in the CFCS were extracted twice using dichloromethane (DCM) in the ratio of 1:1 (v/v) (Zhang et al., 2012). After the extraction process, the residual crude oil in the organic solvent phase was concentrated using a rotary evaporator (EV11, EVATOR) and stored in glass vials for further analysis.

2.15.3. Analysis of hydrocarbon degradation by gas chromatography-mass spectroscopy

The contents of the residual crude oil extracted over a period of 15, 30, 45 and 60 days were analysed using Gas Chromatography-Mass Spectroscopy (GC-MS) (Clarus 600 PerkinElmer, USA) (Singh and Tiwary, 2016). Before being elevated to 280 °C for crude oil analysis, the column temperature was maintained at 50 °C for five minutes. A split ratio of 20:1 was used for all studies. Helium (He) was the carrier gas, and the flow rate was 0.8 mL per minute. The injector was adjusted at a temperature of 250 °C (Bharali et al., 2022).

2.15.4. BS mediated removal of heavy metals from contaminated sand particles

2.15.4.1. Preparation of heavy metals contaminated sand sample

Approximately 500 g of construction grade sand were collected from the premises of Nagaland University, Lumami. The sample was subjected to mechanical sieving to obtain sand particles within the size range of 0.074–0.424 mm. To eliminate organic impurities, the sieved sand was immersed in concentrated nitric acid (HNO_3) for a duration of 60 minutes. Subsequently, the acid-treated sand was repeatedly rinsed with distilled water until the effluent reached a neutral pH, indicating the complete removal of residual acid. The cleaned sand was then oven-dried at 80 ± 2 °C for 24 hours to ensure the removal of all moisture content. 5 g aliquots of oven-dried sand were artificially spiked with 10 mL of a 100 ppm solution of sodium arsenite ($NaAsO_2$) (Qualigen Thermo Fisher) solution and homogenized to achieve uniform heavy metal distribution. The individual mixtures were then completely dried in a hot air oven at 80 ± 2 °C for 24 hours.

2.15.4.2. Batch experiment on heavy metals contaminated sand washing by BS solution

The washing of heavy metal laden sand sample was carried out using BS preparation, specifically the CFCS, at three different concentrations relative to its CMC. To evaluate the efficiency of heavy metal removal at varying BS concentration, 5 g of contaminated sand were accurately weighed and transferred into 250 mL volume Erlenmeyer flasks. Each sample was then treated with 50 ml of BS solution at CMC, below CMC, and above CMC concentration (Sarubbo et al., 2018). The flasks were agitated in a rotary shaker at 150 rpm for 24 h at 37 ˚C (Luna et al., 2016) to facilitate

interaction between the sand matrix and the BS solution, thereby enhancing the desorption of heavy metal ions from the solid phase into the aqueous phase. In order to assess the relative efficacy of the BS, comparative treatments were also carried out. Synthetic surfactant, sodium dodecyl sulfate (0.1 % SDS) was employed as a positive control while distilled water was used as a negative control (Sarubbo et al., 2018). These control treatments allowed for a comprehensive evaluation, facilitating the determination of the optimal BS concentration and its relative performance in promoting the mobilization of heavy metals from the sand. The experiment was performed in triplicate to determine standard deviation.

2.15.4.3. Preparation of sample for ICPMS analysis

Acid digestion was carried out following the handbook of sample preparation for ICPMS analysis by Thermo Fisher Scientific (Scientific, 2021). Briefly, 3 mL of concentrated HNO_3 was added to 100 mL of the sample in a 150 mL Griffin beaker (Merck) and gently heated after covering until the volume was reduced to about 5 mL The mixture was cooled and another 3 mL of concentrated HNO_3 was added and refluxed until digestion was complete which was indicated by the appearance of a light colour. The solution was then uncovered and evaporated again to about 3 mL. A small amount of 1:1 HCl and HNO_3 was added to the mixture after cooling and was refluxed for 15 minutes to dissolve any remaining residues. The beaker walls and cover are rinsed with ultrapure water. Finally, the sample is diluted to up to a volume of 100 mL with ultrapure water and the acid concentration was adjusted to 10 % (v/v) and was in an ICPMS spectrometer (Shimadzu ICPMS-2040/2050). All experiments were performed in triplicates to obtain the standard deviation value.

2.15.4.4. Effect of pH and salinity on heavy metal removal

The influence of pH and salinity on the efficacy of heavy metal removal was systematically investigated (Chen et al., 2017). Precisely 5 g of sand contaminated with 2 mL of stock arsenite solution were accurately weighed and transferred into 250 mL volume Erlenmeyer flasks. Each sample was treated with 50 mL of a BS solution prepared at its CMC. For the pH dependent study, sample pH values were adjusted to 3.0, 5.0, 7.0 and 10.0 using HCl and NaOH. In a parallel set of experiments, salinity levels were modulated to 0.5 %, 1.0 %, 1.5 % and 2.0 % (w/v) by the addition of NaCl. All samples were subjected to agitation at 150 rpm and incubated at 37˚C for a duration of 24 hours. Following incubation, supernatants were separated, subjected to acid

digestion and subsequently analysed for metal content using ICP-MS as described in the section 2.15.4.3. The experiment was performed in triplicate to determine standard deviation.

2.16. Valorisation of waste residual cooking oil (WRCO) as alternate carbon source for BS production

2.16.1. Carbon source

The carbon feedstock utilized in this study was leftover discarded used cooking oil gathered from kitchen waste (Nagaland University, Lumami). The vegetable oil (Dhara Nourish Vit A E Refined Sunflower Oil) was obtained after multiple frying of chicken meat and potato chunks. The gathered WRCO was initially filtered through a clean cheese cloth to eliminate suspended particles, which was subsequently centrifuged at 3000 rpm for 10 minutes to separate fine suspended particles and finally dried in a laboratory hot air oven for overnight period at 50 °C.

2.16.2. Growth condition and BS quantification

The selected bacterial strain was cultivated on mineral salt medium (MSM) supplemented with 2% (v/v) WRCO as the sole carbon source. The growth of the bacterium was monitored continuously for 10 days as described in the section 2.7. The experiment was performed in triplicate to determine standard deviation.

Orcinol assay was used to quantify the total BS yield at the end of the incubation period as described in the section 2.10. The experiment was performed in triplicate to determine standard deviation.

2.16.3. Recovery and partial purification of BS

The BS was extracted from the matured culture after 10 days of incubation using acid precipitation method followed by solvent extraction method as described in the section 2.8. The resultant final brown viscous liquid was collected and stored at 4 °C.

2.16.4. Purification of BS

The partially purified BS, which was previously extracted through solvent extraction method was further purified through TLC and column chromatography technique as described in the section 2.9.

2.16.5. Physicochemical characterization of isolated BS

The properties such as reduction in the surface tension (ST), critical micelle concentration (CMC) and emulsification activity (E_{24}%) of the isolated BS were measured as described in the section 2.4.1, 2.11.1 and 2.11.2, respectively. E_{24}% was determined against different test hydrophobic substrates such as diesel, soybean oil, rice bran oil, waste cooking oil, kerosene and petrol. The experiment was performed in triplicate to determine standard deviation.

The thin layer chromatography (TLC) technique was employed for the qualitative estimation of carbohydrate and lipid components in the extracted BS as described in the section 2.9.1. A FTIR spectrometer was used to record the IR spectrum of the extracted BS for the purpose of identifying functional groups as described in the section 2.12.1. Crystallinity (CI%) of the isolated BS was determined as described in the section 2.12.4. TGA was used to examine the thermo-chemical properties of the extracted BS as described in the section 2.12.2. ESI-MS (Electrospray Ionization Mass Spectrometry) technique was employed to determine the chemical structure of the BS by using a mass spectrometer (Expression-S, Advion) in negative ion mode with methanol as the solvent (Haba et al., 2003). The following parameters were maintained; positive ion polarity, ESI as ion source, nebulizer pressure was 30 psi, temperature was set at 325 °C with a dry gas flow rate of 8 litre/minute, capillary exit was kept at 110 V and the trap drive value was 32.1 (Lan et al. 2015). Total run time was 1.5 minutes and the total scan range was from 0 to 900 m/z (mass to charge ratio.

2.16.6. Ex-situ washing efficiency of BS

Crude oil contaminated acid washed sand samples for the investigation was prepared as described in the section 2.15.1. Washing efficiency of BS produced by the bacterial strain using WRCO at CMC, above CMC and below CMC were determined as previously described in the section 2.15.1. The flask with crude oil contaminated sand and water was kept as control. Gravimetric method was used to determine the amount of residual oil using the equation 2.5 described in the section 2.15.1. The experiment was performed in triplicate to determine standard deviation.

Chapter 3. Results

3.1. Isolation of hydrocarbonoclastic bacteria from environmental samples

A total of thirty different numbers of soil samples were collected from ten hydrocarbons contaminated sampling sites in Mokokchung Town area as shown in Figure 5. From the environmental samples a total of 60 number of bacterial isolates were obtained after the 5th cycle of enrichment cultures and serial dilution technique (Figure. 6). The morphological characteristics were recorded and the same is presented in Table 3.

Figure 6. Isolation of hydrocarbonoclastic bacterial isolates from collected soil samples through (a) Enrichment culture of soil samples and (b) Serial dilution method

Table 3. Colony morphology of obtained hydrocarbonoclastic bacterial isolates

Sl. No.	Colony Code	Shape	Margin	Elevation	Texture	Colour	Optical Density
1.	PNS1a	Round	Entire	Convex	Glistening	Cream	Opaque
2.	PNS1b	Irregular	Lobate	Flat	Butyrous	Cream	Opaque
3.	PNS1c	Irregular	Undulate	Flat	Dull	Cream	Opaque
4.	PNS2a	Round	Entire	Convex	Glistening	Yellow	Opaque
5.	PNS2b	Irregular	Lobate	Growth in Medium	Dull	Cream	Opaque
6.	PNS2c	Round	Lobate	Umbonate	Butyrous	Orange	Opaque
7.	PNS2d	Irregular	Filamentous	Umbonate	Butyrous	Cream	Opaque
8.	PNS3a	Irregular	Lobate	Flat	Butyrous	Cream	Opaque
9.	PNS3b	Irregular	Lobate	Umbonate	Viscid	Dull Yellow	Opaque
10.	PNS3c	Round	Entire	Raised	Butyrous	Dark Yellow	Opaque
11.	PNS3d	Rhizoid	Filamentous	Flat	Butyrous	Cream	Opaque
12.	PNS3e	Irregular	Lobate	Umbonate	Butyrous	Dark Orange	Opaque
13.	PNS3f	Curled	Entire	Flat	Butyrous	Cream	Opaque
14.	Ams1a	Round	Entire	Flat	Butyrous	Cream	Opaque
15.	AMS1b	Round	Entire	Convex	Glistening	White	Opaque
16.	AMS2a	Round	Lobate	Convex	Glistening	Yellow	Opaque
17.	AMS2b	Round	Entire	Convex	Glistening	Orange	Opaque
18.	AMS2c	Round	Entire	Flat	Glistening	Yellow	Opaque
19.	AMS2d	Round	Entire	Flat	Dull/ Cream	Yellow	Opaque
20.	AMS3a	Round	Entire	Flat	Butyrous	White	Opaque
21.	AMS3b	Irregular	Curled	Umbonate	Butyrous	White	Opaque
22.	AMS3c	Round	Irregular	Umbonate	Butyrous	White	Opaque
23.	TSS1a	Round	Entire	Flat	Glistening	Cream	Transparent
24.	TSS1b	Irregular	Undulate	Flat	Dull	Yellow	Opaque
25.	TSS1c	Round	Entire	Convex	Glistening	White	Opaque
26.	TSS1d	Round	Entire	Convex	Glistening	Orange	Opaque
27.	JMS1a	Round	Entire	Convex	Glistening	Orange	Opaque
28.	JMS1b	Round	Entire	Convex	Glistening	Yellow	Opaque
29.	JMS1c	Round	Entire	Flat	Dull	Orange	Opaque
30.	JMS1d	Round	Entire	Convex	Glistening	White	Opaque
31.	JMS1e	Irregular	Lobate	Flat	Dull	Cream	Opaque
32.	Sbis3a	Irregular	Lobate	Flat	Butyrous	Creamy	Opaque

33.	SBIS3b	Irregular	Undulate	Round	Glistening	Creamy	Transparent
34.	SBIS3c	Round	Entire	Flat	Butyrous	White	Opaque
35.	SBIS3d	Round	Entire	Convex	Glistening	Creamy	Opaque
36.	SBIS2a	Round	Entire	Raised	Glistening	Creamy	Opaque
37.	SBIS2b	Round	Lobate	Flat	Glistening	Cream/ Yellow	Opaque
38.	SBIS1a	Round	Entire	Raised	Glistening	Yellow	Opaque
39.	SBIS1b	Irregular	Filamentous	Flat	Glistening	White	Opaque
40.	SBIS1c	Round	Undulate	Raised	Glistening	Creamy	Opaque
41.	SBIS1d	Round	Entire	Raised	Glistening	White	Opaque
42.	SBIS1e	Round	Entire	Umbonate	Glistening	White	Transparent
43.	MJS1a	Round	Entire	Convex	Butyrous	Creamy	Opaque
44.	MJS1c	Irregular	Filamentous	Umbonate	Dull	Creamy	Opaque
45.	SPS3a	Irregular	Irregular	Flat	Butyrous	Yellow	Opaque
46.	SPS3b	Round	Entire	Raised	Glistening	Orange	Opaque
47.	SPS3d	Round	Entire	Flat	Butyrous	White	Opaque
48.	SPS3e	Round	Entire	Convex	Butyrous	Whitish	Opaque
49.	SPS3f	Round	Entire	Convex	Butyrous	Brownish	Opaque
50.	SPS3g	Round	Entire	Raised	Butyrous	Yellow	Opaque
51.	SPS1a	Irregular	Irregular	Raised	Butyrous	White	Opaque
52.	SPS2a	Irregular	Filamentous	Inside Media	Dull	White	Opaque
53.	SPS2b	Round	Entire	Inside media	Butyrous	White	Opaque
54.	SPS2c	Round	Entire	Flat	Glistening	White	Translucent
55.	SPS2d	Round	Entire	Flat	Butyrous	White	Opaque
56.	MMS3a	Irregular	Irregular	Flat	Friable	Brownish	Opaque
57.	MMS3i	Rhizoid	Filamentous	Flat	Butyrous	White	Opaque
58.	LLS2d	Round	Entire	Raised	Glistening	Pinkish	Opaque
59.	LLS2e	Irregular	Lobate	Flat	Butyrous	White	Opaque
60.	MSS2b	Round	Entire	Raised	Butyrous	White	Opaque

3.2. Culturing of obtained hydrocarbonoclastic bacterial isolates

Obtained bacterial isolates were further grown in MSM supplemented with 2% (v/v) n-hexadecane for further screening and characterization. A total of 15 different isolates were obtained from the MSM culture and were checked for reduction in surface tension (ST) of water using a surface tensiometer. Results of reduction in the ST of the cell free culture supernatant (CFCS) of the obtained bacterial isolates are

presented in Table 4. The CFCS of the isolate, AMS1a showed the best surface activity in terms of ST reduction measurement and was selected for further screening of BS production.

Table 4. Measurement of reduction in the ST of the CFCS of the obtained hydrocarbonoclastic bacterial isolates

Colony Code	GPS Co-ordinates	Elevation (m)	Location	Location Type	ST Reduction (mN/m)
SPS3a	26.31368˚N, 94.51033˚E	1185	Sewak	Fuel	38.6
SPS3b	26.31368˚N, 94.51033˚E		Gate	Station	37.3
SPS3d	26.31368˚N, 94.51033˚E				38.1
SPS3e	26.31368˚N, 94.51033˚E				36.9
SPS3f	26.31368˚N, 94.51033˚E				39.4
SPS2a	26.31368˚N, 94.51033˚E				38.5
MMS3a	26.32791˚N, 94.53710˚E	1321	Kapayong	Workshop	35.8
MMS3i	26.32791˚N, 94.53710˚E		Sector		39.4
AMs1a	26.32435˚N, 94.51264˚E	1244	Arkong	Workshop	34.4
AMS2c	26.32435˚N, 94.51264˚E		Ward		35.7
LLS2d	26.32861˚N, 94.53630˚E	1313	Kapayong	Workshop	37.3
LLS2e	26.32861˚N, 94.53630˚E		Sector		40.8
SBIS1a	26.32248˚N, 94.51191˚E	1276	Arkong	Workshop	36.2
SBIS1b	26.32248˚N, 94.51191˚E		Ward		38.5
TSS1d	26.32810˚N, 94.53528˚E	1323	Tsusapang Sector	Workshop	35.6

3.3. Screening of biosurfactant production by selected hydrocarbonoclastic bacterial isolate

Screening assays such as oil displacement, drop collapse test, and penetration assay were carried out to screen the production of biosurfactant (BS). In the oil displacement assay, the CFCS of the selected bacterial isolate was able to effectively displace and spread the crude oil in the petri dish indicating the presence of BS. In the drop collapse assay, the water drops instantaneously destabilized and collapsed with the introduction of CFCS to the water drop. The penetration assay demonstrated that the colored CFCS was able to break and penetrate through the oil barrier into the silica-oil paste at the bottom of the 96 well microplates indicating the presence of BS. The selected bacterial isolate was further screened using CTAB agar and hemolysis assays. The clear zone around the wells in the hemolysis assay indicated the production of BS.

The anionic nature of the BS was confirmed through the CTAB agar test as it showed dark blue halos around the bacterial colonies. The results of the screening assays are presented in Figure 7.

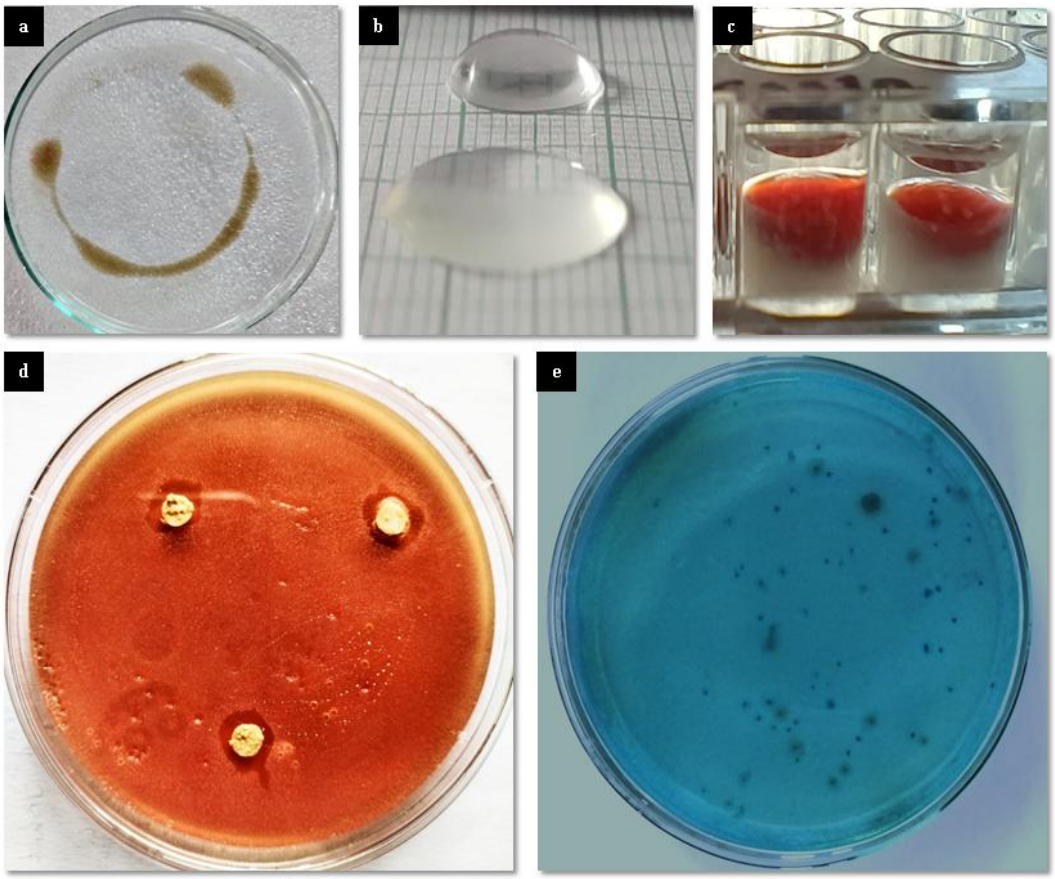

Figure 7. Screening of BS production (a) oil displacement assay, (b) drop collapse test, (c) penetration assay, (d) Hemolysis assay and (e) CTAB agar test

3.4. Determination of oleophilic nature of selected hydrocarbonoclastic bacterial isolate

The selected bacterial isolate was cultured in MSM supplemented with five different types of hydrocarbons. Results clearly showed that the selected bacterial isolated could able to grow and utilize all the tested hydrocarbons and the same is shown in Figure 8. Further, reduction in ST of the CFCS all the bacterial cultures supplemented with test hydrocarbons were determined and are presented in Table 5.

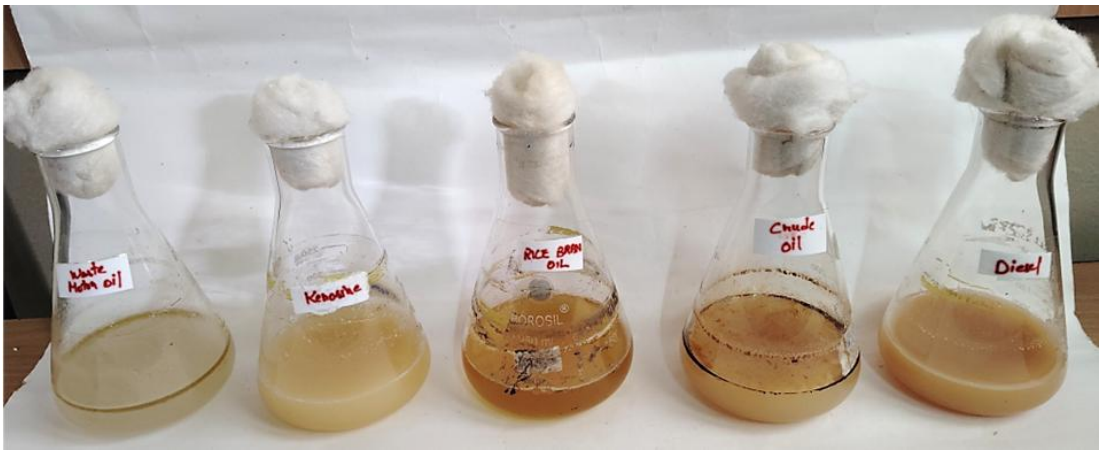

Figure 8. Growth of selected bacterial isolate in MSM supplemented with different hydrocarbons

Table 5. Reduction in ST of the culture medium by the selected bacterial isolate when grown in MSM supplemented with different hydrocarbons

Sl. No.	Type of test hydrocarbon	ST Reduction (mN/m)
1.	Diesel	34.5 ± 0.06
2.	Kerosene	34.9 ± 0.1
3.	Waste Motor/Lubricating oil	35.3 ± 0.1
4.	Crude oil	35.3 ± 0.1
5.	Soyabean oil	34.4 ± 0.06

3.5. Identification of selected hydrocarbonoclastic bacterial isolate

The colony morphology of the selected bacterial isolate, AMS1a was determined using standard method and the results of the same is presented in Table 6. Through Gram staining, the isolate was found to be rod-shaped Gram-negative bacterium (Figure 9). Results of standard biochemical tests of the selected bacterial isolate are presented in Table 6. The selected bacterium was further identified as *Pseudomonas aeruginosa* (AMS1a) through 16s ribosomal RNA gene sequencing and the obtained sequence was submitted in NCBI with the accession number OR642782. In the phylogenetic tree analysis, the topology with the superior log likelihood value was chosen. There were fourteen nucleotide sequences in this investigation and the same is presented in Figure 10.

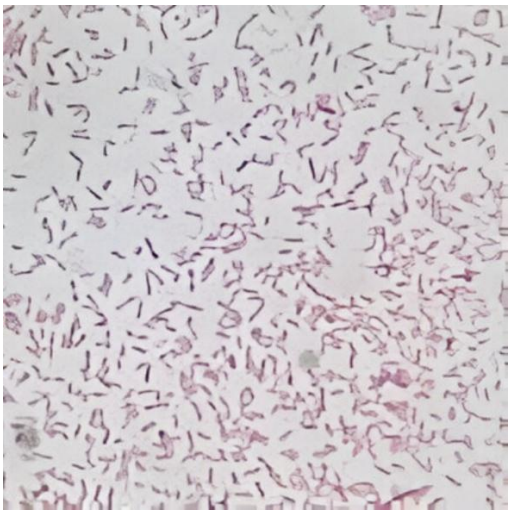

Figure 9. Microscopic image (40X) of Gram reaction of the selected hydrocarbonoclastic bacterial isolate

Table 6. Standard biochemical tests of the selected hydrocarbonoclastic bacterial isolate

Biochemical Tests	**Result**
Gram staining	Negative rods
Spore staining	Negative
Catalase test	Positive
Oxidase test	Positive
Motility test (SIM)	Positive
Urea test	Negative
Indole test	Negative
MR test	Negative
VP test	Negative
Citrate test	Positive
TSI test	Alkaline
H_2S Test (SIM)	Negative
Nitrate test	Positive with Gas
Carbohydrate fermentation after 24 hrs	
Glucose	Positive
Sucrose	Negative
Lactose	Negative
Mannitol	Negative

FESEM coupled with EDX analysis was used to determine the morphological structure and surface elemental composition of the bacterium respectively (Figure 11). The EDX analysis revealed that carbon (C), oxygen (O) and nitrogen were the most abundant elements in the selected bacterial isolate with an atomic percentage of 68.81, 17.77 and 11.37 % respectively.

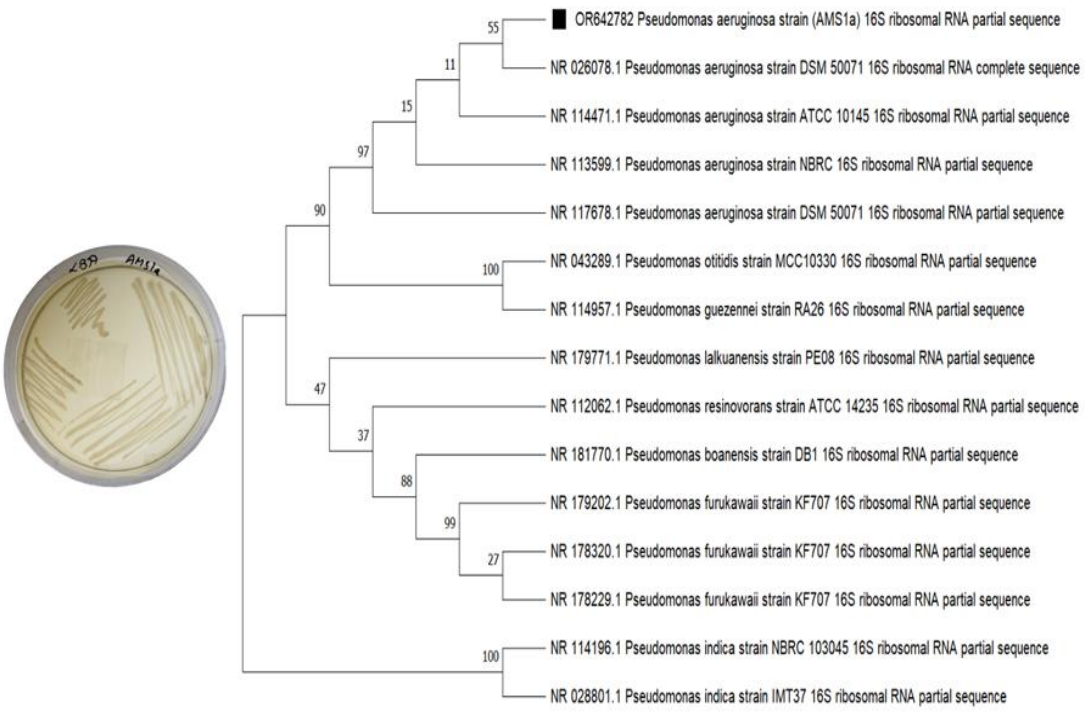

Figure 10. Phylogenetic tree analysis of the selected hydrocarbonoclastic bacterium

3.6. Growth kinetics and BS production

The growth curve of the bacterial strain *P. aeruginosa* (AMS1a) was determined under constant temperature (30 ˚C) and agitation (140 rpm) for a period of 22 days. Figure 12 represents the typical growth curve of the selected bacterial strain in MSM supplemented with 2 % (v/v) n-hexadecane as the sole source of carbon.

It is evident from the growth curve that the bacteria were at lag phase till the 3rd day and went into exponential phase from the 4th day indicating the rapid increase in bacterial population and was continuous up to 11th day. Time duration between 2nd-3rd day, 4th-8th and 9th-12th represents early exponential phase, mid-exponential phase and late exponential phase or initiation of stationary phase, respectively. The stationary phase was sustained till the 14th day. Following the 15th day of incubation, the density of bacteria cells in the culture declined at a steady rate till the 22nd day indicating its death phase.

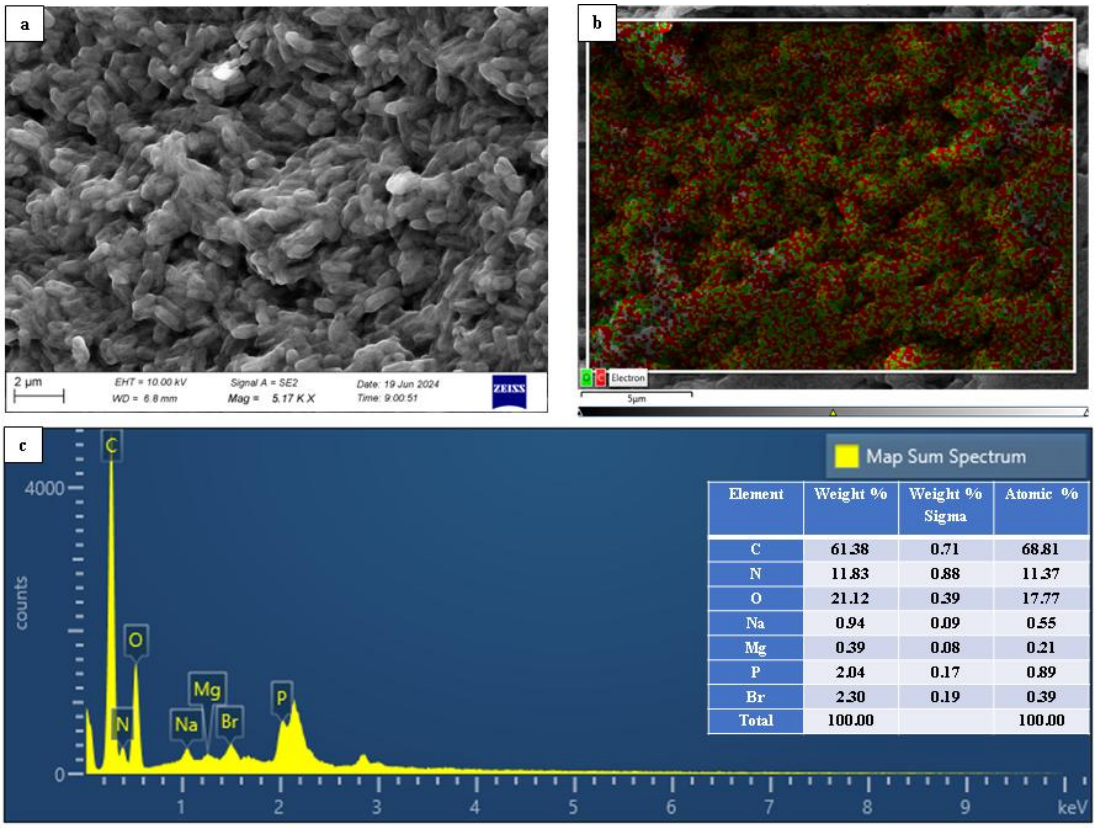

Figure 11. (a) SEM micrograph, (b) EDS layered image of complete surface elemental content and (c) EDS elemental sum spectrum of selected hydrocarbonoclastic bacterium

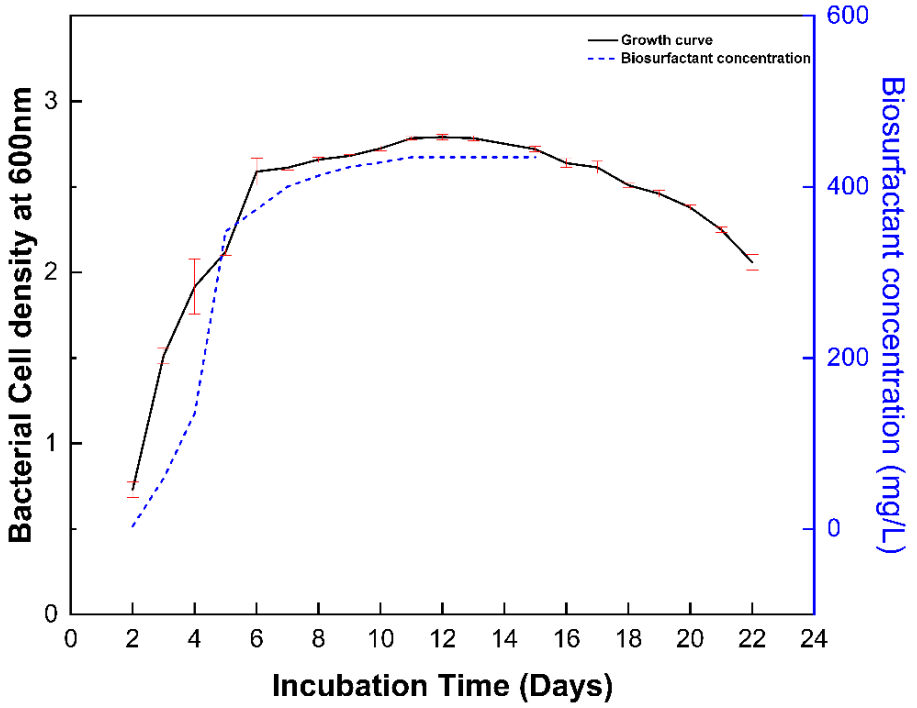

Figure 12. Growth and BS production pattern of *Pseudomonas aeruginosa* (AMS1a) in MSM supplemented with n-hexadecane

3.7. Quantification of BS

It was found that the BS production increased with the increase in bacterial growth in the culture medium and accelerated in the exponential phase. Figure 12 represents the pattern of BS production by the selected bacterial strain over the period of 15 days in MSM. Concentration of the BS maintained a steady level during the stationary phase. The final yield of BS reached a concentration of about 434.7 µg/ml after two weeks of incubation.

3.8. Isolation of BS

The CFCS of the bacterial strain containing BS was acidified at pH 2 for a period of about 24 hours at 4 ˚C, which caused the BSs in the supernatant to protonate and thus resulting in the precipitation of the BS in the solution. The acidified CFCS was then extracted twice using ethyl acetate as the solvent to separate the BS from the aqueous supernatant and the same is presented in Figure 13. Finally, partially purified BS in the form of a dark viscous semi solid was obtained after concentrating the solvent extracted BS in a rotary evaporator.

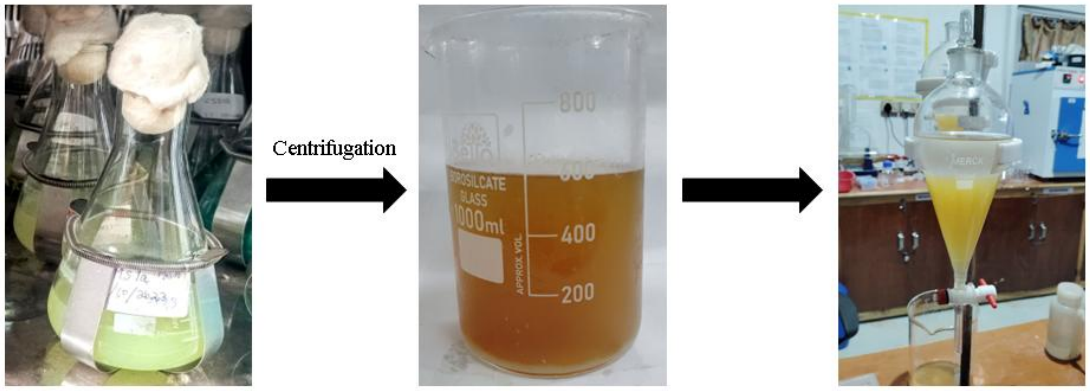

Figure 13. Schematic presentation of BS isolation from the mature bacterial culture

3.9. Purification of isolated BS

TLC was used to determine the purity of the partially purified BS, using chloroform-methanol-water (65: 35: 2, v/v/v) as solvent system. Two major spots and one minor spot were developed after being exposed to UV chamber, iodine fumes and sprayed with acidified anthrone reagent separately. The spots were appeared at R_f 0.3, 0.5 and 0.7 and the same is presented in Figure 14.

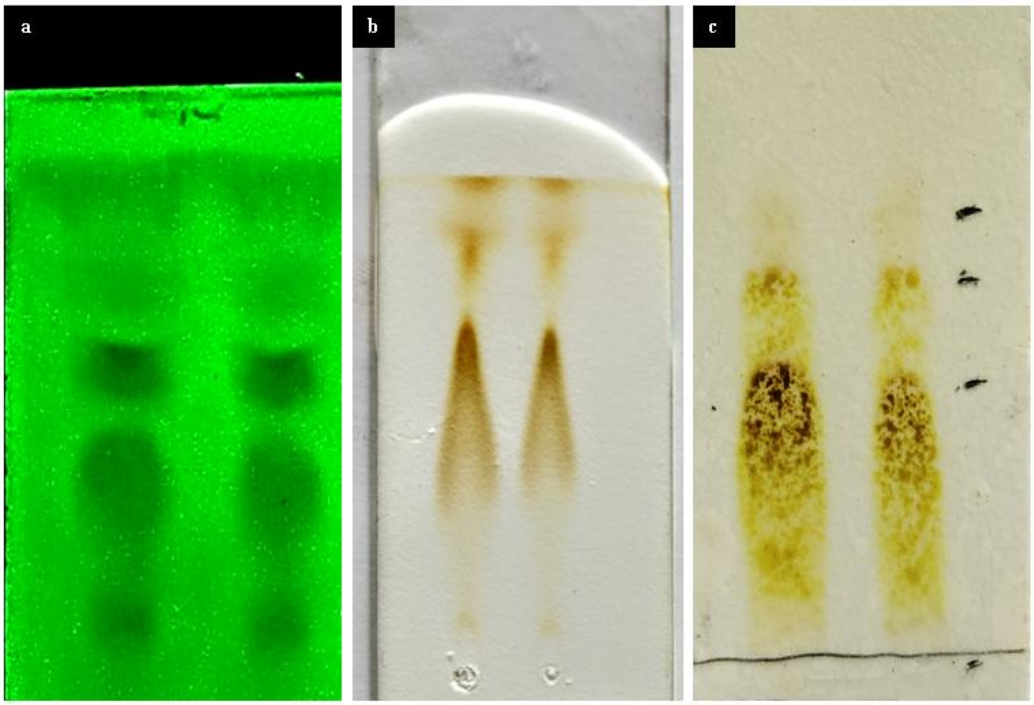

Figure 14. TLC of partially purified BS after exposed to (a) UV light, (b) Iodine fumes, and (c) Anthrone reagent

The neutral lipids present in the partially purified BS was initially eluted down the chromatography column with chloroform (100 %) (Figure 15a). A solvent system comprising of chloroform: methanol in the ratio of 50:3 (v/v) was used to separate the first fraction of BS with R_f value, 0.7. This was followed by a mobile solvent system comprising of chloroform: methanol in the ratio of 50:5 (v/v) to separate the BS fraction with R_f value, 0.5. Finally, a mobile system consisting of 1:1 (v/v) ratio of chloroform: methanol was used to separate the final BS fraction with R_f value 0.3. All the fractions of the BS were confirmed by TLC prior to introduction of the subsequent mobile system. Using a rotary evaporator, the solvent system present in the separated BS fractions were evaporated and recovered (Figure 15b).

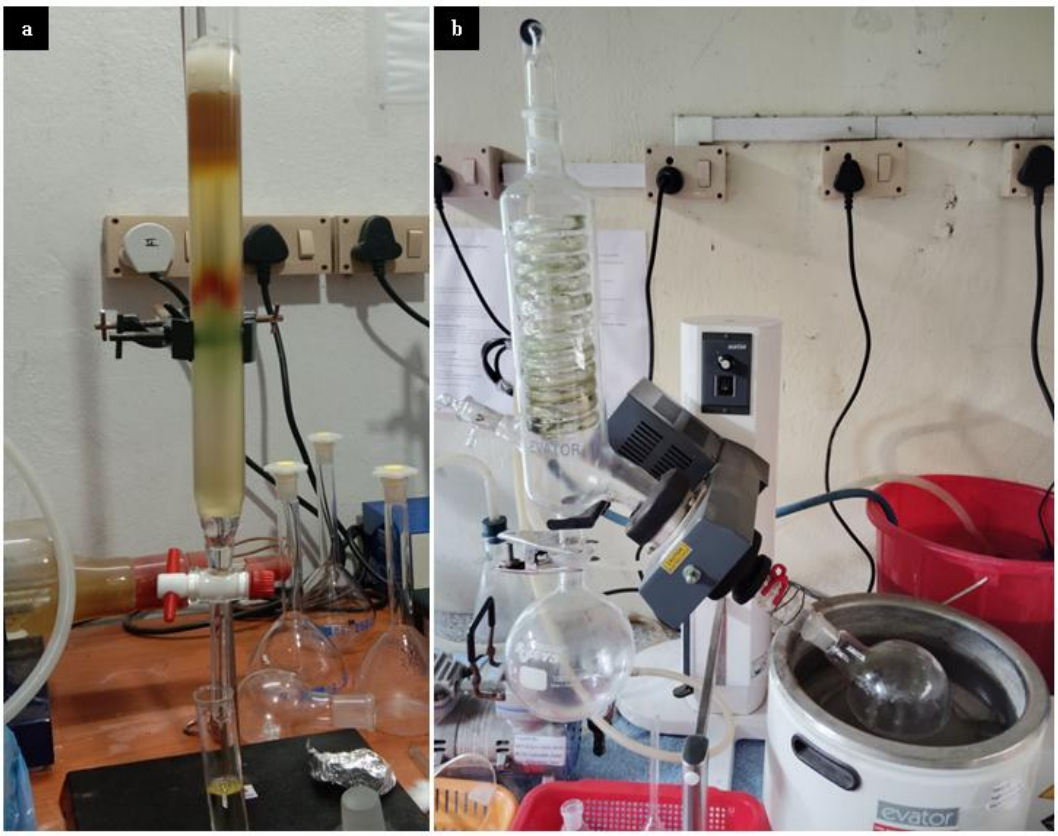

Figure 15. (a) Purification of partially purified BS through column chromatography and (b) Recovery of purified fraction of BS through a rotary evaporator system

3.10. Determination of surface activity

3.10.1. Determination of CMC

The CMC of the BS produced by the selected *P. aeruginosa* (AMS1a) strain was found to be 195.6 mg/L, corresponding to a reduction in the ST of distilled water from 72 mN/m to 34.4 mN/m. Figure 16 illustrates the CMC of the isolated BS.

3.10.2. BATH assay

Using a UV-Vis spectrophotometer, the degree of adherence of bacterial cells to model hydrocarbon *i.e*. n-hexadecane was found to be about 50 % ± 0.01 indicating the degree of hydrophobicity of the bacterial cell surface while growing on hydrophobic substrate like n-hexadecane. Further, the result asserts the production of BS by the selected bacterium. Indicating and asserting an important and distinct characteristic feature of BS producing bacteria.

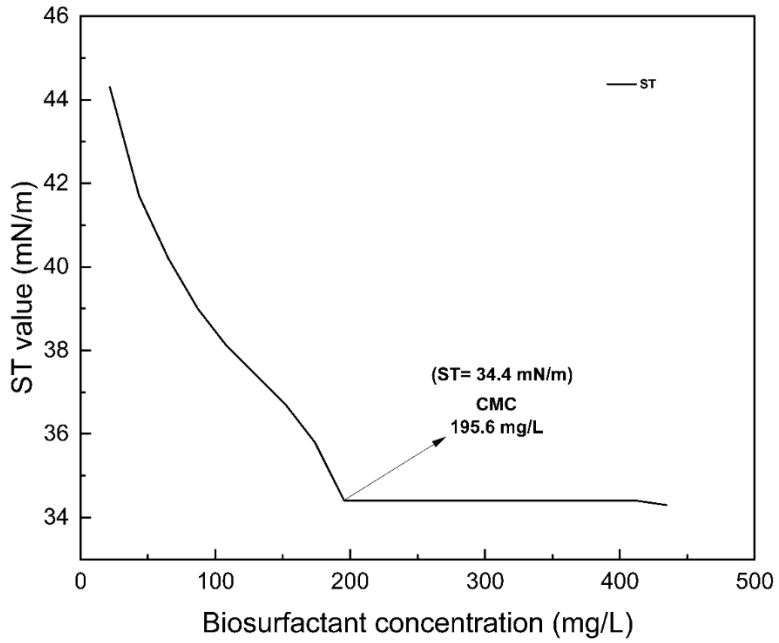

Figure 16. CMC of the BS isolated from *P. aeruginosa* (AMS1a) strain

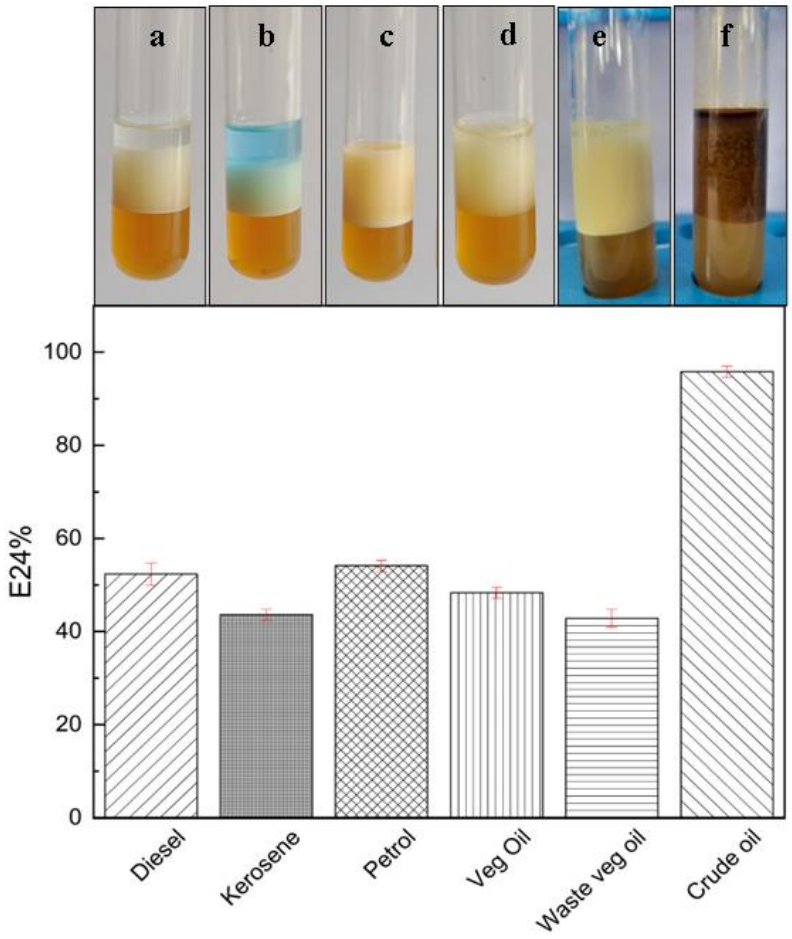

Figure 17. Emulsification index (E_{24}%) of the BS produced by the selected bacterial strain against different test hydrophobic substrates (a) Diesel, (b) Kerosene, (c) Petrol, (d) Vegetable oil, (e)Waste Vegetable oil, and (f) Crude oil

3.10.3. Emulsification activity

Emulsification indices (E_{24}%) of the tested BS against six different hydrophobic substrates were determined. The BS was able to form stable emulsion with all the tested hydrophobic substrates used in the experiment as evident from the height of emulsion shown in Figure 17.

3.11. Physicochemical characterization of the isolated BS

3.11.1. FTIR

The functional groups in the isolated BS were further examined using an FTIR spectroscopy (Figure 18). The existence of an aliphatic long fatty acid chain was indicated by the presence of distinctive peaks at 878, 1402, 2856, and 2931 cm^{-1}. The distinct peaks observed in the IR spectrum *i.e.* 1260 cm^{-1}, 1644 cm^{-1}, and 3410 cm^{-1} refers to the significant functional groups, namely the carbonyl group (C–O), alkene (C = C), and OH bond, respectively. The vibration at 1124 cm^{-1} was observed to correlate to the C–O stretching, which predicted the existence of sugar moiety, while the presence of the more significant band at 1735 cm^{-1} implied the presence of carboxyl group, which showed the linking group between the sugar and fatty acid. The peak position of various functional groups of BS molecule are presented in Table 7.

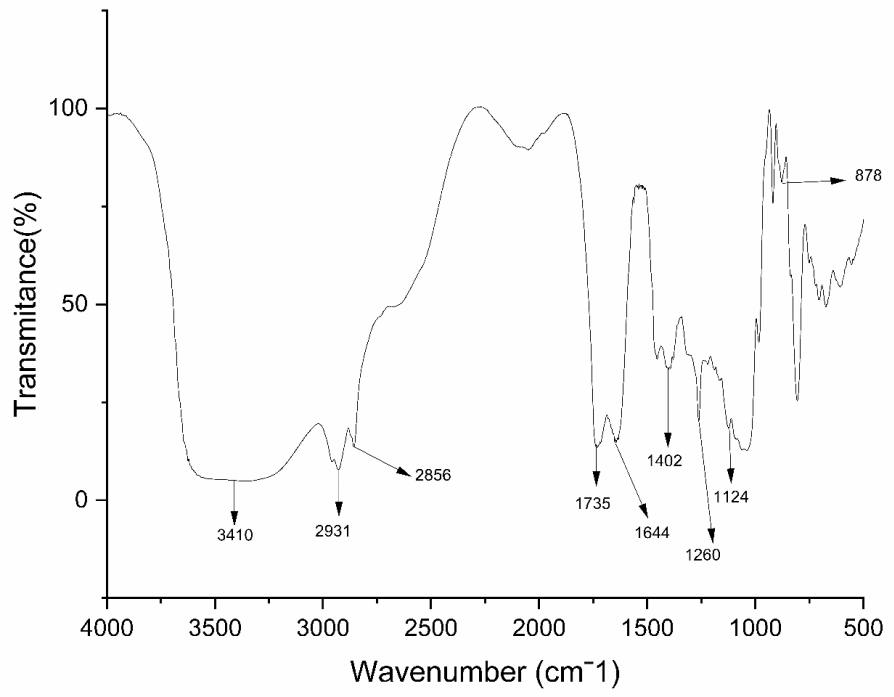

Figure 18. FTIR spectrum of the BS isolated from *P. aeruginosa* (AMS1a) strain

Table 7. Peak position of various chemical functional groups exists in the BS isolated from *P. aeruginosa* (AMS1a) strain

Peak Position (cm^{-1})	Functional Group	Peak Intensity
3200-3550	O-H stretching	Strong, Broad
2500-3300	O-H stretching	Strong, Broad
2840-3000	C-H stretching	Medium
1720-1740	C=O stretching	Strong
1626-1662	C=C stretching	Medium
1395-1440	O-H bending	Medium
1250-1310	C-O stretching	Strong
1087-1124	C-O stretching	Strong
860-900	C-H bending	Strong

3.11.2. TGA

The thermal degradation analysis of the BS revealed three distinct regions of mass loss. The obtained data are presented in Figure 19. The initial phase of degradation, showing a weight reduction of approximately 2.53 %, took place within the temperature range of 50 to 170 °C. The most substantial mass loss, about 31.27 %, occurred during the temperature range of 170 to 440 °C. By the end of the thermal scan at 500 °C, a residual mass of 63.33 % remained.

DTG analysis is performed to determine the rate of BS mass loss relative to temperature. The BS shows a maximum degradation temperature of approximately 235 °C and a peak mass loss rate of around 6 % per minute. The same is presented in Figure 19.

DTA analysis is conducted to ascertain the disintegration heat. The DTA thermogram displays a small exothermic peak at 75 °C, followed by significant exothermic peak at 180 °C, indicating a phase transition and the thermal degradation of the hydrocarbon component of the BS molecule. The DTA spectrum of the analysed BS sample is presented in Figure 19.

3.11.3. DSC

In the DSC thermogram of the BS, two distinct peaks can be observed. The first peak at about 72 ˚C shows the enthalpy of dehydration while the second peak at

around 180 ˚C represents the enthalpy of decomposition. The same is presented in Figure 20.

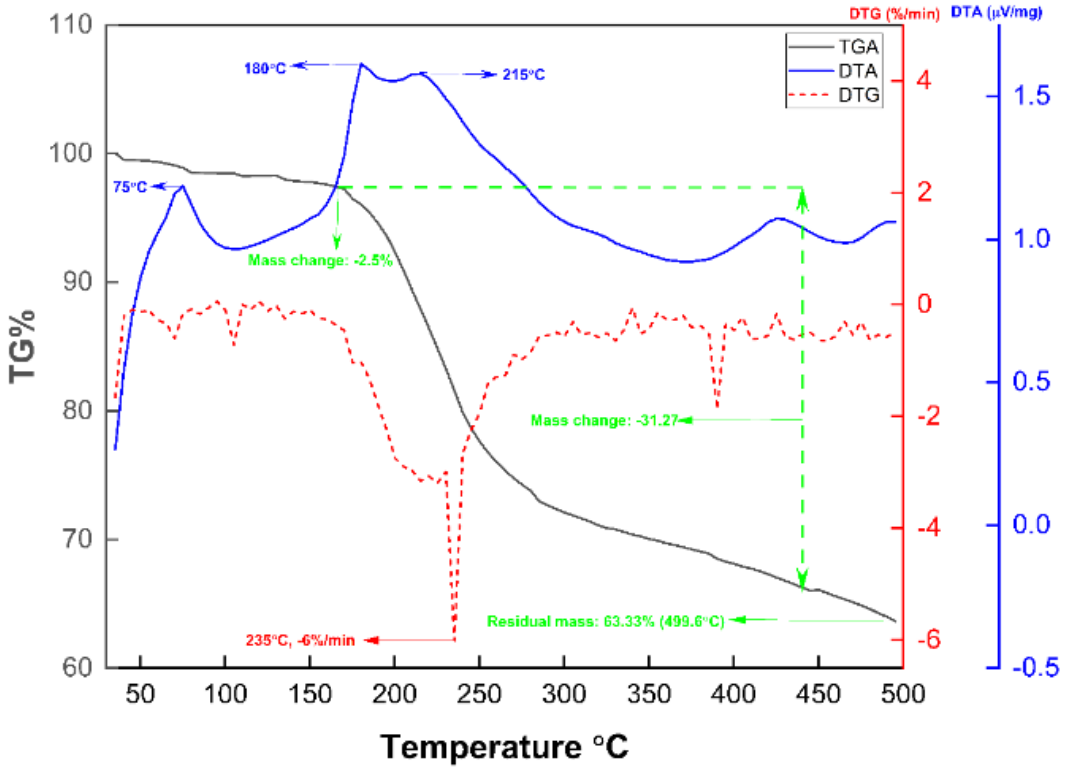

Figure 19. Thermal analysis of the BS isolated from *P. aeruginosa* (AMS1a) strain

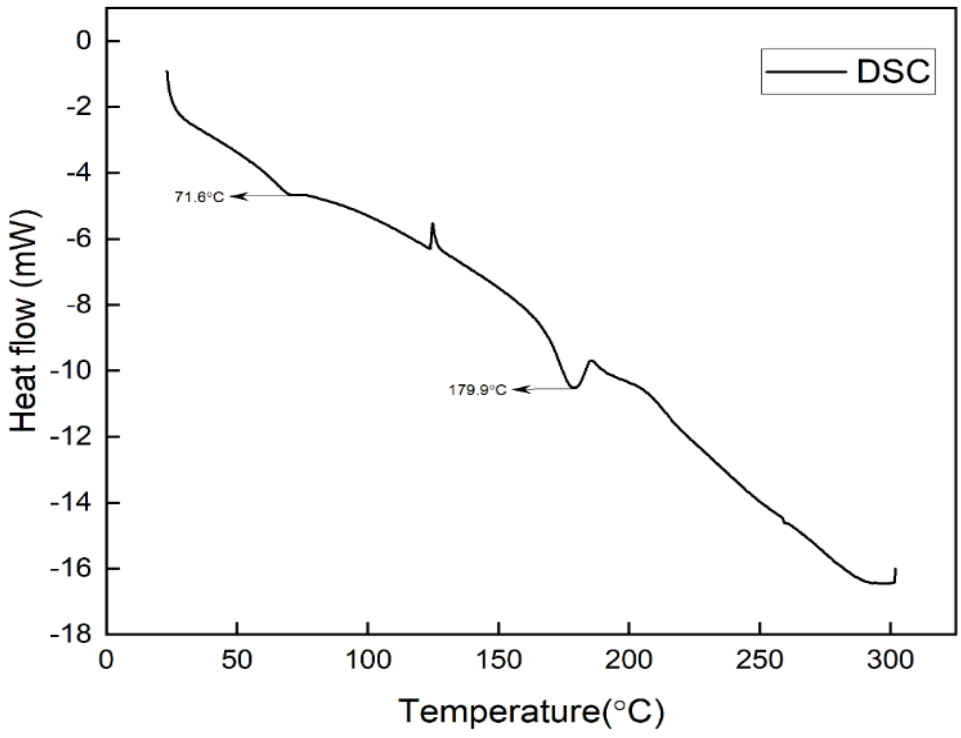

Figure 20. DSC thermogram of the BS isolated from *P. aeruginosa* (AMS1a) strain

3.11.4. Zeta potential

The BS, exhibiting a zeta potential of -4.49 mV, reveals a preponderance of negative charges on its surface (Figure 21). The results demonstrate the considerable negative surface charge of the BS.

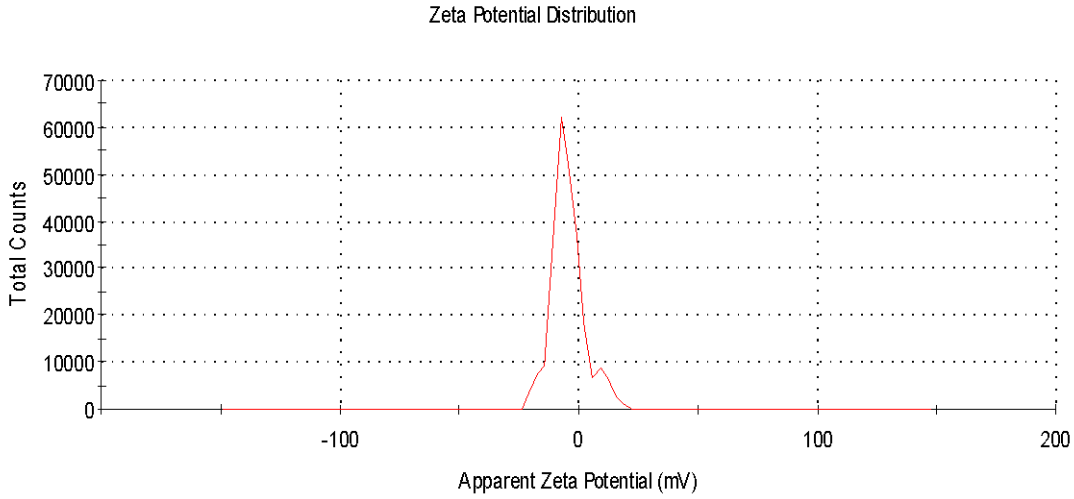

Figure 21. Zeta potential of BS isolated from *P. aeruginosa* (AMS1a) strain

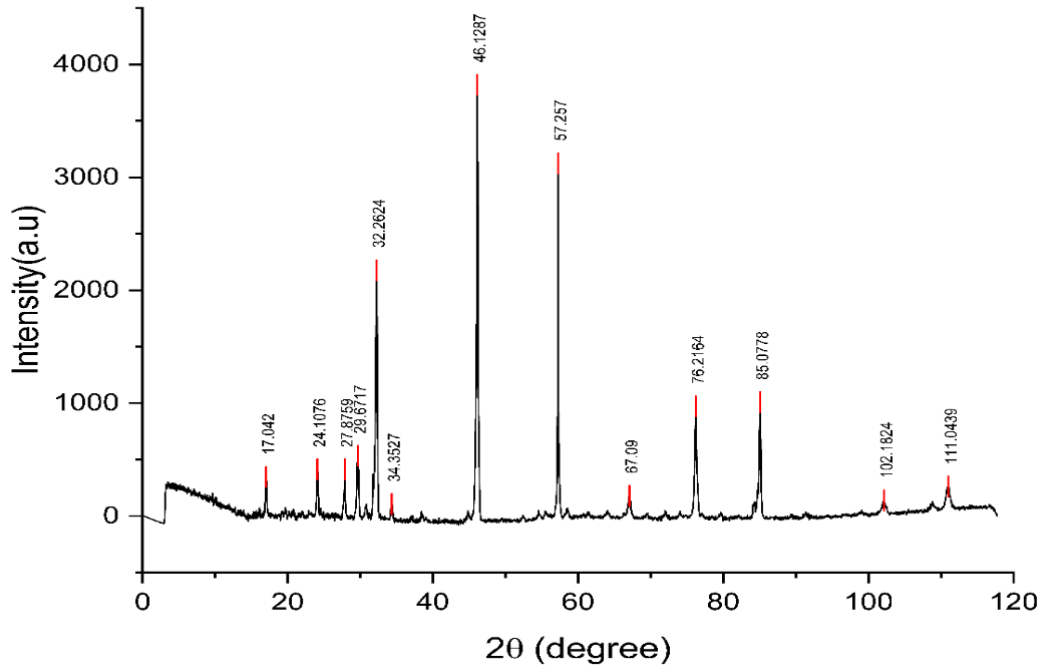

Figure 22. X-ray diffractogram of BS isolated from *P. aeruginosa* (AMS1a) strain

3.11.5. XRD

XRD analysis of the BS was performed to determine the degree of crystallinity. The X-ray diffractogram of the isolated BS is presented in Figure 22 and revealed

strong and narrow characteristic diffraction peak at 17.04, 24.1, 27.9, 29.6, 32.2, 34.3, 46.1, 57.2, 67.09, 76.2, 85.07, 102.1 and 111.04 in 2θ area corresponding to interplanar spacing of 5.19, 3.68, 3.19, 3.00. 2.77, 2.60, 1.96, 1.60, 1.39, 1.24, 1.13, 0.99 and 0.93 Å, respectively. The crystallinity index (C.I) was calculated using the formula mentioned in section *2.12.4* of chapter 2 and was found to be 41.1 %.

3.11.6. EDX

The superficial features of the isolated BS was investigated through *EDX* spectroscopy. The result from the EDX analysis of the crude BS (acid precipitated) shows that carbon and oxygen as the major element present with an weight perecntage of 33.93 and 22.56 % respectively (Figure 23). However, the weight percentage of the major elements, carbon and oxygen was found to be comparatively higher in the case of partially purified BS (solvent extracted) with a weight percentage of 60.08 and 27.18 % respectively as revealed from EDX elemental map sum spectrum in Figure 24.

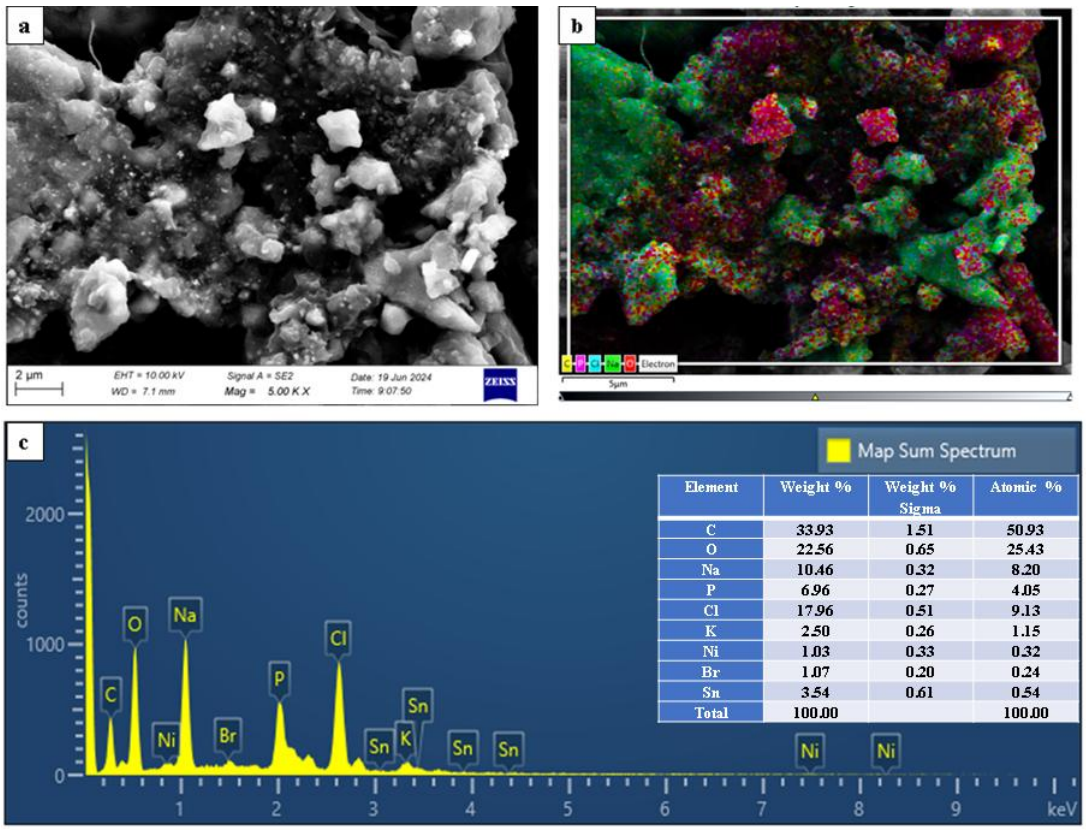

Figure 23. (a) SEM micrograph, (b) EDX layered image of major elements and (c) EDX elemental map sum spectrum of the of crude BS

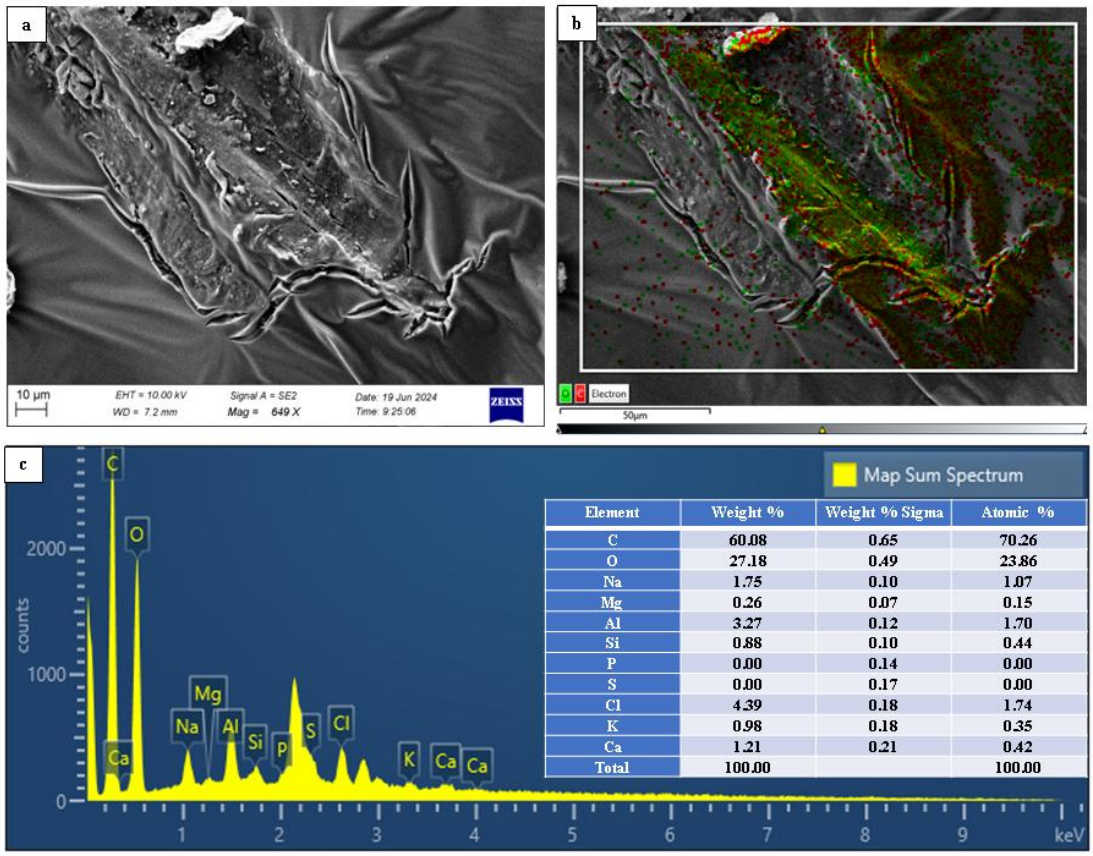

Element	Weight %	Weight % Sigma	Atomic %
C	60.08	0.65	70.26
O	27.18	0.49	23.86
Na	1.75	0.10	1.07
Mg	0.26	0.07	0.15
Al	3.27	0.12	1.70
Si	0.88	0.10	0.44
P	0.00	0.14	0.00
S	0.00	0.17	0.00
Cl	4.39	0.18	1.74
K	0.98	0.18	0.35
Ca	1.21	0.21	0.42
Total	100.00		100.00

Figure 24. (a) SEM micrograph, (b) EDX layered image of major elements and (c) EDS elemental map sum spectrum of the BS of partially purified BS

3.11.7. NMR

As shown in the Figure 25, the presence of chemical shift value in ^{1}H NMR at 1.24 ppm indicated the methyl group (-CH_3) corresponding to the sugar moiety. While another peak at 0.86 ppm corresponds to the (-CH_3) group of the long chain aliphatic group. The presence of sugar moiety was confirmed by the presence of peaks at 4.93 (-1'-H), 3.63 (-5'-H), and 4.14-4.29 ppm (-2', 3', 4'-H). The sharp peaks present at 1.24 ppm corresponds to the long chain hydrocarbon of the lipid group. Other characteristic peaks were also shown for a -COO-CH- (5.81 ppm), -O-CH- (4.30 ppm) and -CH_2-COO- (2.32, 2.8 ppm) which confirms the presence of rhamnolipid (RL) *i.e.* mono-RL having two long chain fatty acids in the analysed BS sample (Table 8). Similarly, characteristic peaks at 0.82 ppm (-CH_3), 1.24-1.21 ppm {-$(CH_2)_n$ and -CH_3 (ring)}, 5.34 ppm (-COO-CH-), 4.16 ppm (-O-CH-), and 2.35, 2.47 ppm (-CH_2-COO-) confirms the structure of di-RL and its presence in the analysed BS sample (Table 8).

Table 8. ^{1}H NMR of RL isolated from *P. aeruginosa* (AMS1a) strain

Assignments	Chemical shifts (in ppm)	
	Mono-RL	**Di-RL**
-$(CH_2)_n$-	1.24	1.24
-CH_3 (aliphatic long chain)	0.86	0.82
-CH_3 (ring)	1.24	1.21
-COO-CH-	5.81	5.34
-CH_2-COO-	2.8, 2.32	2.35, 2.47
-O-CH-	4.30	4.16
1´H-	4.93	4.83
2´,3´,4´H-	4.29, 4.26, 4.14	3.57-3.66
5´H-	3.63	3.37

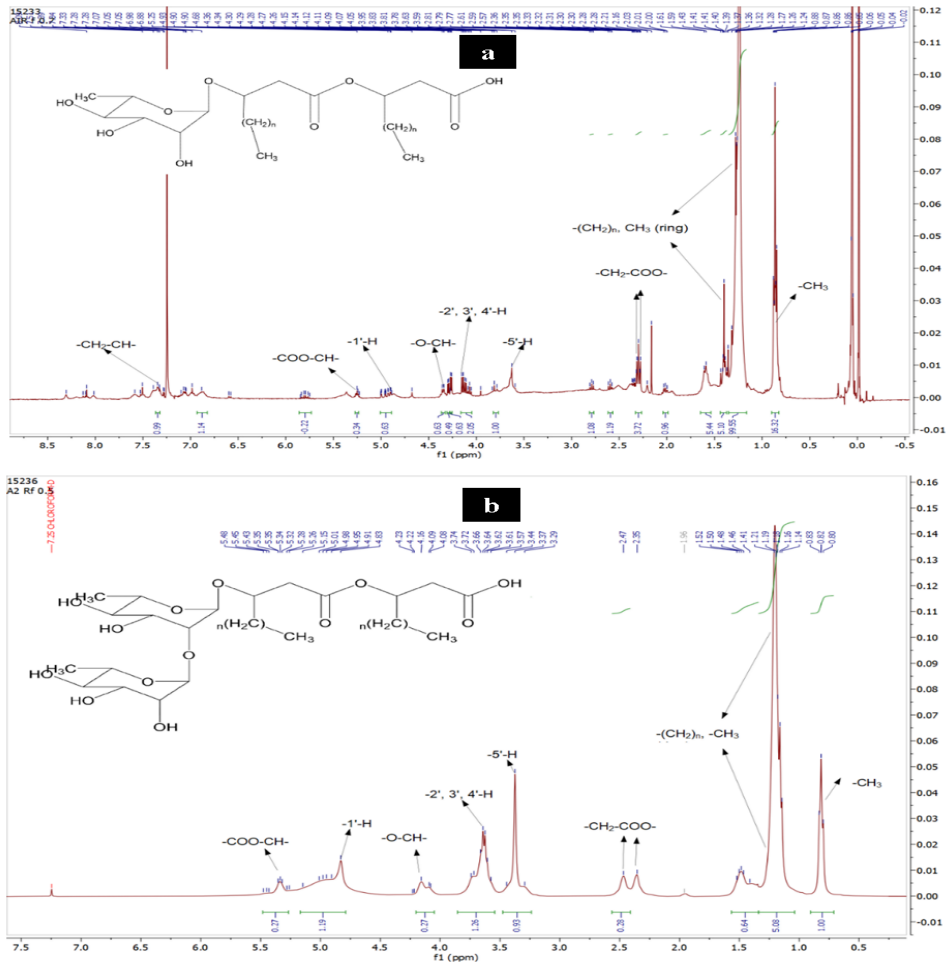

Figure 25. ^{1}H NMR of RL (a) mono-RL and (b) di-RL isolated from *P. aeruginosa* (AMS1a) strain

The ^{13}C NMR of RL (Figure 26) shows that peaks at 170.85 and 171.61 ppm shows the easter group (C=O) of mono and di-RL respectively. The presence of carboxylic group was confirmed by the peaks at 173 ppm for mono-RL and 174.20 ppm for Di-RL. Peaks at 62.52-82.95 ppm and 68.13-73.36 ppm corresponds to the rhamnose rings in both mono and di-RL respectively (Table 9).

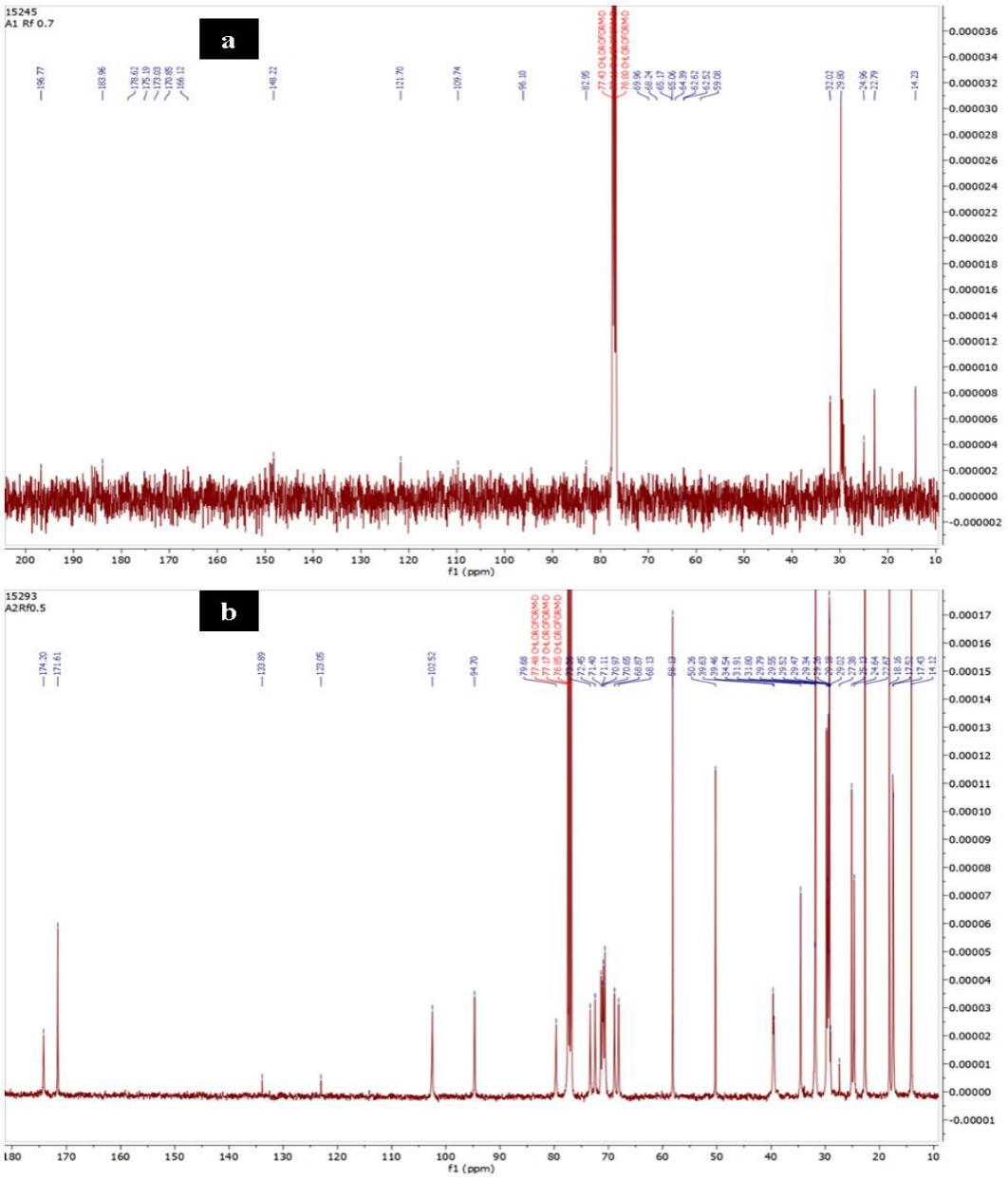

Figure 26. ^{13}C NMR of RL (a) mono-RL and (b) di-RL isolated from *P. aeruginosa* (AMS1a) strain

Table 9. ^{13}C NMR of RL isolated from *P. aeruginosa* (AMS1a) strain

Assignments	**Chemical shifts (δ)**	
	Mono-RL	**Di-RL**
C=O (ester group)	170.85	171.61
C=O (carboxylic group)	173.03	174.20
CH_3 (rhamnose)	22.79	22.67
α-CH_2 and β-CH_2	24.96-33.02	29.18-31.91
Rhamnose ring carbons	62.52-82.95	68.13-73.36

3.11.8. LC-MS

LC-MS was performed using the purified BS obtained from column chromatography separation. The total ion chromatogram (TIC) obtained from the MS showed a total of seven dominant peaks with a retention time (RT) ranging from 22.059 to 24.907 minutes as shown in Table 10. These peaks detected from the TIC corresponded to a mixture of mono-RL and di-RL. The peak detected at m/z 531 corresponded to Rha-C_{10}-C_{12}, while the rest of the signals were found to be di-RL showing the presence of Rha-Rha-C_8-C_{10}/ Rha-Rha-C_{10}-C_8 (m/z 621.387), Rha-Rha-C_{10}-$C_{12:1}$ (m/z 675.423), Rha-Rha-C_{10}-C_{10} (m/z 649.4), Rha-Rha-C_{10}-$C_{14:1}$ (m/z 703.45), Rha-Rha-C_{10}-C_{14}/Rha-Rha-C_{14}-C_{10} (m/z 705.4701), and Rha-Rha-C_{12}-C_{12} (m/z 705.4701). The different assignments for the pseudo-molecular ion peaks and other characteristic peaks shown by the cleavage of the rhamnose moieties have been presented in Table 10. In the case of di-RLs such as Rha-Rha-C_{10}-C_{14}/Rha-Rha-C_{14}-C_{10} with m/z 705.4694, the fragmentation of the two fatty acid chains leads to two peaks at m/z 225 and m/z 169.2. Another cleavage at the ether linkage of rhamnose and fatty acid chains give two characteristic peaks at m/z 309 for the di-rhamnose moiety and m/z 393 for the two fatty acid chains which has been depicted in Figure 27.

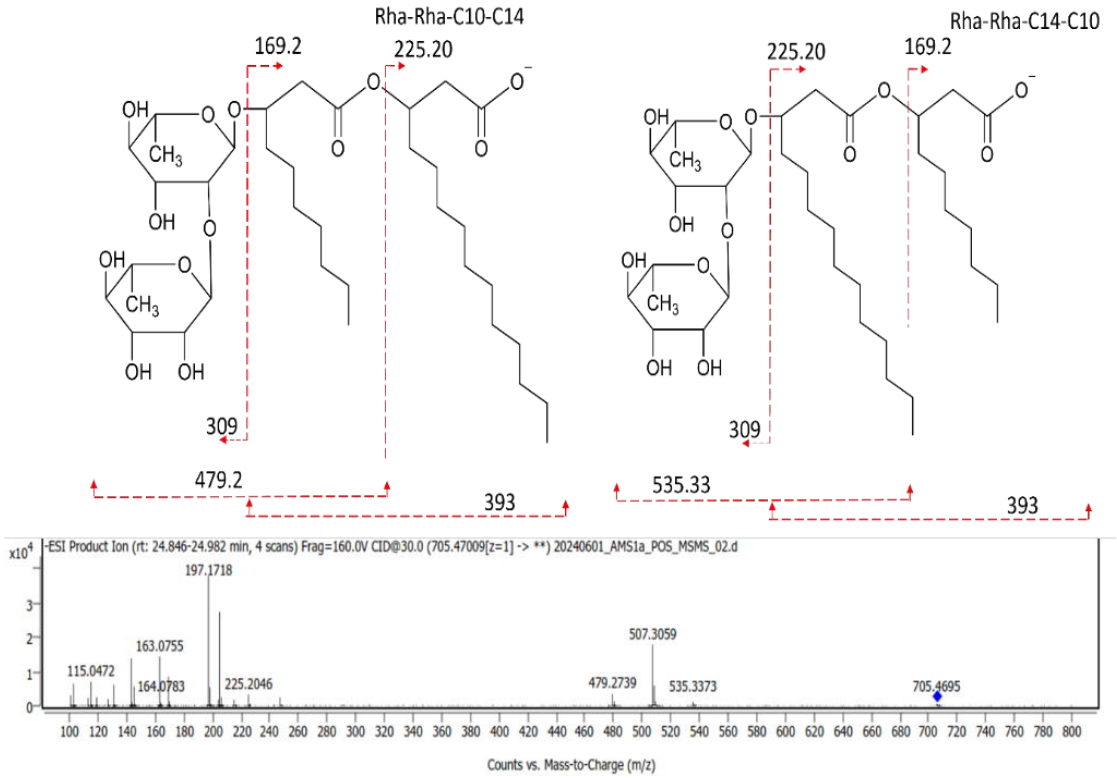

Figure 27. Diagrammatic representation showing the different cleavage sites of di-RL [Rha-Rha-C_{10}-C_{14}/Rha-Rha-C_{14}-C_{10} (m/z 705.4695)] and their corresponding m/z peaks

Table 10. The different RL congeners present in the analysed BS produced by *P. aeruginosa* AMS1a and their peak assignments

				Characteristic fragments								
Sl. No.	**RT**	**m/z [M-H]⁻**	**RL/HAA**	**Rha-Rha-FA1**	**Rha-Rha-FA2**	**Rha-FA1**	**Rha-FA2**	**FA1-FA2**	**FA2-FA1**	**FA1**	**FA2**	**Others**
1	22.06	621.37	Rha-Rha-C_8-C_{10}; Rha-Rha-C_{10}-C_8	-	479.27	-	-	-		141.1	169.13	204.9, 205.08, 247.1

2	23.05	649.4	Rha-Rha- C_{10}-C_{10}		479.27	-	-	-	-	169.2	-	163.07, 205.08, 247.10
3	23.5	675.423	Rha-Rha-C_{10}-$C_{12:1}$		479.27	-	-	-	-	169.2	195.1	247.1, 205
4	24.24	531.379	Rha-C_{10}-C_{12}		-	-	333.21		-	169.13	197.17	163.07, 205.08
5	24.5	703.45	Rha-Rha-C_{10}-	$C_{14:1}$	479.27	-	333.21	-	-	169.2	197.17	163.07, 204.98, 248.97
6	24.9	705.4701	Rha-Rha-C_{10}-C_{14}	Rha-Rha-C_{14}-C_{10}	479.27	535.33	-	-	-	169.2	225.20	205.08, 163.07, 247.10
7	24.9	705.4701	Rha-Rha-	C_{12}-C_{12}	507.3058	-	-	-	-	197.17	-	205.08, 163.07, 247.10

(Rha = Mono-rhamnose; Rha-Rha = Di-rhamnose; FA1 = Fatty acid short chain; FA2 = Fatty acid long chain; HAA = 3-(3-hydroxyalkanoyloxy) alkanoic acid; RT = Retention time; m/z $[M-H]^-$ = mass to charge ratio)

3.12. Stability studies of the isolated BS

3.12.1. Effect of environmental variables on E_{24} %

The BS exhibited and retained a stable E_{24}% within 54.1 % to 62.5 % at temperature range of 4 ˚C to 121 ˚C demonstrating the absence of any significant effect of temperature on the emulsification activity and the same is presented in Figure 28a. At varying salinity (2 %-10 %), the BS was able to maintain a stable E_{24}% of 50 % to 65.6 % highlighting the stable nature of the BS and the same is presented in Figure 28b. The BS was able to maintain a stable E_{24}% of 54 % to 60 % at the pH range of 5 to 10 and the same is presented in Figure 28c. However, at acidic pH of 3, the emulsification activity decreased to 37.5 %. The BS showed a stable emulsification activity with the E_{24}% value of 62 % to 71.4 % with all the three types of heavy metal used (As, Cd and Cr) at varying concentration (100-500 ppm) as shown in Figure 28d. Over a period of 30 days, no significant change in the emulsification activity was observed as shown in Figure 28e. The BS was able to maintain an average E_{24}% value of about 51.6 % ± 0.07 for a period of 30 days of incubation. The compound microscopic image of stable emulsion after 30 days at 10 X magnification is presented in Figure 28f.

3.12.2. Effect of environmental variables on surface activity

The BS was able to maintain a consistent reduction ST of distilled water at an average about 35 mN/m ± 0.05 at a temperature range of 25 ˚C to 121˚C. However, it was observed that there was a slight increase in the ST value, 36.1 ± 0.15 mN/m at 4˚C and the same is presented in Figure 29a. As shown in Figure 29b, the BS was able to maintain the reduction of ST within the value of 34.2 mN/m ± 0.15 to 35.6 mN/m ± 0.05 at the salinity range of 2 % to 10 %. It was found that there was a small but steady reduction of ST values with the increase in salinity. At the pH range of 3 to 10, the ST value of the BS increased marginally and consistently with the increase in pH value. Maximum reduction in the ST of 31.5 mN/m ± 0.1 was observed at pH 3 and steadily increase till 36.6 mN/m ± 0.05 at pH 10 and the same is presented in Figure 29c. The BS maintained a stable reduction in the ST within the range of 34.4 mN/m ± 0.05 to 35.8 mN/m ± 0.11 with all the three types of heavy metal used (As, Cd and Cr) at varying concentration (100-500 ppm) as shown in Figure 29d.

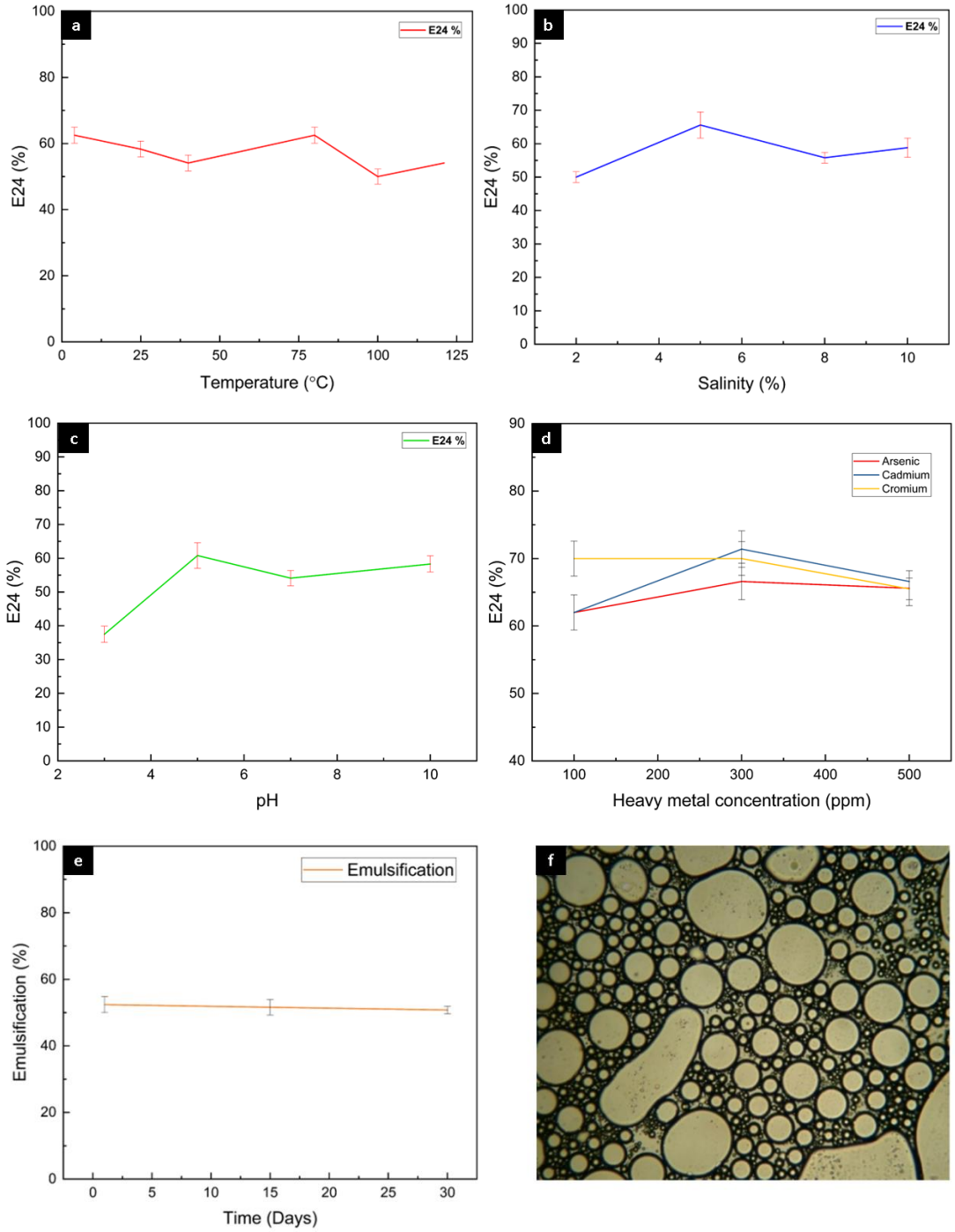

Figure 28. The effect of (a) Temperature, (b) Salinity, (c) pH, (d) Heavy metal salts, (e) Time on the emulsifying capacity of the BS, and (f) Microscopic image of a stable emulsion formed in the presence of BS

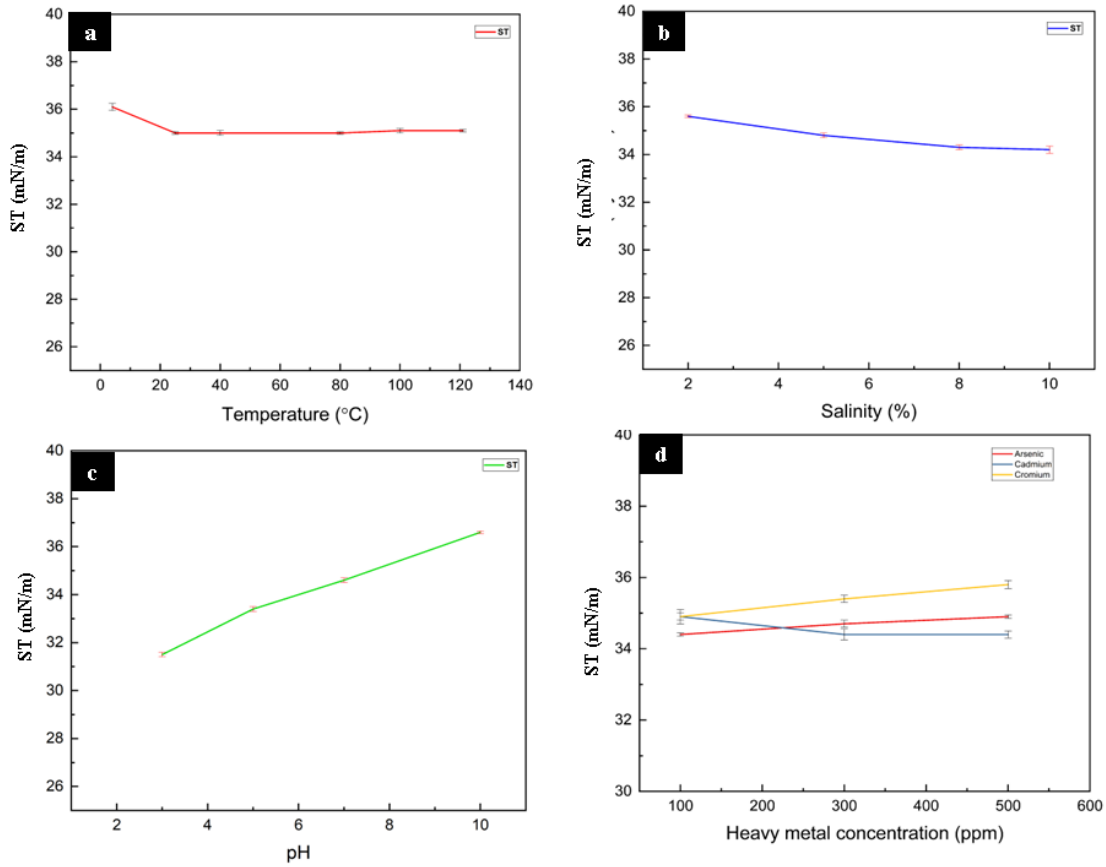

Figure 29. The effect of (a) Temperature, (b) Salinity, (c) pH and (d) Heavy metal salts on the surface activity of the BS

3.13. Biological activity of the isolated BS

3.13.1. Antibacterial activity

Disc diffusion assay was employed to determine the antibacterial activity of the isolated BS against seven different test bacterial strains. The BS exhibited significant antibacterial activity against all test strains. However, the degree of efficacy varied among the bacterial strains. The zone of inhibitions expressed in millimeter (mm) produced by the BS against the test bacterial strains are shown in Figure 30.

The IC_{50} values of BS against the different bacterial strains ranged from 0.021 mg/mL to 1.268 mg/mL and are presented in Table 11.

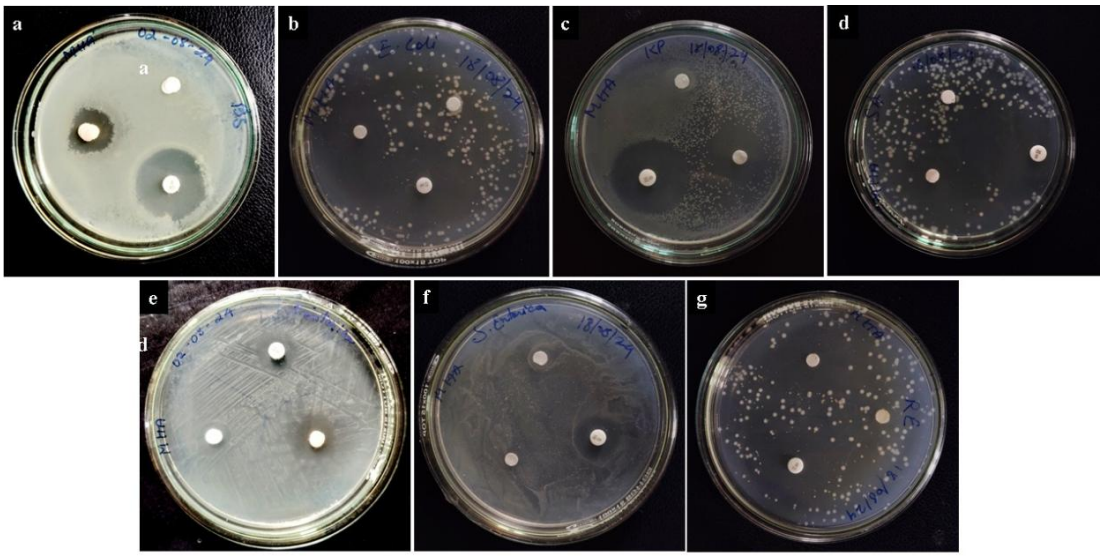

Figure 30. Antibacterial activity of BS produced by produced by *P. aeruginosa* (AMS1a) strain against (a) *Bacillus subtilis*, (b) *Escherichia coli*, (c) *Klebsiella pneumonia*, (d) *Staphylococcus aureus*, (e) *Listeria monocytogenes*, (f) *Salmonella enterica*, and (g) *Ralstonia eutropha*

Table 11. IC_{50} values of BS produced by produced by *P. aeruginosa* (AMS1a) against test bacterial strains

Sl. No.	Bacterial strain	IC_{50} (mg/ml)
1.	*Bacillus subtilis*	0.516
2.	*Escherichia coli*	1.268
3.	*Klebsiella pneumonia*	0.021
4.	*Staphylococcus aureus*	0.140
5.	*Listeria monocytogenes*	0.464
6.	*Salmonella enterica*	0.943
7.	*Ralstonia eutropha*	0.276

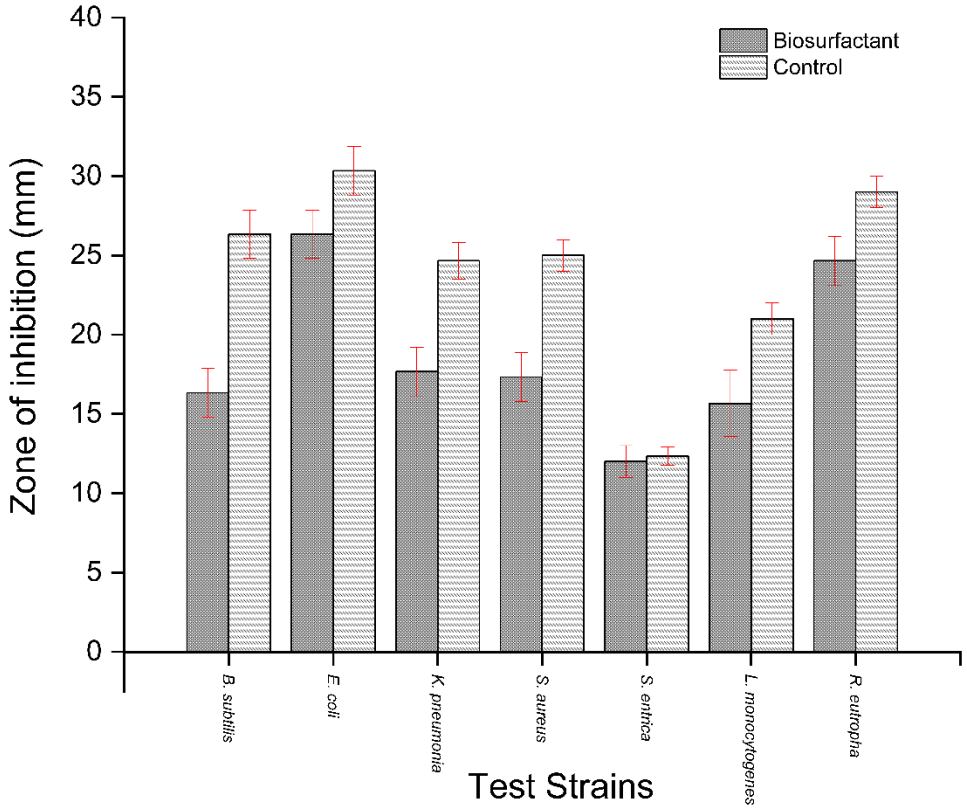

Figure 31. Zone of growth inhibition (mm) formed by the BS produced by *P. aeruginosa* (AMS1a) against test bacterial strains

3.13.2. Phytotoxicity assessment

. In the phytotoxicity assessment test using *Vigna radiata* seeds, the percentage of relative seed germination (RSG) of the BS at CMC and below CMC concentration was similar to the control (100 %) and was slightly reduced to about 93.3 % ± 6.7 at above CMC concentration. In comparison with the synthetic surfactant, SDS with RSG percentage of only 86.7 % ± 6.7, evident that the BS had significantly lower toxicity on the germination of the *V. radiata* seeds. Similarly, except in the case of SDS, the percentage relative root length (RRL) was above 50 % in all the concentration of the BS. Additionally, the percentage of RRL of the BS at below CMC concentration was much higher at 99.4 % ± 3.4 as compared to the control (0.1 % SDS) at 34.5 ±5.6 (Figure 32). It is therefore evident from the study that the synthetic surfactant induces consequential phytotoxicity with germination index of only about 30 %. Phytotoxicity induced by BS was insignificant at CMC and below CMC concentration with germination index of 84 % ± 4.8 and 99.4 % ± 3.4 respectively while the BS at higher concentration had a germination index value of 52.9 % ± 9.7 (Figure 33).

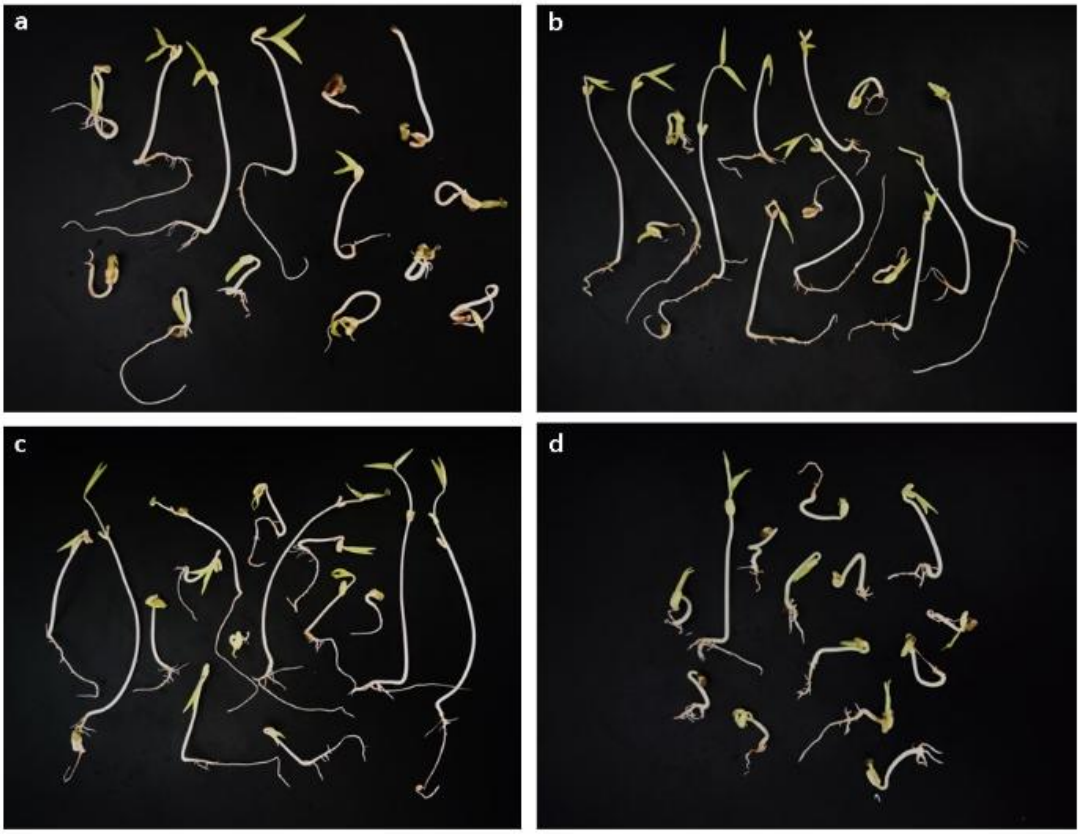

Figure 32. Effect of BS on the *Vigna radiata* seeds germination at (a) above CMC, (b) below CMC, (c) at CMC and (d) in the presence of SDS (0.1 %)

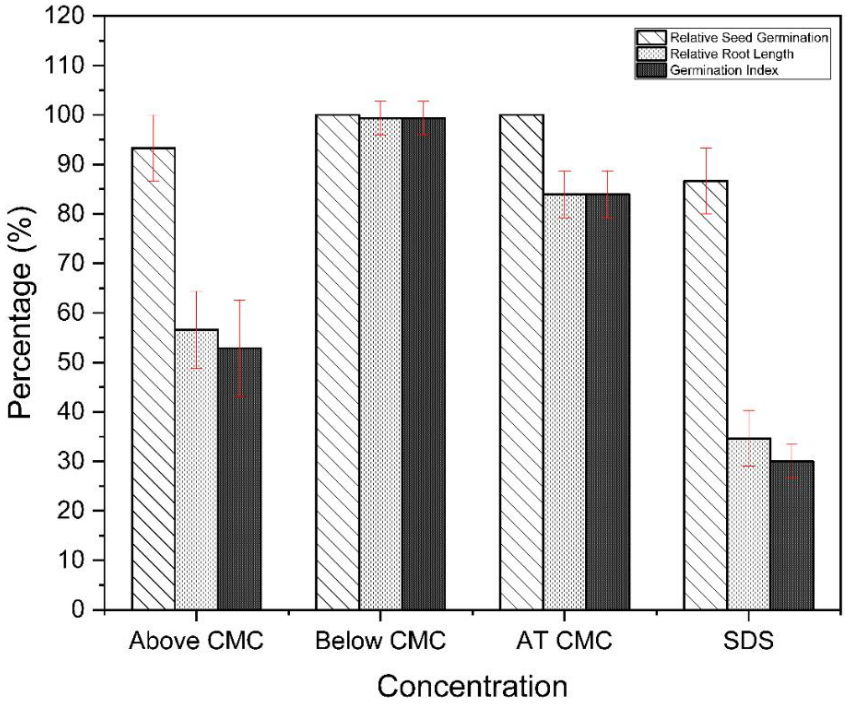

Figure 33. Phytoxicity of the BS at above CMC, below CMC, at CMC, and (d) in the presence of SDS (0.1 %)

3.13.3. Larvicidal activity

The larvicidal activity of the BS was determined by exposing it to *A. salina* larvae for 24 hours. The BS at lower concentration showed weak toxicity on the larvae and increased with upsurge in concentration. The LC_{50} was found to be at the concentration of 592.42 µg/L (Figure 34).

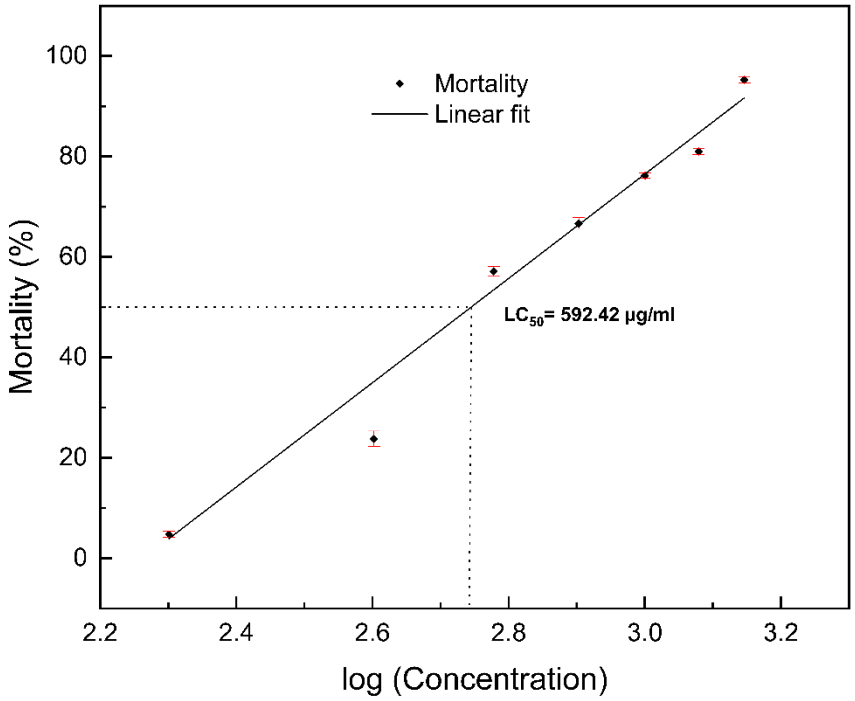

Figure 34. Larvicidal activity of the BS at various concentrations

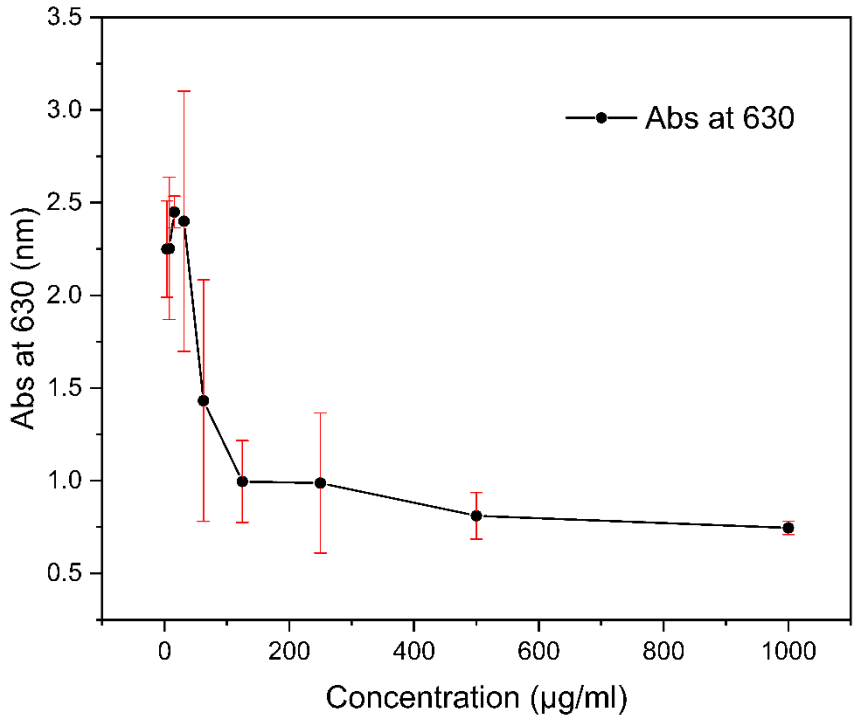

Figure 35. Anti-biofilm activity of the BS at various concentrations

3.13.4. Anti-biofilm activity

In the anti-biofilm assay, a reduction in optical density (OD) with increasing concentrations of the BS can be observed as shown in Figure 35, thus demonstrating the inhibitory effect of the BS on biofilm activity.

3.13.5. Cytotoxicity assessment of BS

3.13.5.1. MTT based cell viability assay

The results from the *in vitro* cell cytotoxicity test demonstrated the biocompatibility and benign nature of BS as there was no significant cytological change ($p < 0.05$) in the viability of the rat primary hepatocyte cells even when exposed up to a concentration of 100 µg/ml as shown in Figure 36a. Bright field image of primary hepatocytes indicates that cell exposed to the maximum dose (100 µg/ml) of BS for 24 hours exhibits mostly normal morphology with clear and intact cytoplasm and well defined plasma membranes (Figure 36b). This indicates the non-cytotoxic nature of the BS.

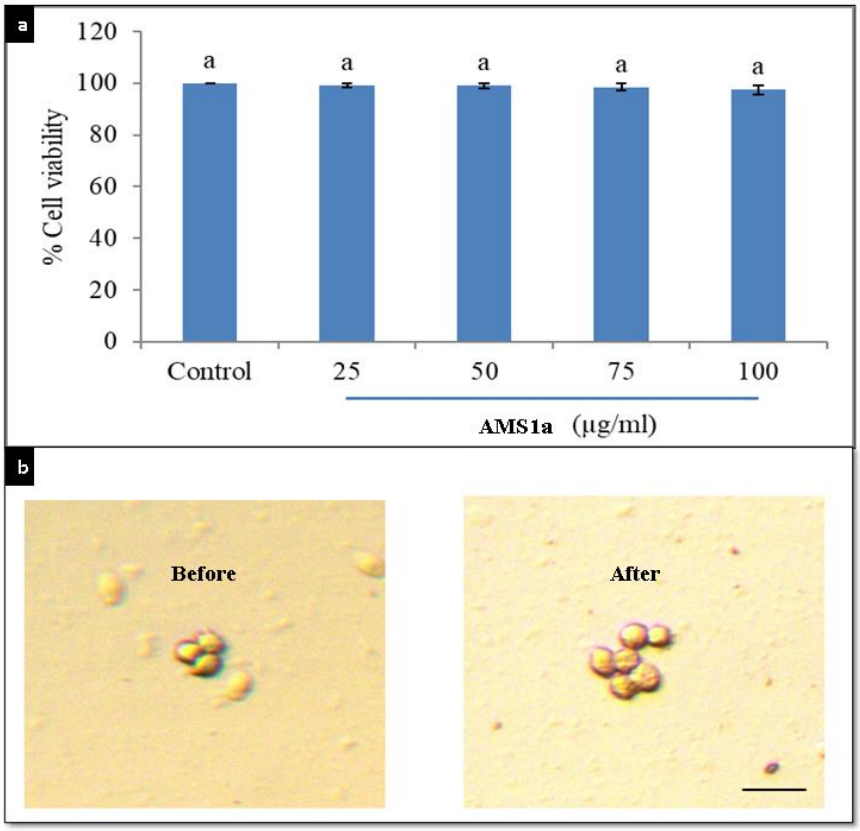

Figure 36. (a) Viability of primary rat hepatocyte cells after exposure to the various concentration of BS and (b) Bright field microscopic images of viable cells before and after treatment with the BS

3.13.5.2. Superoxide generation

The results from the superoxide generation assay indicates that the BS does not induce notable oxidative stress on the primary hepatocytes cells, however there was a slight but insignificant ($p < 0.05$) increase in the arbitrary unit (a.u) value with the increase in BS concentration as shown in Figure 37.

3.13.5.3. Total ROS generation

The findings from the cellular oxidative stress assay (section 3.11.5.2.) showed comparable results to that of the superoxide generation assay where a slight but negligible increase in the ROS generation value can be seen with the increase in concentration of BS. However there was no substantial increase ($p < 0.05$) in the overall oxidative stress of the cells as shown in Figure 38.

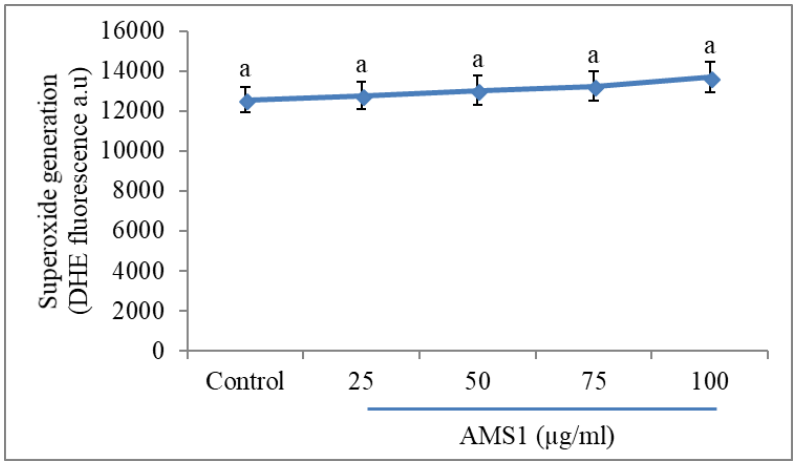

Figure 37. Superoxide generation in the primary rat hepatocyte cells after exposure to the various concentrations of BS

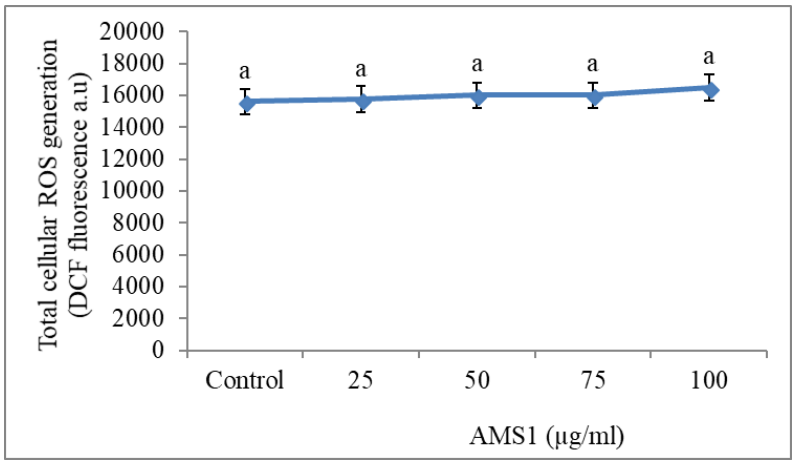

Figure 38. Oxidative stress in the primary rat hepatocyte cells after exposure to the various concentrations of BS

3.13.6. Determination of binding affinity of RL BS with surface-binding protein, E8L of Mpox virus through molecular docking

In order to determine the efficacy of RL BSs in the treatment of Mpox virus, computational method like molecular docking and ADME were utilized. The E8L protein was prepared by homology modelling using the amino acid sequence provided in the NCBI database and structure assessment was done showing all the amino acid residues on the favourable region. Figure 39a shows the Cell surface-binding protein OPG105 of Mpox virus and Figure 39b shows the Ramachandran plot of receptor protein showing 96.54 % in favourable region and 0.87 % in Ramachandran outliers.

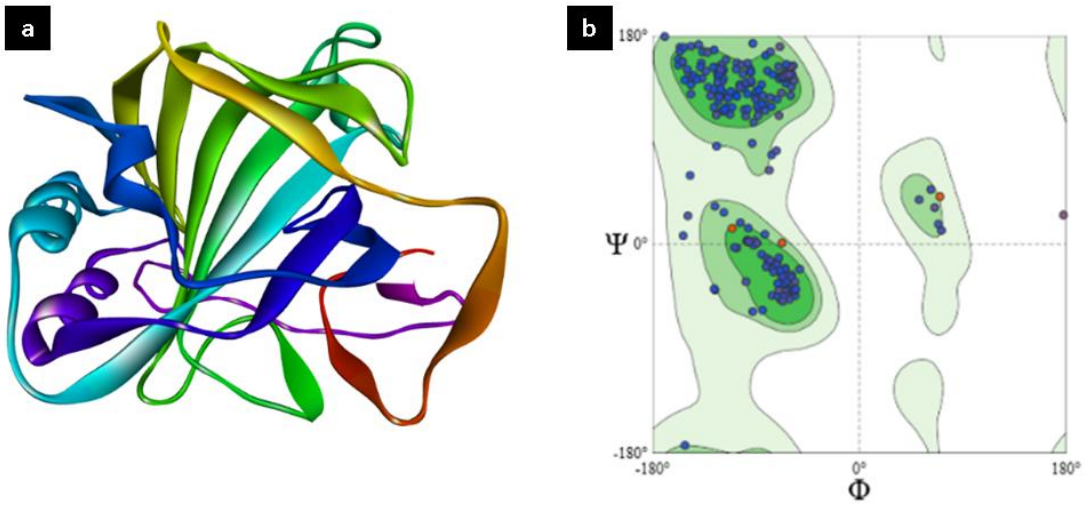

Figure 39. (a) 3D structure of the Cell surface-binding protein OPG105 of Mpox virus and (b) Ramachandran plot of receptor protein

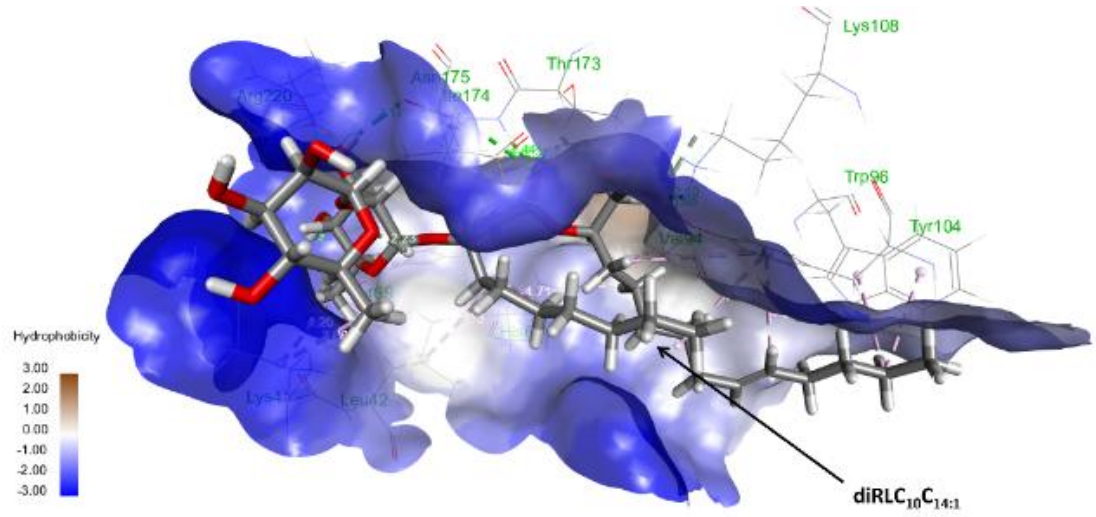

Figure 40. Rha-Rha-$C_{10}C_{14:1}$ BS inside the hydrophobic cavity of receptor protein

ADME predictions were obtained from SwissADME server and the results have been presented in Table 12. Based on the predictions, all RLs are found to be non-BBB permeant which indicates that they do not cross the blood brain barrier and will not show any kind of toxicity or inhibitory action in the central nervous system. Except mono-RL, all di-RLs failed to show drug-likeness.

The docking results revealed that the RLs bind exceptionally well with the receptor protein as compared to chondroitin sulphate and other standards used (Table 13). Among the RLs, Rha-Rha-C_{10}-$C_{14:1}$ was found to show the best MolDock score of -193.648 kcal/mol as compared to chondroitin sulphate with MolDock score of -142.195 kcal/mol. Other standards like aztreonam had a MolDock score of -143.583 kcal/mol while tecovirimat and lidocaine showed MolDock score of -99.4547 and -84.7327 kcal/mol, respectively. Figure 40 shows the surface of hydrophobic region in Rha-Rha-C_{10}-$C_{14:1}$ inside the cavity of E8L protein.

Table 12. Druglike-ness and ADME profile of RLs obtained from *P. aeruginosa* (ASM1a)

Ligand	Mol. Wt (g/mol)	HBA[a]	HBD[b]	RBC[c]	TPSA[d]	Log $P_{o/w}$[e]	Lipinski rule	BBB permeability	Solubility
Rha-Rha-C_{10}-$C_{14:1}$	704.89	13	6	25	201.67 Å²	3.78	No	No	Moderately soluble
Rha-Rha-C_{10}-C_{12}	678.85	13	6	24	201.67 Å²	3.42	No	No	Moderately soluble
Rha-Rha-C_{10}-C_{14}	706.90	13	6	26	201.67 Å²	4.10	No	No	Poorly soluble
Rha-Rha-C_8-C_{10}	706.90	13	6	26	201.67 Å²	3.91	No	No	Poorly soluble

Rha-Rha-C_{12}-C_{12}	706.90	13	6	26	201.67 Å²	3.91	No	No	Poorly soluble
Rha-Rha-C_{14}-C_{10}	706.90	13	6	26	201.67 Å²	4.11	No	No	Poorly soluble
Rha-C_{10}-C_{10}	504.65	9	4	20	142.75 Å²	3.47	Yes	No	Moderately soluble

([a]Hydrogen bond acceptor; [b]Hydrogen bond donor; [c]RBC- Rotatable bond count; [d]TPSA- Topological polar surface area; [e]Log $P_{o/w}$-(octanol/water)

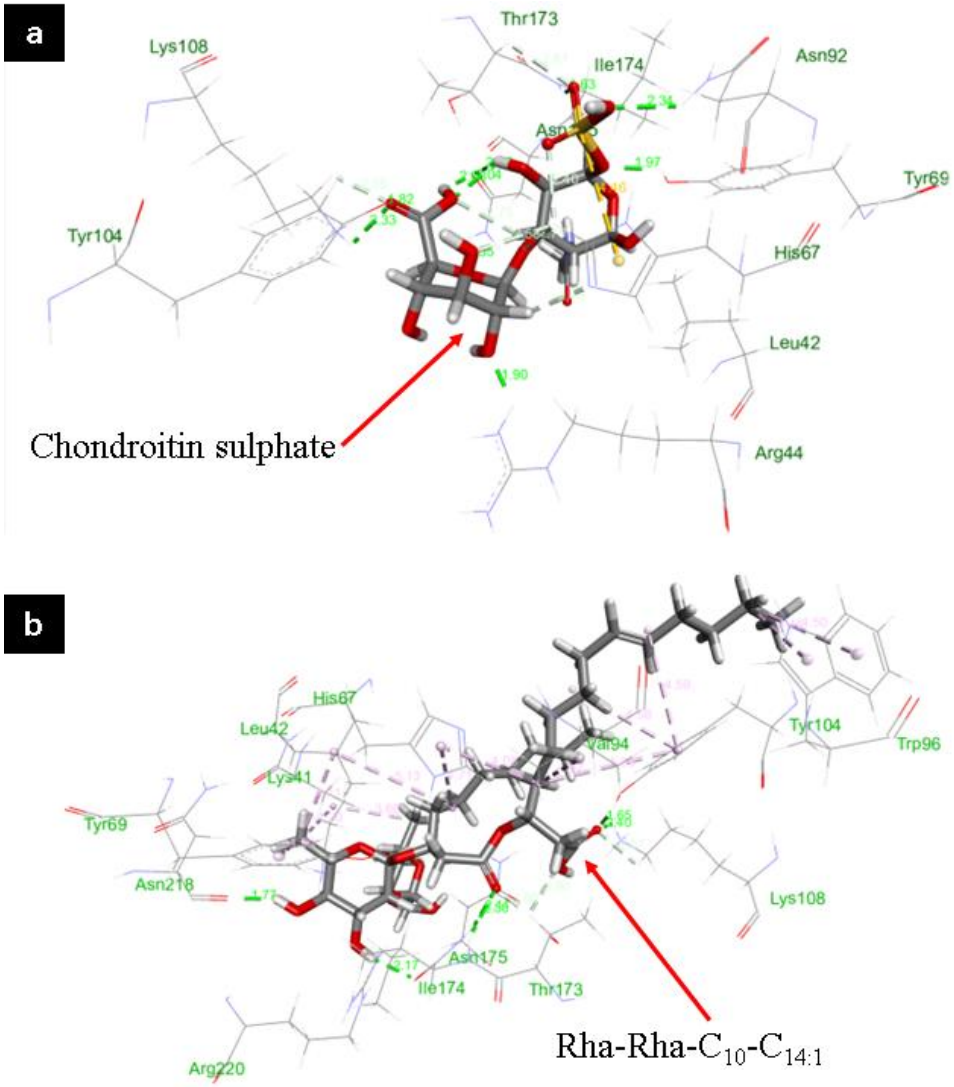

Figure 41. Docking interactions of (a) Chondroitin sulphate and (b) Rha-Rha-C_{10}-$C_{14:1}$ within receptor active sites of E8L protein

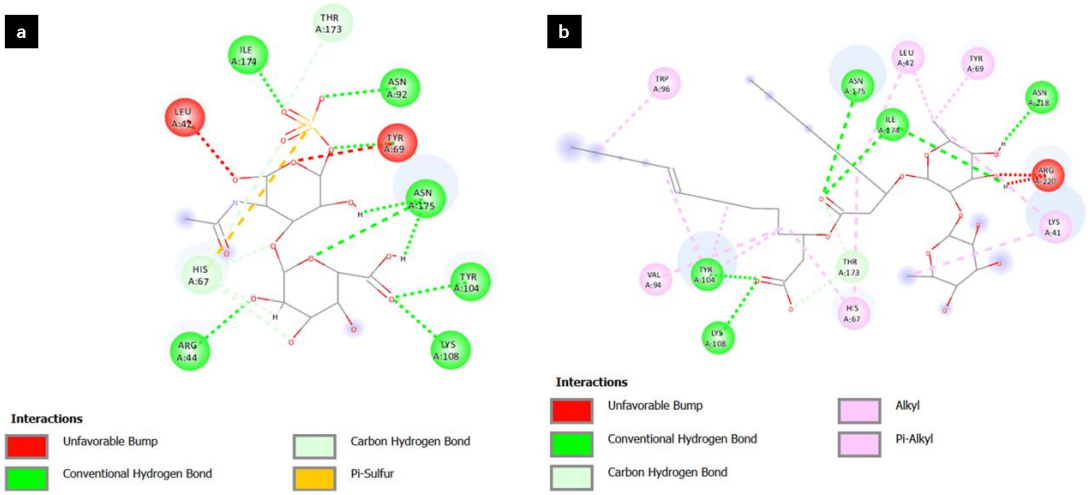

Figure 42. Ligand maps depicting ligand interaction of (a) Chondroitin sulphate and (b) Rha-Rha-C_{10}-$C_{14:1}$ with amino acid residues

Table 13. Docking of receptor protein with RLs, chondroitin sulphate and other standards

Ligand	Mol Dock Score	Rerank Score	Interaction	Protein	Internal	H Bond	LE1	LE3	Docking Score
Rha-Rha-C_{10}-$C_{14:1}$	-193.648	-104.726	-198.861	-198.861	5.21278	-9.567	-3.952	-2.13727	-183.712
Rha-Rha-C_8-C_{10}	-175.67	-125.033	-187.557	-187.557	11.8872	-7.40856	-3.5851	-2.5517	-158.562
Rha-Rha-C_{10}-C_{12}	-173.684	-105.496	-159.881	-159.881	-13.8035	-5.1475	-3.69541	-2.24459	-144.995
Rha-Rha-C_{14}-C_{10}	-172.19	-94.3419	-200.033	-200.033	27.8425	-8.98207	-3.51409	-1.92535	-149.799
Rha-Rha-C_{10}-C_{14}	-171.203	-107.414	-194.974	-194.974	23.7702	-9.10258	-3.49395	-2.19213	-159.261

Rha-Rha-C_{12}-C_{12}	-165.614	-90.9244	-189.587	-189.587	23.973	-5.38342	-3.37988	-1.8556	-136.74
Rha-C_{10}-C_{10}	-158.261	-115.765	-162.823	-162.823	4.56199	-7.66033	-4.52173	-3.30758	-141.995
Aztreonam	-143.583	-97.6636	-129.248	-129.248	-14.3352	-6.82868	-5.12797	-3.48799	-154.891
Chondroitin sulfate	-142.915	-77.4171	-123.474	-123.474	-19.4406	-12.0968	-4.76382	-2.58057	-164.594
Tecovirimat	-99.4547	-57.8584	-120.993	-120.993	21.5387	-2.48171	-3.68351	-2.1429	-104.573
Lidocaine	-84.7327	-59.6596	-99.2397	-99.2397	14.507	-2.63984	-4.98428	-3.50939	-84.0847

Table 14. Hydrogen bonding interactions and active amino acid residues

Ligand	**H bonds**	**Residues**
Chondroitin sulfate	12	Lys 108, His 67, Asn 175, Asn 92, Ile 174, Thr 173, Tyr 104, Arg44,
Tecovirimat	7	Lys 108, His 67, Asn 175, Asn 92, Ile 174, Tyr 69,
Aztreonam	5	Asn 175, Lys 41, Thr 173, Tyr 104, Asn 218
Lidocaine	5	Asn 218, Arg 220, Ile 174, Tyr 69
Rha-Rha-C_{10}-$C_{14:1}$	8	Lys 108, Asn 175, Asn 218, Tyr 104, Thr 173, Ile 174
Rha-Rha-C_8-C_{10}	5	Lys 108, Asn 175, Lys 41, Ser 177
Rha-Rha-C_{10}-C_{12}	3	Arg 220, Lys 108, Lys 41
Rha-Rha-C_{14}-C_{10}	13	Lys 108, His 67, Asn 218, Asn 175, Ile 174, Lys 41, Ser 177

Rha-Rha-C_{10}-C_{14}	13	Lys 108, Asn 175, Asn 218, Lys 41, Thr 173, Ile 174, Ser 177
Rha-Rha-C_{12}-C_{12}	4	Lys 41, Thr 39, Tyr 219, Arg 44
Rha-C_{10}-C_{10}	6	Asn 218, Asn 175, Lys 41, His 67

To reinforce the docking results, chondroitin sulphate along with other ligands were docked with the receptor protein on the active cavities predicted by the MVD software, and the results indicated that chondroitin sulphate as well as other ligands shared the same binding cavities (Figure 41) and amino acid residues (Figure 42). Table 14 represents the interaction of different ligands of with active amino acid residues. The complete information which includes the active binding residues with ligand atoms and their bond distances have been presented in appendix section.

3.14. Bioremediation application

3.14.1. Sand washing experiment

In the crude oil washing experiment, the BS performed much more consistently and efficiently after 24 hours of washing (Figure 43a) when compared to the synthetic surfactant with an average removal rate of 81.2 % ± 1.5, 78.6 % ± 2.7, and 81.6 % ± 2.2 at CMC, below CMC and above CMC respectively. The same is illustrated in Figure 43b. The synthetic surfactant (positive control), SDS (0.1% w/v) was able to remove an average of 72.9 % ± 2.3 of the crude oil and the control, distilled water (negative control) was able to remove about 55.4 % ± 4.2 of crude oil.

3.14.2. Crude oil degradation

After an incubation period of 15, 30, 45 and 60 days (Figure 44), the ability of the selected hydrocarbonoclastic *P. aeruginosa* (AMS1a) strain to degrade crude oil was validated using GC-MS analysis. Figure 45a, b, c and d display the respective chromatograms for 15, 30, 45 and 60 days. The results demonstrate that only selected hydrocarbons including medium to long-chain hydrocarbons are degraded into simpler and shorter molecules throughout the degradation process. The use of crude oil, a complex hydrocarbon mixture, as the exclusive carbon source results in the formation and accumulation of by-products during the 60-day degradation process, leading to the emergence of multiple additional compounds which is confirmed through the appearance of multiple newer peaks in the chromatogram of 45- and 60-days treatment.

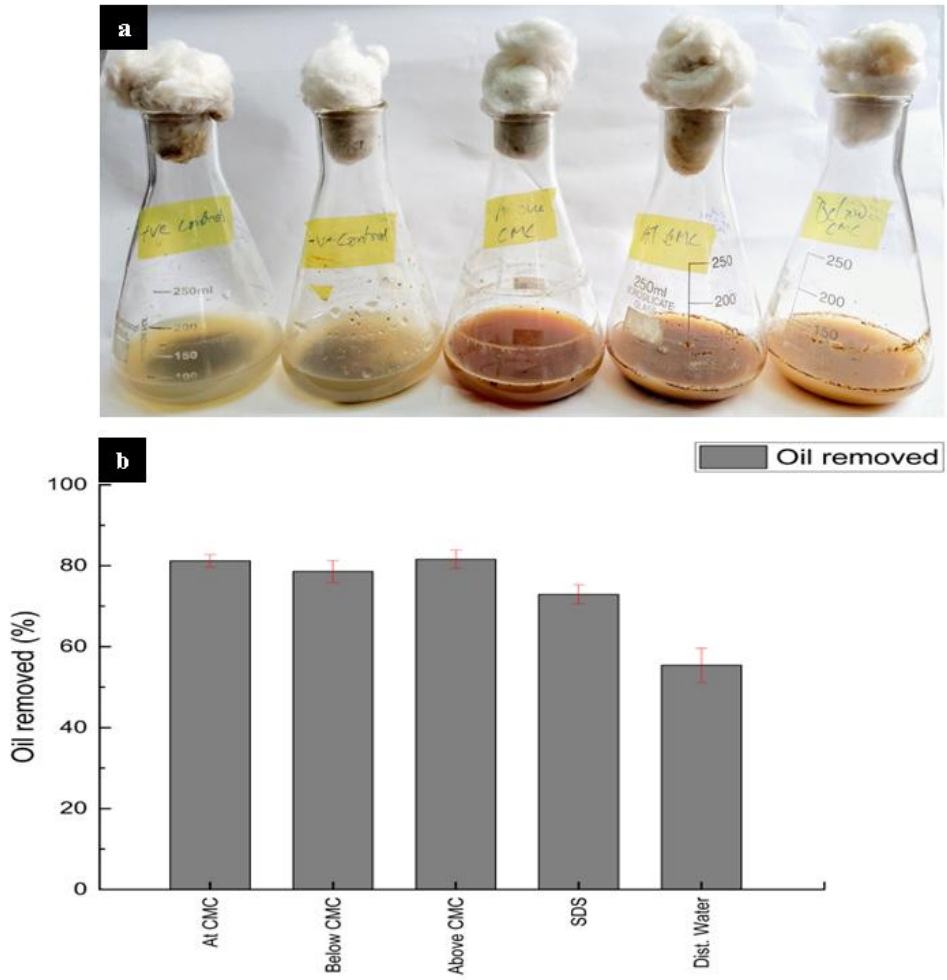

Figure 43. (a) Washing of crude oil contaminated sand samples with BS and (b) efficacy of BS at different concentrations in removal of crude oil (%) from the contaminated sand samples

Figure 44. Growth of *P. aeruginosa* (AMS1a) strain in MSM supplemented with crude oil during (a) 15 days, (b) 30 days, (c) 45 days, and (d) 60 days of incubation

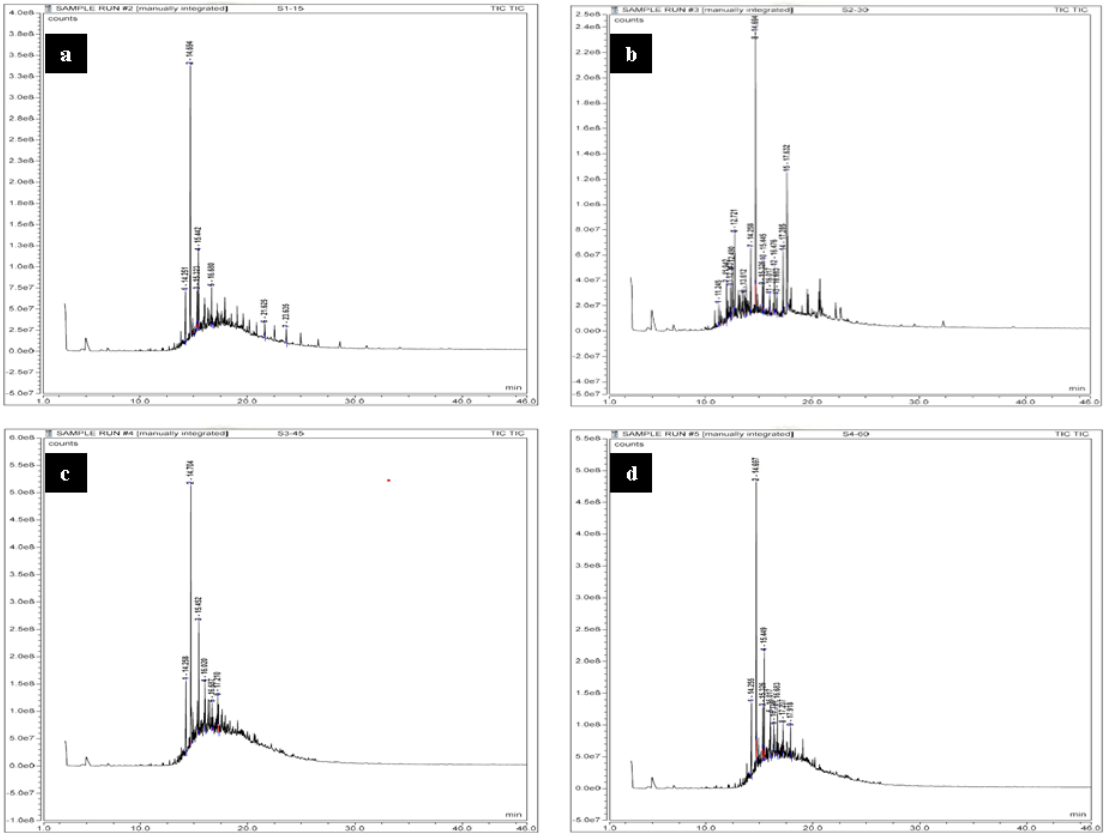

Figure 45. GC-MS chromatograms of the residual crude oil in the culture medium after (a) 15 days, (b) 30 days, (c) 45 days and (d) 60 days of treatment with *P. aeruginosa* (AMS1a) strain.

3.14.3. BS mediated removal of Arsenite

3.14.3.1. Effect of BS concentration on heavy metal removal

The sand washing experiment was performed using the CFCS containing RL BS exhibited significant Arsenite [As (III)] removal efficiencies of 82.2 ± 2.7 %, 79.5 ± 6.5 %, and 91 ± 6.6 % at concentrations equivalent to the CMC, above CMC and below CMC, respectively (Figure 46). Conversely, the use of a synthetic surfactant as a positive control, SDS at the concentration of 0.01 % (w/v) showed significantly reduced Arsenite removal efficiency of just 45.7 %. The negative control with distilled water also achieved an even lower removal efficiency of 32.9 % under the same experimental conditions.

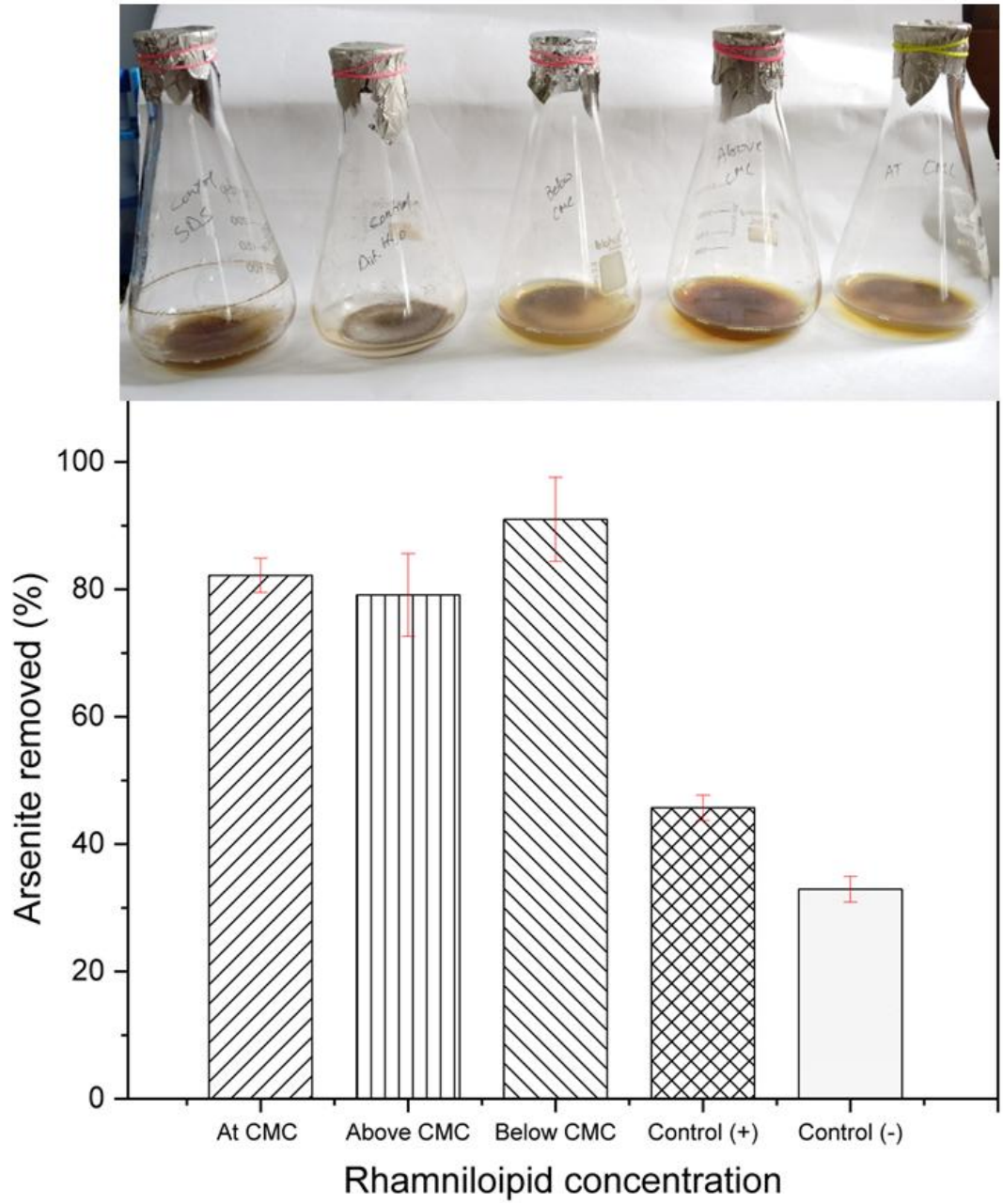

Figure 46. Efficacy of BS at different concentrations in removal of arsenite (%) from the contaminated sand samples

3.14.3.2. Effect of pH and salinity on heavy metal removal

The Arsenite removal efficacy of the CFCS at CMC concentration in the sand washing experiment conducted under varying salinity ranges of 0.5, 1, 1.5 and 2 % was of found to be 78.9 % ± 4.2, 79.3 % ± 3.9, 79.7 % ± 4.4 and 89.9 % ± 10 respectively (Figure 47a). Similarly, the Arsenite removal efficacy of the CFCS (CMC) was found to 89.3 % ± 7.3, 74.2 % ± 1.5, 67.7 % ± 1.3 and 57.99 % ± 4 at a pH of 3, 5, 7 and 10 respectively (Figure 47b).

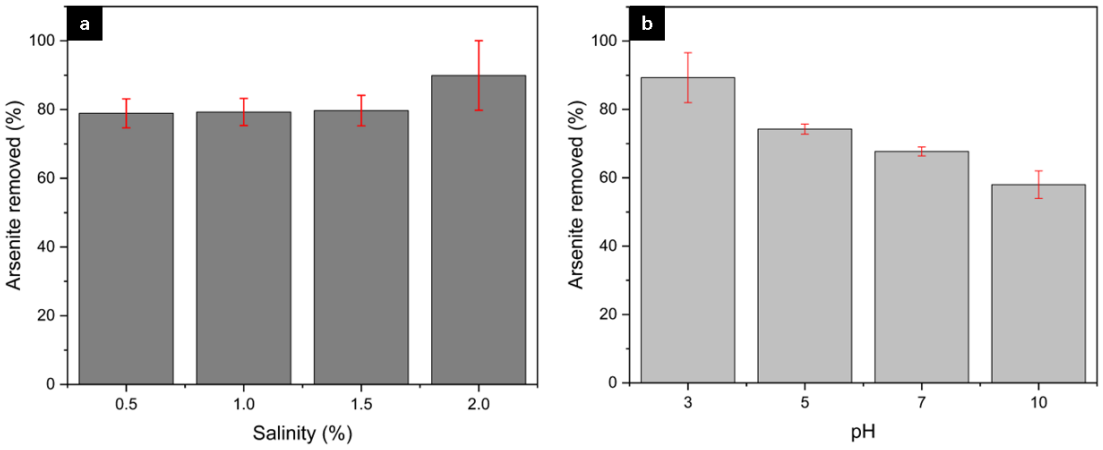

Figure 47. Effect of (a) salinity and (b) pH on the removal efficacy of arsenite

3.15. Valorisation of waste residual cooking oil (WRCO) as alternate carbon source for BS production

3.14.1 Growth behaviour

Figure 48 depicts the bacterial growth in MSM supplemented with WRCO as sole carbon source. From the results, it can be noted that the bacterium was in the early exponential growth phase till third day of incubation and entered into the exponential phase that lasted till the 5th day. Following the 5th day of incubation, the bacteria entered into the decline-phase that can be referred as late exponential phase with rapid and continuous decline in the OD of the culture till the 10th day of incubation. No distinct stationary phase was seen in the growth curve.

3.15.2. Physical Characterization

3.15.2.1. ST and CMC

The BS generated by the bacterial strain in the presence of WRCO reduced the ST of the distilled water from 72 mN/m to about 34.3 mN/m. After diluting the extracted BS solution multiple times in sterile distilled water, the CMC value was determined. Figure 49 illustrates the decrease in ST caused by the BS solution at different dilutions. A 177.74 mg/L CMC and 34.3 mN/m ST for BS were recorded and no further decrease in ST was noticed after the CMC was reached (Figure 48).

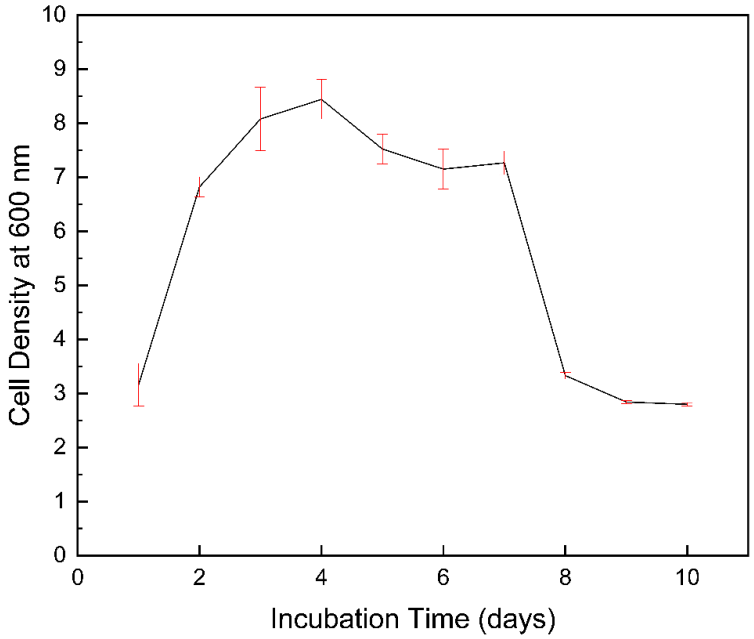

Figure 48. Growth of *P. aeruginosa* (AMS1a) strain in MSM supplemented with WRCO as sole carbon source

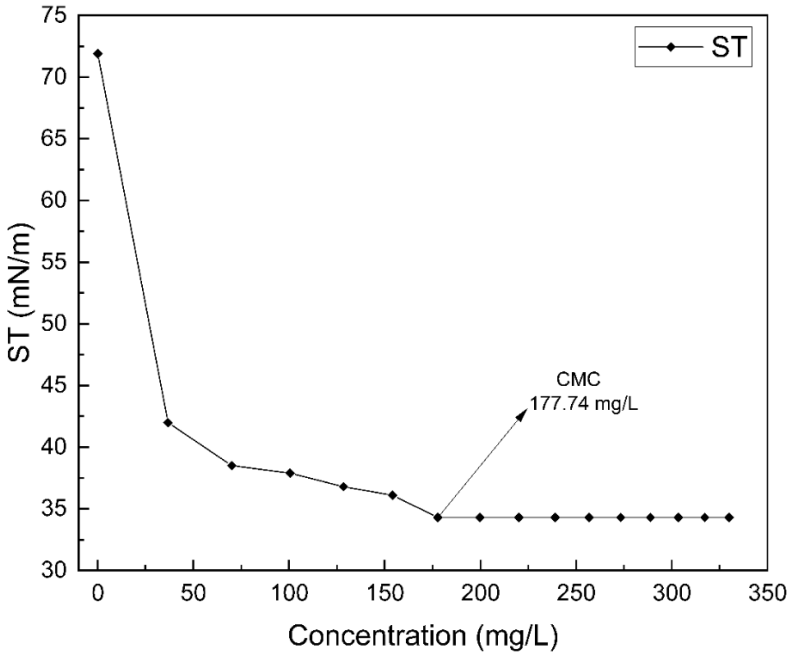

Figure 49. CMC of the BS produced by *P. aeruginosa* (AMS1a) in the presence of WRCO as carbon source

3.15.2.2. Emulsification activity (E_{24}%)

The emulsification activities of the BS present in the CFCS that was produced using WRCO were assessed against the different hydrocarbons and the same is presented in Figure 50. Results showed that, the CFCS containing BS can emulsify

different hydrocarbons to a greater extend. The CFCS of the bacterial strain exhibited appreciable emulsification indices against diesel, soyabean oil, rice bran oil, waste cooking oil, kerosene, and petrol were in the range of 56.7 %, 51.4 %, 63.6 %, 50 %, 55.4 %, and 56.4 %, respectively.

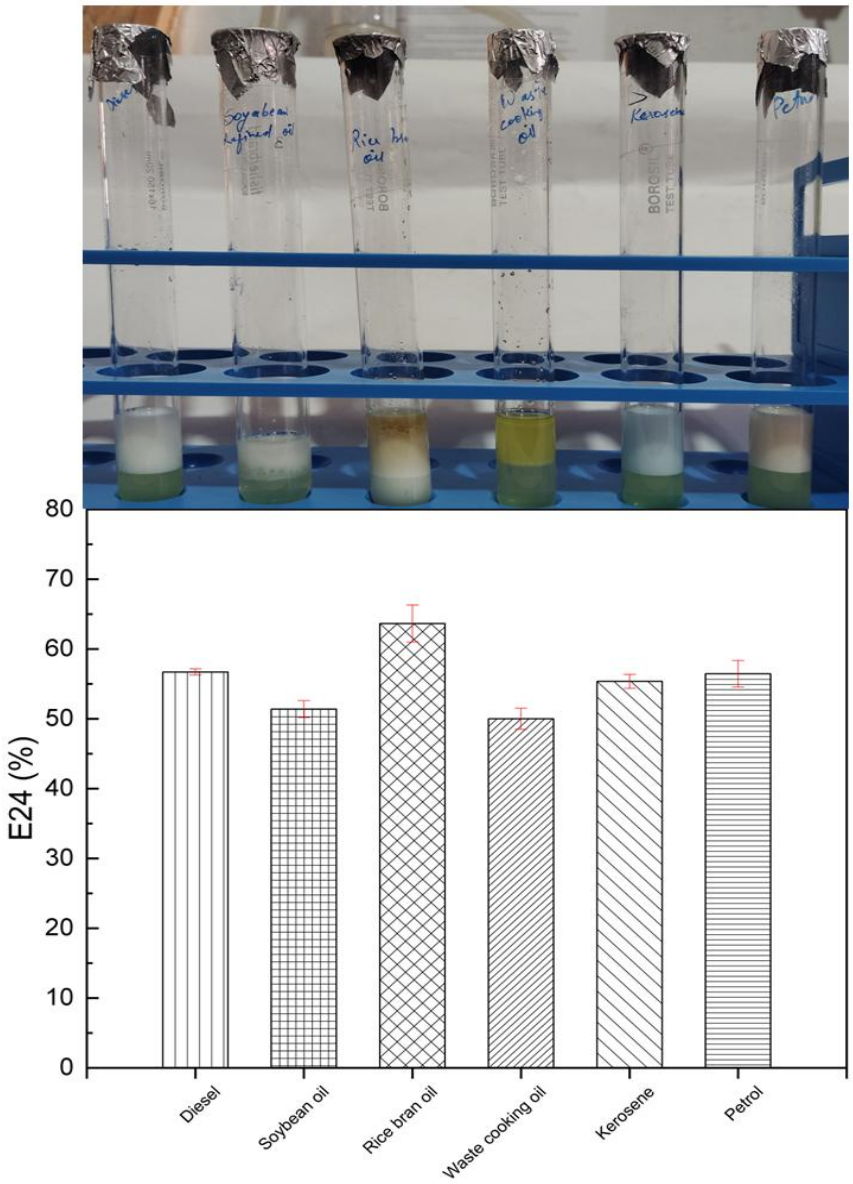

Figure 50. Emulsification indices (E_{24}%) of the BS produced by *P. aeruginosa* (AMS1a) using WRCO as carbon source against different test hydrophobic substrates (a) Diesel, (b) Soybean oil, (c) Rice bran oil, (d) Waste cooking oil, (e) kerosene, and (f) Petrol

3.15.2.3. XRD

Numerous peaks were observed in XRD spectrum at 2θ values varying from 7.66 to 84.38, with d spacing values varying from 11.5 to 1.15 Å, respectively (Figure

51). Crystallinity index (C.I) of the BS was calculated to be 11.15 %. Results clearly revealed the amorphous aspect of the extracted BS.

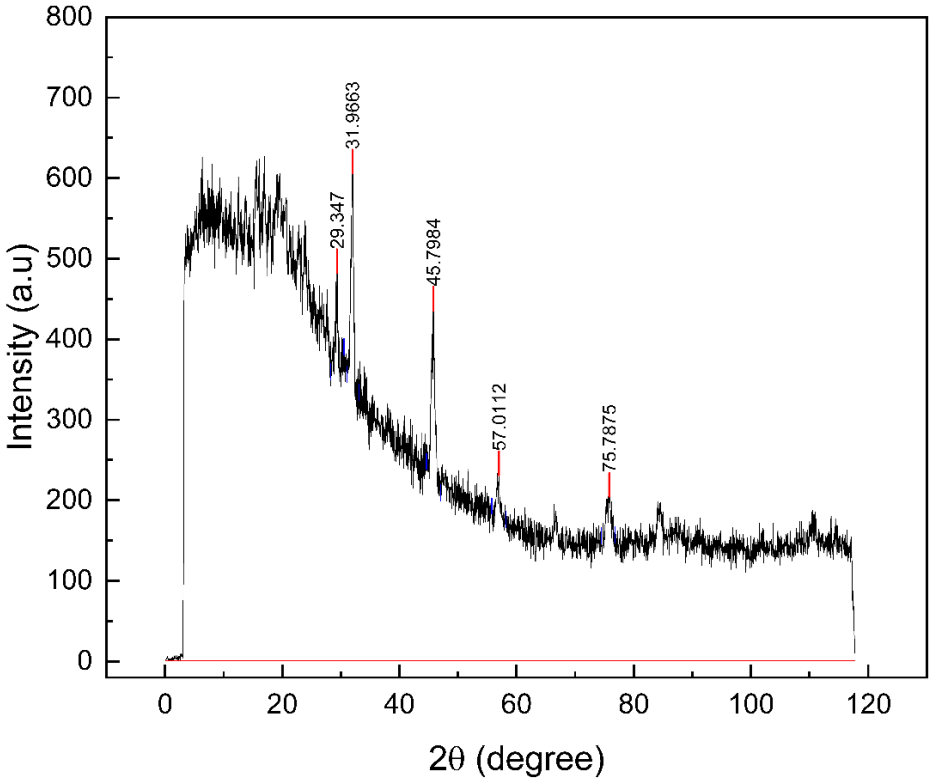

Figure 51. X-ray diffractogram of BS produced by *P. aeruginosa* (AMS1a) using WRCO as carbon source

3.15.2.4. Thermal analysis of BS

The thermal degradation analysis of the BS revealed two distinct regions of mass loss as shown in Figure 52. The first phase of degradation of approximately 2.53 % was shown within the temperature range of 100 to 120 °C. The most significant mass loss of about 94.42 % was seen at the temperature range of 200 to 750 °C. By the end of the thermal scan at 800 °C, a residual mass of 3.35 % remained. As evident from the DTG, the BS shows a maximum degradation temperature of about 257.2 °C approximately and a peak mass loss rate of around 13.3 % per minute. The DTA thermogram displays an exothermic peak at 83.2 °C, followed by significant exothermic peak at 257 °C, indicating a phase transition and the thermal degradation of the hydrocarbon component of the BS molecule.

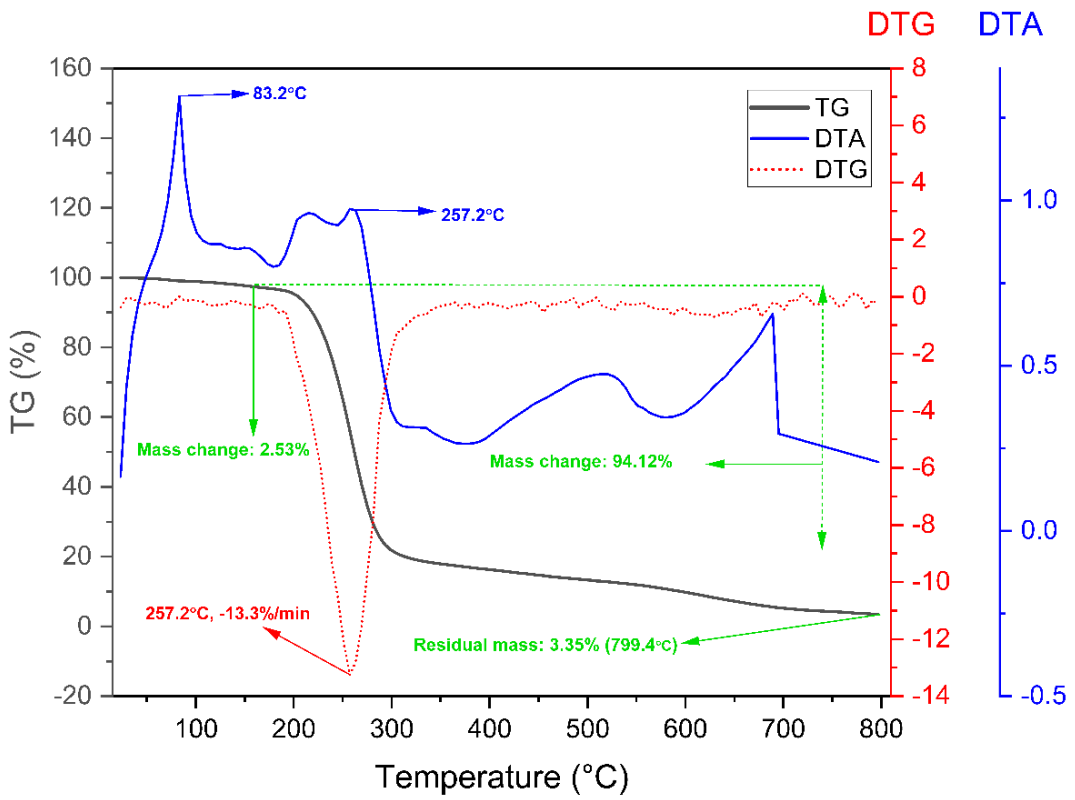

Figure 52. Thermogram of the BS produced by *P. aeruginosa* (AMS1a) using WRCO

3.15.3. Isolation, purification and chemical characterization of BS

3.15.3.1. Isolation and purification

CFCS was acidified at pH 2 for about 24 hours at 4 °C for precipitation of BS. The acidified CFCS was then extracted twice with ethyl acetate to separate the BS from the aqueous phase and the extracted BS was concentrated using a rotary evaporator resulting in a dark viscous partially purified BS. The partially purified BS was then cleaned through silica column using 100 % chloroform to remove the neutral lipids in the mixture. TLC was carried out using a solvent system of chloroform, methanol and water in the ratio of 65:35:2 (v/v/v) to determine the different fractions of BS in the partially purified mixture. After developing the plate, it was exposed to UV light, iodine fumes and sprayed separately with acidified anthrone reagent. This revealed two major spots and one minor one, showing up at R_f values of 0.3, 0.5, and 0.7 (Figure 53). Yellowish green spots were observed in TLC plates after spraying with anthrone reagent indicating the presence of carbohydrate units (Figure 53a). When identical plates were exposed to iodine fumes, yellowish brown spots suggestive of lipids appeared in about the identical region and the same is presented in Figure

53c. However, no spots developed when exposed to ninhydrin, which confirmed the non-appearance of amino acid in the extracted BS.

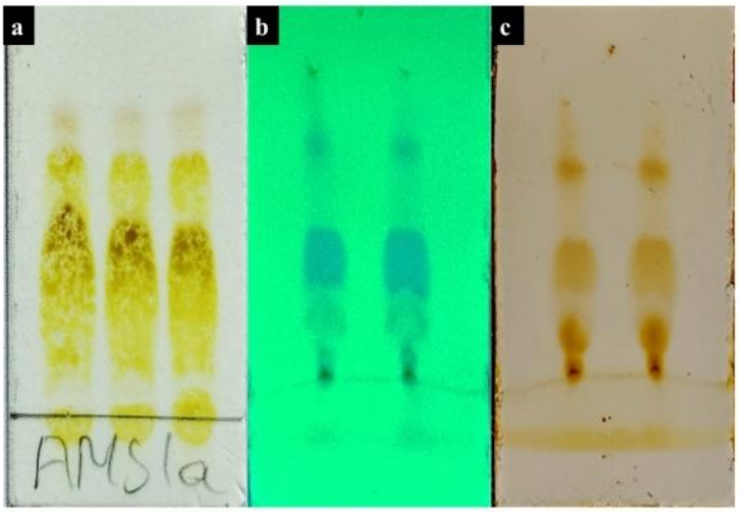

Figure 53. TLC separation of BS produced by *P. aeruginosa* (AMS1a) using WRCO as carbon source after exposed to (a) Anthrone reagent, (b) UV light, and (c) Iodine fumes

3.15.3.2. FTIR analysis

Figure 54 shows the IR spectrum of the isolated BS, which displays wide-ranging absorption bands. Prominent distinctive peak at 3435 cm^{-1}, confirmed the occurrence of –OH stretching of the hydroxyl group, whereas spectra at 2945 cm^{-1} revealed the occurrence of –CH aliphatic and −C=O stretching vibrations of the ester carbonyl group at 1743 cm^{-1}. Peaks at 1640 cm^{-1} corresponds to double bond C=C stretching and the sorption band 711 cm^{-1} also indicated the existence of a strong C-H bending.

3.15.3.3. ESI-MS analysis

The mass spectrum of the BS is depicted in Figure 55. The ions observed in the spectra were recognized as mono–RLs and di–RLs having different fatty acyl chains. Rha–Rha–C_{12}–C_{10} which correspond to pseudomolecular ions at m/z around 655.8 have been detected as di-RL and Rha–C_{10}–C_{12} which corresponds to the pseudomolecular ion at m/z 533.4 have been identified as mono-RL.

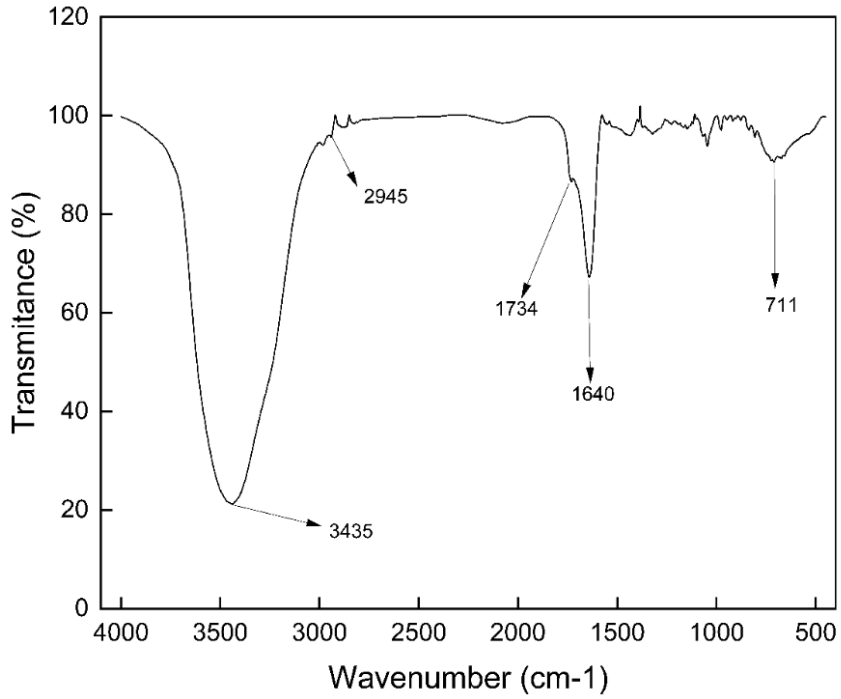

Figure 54. FTIR spectrum of BS produced by *P. aeruginosa* (AMS1a) using WRCO

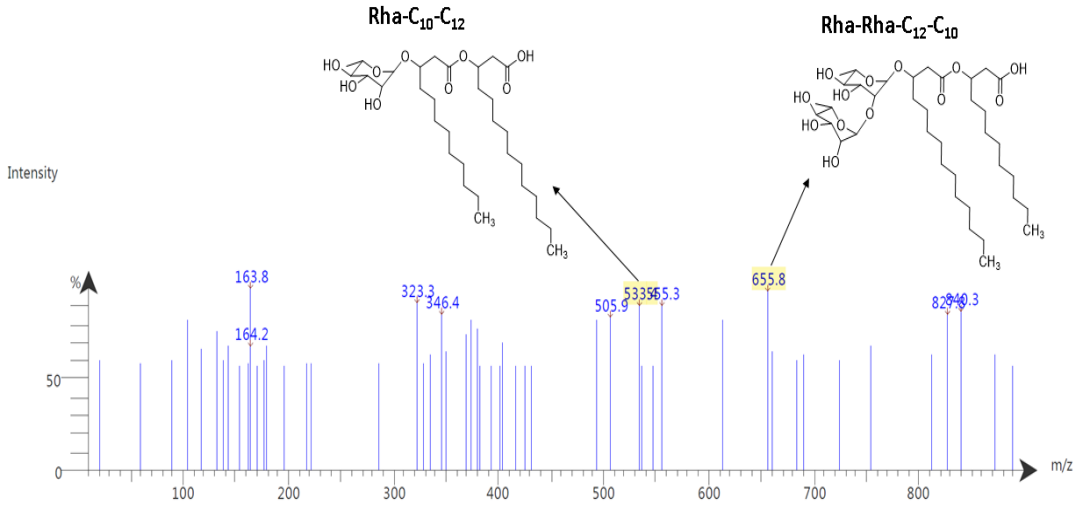

Figure 55. ESI-MS spectrum of BS produced by *P. aeruginosa* (AMS1a) using WRCO

3.15.4. Soil washing experiment

Figure 56a illustrates the outcomes of the investigation into the ability of BS solutions to remove crude oil pollutant from contaminated sand. The BS produced by *P. aeruginosa* (AMS1a) using WRCO performed exceptionally well in the crude oil washing experiment with an average crude oil removal efficiency of 81.93 % ± 2.2, 89.87 % ± 2.5 and 71.87 % ± 2.7 at CMC, above CMC and below CMC concentration, respectively (Figure 56b). In comparison, synthetic surfactant, SDS (positive control)

at 0.1 % (w/v) concentration was able to remove about 61.93 % ± 1.4 and the negative control (distilled water) showed a removal efficiency of about 50.2 % ± 2.7. It can also be observed from the results that the BS at higher concentration (at CMC and above CMC) exhibited higher removal efficiency when compared to concentration below CMC.

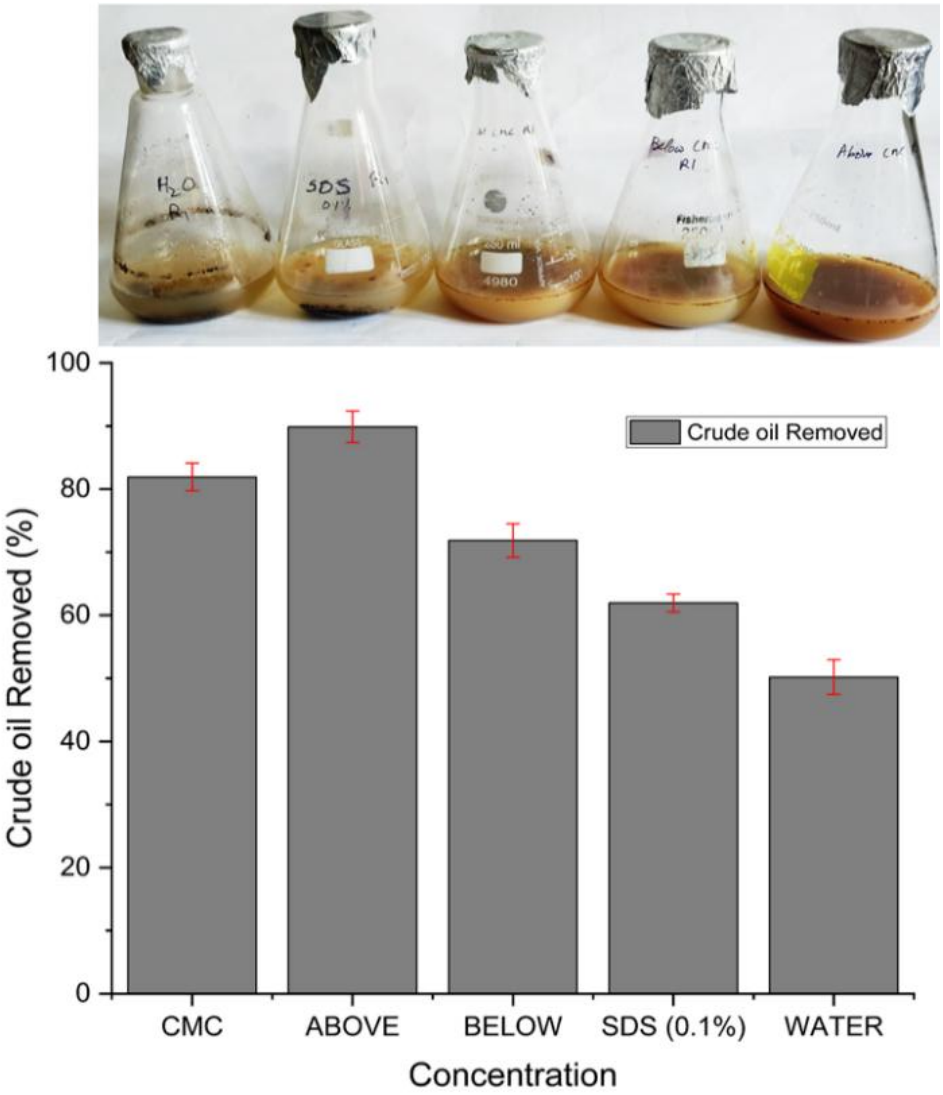

Figure 56. (a) Washing of crude oil contaminated sand samples with BS produced by *P. aeruginosa* (AMS1a) using WRCO and (b) Efficacy of BS at different concentrations in removal of crude oil (%) from the contaminated sand samples

Chapter 4. Discussion

4.1. Isolation of oleophilic hydrocarbonoclastic bacteria from environmental samples

In the present study, a total of 30 different hydrocarbon contaminated soil samples were collected around the automobile servicing station within Mokokchung town of Nagaland, India. Contaminated sampling sites such as automobile workshops, car wash and fuel stations were selected for the isolation of oleophilic hydrocarbonoclastic bacteria since microorganisms found in such contaminated environments are known to produce biosurfactants to emulsify and solubilise the available insoluble hydrophobic hydrocarbon substrates and utilize it as a carbon and energy source (Healy et al., 1996). In the present investigation, Bushnell-Hass (BH) medium was used for the enrichment culture as it does not contain any usable carbon source and selectively supports the growth of hydrocarbon degrading bacteria making it ideal for the isolation of hydrocarbon degrading or utilizing bacterial species (Allred et al., 1963; de Jesús Cortés-Sánchez et al., 2013). The total number of bacterial isolates obtained from the oil contaminate soil samples were determined at the end of enrichment culture method using n-hexadecane as sole source of carbon. Altogether, a total of 60 morphologically district different oleophilic hydrocarbonoclastic bacterial isolates were obtained. In accordance with the present investigation, Bekele et al. (2022) isolated two potent diesel degrading strains of *P. aeruginosa* (AAUW23 and AAUG11) and one *B. subtilis* (AAUG36) using enrichment culture technique. Using an enrichment culture technique and burnt motor oil and diesel as the only sources of carbon, Hossain et al. (2022) utilized soil samples collected from a petrol pump disposal site. They were able to identify three distinct bacterial isolates that were closely linked to *Enterobacter* sp., *Pseudomonas* sp., and *Acinetobacter* sp., respectively. During isolation and screening, the enrichment culture approach promotes the proliferation of the specific microorganisms with the characteristics of interest and raises the number of such target species. The selection of species unique to the metabolism of specific compounds using a certain carbon and/or energy source is one of the simplest methods for isolating novel species (Bhatt et al., 2023). Rahman et al. (2002a) documented a crude oil metabolizing *Pseudomonas* sp. DS10-129, which was isolated from soil samples obtained from gasoline and diesel stations. Rahman et al. (2002b) successfully obtained 130 bacterial isolates capable of degrading oil using

the enrichment culture approach out of which two *Pseudomonas* sp. were identified as proficient in using crude oil and producing biosurfactant (BS). Colombo Fleck et al. (2000) used the enrichment culture approach to isolate several bacterial strains that have the ability to produce BS and metabolize crude oil. The current study aimed to isolate indigenous BS producing oleophilic hydrocarbonoclastic bacterium to determine the bioremediation potential of the isolated BS. Moreover, there were no previous studies on the BS potential from the Indian State of Nagaland. Therefore, successful isolation of a native BS producing bacterium provides great promise for bioremediation potential of environmental pollutants in Nagaland, India as the native strain is evidently best adapted to the climatic and other environmental conditions of Nagaland, and therefore could reasonably be expected to naturally provide the optimum bioremediation potential.

4.2. Culturing and screening of BS producing hydrocarbonoclastic bacterial isolate

The obtained oleophilic hydrocarbonoclastic isolates from the enrichment culture approach was further inoculated in MSM supplemented with n-hexadecane as sole carbon source. This approach was used based on the fact that hydrocarbonoclastic bacteria are capable of producing biosurfactant while catabolizing long chain alkanes and utilizes hydrocarbon as a source of carbon and energy (Dashti et al., 2008; Meng et al., 2017). The culture medium of the bacterial isolate exhibiting the maximum reduction in surface tension (ST) was selected for further screening and production of BS. Similar strategy was previously used by Bordoloi and Konwar (2008) and Bharali et al. (2022) for the isolation of potential hydrocarbon utilizing bacterial strains. A total of 15 different bacterial isolates were obtained from the MSM culture. The *Du Noüy* ring technique is widely employed for screening of BS producing bacteria due to its simplicity, reliability and measures the force required to detach a platinum ring from an interface or surface of a liquid (Walter et al., 2010). Cooper (1986) states that a culture is considered potential if it is able to decrease the ST of a liquid medium to 40 mN/m or below. In the oil spreading assay, the CFCS was able to easily displace the oil layer in the petri dish indicating the production of BS. The extent of the displaced oil on addition of CFCS of the selected isolate is directly related to the activity of BS. Morikawa et al. (2000), Cheng et al. (2017) and El-Housseiny et al. (2020) have established that the oil spreading approach is a dependable method for quantifying the

surface activity of BS. Furthermore, they have demonstrated that this methodology is very sensitive and capable of detecting even small quantities of BS. When surfactant is present, the liquid drop expands or even collapses due to the reduction in the force or interfacial tension that exists between the liquid drop and the hydrophobic surface (Jain et al., 1991). The integrity of drops is contingent upon the quantity of surfactants and correlated to the degree of tension on the surface and interface (Walter et al., 2010). The CFCS containing safranin stain was able to penetrate through the oil layer into the silica-oil paste at the bottom of the 96 well microplates indicating the presence of BS. The penetration assay is appropriate for screening with high throughput and is based on the interaction between two insoluble phases, leading to a change in colour (Maczek et al., 2007; Walter et al., 2010). BSs have the ability to induce the rupture of the red blood cells (Walter et al., 2010). The clear zone produced by the chosen bacterial isolate in the blood agar plate exhibited β haemolysis and was confirmed to be positive for BS production. Mulligan et al. (1984) suggested using the blood agar assay as an initial assessment technique, which should be supplemented by additional techniques that rely on the measurement of surface activity. The CTAB agar plate method is a convenient screening technique used to identify the presence of exogenous glycolipids or other anionic surfactants (Siegmund and Wagner, 1991). The dark blue halos around the bacterial colonies indicated the anionic nature of the BS. When bacteria on the solid culture medium produce anionic surfactants, they react with cationic surfactant, CTAB and methylene blue dye to produce a dark blue, insoluble ion pair. As a result, BS producing bacterial colonies are encircled by dark blue halos (Mulligan et al., 1984; Tuleva et al., 2002; Walter et al., 2010).

The oleophilic nature of the selected hydrocarbonoclastic isolate was further studied by culturing it with different hydrocarbon substrates *viz*. waste motor oil, kerosene, diesel, crude oil, and rice bran oil as sole carbon source, individually. The selected hydrocarbonoclastic isolate could able to grow competently in the presence of all the tested hydrocarbon substrates. Further, the substantial reduction in the ST of the CFCSs supplemented with test hydrocarbon substrates at the end of 14 days confirm the presence of BS, thus indicating the utilization capacity of various hydrocarbon substrates as carbon source thereby confirming the hydrocarbonoclastic nature of the bacterial isolate.

4.3. Identification of selected bacterial isolate

The bacterial isolate was found to be Gram negative, rod shaped, motile and non-sporing bacterium. The standard biochemical tests revealed that the bacterial isolate was positive for catalase, oxidase, citrate, nitrate and glucose fermentation test. Clustal Omega alignment analysis show that the bacterial isolate AMS1a sequence has a 100 % similarity to various 16S rRNA gene sequences across *Pseudomonas* sp., particularly *P. aeruginosa*. The results of this analysis indicate that all 16S rRNA gene sequences obtained from NCBI are closely related to the isolate AMS1a. Specifically, the isolate AMS1a sequence exhibits considerable homology (> 97 %) compared to other Pseudomonas sequences. Based on phylogenetic analysis, the isolate AMS1a gene sequence shows a closer relationship to the *P. aeruginosa* DSM 50071 and ATCC 10145 sequences. *P. aeruginosa* ATCC 10145 was selected as the root of the phylogenetic tree because it was found to be closely related to the isolate AMS1a in the alignment test conducted using Clustal Omega. *P. aeruginosa* is a prevalent Gram-negative bacterial species among the hydrocarbonoclastic oleophilic prokaryotes. It is recognized for its versatile metabolism and capacity to inhabit numerous environments (Mielko et al., 2019). Various species of Pseudomonas capable of generating BSs have been reported from diverse polluted environments such as petroleum hydrocarbon contaminated fields (Bharathi and Vasudevan, 2001; Bordoloi and Konwar, 2008; Saravanan and Vijayakumar, 2012), metal contaminated sites (Cerqueira dos Santos et al., 2024), pesticide-affected regions (Wang et al., 2022), and habitats contaminated with industrial effluent (Al-Ansari et al., 2021; Wang et al., 2023).

4.4. Growth kinetics and BS production

The current study showed an uneven sigmoidal growth curve over a 14-day incubation period which closely aligns with previously documented growth curves of other Pseudomonas species (Janek et al., 2013; Goswami et al., 2015; Ramírez et al., 2015). In comparison to earlier published studies, the selected bacterial strain exhibited optimal growth at 30 ºC. This may be attributable to the abiotic factors of the contaminated sampling site from which bacterial strain was isolated. According to the records, the temperature in the Mokokchung township region does not exceed 32 ºC during summer, with an average summer temperature of 27 ºC (https://www.cgwb.gov.in/old_website/District_Profile/Nagaland/Mokok.pdf).Cerqueira dos Santos et al. (2024) isolated a strain of *P. aeruginosa* BM02 from acidic soil

in a Brazilian municipality with temperatures ranging from 28 ± 6 °C, which is very near the ideal temperature for BS synthesis. Wei et al. (2005) and Chen et al. (2007) reported optimum activity of rhamnolipid (RL) biosurfactant production by *P. aeruginosa* J4 between 30-37 ºC which decreased with further increase in the temperature. Temperatures between 28-40 °C were reported for the production of RL by various strains of *P. aeruginosa* (Müller et al., 2012; Henkel et al., 2012). Such discrepancies in the reported optimum temperature for *P. aeruginosa* strains distinctly indicates their apparent physiological variations.

The bacterial strain exhibited progressive growth and persisted throughout the fermentation process from 0 to 12th day and entered a decline phase thereafter. It has been proposed that cells enter into the decline phase due to the consumption of available nutrients in the culture medium, resulting in the build-up of toxic substances and a restricted supply of dissolved oxygen, which may impede bacterial growth (Lan et al., 2015). The ST measurements of the culture medium throughout the experiment showed a steady decline indicating the gradual production and accumulation of surface-active compounds such as BS. The growth of hydrocarbonoclastic oleophilic bacteria can be accompanied by the production of BSs which can aid in the attachment of cells to hydrophobic substrate molecules and facilitate their metabolism (Bharathi and Vasudevan, 2001). A spike in BS biosynthesis was noticed even after the bacterial population had entered into stationary phase. The reason for this could be attributed to the biosynthesis of BS as a secondary metabolite (Rahman et al., 2002a). Multiple studies have demonstrated that certain bacteria are capable of decreasing the ST of their culture medium by producing BS during the shift from exponential to stationary growth phases (Yin et al., 2009, Safari et al., 2023). The yield of the BS was found to be about 434.7 mg/L. Similarly, Cheng et al. (2017) reported a biosurfactant yield of 827 mg/L from *P. aeruginosa* grown in MSM culture supplemented with 2 % glucose as a carbon source. Rahman et al. (2010) also reported a BS yield of 106 mg/L for a culture medium supplemented with glycerol as a carbon source. The disparity in the yield of BS from *P. aeruginosa* species is greatly attributed to factors such as carbon source, nitrogen source, salt concentration and aeration that influences the type and overall yield of BS (Md, 2012).

4.5. Isolation and partial purification of BS

The BS from the CFCS was isolated initially isolated though acid precipitation at pH 2 followed by solvent extraction using ethyl acetate. Acid precipitation and solvent extraction is a common method used for BS isolation due to its simplicity and high purity (Chio et al., 2023). However, solvent extraction method involves the use of unsustainable and costly organic solvent contributing to the high separation and purification cost (Zhang et al., 2022). Previous studies have reported that different bacterial strains produced RLs with varying compositions (Abdel-Mawgoud et al., 2010). The composition of the partially purified BS was analysed through thin layer chromatography technique, where spot appeared in the TLC plates with higher R_f value that holds the mono-RLs, whereas the lower R_f value contains the di-RLs. These findings are consistent with other reported studies of Abdel-Mawgoud et al. (2008), George and Jayachandran (2009) and Lotfabad et al. (2009). Moreover, in the present study, a minor lower spot with a R_f value of 0.3 was also observed. Similar observation was reported by Lotfabad et al. (2010), where a lower R_f value of 0.31 refers to the di-RL structure, while the higher spot for mono-RLs had a R_f value of 0.76 (Lotfabad et al., 2010). Cheng et al. (2017) characterized the BS produced by *P. aeruginosa ZS1* isolated from petroleum sludge in Zhoushan islands, China through TLC technique. They were able to separate mono RLs, Rha-C_{10}-C10 and di RLs, Rha-Rha-C_{10}-C_{10} homologues from a RLs mixture. Abdel-Mawgood et al. (2008) obtained a lower spot (di-RL) and a higher spot (mono-RL) with respective R_f values of 0.4 and 0.68. El-Housseiny et al. (2020) described the characterization of BS from *P. aeruginosa* P6 through TLC analysis and showed two spots, one major spot with R_f value 0.56 and another minor one with R_f value of 0.71, which corresponds to di RLs and mono RLs. Both mono and di RLs are the two main types of RLs produced by most of the *P. aeruginosa* species (Lang and Wullbrandt, 1999; Maier and Soberon-Chavez, 2000). Column chromatography was performed to separate the individual homologues of RLs using a chloroform-methanol solvent system at different ratios. Many compounds may be efficiently purified and their structural and functional analyses carried out with such chromatography technique. Perfect outcomes are obtained in the identification and isolation of RLs congers using this approach (Sim et al., 1997). Moreover, column chromatography uses a cheap, disposable stationary phase that may be disposed away after use to avoid deterioration and cross contamination. Also, recovering the mobile phase for usage later on is much simpler.

4.6. Surface activity of isolated BS

4.6.1. Determination of CMC

According to the findings, the CMC of the extracted BS was measured to be 195.6 mg/L, which is equivalent to a ST of 34.4 mN/m. The CMC of RLs is significantly lower than that of synthetic surfactant like SDS which has a CMC value of 2200 mg/L (Khademolhosseini et al., 2019). The CMC values of mono and di-RLs, as well as their combinations produced by different bacterial species are reported to vary between 1 and 400 mg/L (Kopalle et al., 2022; Arkhipov et al., 2023). Greater values of CMC indicate a greater quantity of surfactant is required to reduce ST. Therefore, a lesser quantity of BS is required to achieve the maximal ST reduction. This is one of the important aspects that contribute to the greater utility of BSs compared to chemical surfactants. According to Manivasgan et al. (2014), a fine-quality BS has the ability to decrease the ST of water from 72.75 mN/m to 35 mN/m. Effective BSs, according to Zhang and Miller (1992), can reduce the ST of water to less than 40 mN/m.

Moreover, variations in the purity and content of the BSs might have contributed to the disparate CMC values. For RLs derived from different microbial sources, CMC values ranging from 10 to 230 mg/L have been reported (Zhang and Miller, 1992; Nitschke et al., 2005; Abdel-Mawgoud et al., 2010). It is well known that the distribution of homologues affects the characteristics of RLs. In general, the CMC tends to reduce as the length of the surfactant chain increases and with the increase the di-RL content (Perfumo et al., 2006). But this trend was not seen in the current investigation. The possible explanation for this phenomenon is that the BS examined in this study are not composed of one primary congener but rather contain an assortment congener with varying chain lengths. Additionally, the LC-MS results for the extracted BS indicated the presence of a combination of di and mono RL congeners which might potentially impact its CMC values.

4.6.2. BATH assay

The findings of BATH assay showed the cell surface hydrophobicity (CSH) of the bacterium with a 50 % ± 0.01 degree of adherence to n-hexadecane which is a potential proof of cell affinity for hydrophobic substrates (Zhang and Miller, 1994). This procedure is regarded as an indirect approach to investigate bacteria that produce BS since it is predicated on the concept that such bacteria have an attraction for hydrophobic substrates (Rosenberg et al., 1980). As per Mohebali et al. (2007), the

BATH assay determines the degree of partitioning of bacterial cells into aqueous and hydrophobic phases. The chosen bacterial strain in the present study has substantial hydrophobicity at its surface as indicated by the mean value of 50 % ±0.01 obtained from the BATH experiment. According to Singh and Tiwary (2016), the BATH assay revealed that the *Pseudomonas otitidis* strain had 69.3 % CSH, suggesting a highly hydrophobic surface on its cell surface. Notably, the BATH assay does not indicate an absolute quantity of CSH but rather, it is linked to the segregation of bacterial cells into aqueous and hydrophobic phases. According to Al-Tahhan et al. (2000), the results of BATH assays, are more relative and may be used to evaluate how different environmental factors impact behaviour of bacterial cells. In addition, Zhong et al. (2008) found that CSH depends on the proportion of hydrophobic to hydrophilic areas on the cell membrane. According to Liu et al. (2014b), CSH is an important component that influences the effectiveness of several bioprocesses, including interactions between cells and nutrient uptake. Faisal et al. (2023) mentioned that the generation of BS renders the surface of cells hydrophobic, thereby improving their adherence to the larger oil droplets. RLs were shown to enhance the CSH of the sluggish degraders during the breakdown of octadecane, but have no impact on the CSH of the swift degraders (Zhang and Miller, 1994). Moreover, they also suggest that the cell hydrophobicity and aqueous dispersion of octadecane regulate the bioavailability of octadecane in the presence of RL. According to Zhong et al. (2008), di-RL was shown to increase *P. aeruginosa* CSH more than mono RL.

4.6.3. Emulsification activity

Emulsification activity is regarded as a critical parameter among the physicochemical qualities utilized to assess the commercial usability of BSs (Mendes et al., 2015). This is regarded as an indirect approach for evaluating BS production. The findings demonstrated a varied emulsifying capacity, extending from 42.8 % ± 1.9 to 95.83 % ± 1.2 % against a wide range of hydrophobic substrates, reflecting the capability of the selected bacterial strain to produce BS that improve the interaction of hydrophobic substances with water. According to Patel and Desai (1997) and Lovaglio et al. (2011), RLs have a great ability to emulsify a wide range of n-alkanes, aromatic hydrocarbons, petroleum derived compounds, crude oil, and vegetable oils. With regard to the investigation conducted by Sun and colleagues (2018), *Pseudomonas* sp. CQ2 from Changqing oil field, China produces a BS with an E_{24}% reach as high as

61.5 %. As reported by Kumari et al. (2012), the BS generated by *Pseudomonas* sp. BP10 has a high emulsification activity of up to 75 %. Hydrocarbons are pseudo-solubilized or emulsified at varying rates by the majority of microbial surfactants, which are substrate specific (Etoumi et al., 2008). A number of studies have found emulsifying indices ranging from 50 % to 75 % for various RL mixtures (Wei et al., 2005; Abdel-Mawgoud et al., 2008; Benincasa and Accorsini, 2008; George and Jayachandran, 2009; Lotfabad et al., 2009; Bharali and Konwar, 2011; Abbasi et al., 2012; Aparna et al., 2012). The resulting oil-in-water (O/W) emulsions turned out to be dense and have persisted for over a week at room temperature, indicating the usefulness of the BSs in for bioremediation process to improve the bioavailability of the intractable hydrocarbons. Besides that, as noted by Maier and Soberon-Chavez (2000) and Abdel-Mawgoud et al. (2008), the capacity of the BSs to emulsify fossil fuels products particularly kerosene, n-hexadecane, octadecane, diesel, and lubricating oil may facilitate their microbial assimilation. The excellent emulsification activity demonstrated by the RL BS against different test hydrocarbon in the present study accredits it as a powerful emulsifying agent to be potentially used in environmental application such as MEOR and oil mobilizing agents (El-Housseiny et al., 2020). Furthermore, the bioremediation of petroleum-contaminated settings may benefit from the capacity of the BS to emulsify various hydrocarbon oils because it may facilitate the assimilation of such hydrophobic compounds by BS producing microorganisms (Maier and Soberon-Chavez, 2000; Abdel-Mawgoud et al., 2008).

4.7. Physicochemical characterization of isolated BS

4.7.1. FTIR

The recovered BS was analysed using FTIR to determine its functional groups. The FTIR investigation identified significant absorption bands in the tested BS at certain wavenumbers: 3410, 2931, 2856, 1735, 1644, 1402, and 1206 cm^{-1}. The results provide compelling evidence that the detected wavenumbers align with the various functional categories of the RL as reported in the literature (Arutchelvi and Doble, 2010; Cortés-Sánchez et al., 2012). Lan et al. (2015) and Ibrahim (2018) reported that the aforementioned primary chemical structure groups align with the structural features of RL, as determined by FTIR analysis. The wavenumbers below 1200 cm^{-1} encompasses many types of C–H, C–O, and $–CH_3$ vibrations that cannot be further classified (Zhao et al., 2013). It is also crucial to point out that there were slight

differences observed in the infrared spectra compared to the spectra previously published. This variation may be ascribed to the specific constitution of RL mixtures obtained from varied strains of *Pseudomonas* sp., as well as differences in the culture and purification conditions employed.

4.7.2. Thermal characterization

The high thermal stability of the RL is evident from the TGA thermogram with 63.33 % residual mass at the end of the thermal scan at 500 ˚C. During the thermal degradation process, the initial mass loss of about 2.53 % at temperature range of 50 ˚C to 170 ˚C is the result of the evaporation of water indicating the hydroscopic nature and the ability of the BS to absorb moisture from the surroundings (Singh and Tiwary, 2016; Gil et al., 2022). The second significant mass loss of about 31.27 % at temperature range of 170 ˚C to 440 ˚C is presumably due to the breakdown of RL (Gil et al., 2022). The rate of BS disintegration of about 6 % per minute was determined by DTG and the heat of disintegration was confirmed by the DTA thermogram. The enthalpy of dehydration and the enthalpy of decomposition of the RL can be observed through the peaks at 72 ˚C and 180 ˚C respectively in the DSC thermogram. Gogoi et al. (2016) also report a similar observation, where the crystallization and melting temperature of RL from *P. aeruginosa* was found to be 99 and 134 °C respectively.

4.7.4. Zeta potential

Fundamental information about the electrokinetic and surface charge characteristics of a material may be obtained from the zeta potential, which is calculated by analysing the mobility pattern of electrically charged particles in an electric field. According to Maillard et al. (2021), it is an invaluable instrument for comprehending the adhesion, aggregation, and interactions of biomolecules with various materials or surfaces. The isolated BS exhibits a zeta potential of −4.49 mV. Such lower zeta potential value indicates that BS particles are more likely to aggregate and accordingly their dispersion in the aqueous solution will be unstable. The negative charge of BS is primarily attributable to the carboxylic acid unit in their hydrophobic head region (Raza et al., 2010). The findings of the present study show that the BS has a noticeable negative surface charge and may interact with cationic pollutants, such as heavy metal ions like Cd^{2+}, Pb^{2+}, As^{3+}etc. in an efficient manner. According to Gong et al. (2022), pH of the solution has an effect on the zeta potential of RL. The fall in

pH lowered the zeta potential and foaming attributes of RL solutions while promoting the aggregation nature of RL molecules.

4.7.5. XRD

The presence of pronounced peaks in the XRD chromatogram verifies the 41.1 % crystalline characteristics in the isolated BS. The results of the current XRD study of BS were discovered to be consistent with Domdi et al. (2021). Through XRD analysis, they were able to determine the presence of crystalline nature in the RL which was isolated from *P. aeruginosa* PU1 strain. According to Sultana et al. (2024), XRD analysis of the refined RL-like BS made from a novel oil degrading bacterium, *Bacillus velezensis* S2, revealed no notable peak aside from a broad diffracted background, indicating that the core structure of RL is amorphous in nature.

4.7.6. EDX

The elemental composition of the dehydrated BS was determined in the current investigation using the SEM-EDX map sum spectrum. Carbon and oxygen were found to be the major elements present in the isolated BS. This investigation demonstrated that the BS included carbon and oxygen, as well as sodium, phosphorus, chlorine, and potassium, but not nitrogen. Hence, the BS belongs to the glycolipid group and cannot be placed in the lipopeptide or polymeric surfactant groups. Moreover, the presence of other elements in the EDX spectrum indicates the possibility of contaminants either from the growth medium or from the process of separating the BS using the acid precipitation technique. The existence of tightly packed bulky, irregular shapes of clump-like formations was shown by SEM micrographs of the acid precipitated BS. In comparison, the SEM micrographs of the solvent extracted BS was visually much smoother. Sabturani et al. (2016) and Haque et al. (2020) advocate the use of SEM-EDX to determine the chemical composition of BS produced by *P. aeruginosa* UKMP14T and *P. aeruginosa* ENO14, respectively. According to Sabturani et al. (2016), the combination of SEM-EDX is highly helpful in validating the primary elements and facilitates identification work. By offering reliable preliminary data as a point of reference, this will assist to narrow down the next phase in the structural characterisation investigation.

4.7.7. NMR

The identified signals in the ^{1}H and ^{13}C NMR investigations align with the functional groups of the RL as described in the literature (Cortés-Sánchez et al., 2012; Araujo et al., 2020). Therefore, according to the explanations obtained through NMR studies, it can be concluded that the BS was composed of RL. The inadequate clarity of the NMR spectra suggests that the substance being studied may include a combination of several RL congeners. The current results were corroborated by Monteiro et al. (2007) and Wei et al. (2005), who utilized ^{1}H and ^{13}C NMR analysis to determine the chemical composition of the pure BS.

4.7.8. LCMS

The mass spectrometry data indicated the presence of both mono- and di-rhamnose groups, as well as mono- and di-lipid groups. There was a significant variation in the length and composition (saturated or unsaturated) of the lipid chains, with a particular focus on the presence of saturated C_{10} and C_{12} fatty acids in mono-RL, and saturated C_8, C_{10}, C_{12}, and C_{14} fatty acids in di-RL. The previously investigations reports that the most prevalent *P. aeruginosa* RL comprises fatty acids ranging from C_8 to C_{14}, with C_{10} being the most often seen. In their study, Christova et al. (2011) identified mono- and di-RL congeners as anions with m/z values of 503 and 649. These values matched to the deprotonated molecules of Rha-C_{10}-C_{10} (mono-RL) and Rha_2-C_{10}-C_{10} (di-RL) respectively. Déziel et al. (1999 and 2000) observed that the ions with the greater abundance were found at m/z 649.9 and 503.6. These ions have been identified as the Rha_2-C_{10}-C_{10} and Rha-C_{10}-C_{10} congeners, respectively. It is important to note that there was no estimation of each individual congener, thus it is possible that some of them, particularly the less frequent ones, might also be contained in minimal proportions. The NMR investigation did not reveal the existence of unsaturated chain congeners, regardless of the slight signals in the 7.0–8.2 ppm region however, these congeners were found using mass spectrometry.

4.8. Stability studies

4.8.1. Effect of environmental variables on E_{24} %

The efficacy of BS relies on its capacity to maintain stability throughout diverse environments, accounting for fluctuations in pH, temperature, and salinity (Gudiña et al., 2010). The current work assessed the strength of the obtained BS by

exposing the CFCS to severe environmental variables like pH, temperature, and salt. BS demonstrated stability throughout all evaluated variables with no occurrence of precipitate formation or a significant decline in surface active behaviour. The findings indicated that the BS was able to continue operating and retain its active property within a wide temperature range (4 °C to 121 ˚C). Moreover, there was minimal variation in the E_{24}% observed when subjected to varying temperature with overall values ranging between 54.1 % to 62.5 %. In similar research, Cerqueira dos Santos et al. (2024) examined the effects of RL isolated from *P. aeruginosa* BM02 on its stability under wide range of temperatures and the results showed that the RL was stable even at severe temperatures ranging from 40 °C to 120 °C with minimal variations in its E_{24}% value (65 to 71 %). We also examined the impact of elevated temperatures on the emulsifying activity of CFCS and found that autoclaving led to a marginal but insignificant decrease in its E_{24}% value. The proficient temperature stability and strong emulsifying activity of the investigated RLs render them suitable for implementing microbial enhanced oil recovery (MEOR) and bioremediation in oil contaminated areas characterized by extreme temperatures (Zhou et al., 2019). The E_{24}% of the BS remain stable above 50 % at pH range of 5 to 10. However, a decrease in the E_{24}% value was observed at pH 3. This might be because, RLs at high acidic condition precipitates into the aqueous solutions resulting in lowered emulsifying activity (Lovaglio et al., 2011; El-Housseiny et al., 2020). When salt crystals are dissolved in water, it produces its own electrical charges during dissolution and these charges gets absorbed to the emulsion droplets and influences the stability of the emulsion (Zargar et al., 2022). The stable emulsification capacity of the RL under varying NaCl salinity (2 -10 %) was demonstrated by maintaining a relatively stable emulsion of above 50 %. The RL was also relatively stable under different concentration of heavy metals salts (100-500 ppm), maintaining an E_{24}% of above 60 % with all the three heavy metal salts used. This shows that the RL under study can be a stable and efficient bioremediating agent in highly contaminated environmental conditions. A similar study on the emulsification activity conducted by Peter and Singh (2014) where, RL from *Pseudomonas fluorescens* was reported to exhibit maximum emulsification activity of 90 % with palm oil, sunflower oil and coconut oil at the optimum temperature of 4 °C at pH 6 and 7. Additionally, it showed the highest emulsification of 94.44 % in palm oil at 5 % NaCl concentration. Additionally, the use of RL in its crude form *i.e.* cell free culture supernatant (CFCS) in bioremediation

applications is advantageous as it will reduce expenses typically given away to the steps of separation and the purification process (El-Housseiny et al., 2020).

4.8.2. Effect of environmental variables on surface tensiometric behaviour

The property of RLs to reduce the ST of liquids has a number of bioremediation applications (Safari et al., 2023). Therefore, it is necessary to determine the stability of the surface activity of RLs under varying environmental factors such as, pH, temperature, salinity and presence of environmental contaminants such as heavy metals so as to determine the stability and efficacy during bioremediation. In the current study, the optimal surface activity was achieved within a pH range of 6 to 8. A substantial decrease in surface activity was seen under extremely acidic (pH 2) settings. This phenomenon arises as a result of precipitation of RLs in high acidic circumstances, resulting in structural distortion and diminished capacity to decrease ST as under high acidic settings, the groups with negative charges at the polar ends of RL molecules undergo protonation (El-Housseiny et al., 2020). The impact of the ionic concentration on tensio-active surface property was also examined, revealing that surface activity was relatively stable at salinity ranges of 2 % to 10 % maintaining a ST reduction of 34.2 mN/m ± 0.15 to 35.6 mN/m ± 0.05. Thus, the obtained RLs have demonstrated their superiority as a preferred option for the bioremediation processes of high salinity areas, such as polluted coastal environments. In a similar study by Reddy et al. (2016) it was noted that the ST exhibited a progressive rise from 30 to 38 mN/m when the salt content rose from 6 to 20 %. The RL also exhibited stable ST reduction with different heavy metal salts (As, Cd and Cr) at different concentrations (100-500 ppm) by maintaining a ST value within the range of 34.4 mN/m ± 0.05 to 35.8 mN/m ± 0.11 and highlighting its stable surface activity and potentiality to be an efficient bioremediating agent in environments with elevated heavy metal contamination. The surface activity of the BS maintained a consistent ST reduction value of about 35 mN/m ± 0.05 at a temperature range of 25 °C to 121°C however, there was an increase in the ST value at 4 °C. This might be due to the precipitation of RLs at low temperatures (4 °C) that adversely affects their surface activity (El-Housseiny et al., 2020). With regard to its notable thermal stability and surface activity, the studied BS can be effectively used for remediation and enhanced oil recovery (EOR) application in oil ladened sites with high temperatures. In line with the present investigation, Cerqueira dos Santos et al. (2024) found that the BS derived

from *P. aeruginosa* BM02 remained stable under all tested conditions. The best surface tensiometric activity was observed at pH 3.0, with a 2 % NaCl concentration and a temperature of 80 °C. Joshi et al. (2008) found that the stability of the BS was maintained at a temperature of 80 °C and within pH and NaCl ranges of 6 to 12 and 1 to 7 %, respectively. However, the surface activity of the BS declined as the NaCl concentration increased to 10 % and the pH level decreased down to the acidic range resulting in the formation of precipitates. Khademolhosseini et al. (2019) conducted a study on a RL produced by *P. aeruginosa* HAK01. They revealed that the BS possessed excellent stability under various conditions including temperatures ranging from 40 to 121 °C, pH values between 3 and 10 and salt levels up to 10 % (w/v) NaCl. Based on their findings, they propose that the BS might be utilized in microbial enhanced oil recovery (MEOR) applications.

4.9. Biological activity

4.9.1. Antibacterial activity

The results of antibacterial assay highlight the broad spectrum activity of the RL under study. *P. aeruginosa* are known to produce numerous metabolites including RLs which are directly or indirectly involved with the bactericidal activity of a wide spectrum of Gram-positive and Gram-negative bacteria. RLs enhance the bactericidal activity by acting as a carrier system to deliver the toxic compounds produced by *P. aeruginosa* to the target bacterium (Gdaniec et al., 2021). When RLs come in contact with Gram-negative bacteria, the O antigen component of the lipopolysaccharides present in the outer membrane interacts with the hydrophilic moiety of RLs, thus leading to the increase in hydrophobicity of the membrane due to the unavailability of polar sugar residues on the surface of the bacteria (Zhong et al., 2014; Gdaniec et al., 2021). The exact mechanism of RL interaction with Gram-positive bacteria is quite ambiguous, however, RLs are known to interact with numerous Gram-positive bacteria whose membranes are composed of a variety of phospholipid compounds (Gdaniec et al., 2021). Apart from Gram positive and Gram-negative bacteria, RLs are known to show antifungal activity against a wide number of fungi and even protists *viz*. amoeba at higher concentrations (Cosson et al., 2002; Goswami et al., 2015; Gdaniec et al., 2021). RLs are reported to assist in increasing the fluidity of fungal membranes (Monnier et al., 2019; Gdaniec et al., 2021). Further, RLs are reported to play a defensive role by shielding *P. aeruginosa* from the defense mechanism of its

hosts through hindering macrophages phagocytosis and lysis of polymorphonuclear neutrophils (Gdaniec et al., 2021). The outcomes of the present investigation suggest the potential use of RL BS in therapeutics in addition to its typical bioremediation applications. Moreover, antimicrobial investigations are crucial for understanding the potential adverse effects of biosurfactants on other microorganisms residing in contaminated settings during bioremediation applications.

4.9.2. Phytotoxicity assessment

Evaluation of the toxicity induced by BSs on plants is a crucial and critical step that must be undertaken before implementing bioremediation applications. This evaluation helps to determine whether the BSs might adversely affect plant health, growth or productivity when introduced into the environment at the time of bioremediation process. Through identification of any potential phytotoxic effects, researchers can ensure that the bioremediation process is not only effective in cleaning up contaminants but also safe for surrounding vegetation (Gidudu and Chirwa, 2022). This precautionary approach ensures ecological balance and supports sustainable environmental management practices. The results from the study indicated that the synthetic surfactant which exhibited notable phytotoxicity while the BS did not induce consequential phytotoxicity towards the *Vigna radiata* seeds at CMC and below CMC concentrations. However, at higher concentration of BS (above CMC), it induced some phytotoxicity to the *V. radiata* seeds which is evident by the lower germination index of 52.7 %. Nevertheless, compared to synthetic surfactant SDS, phytotoxicity of BS to *V. radiata* seeds is quite low at concentration above CMC. Similar results were report by Santos et al. (2017) where a BS produced by *Candida lipolytica* showed continuous decrease in germination index when exposed to *Brassica oleracea* var. *botrytis L.*, *Brassica oleracea* var. *capitata*, and *Lactuca sativa* L. seeds with increase in concentration of the BS.

4.9.3. Larvicidal activity

The BS showed a LC_{50} concentration of 592.42 µg/mL. Similar results have been reported by Silva et. (2010) where a BS produced by *P. aeruginosa* was tested for its toxicity against brine shrimp and showed a LC_{50} value of 525 mg/L after 24 hours. Diab et al. (2020) also reported a BS produced by *P. aeruginosa* with a LC_{50} value of 100 ppm against *A. salina* larvae after 24 hours and observed that the LC_{50}

value of the BS was significantly reduced when the concentration was reduced to 5 %. All these reports demonstrate the low toxic nature of BSs. However, they can also be an effective biocontrol agent against various unwanted disease-causing pests (Silva et al., 2015). Sabarinathan et al. (2021) reported that BS produced by *Pseudomonas plecoglossicida* BP03 showed LC_{50} value ranging from 62.983 ppm to 99.480 ppm against different stages of *A. sunadicus* larva highlighting its potential larvicidal activity. Harikrishnan et al. (2023) also reported a BS derived from *Enterobacter cloacae* with an LC_{50} value of 26.49 mg/L against mosquito larvae, *Culex quinquefasciatus* demonstrating it to be an effective biocontrol agent. Fernandes et al. (2020) also reported a BS from *Wickerhamomyces anomalus* CCMA 0358 with 100 % mortality rate against *Aedes aegypti* larvae in 24 hours. The interaction of BSs with the hydrophobic region of the respiratory siphon enhances the larvae's exposure to the aqueous environment by facilitating the penetration of water into their spiracular cavity. Furthermore, the presence of BSs influences the tracheal structures located near the water's surface, thereby assisting the larvae in ascending for respiration. The presence of BS causes a significant reduction in ST and consequently, the larvae lose their ability to remain buoyant on the water surface causing them to sink to the tank's bottom. This displacement disrupts hydrostatic equilibrium, imposes excessive energy demands and ultimately results in mortality due to drowning (Harikrishnan et al., 2023). Thus, the result from the study indicates that application of BS at lower concentration may not possess any detrimental effect on the biotic component of the environment during bioremediation. However, at higher concentration, it might exhibit selective toxicity towards certain organisms.

4.9.4. Antibiofilm activity

Biofilms are complex three-dimensional structures composed of heterogeneous microbial populations which are anchored to a surface through a self-produced matrix of extracellular polymeric substances (EPS) and often causes harmful contamination to various medical equipment such as catheters and pacemakers leading to infections and related medical complications (Yamasaki et al., 2020). From the result obtained, a progressive reduction in optical density (OD) was observed with increasing concentrations of the BS which indicates a dose dependent inhibitory effect on biofilm formation and activity. The decrease in the OD indicates that the BS affects the formation of biofilm by interfering with the ability of the bacterial cells to adhere to

surfaces and hindering to establish a robust biofilm matrix (Al-Razn et al., 2021). Moreover, at higher concentrations, the BS may even disrupt the structural integrity of the EPS which are critical for biofilm stability and maintenance. Sen et al. (2020) also reported a dose dependent antibiofilm activity form RL BS against two dermatophytic fungi and was able to successfully disrupt the mature biofilms of the pathogens highlighting its potential antibiofilm property. Biofilms also plays an important role in the degradation of organic pollutants owing to their eco friendliness, cost effectiveness and sustainability. The efficacy of microbial bioremediation within biofilms is largely attributed to the presence of diverse functional groups on the biofilm matrix which enhances the biodegradation process (Ali et al., 2023). The results verified that the biosurfactant had a dose dependent inhibitory effect on the biofilm. Hence, the biofilm forming ability of beneficial bacterial species associated with the remediation of pollutants present in the polluted environment will not be directly harmed by the addition of BS at concentration around its CMC during the bioremediation.

4.9.5. Cytotoxicity assessment

In order to improve the degradation of the pollutant, BSs are generally applied to the contaminated environment throughout the bioremediation process. Humans or animals adjacent to or involved with such a contaminated environment are therefore at a high risk of being exposed to the applied BS. To verify the safety of BSs application, it is essential to ascertain their cytotoxicity and the cellular stress that results from exposure to them. *P. aeruginosa* species are known for producing a wide array of bacterial metabolites such as exotoxins that frequently inflicts negative impact to the host organisms and often bring about numerous epidemic diseases (Patowary et al., 2016). BSs in general are reported to be less toxic towards living cells and more biodegradable in nature as compared to their chemical counterpart (Ferreira et al., 2017). A compound can be regarded as nontoxic in nature if it shows a cell viability of more than 80 % (Patowary et al., 2019). The viability of rat primary liver cells against the RL BS treatment produce by the selected *P. aeruginosa* AMS1a strain was found to be over 97 % in all the different concentration used. Additionally, it was confirmed that there was no substantial cellular oxidative stress ($p < 0.05$) even at concentration of 100 µg/L which implies the benign nature towards living cell and can be a non-toxic agent. Non cytotoxic nature of RLs towards mouse fibroblast cells has been already reported through several studies (Bharali et al., 2018; Patowary et al.,

2019). However, it has also been reported that at higher concentration of RLs, it can exhibit cytotoxic effects on living cells (Stipcevic et al., 2005). Depending on the chemical nature, RLs exhibits varying levels of cytotoxicity on living cells. It has been reported that mono-RLs do not induce cytotoxicity towards human keratinocyte even at higher concentration of 300 µg/L while di-RL can induce cytotoxicity at concentrations above 40 µg/L (Adu et al., 2023) The findings of Andreadou et al. (2016) suggested that exposure of lymphocytes to RLs can cause chromosomal fragility and may also lead to chromosomal aberrations. Haussler et al. (1998) previously reported that RL showed a time and concentration reliant cytotoxicity against nonphagocytic and phagocytic cells. In this regard, the cytotoxicity of RLs at higher concentration as well as the type of RL used, can prove to be an effective anti-cancer agent in the biomedical field (Sanjivkumar et al., 2021). Additionally, RLs can prove to be a safe and non-cytotoxic remediating agent for bioremediation of various environmental pollutants.

4.9.6. Binding affinity studies of RL with Monkeypox virus protein

BSs are known for their antiviral and therapeutic properties against viruses such as human immunodeficiency virus (HIV), zika virus, herpes simplex virus (HSV), coronavirus, respiratory syncytial virus (RSV) (Almuhayawi et al., 2024; Cerqueira dos Santos et al., 2024) and even against viral plant pathogen such as telosma mosaic virus (Yang et al., 2024). However, there are no specific scientific reports of the use of RLs or BS in general as antiviral agent against Monkeypox virus (MPXV) till date. Mpox is a contagious disease caused by the MPXV, a rare zoonotic pathogen that was initially identified in 1958 in a laboratory of primates in Denmark. MPXV is distinguished by its large enveloped structure and double stranded DNA with a genome approximately 197 kb in length (He et al., 2023). It is a part of the Poxviridae family and belongs to the genus ortho poxvirus (Azari et al., 2024). The reemergence of the MPXV in 2022 raised serious concerns about the potential onset of a new pandemic and in response to the unexpected surge of Mpox cases outside of Africa, the WHO declared it a public health emergency in July 2022 (Bhardwaj et al., 2024). At present, there are no specific and effective antiviral therapeutics available for treatment and prevention of Mpox. However, vaccines such as MVA-BN (JYNNEOSTM), LC16 and ACAM2000 are currently used with limited adoption owing to potential adverse side effects (Loganathan et al., 2024).

Ortho poxviruses, including MPXV, replicate in the cytoplasm rather than the nucleus of infected cells. The virus enters the host cells after initially attaching to the cell surface. This attachment occurs through interactions between viral ligands and cell surface receptors such as chondroitin sulfate (Loganathan et al., 2024). Vaccinia virus (VACV) and also known to be genetically similar to MPXV. A number of studies on MPXV employ VACV models because of their genetic similarity (Shchelkunova and Shchelkunov, 2022). The Glycosaminoglycan (GAG) binding proteins A27, H3 and D8 are found in VACV. It has been reported that the VACV uses the proteins A27 and H3 for interaction with heparan sulphate and the D8 protein to interact with chondroitin sulphate. The deletion of D8 protein has been found to significantly disrupt the GAG mediated attachment of mature virus particles to the cell surface (Chaudhuri, 2024). This is because the interaction between D8 and chondroitin sulfate is essential for both the attachment of the virus to the cell surface and the entry of the mature virus particle into the host cell through the fusion of the host cell membrane with the virion membrane that takes place at low pH in case of MPXV (Matho et al., 2014). The E8L protein of MPXV is an ortholog of the D8 protein and shares a high degree of sequence and structural similarity with the D8 protein of VACV. This similarity suggests that E8L performs a similar function making it a promising target for therapeutic intervention (Chaudhuri, 2024). The purpose of the investigation was to ascertain whether the RLs could bind to the active sites of chondroitin sulphate by docking them inside the active pockets of the cell surface binding protein OPG105 of MPXV. To achieve this, RLs and other viral drugs currently used in the treatment of MPXV were docked to determine whether these ligands were able to bind on the active sites of chondroitin sulphate. Results from the docking studies revealed that the RLs bind exceptionally well with the receptor protein of virus as compared to chondroitin sulphate and other standards used which presents a promising potential application of RLs as a green therapeutic against ortho poxviruses such as Mpox virus. Though, a little is known about bacteriophages, the function of viruses in bioremediation is still unknown. Therefore, this might be a domain for further study.

4.10. Bioremediation application

4.10.1. Soil washing experiment

The percentage of crude oil removed from the contaminated sand by the CFCS was found to relatively higher than that of the synthetic surfactant (SDS). Similar

findings with efficient crude oil removal capacity by a RL produced by *P. aeruginosa* has been reported in previous studies (Urum and Pekdemir, 2004; Aparna et al., 2012; Pourfadakari et al., 2020). This shows that the BS from *P. aeruginosa* is highly effective in crude oil removal and can be an efficient alternative for bioremediation of hydrocarbon oil contamination. The removal of crude oil from contaminated soil in the presence of BS can be explained by two proposed mechanisms; mobilization and solubilization. Mobilization occurs when the surfactant concentration is below the CMC. In this phase, the capillary forces, surface and interfacial tension, contact angle and wettability are reduced. Below the CMC concentrations, surfactants lower the surface and interfacial tension between water, oil, air and soil systems. When surfactants interact with the oil in the soil, they increase the contact angle and reduce the capillary forces that hold the oil to the soil by decreasing the interfacial tension. The mobilization step also depends on the ionic charge of the surfactant, as surfactants adsorb onto soil. This adsorption can lead to a reduction in surfactant concentration, making it less effective or even ineffective for soil treatment. When the concentration rises above the CMC, the solubility of the oil increases greatly due to the formation of surfactant micelles. These micelles have hydrophobic ends that cluster inside and hydrophilic ends that face the water. This structure provides a suitable environment for hydrophobic organic molecules, a process referred to as solubilization (Urum et al., 2004). Thus, it can be concluded that the main mechanism involved in the removal of crude oil by RL in the current study was greatly attributed to the mobilization phenomenon as there was no substantial increase in the oil removal capacity at concentrations above CMC. Gaur et al. (2021) demonstrated the excellent oil recovery capacity of BS produced by *P. aeruginosa* from soil contaminated with engine oil through centrifugation at 6000 rpm for 20 minutes. Bharali et al. (2022) also conducted a study on the efficiency of BSs produced by four different strains of *P. aeruginosa* to recover residual crude oil from petroleum sludge and reported that the BSs were able to recover about 63.4 to 73.5 % of residual oil from the sludge.

4.10.2. Crude oil degradation

The crude oil degradation potential of the bacterium was confirmed by the GC-MS analysis. Selected complex and medium to long chain hydrocarbons are broken to simpler and shorter compounds during the degradation process. As a result of the utilization of the complex mixture of hydrocarbon as the sole carbon source,

generation of bacterial by-products can be observed during the entire degradation process of 60 days leading to the degradation and formation of new compounds (*Appendix-I*). Additionally, degradation of the large hydrocarbon molecules leads to their breakage and results in the generation of several smaller molecules which further serves as precursors for formation of other complex and stable compounds. It is also evident from the GC-MS data that the bacterium was unable to breakdown the complex and highly branched hydrocarbons such as Pentadecane,2,6,10-trimethyl; Heptadecane,2,6,10,14-tetramethyl; Heptadecane,2,6,10,15-tetramethyl; Tetradecane,2,6,10-trimethyl-; Dodecane, 2,6,10-trimethyl; Octadecane, 3-ethyl-5-(2-ethylbutyl); Heptadecane,9-hexyl; Tricyclo[7.4.1.1(2,7)]pentadeca-2,4,6,9,11,13-hexaene-8-ol; 10-Acetoxy-2-hydroxy-1,2,6a,6b,9,9,12a-heptamethyl-1,3,4,5,6 etc, even after a period of 60 days. From the previous studies, it has been well established that every bacterial strain has its limitations where it can degrade only a selected number or size of hydrocarbons (Rehman et al., 2021). A multitude of variables contributes to this constraint. This restriction is the result of many reasons. Primarily, crude oil is made up of a wide variety of hydrocarbons with unique chemical structures and traits, making the composition extremely complicated. Secondly, nutrient availability and environmental variables can influence the efficacy of bacterial decomposition. For instance, some hydrocarbons may be more susceptible to bacterial enzymes, whereas others may exhibit greater resistance to breakdown due to their chemical characteristics or spatial configuration within the oil matrix. Moreover, toxic chemicals in crude oil including heavy metals and aromatic and polyaromatic compounds can impede bacterial growth and catalytic activity thereby restricting their capacity to completely breakdown the oil (Chuah et al., 2023). Hence, for effective degradation of crude oil components its it is preferred to use consortium of bacteria with different degradation potential (Primeia et al., 2020).

4.10.3. BS mediated removal of heavy metal

The results of the CFCS mediated removal of arsenite highlights the superior efficacy of the RL BS in promoting the desorption and removal of arsenite from sand matrices compared to the synthetic surfactant and water alone. The findings also confirm that the BS has the highest efficient in mobilizing arsenite from polluted sand at sub CMC levels. This indicates that raising the concentration of RL BS above the CMC does not relate to improved arsenite removal. In fact, the effectiveness seems to

slightly reduce at above CMC concentrations with the lowest removal efficiency observed of 79.5 ± 6.5 %. Such behaviour may be attributed to the micelle saturation or surfactant aggregation effects that hinder additional solubilization or mobilization of arsenite at higher BS concentrations. Anionic BSs such as RLs interacts with positively charged heavy metal ions in the soil to form metal BS complexes via ionic bonds. These ionic bonds are comparatively much stronger than the bond between the metal and the soil. Thus, the metal BS complex is desorbed from the soil into the solution during the process of washing due to the reduction of interfacial tension and is flushed out from the soil (Pacwa-Płociniczak et al., 2011; Santos et al., 2016). During remediation process, as the concentration of RL increases, the number of H^+ increases due to the continuous ionization of the carboxylic and hydroxylic groups. Ultimately, the metal and RL having stronger attractive force pulls the metal ions from the soil surface and forms the complex (Dahrazma, 2005). RLs are also capable of removing the anionic metals or oxoanions like arsenic/chromium from soil particles, by substituting the anionic metals from the adsorption sites, increasing the electrostatic repulsion between soil sediments and anionic metal, thereby mobilizing the metal ions (Wang and Mulligan, 2009b).

4.10.4. Effect of pH and salinity on heavy metal removal

Anionic biosurfactants like RLs can form chelating compounds with the positively charged heavy metal ions due to their complexation ability (Santos et al., 2016; Mulligan, 2021). However environmental factors such as salinity and pH may influence the performance of BS mediated bioremediation of heavy metals. In the sand washing experiment under varying salinity range of 0.5 % to 2 %, the BS at CMC showed a maximum arsenite removal efficacy of 89.9 % ± 10 at 2 % salinity. It can also be observed that the arsenite removal efficiency was relatively consistent in the range of 78.9 % to 79.7 % at salinity levels below 2 %. This increase in removal efficacy at higher salinity may be due to the addition of salt ions which causes a reduction in the electrostatic repulsion between the charged head groups of the RL molecules thus allowing the molecules to pack more closely together leading to the formation of larger aggregates with unique and specialized RL structures (Chen and Lee, 2022) which might result in increased interaction with the metal ion. In the soil washing experiment under a pH range of 3 to 10, a gradual decrease in the removal efficacy of the BS at CMC was observed with the increase in pH. Among the four

different pH condition, the lowest removal efficacy was seen at the highest pH vale of 10. This might be because, the pH of the solution can greatly influence the complexation of BS with the heavy metal ion as it plays a key role in determining the self-assembly behaviour and structural organization of RLs (Champion et al., 1995). Additionally, increased level of pH of the solution has been reported to reduce interfacial tension (Lin et al., 1987) which might play a role in enhancing the removal efficacy of the BS. In contrast, Zhang and Miller (1992) reported a significant decrease in surface activity of RL with decrease in pH which resulted in the increase in ST reduction from 30 mN/m to 40 mN/m.

4.11. Valorisation of WRCO as alternate carbon source for biosurfactant production.

4.11.1. Production of BS

Given the notably high production cost of RLs, it is crucial to identify sustainable and affordable feedstocks that can enhance yield. One promising approach is the utilization of waste materials from the agriculture and food industries, particularly waste residual cooking oil (WRCO), which is commonly discarded as waste. During deep frying, oxidation occurs more rapidly than hydrolysis, leading to the formation of hydroperoxides and variety of low molecular weight volatile compounds such as short-chain alkanes, alkenes, carboxylic acids, ketones and aldehydes (Choe and Min, 2007). These compounds present in WRCO can serve as viable carbon sources due to the adaptability of *P. aeruginosa* to diverse and complex hydrocarbons. A clear indication of BS production in the presence of WRCO was observed through the gradual decrease in ST of the culture medium from 72 mN/m to approximately 34.3 mN/m over a 10 day incubation period. Interestingly, the growth pattern of *P. aeruginosa* strain AMS1a differed when using WRCO compared to n-hexadecane with a slightly lower reduction in ST of water and CMC. This may be attributed to the varied types and proportions of hydrophobic compounds present in WRCO in contrast to the uniform composition of pure n-hexadecane. These findings suggest that the selection of carbon sources for RL biosynthesis appears to be predominantly strain dependent (Wu et al., 2008; Panesar et al., 2009). In addition, RL production is significantly affected by various culture conditions such as temperature, ionic strength, agitation and the concentration of the carbon substrate. Previous studies (Lang and Wullbrandt, 1995; Henkel et al., 2012) have highlighted that both the

quantity and nature of BSs produced are influenced by the type of carbon source used. Research by Salihu et al. (2009) and Saharan et al. (2011) indicates that temperature also affects bacterial physiology, thereby influencing BS synthesis. Wei et al. (2005) and Chen et al. (2007) found that optimal RL production by *P. aeruginosa* strains occurred within the 30 to 37 °C range, with reduced production at higher temperatures. Reports indicate that different strains of *P. aeruginosa* can produce RL across a broad temperature range of 28 to 40 °C (Müller et al., 2011; Saharan et al., 2011; Henkel et al., 2012), reflecting physiological diversity among strains. Leahy et al. (1990) reported that using hydrocarbons at lower concentrations mitigates toxicity, prevents enzyme deactivation and reduces oxygen limitation. Furthermore, pH plays a vital role in determining the behaviour of surface-active compounds (Silva et al., 2010). According to Yateem et al. (2002), RL molecules with a pKa of 5.6 were at least 50 % uncharged in acidic conditions (pH < 6.0) but as pH increased beyond 6.8, the molecules acquired a negative charge enhancing their surface activity. Cunha et al. (2004) observed that increasing the agitation speed during the cultivation of *Serratia* sp. SVGG16 on ethanol blended gasoline adversely affected the reduction in ST achieved by the produced BSs.

4.11.2. Physicochemical characterization

The observed ST value of the BS produced using WRCO was found to be slightly better than that obtained with n-hexadecane. According to previous reports, the CMC of RLs typically ranges from 10 to 200 mg/L attributed largely on factors such as the bacterial strain, carbon source, culture medium composition and other parameters, including temperature, pH and agitation rate (Nitschke et al., 2005). The results of ST and CMC measurements from this study slightly differed from previously reported values (Haba et al., 2000; De Lima et al., 2009; George and Jayachandran, 2013; Lan et al., 2015). This variation may be attributed to the presence of WRCO derived components in the crude RL mixture such as fatty acids, which can associate with RL molecules and persist even after purification, thereby influencing ST and CMC. Additionally, the type of RL produced, relative abundance of individual RL congeners synthesized by different *Pseudomonas* strains and the degree of purity can significantly affect ST, CMC and emulsification activity (Radzuan et al., 2017). As noted by Sabturani et al. (2016), a higher number of RL congeners does not necessarily correlate with a lower CMC. Instead, the specific types of congeners present and the

extent to which each congener contributes to overall surface activity primarily determine the CMC of a BS. Emulsifying capacity is a key characteristic of surfactants. Indicators of surface activity typically include the stabilization of oil–water emulsions in addition to reductions in surface and interfacial tension (Hao et al., 2004). In this study, the CFCS demonstrated clear emulsification activity against different hydrophobic substrates however, the degree of emulsification varied across the different substrates. Previous studies have shown that most microbially produced surfactants exhibit substrate specific effects leading to different rates of hydrocarbon solubilization or emulsification (Etoumi et al., 2007). The ability of the BS to emulsify specific crude oil by-products such as diesel, kerosene and petrol can enhance microbial uptake, which is advantageous for the remediation of crude oil contaminated environments (Maier and Soberon-Chavez, 2000; Abdel-Mawgoud et al., 2009). RLs can further accelerate biodegradation by promoting emulsification (Shao et al., 2017). Additionally, the capacity of BSs to emulsify plant-based oils suggests their potential applications in the cosmetics and pharmaceutical industries (Silva et al., 2010). Prior research has also indicated that RLs are predominantly substrate specific, emulsifying or solubilizing various hydrocarbons at different rates (Moussa et al., 2014). Furthermore, Pornsunthorntawee et al. (2008) reported that the carbon source used for RL production significantly affects their emulsification properties.

Both chromatographic and spectroscopic techniques were employed to chemically characterize the isolated BS. The appearance of different spots on the TLC plates at around R_f 0.3, 0.5 and 0.7 indicated the presence of both mono and di-RLs. Column chromatography was used to separate the BS components from the crude extract and the observed separation pattern was consistent with previous findings for RLs isolated from various *P. aeruginosa* strains (Amani et al., 2013; George and Jayachandran, 2013; Thio et al., 2022). IR spectroscopic analysis of the BS revealed adsorption bands characteristic of RLs indicating the presence of rhamnose sugar rings and long fatty acyl chains. Although slight differences were observed in the relative intensities of individual IR bands, the IR spectra of the RL displayed key absorption bands similar to those reported in earlier studies (Lotfabad et al., 2010; Hazra et al., 2011; Moussa et al., 2014). Additional minor bands in the spectra were likely due to the presence of polypeptides or polysaccharides, potentially carried over from cellular debris during the extraction process (Bharali et al., 2018). ESI-MS confirmed the presence of mono and di RLs with varying fatty acyl chains. These results are in

agreement with previous studies, which identified mono RLs at 499.2 and 527.3 m/z (Ndlovu et al., 2017). Similarly, Lan et al. (2015) reported that BSs produced by *Pseudomonas* SWP-4 using waste cooking oil contained both mono and di RLs corresponding to Rha–Rha–C_{10} and Rha–Rha–C_{10}–C_{10} respectively. Variations in RL congener ratios and the predominance of specific congeners have been shown to be influenced by factors such as the carbon source, culture conditions, fermentation duration and the specific *P. aeruginosa* strain used (Aparna et al., 2012; Sabturani et al., 2016). Furthermore, XRD analysis revealed a turbostratic pattern confirming the amorphous nature of the extracted BS consistent with earlier reports (Chandankere et al., 2014; Ahmad et al., 2021).

4.11.3. Soil washing experiment

In the washing experiment, BS produced using WRCO achieved a crude oil removal efficiency of 71.87 to 89.87 % across different concentrations. However, the addition of BSs at concentrations above the CMC did not significantly improve crude oil removal from contaminated sand. This behaviour can be explained based on interfacial tension (IFT) and capillary forces that exist between sand particles and crude oil. As IFT between the sand and oil decreases, the capillary forces binding them are reduced. The reduction in IFT increases the contact angle between oil and soil particles, thereby altering the system's wettability. Consequently, crude oil is mobilized from the sand oil mixture into the aqueous phase. This behaviour is strongly associated with BS concentration up to the CMC (Desai and Banat, 1997). Variations in oil removal efficiency observed with BS from different bacterial strains indicate that oil and sand separation depend not only on the physicochemical properties of the BS but also on the combined interactions of the surfactant, crude oil and sand (Urum and Pekdemir, 2004). Pi et al. (2017) reported that RLs significantly enhance hydrocarbon solubilization and desorption which may facilitate microbial degradation of hydrocarbon pollutants. Previous studies have shown that crude RLs can be directly applied in the bioremediation of various contaminants including petroleum hydrocarbons, heavy metals and pesticide residues without the need for purification (Shen et al., 2016; Chen et al., 2017; Radzuan et al., 2017). Although synthetic surfactants such as SDS can also remove crude oil from contaminated sand however they are more persistent than petroleum hydrocarbons making them potentially toxic to the environment and can generate secondary contaminants (Desai and Banat, 1997;

Christofi and Ivshina, 2002; Urum and Pekdemir, 2004). Furthermore, strict environmental regulations have increased the demand for safer and more sustainable alternatives. The results of this study demonstrate the potential of RLs including their crude form for the effective removal of crude oil from soil highlighting their applicability in bioremediation. Zeng et al. (2007) compared RLs with synthetic surfactants such as CTAB, Triton X-100 and SDS and found notable differences in biodegradability and toxicity. Unlike synthetic surfactants, RLs were shown to be non-toxic and biodegradable by *Bacillus subtilis* and other compost microorganisms. Additionally, Kumar et al. (2015) reported that RLs mitigated the toxic effects of petroleum hydrocarbons in polluted soil, thereby promoting plant growth. Similarly, Varjani and Upasani (2016) demonstrated that RLs produced by *P. aeruginosa* NCIM 5514 were capable of mobilizing crude oil, indicating their potential role in microbial enhanced oil recovery (MEOR) processes.

Chapter 5. Summary and Conclusion

The present study reports successful isolation, characterization and taxonomic identification of a novel hydrocarbonoclastic bacterial strain, *Pseudomonas aeruginosa* (AMS1a) from petroleum contaminated terrestrial sediment around an automobile repair shop in Mokokchung Town, Nagaland, India. To the best of our knowledge, this is the first description of a naturally occurring indigenous hydrocarbonoclastic bacterium that produces biosurfactant (BS) from the Indian state of Nagaland. The strain was identified as a potent hydrocarbonoclastic bacterium possessing proficient oleophilic trait and high BS production potential. The ability to grow on complex hydrocarbon mixtures as sole source of carbon and energy demonstrates its metabolic adaptability and ecological competence to xenobiotic laden environments. Preliminary screening indicated the competence of AMS1a strain for effective surface activity through the *Du Noüy* ring method. Its BS producing ability was screened using standard assays *viz*. reduction of surface tension, oil displacement, drop collapse test, penetration assay, CTAB and haemolysis assay. The cell free culture supernatant of the strain could reduce the surface tension of distilled water from an initial value of 72 mN/m to 34.4 mN/m and it formed stable oil-in-water (O/W) emulsions with different test–hydrophobic substrates, which clearly indicates the presence of a highly surface-active amphiphilic extracellular metabolite. Further, BATH assay evidently supports the oleophilic responsiveness and BS production potentiality of the AMS1a strain in the presence of complex hydrophobic carbon feedstock.

The chemical structure of the BS was established by an integrated analytical approach comprising thin layer chromatography (TLC), column chromatography, fourier transform infrared spectroscopy (FTIR), nuclear magnetic resonance spectroscopy (^{1}H and ^{13}C NMR) and liquid chromatography coupled with tandem mass spectrometry (LC-MS/MS). The BS was identified by these analyses to be a heterogeneous mixture of mono-rhamnolipids (mono-RLs) and di-rhamnolipids (di-RLs), characteristic of glycolipids that are normally secreted by *Pseudomonas aeruginosa* species. FTIR spectrum showed neat absorption bands for ester and hydroxyl functional groups, and NMR spectra for rhamnose sugar moieties and fatty acid chains. LCMS-MS profiling showed molecular ion peaks for disparate RL congeners, further confirming the structural diversity of the BS. The amorphous nature

of the isolated BS was revealed through XRD diffractogram and its anionic nature was further confirmed through Zeta potential analysis. TGA and DSC analysis highlighted the high thermal stability of the BS with a residual mass of 63.33 % at 500 °C.

The BS from AMS1a strain exhibited strong surface activity with structural stability and functionality against the broad range of physicochemical parameters. Stability tests determined the resilience of the BS to extreme conditions of the environment, such as broad temperature ranges (4–121°C), pH ranges (3–11), high salinity (2-10 % NaCl) and exposure to heavy metal ions like arsenite, cadmium, and lead. Such physicochemical stability indicates the potential application of the BS at the commercial scale in industries requiring sturdy and enduring surface-active agents, such as petroleum recovery, environmental remediation, pharmaceuticals, food processing and cosmeceuticals. Furthermore, the RL isolated from AMS1a strain proved its non-toxic nature in both the *in vitro* and *in vivo* experiments and highlighted its promising potential in bioremediation applications, particularly in the biodegradation of petroleum hydrocarbons and the removal of heavy metals such as arsenite from contaminated soils via soil washing techniques. Additionally, molecular docking analyses revealed promising antiviral potential, particularly due to the exceptional binding affinity of Rha-Rha-C_{10}-$C_{14:1}$ congener against the E8L protein of Monkeypox virus (MPXV) as compared to chondroitin sulphate and other standards used in the study which presents a promising potential application of RLs as therapeutics against Ortho poxviruses such as MPXV.

Despite its great bio-functional properties, BS production on a laboratory scale was suboptimal, limiting its application at industrial level. Although the bacterial strain was able to successfully utilize cheap alternate carbon substrates such as WRCO, production of the BS is inherently complex with many interdependent variables like nutrient availability, carbon source, pH, oxygenation rate, agitation rate and fermentation time. Lack of optimal culture conditions and high cost of downstream processing (extraction and purification) hinders scale-up production to commercial level. A notable limitation of the present study is that, no systematic bioprocess optimization strategy has been exclusively discussed for the maximization of BS production in bioreactor operations. Moreover, the effect of the fermentation condition on the physicochemical characteristics and functional activity of the BS has not been taken into consideration. These are important factors for the design of BS formulations for specific industrial applications and need to be dealt with cautiously

in future research. In addition, the capacity for degradation of crude oil by the bacterial strain was first established with unrefined petroleum as a single carbon substrate, but the catabolic potential of the strain against individual hydrocarbon fractions such as aliphatic hydrocarbons (C_{10}–C_{35}), monocyclic and polycyclic aromatic hydrocarbons (PAHs) and heteroatom containing (NSO) compounds remains to be further studied in detail. Large scale genomic and transcriptomic description would be required to decipher the molecular machinery of hydrocarbon degradation, BS synthesis and stress resistance. This would be capable of enabling the identification of the biosynthetic gene clusters (BGCs), regulatory genes and the major metabolic pathways, thus making rational strain design for enhanced performance possible. Furthermore, the identification of the substrate specificity and degradation kinetics of the strain will be important to the design of targeted bioremediation strategies and to interpretation of ecological interactions in petroleum contaminated ecosystems.

Addressing these research gaps will provide an opportunity for the advancement of BS technology. Optimization of the conditions of cultivation (e.g., use of statistical design of experiments such as response surface methodology), discovery of low cost and sustainable feedstocks (e.g., agro-industrial wastes) and novel BS recovery technologies (e.g., foam fractionation, membrane separation, ultrafiltration, electrokinetic extraction etc.) are opportunities for future research. Synthetic biology and metabolic engineering approaches can also be exploited to create recombinant microbials with better yield of BSs, reduced formation of byproducts and engineered functionalities. Lastly, expanding the elementary expertise and technological versatility of microbial mediated BS production is of enormous potential for its incorporation into a wide range of industrial and environmental processes such as green nanomaterial production, biomedical device coatings, antimicrobial products and formulations, and green cleanup systems for polluted terrestrial and aquatic ecosystems.

References:

Abbasi, H., Hamedi, M. M., Lotfabad, T. B., Zahiri, H. S., Sharafi, H., Masoomi, F., ... & Noghabi, K. A. (2012). Biosurfactant-producing bacterium, *Pseudomonas aeruginosa* MA01 isolated from spoiled apples: physicochemical and structural characteristics of isolated biosurfactant. *Journal of Bioscience and Bioengineering*, *113*(2), 211-219.

Abdel-Mawgoud, A. M., Aboulwafa, M. M., & Hassouna, N. A. H. (2008). Characterization of surfactin produced by *Bacillus subtilis* isolate BS5. *Applied Biochemistry and Biotechnology*, *150*, 289-303.

Abdel-Mawgoud, A. M., Aboulwafa, M. M., & Hassouna, N. A. H. (2009). Characterization of rhamnolipid produced by *Pseudomonas aeruginosa* isolate Bs20. *Applied Biochemistry and Biotechnology*, *157*(2), 329-345.

Abdel-Mawgoud, A. M., Lépine, F., & Déziel, E. (2010). Rhamnolipids: diversity of structures, microbial origins and roles. *Applied Microbiology and Biotechnology*, *86*, 1323-1336.

Acharjee, S. A., Bharali, P., Ramachandran, D., Kanagasabai, V., Gogoi, M., Hazarika, S., ... & Vishawkarma, V. (2024). Polyhydroxybutyrate (PHB)-Based sustainable bioplastic derived from *Bacillus* sp. KE4 isolated from kitchen waste effluent. *Sustainable Chemistry and Pharmacy*, *39*, 101507.

Adu, S. A., Twigg, M. S., Naughton, P. J., Marchant, R., & Banat, I. M. (2023). Characterisation of cytotoxicity and immunomodulatory effects of glycolipid biosurfactants on human keratinocytes. *Applied Microbiology and Biotechnology*, *107*(1), 137-152.

Akün, M. E. (2020). Heavy metal contamination and remediation of water and soil with case studies from Cyprus. In *Heavy Metal Toxicity in Public Health*. IntechOpen.

Alaidaroos, B. A. (2023). Advancing eco-sustainable bioremediation for hydrocarbon contaminants: challenges and solutions. *Processes*, *11*(10), 3036.

Al-Ansari, M. M., Benabdelkamel, H., AlMalki, R. H., Rahman, A. M. A., Alnahmi, E., Masood, A., ... & Choi, K. C. (2021). Effective removal of heavy metals from

industrial effluent wastewater by a multi metal and drug resistant *Pseudomonas aeruginosa* strain RA-14 using integrated sequencing batch reactor. *Environmental Research*, *199*, 111240.

Ali, A., Zahra, A., Kamthan, M., Husain, F. M., Albalawi, T., Zubair, M., ... & Noorani, M. S. (2023). Microbial biofilms: applications, clinical consequences, and alternative therapies. *Microorganisms*, *11*(8), 1934.

Ali, H., Khan, E., & Ilahi, I. (2019). Environmental chemistry and ecotoxicology of hazardous heavy metals: environmental persistence, toxicity, and bioaccumulation. *Journal of Chemistry*, *2019*(1), 6730305.

Allred, R. C., DeGray, R. J., Edwards, R. W., Hedrick, H. G, Klemme, D. E., Rogers, M., Wulf, M., & Hodge, H, SIM Special Publications 1963, 1.

Almuhayawi, M. S., Elshafey, N., Hagagy, N., Selim, S., Al Jaouni, S. K., Sofy, A. R., ... & Elnosary, M. E. (2024). Exploring biosurfactant from *Halobacterium jilantaiense* as drug against HIV and zika virus: fabrication, characterization, cytosafety property, molecular docking, and molecular dynamics simulation. *Frontiers in Bioengineering and Biotechnology*, *12*, 1348365.

Al-Razn, R. S., & Abdul-Hussein, Z. R. (2021). Anti-biofilm activity of rhamnolipid extracted from *Pseudomonas aeruginosa*. *Annals of the Romanian Society for Cell Biology*, *25*(6), 1731-1743.

Al-Tahhan, R. A., Sandrin, T. R., Bodour, A. A., & Maier, R. M. (2000). Rhamnolipid-induced removal of lipopolysaccharide from Pseudomonas aeruginosa: effect on cell surface properties and interaction with hydrophobic substrates. *Applied and Environmental Microbiology*, *66*(8), 3262-3268.

Amani, H., Müller, M. M., Syldatk, C., & Hausmann, R. (2013). Production of microbial rhamnolipid by *Pseudomonas aeruginosa* MM1011 for ex situ enhanced oil recovery. *Applied Biochemistry and Biotechnology*, *170*(5), 1080-1093.

Andrä, J., Rademann, J., Howe, J., Koch, M., Heine, H., Zähringer, U. & Brandenburg, K. (2006). Endotoxin-like properties of a rhamnolipid exotoxin from *Burkholderia (Pseudomonas) plantarii*: immune cell stimulation and biophysical characterization. *Biological Chemistry*, 387(3), 301-310.

Andreau, K., Leroux, M., & Bouharrour, A. (2012). Health and cellular impacts of air pollutants: from cytoprotection to cytotoxicity. *Biochemistry Research International*, *2012*(1), 493894.

Anetor, G. O., Nwobi, N. L., Igharo, G. O., Sonuga, O. O., & Anetor, J. I. (2022). Environmental pollutants and oxidative stress in terrestrial and aquatic organisms: examination of the total picture and implications for human health. *Frontiers in Physiology*, *13*, 931386.

Aparna, A., Srinikethan, G., & Smitha, H. (2012). Production and characterization of biosurfactant produced by a novel Pseudomonas sp. 2B. *Colloids and Surfaces B: Biointerfaces*, *95*, 23-29.

Arathi, A., Akhil, V., & Mohanan, P. V. (2021). Application of biosurfactants in the disruption of cell biomass. In *Green sustainable process for chemical and environmental engineering and science* (pp. 317-328). Elsevier.

Arkhipov, V. P., Arkhipov, R., & Filippov, A. (2023). Rhamnolipid biosurfactant: use for the removal of phenol from aqueous solutions by micellar solubilization. *ACS Omega*, *8*(33), 30646-30654.

Arutchelvi, J., & Doble, M. (2010). Characterization of glycolipid biosurfactant from *Pseudomonas aeruginosa* CPCL isolated from petroleum-contaminated soil. *Letters in Applied Microbiology*, *51*(1), 75-82.

Asfora Sarubbo, L., Moura de Luna, J., & de Campos-Takaki, G. M. (2006). Production and stability studies of the bioemulsifier obtained from a new strain of *Candida glabrata* UCP 1002. *Electronic journal of Biotechnology*, *9*(4), 0-0.

Azari, P. P., Rukerd, M. R. Z., Charostad, J., Bashash, D., Farsiu, N., Behzadi, S., ... & Nakhaie, M. (2024). Monkeypox (Mpox) vs. Innate immune responses: Insights into evasion mechanisms and potential therapeutic strategies. *Cytokine*, *183*, 156751.

Banat, I. M., Franzetti, A., Gandolfi, I., Bestetti, G., Martinotti, M. G., Fracchia, L., ... & Marchant, R. (2010). Microbial biosurfactants production, applications and future potential. *Applied Microbiology and Biotechnology*, *87*, 427-444.

Barathi, S., & Vasudevan, N. (2001). Utilization of petroleum hydrocarbons by Pseudomonas fluorescens isolated from a petroleum-contaminated soil. *Environment International*, *26*(5-6), 413-416.

Behrens, B., Engelen, J., Tiso, T., Blank, L. M., & Hayen, H. (2016). Characterization of rhamnolipids by liquid chromatography/mass spectrometry after solid-phase extraction. *Analytical and Bioanalytical Chemistry*, *408*(10), 2505-2514.

Bekele, G. K., Gebrie, S. A., Mekonen, E., Fida, T. T., Woldesemayat, A. A., Abda, E. M., ... & Assefa, F. (2022). Isolation and characterization of diesel-degrading bacteria from hydrocarbon-contaminated sites, flower farms, and soda lakes. *International Journal of Microbiology*, *2022*(1), 5655767.

Benincasa, M., & Accorsini, F. R. (2008). *Pseudomonas aeruginosa* LBI production as an integrated process using the wastes from sunflower-oil refining as a substrate. *Bioresource Technology*, *99*(9), 3843-3849.

Bergey, D. H. (1994). *Bergey's manual of determinative bacteriology*. Lippincott Williams & Wilkins.

Bharali, P., & Konwar, B. K. (2011). Production and physico-chemical characterization of a biosurfactant produced by *Pseudomonas aeruginosa* OBP1 isolated from petroleum sludge. *Applied Biochemistry and Biotechnology*, *164*, 1444-1460.

Bharali, P., Bashir, Y., Ray, A., Dutta, N., Mudoi, P., Alemtoshi, ... & Konwar, B. K. (2022). Bioprospecting of indigenous biosurfactant-producing oleophilic bacteria for green remediation: an eco-sustainable approach for the management of petroleum contaminated soil. *3 Biotech*, *12*(1), 13.

Bharali, P., Das, S., Ray, A., Pradeep Singh, S., Bora, U., Kumar Konwar, B., ... & Sahoo, D. (2018). Biocompatibility natural effect of rhamnolipids in bioremediation process on different biological systems at the site of contamination. *Bioremediation Journal*, *22*(3-4), 91-102.

Bharali, P., Singh, S. P., Dutta, N., Gogoi, S., Bora, L. C., Debnath, P., & Konwar, B. K. (2014). Biodiesel derived waste glycerol as an economic substrate for biosurfactant production using indigenous *Pseudomonas aeruginosa*. *RSC Advances*, *4*(73), 38698-38706.

Bhardwaj, P., Sarkar, S., & Mishra, R. (2024). Mpox and related poxviruses: A literature review of evolution, pathophysiology, and clinical manifestations. *Asian Pacific Journal of Tropical Biomedicine*, *14*(8), 319-330.

Bhatt, A. K., Bhatia, R. K., & Bhalla, T. C. (Eds.). (2023). *Basic biotechniques for bioprocess and bioentrepreneurship*. Academic Press.

Bialy, H. E., Gomaa, O. M., & Azab, K. S. (2011). Conversion of oil waste to valuable fatty acids using oleaginous yeast. *World Journal of Microbiology and Biotechnology*, *27*(12), 2791-2798.

Biktasheva, L., Gordeev, A., Selivanovskaya, S., & Galitskaya, P. (2022). Di-and mono-rhamnolipids produced by the *Pseudomonas putida* PP021 isolate significantly enhance the degree of recovery of heavy oil from the Romashkino Oil Field (Tatarstan, Russia). *Processes*, *10*(4), 779.

Bodour, A. A., & Miller-Maier, R. M. (1998). Application of a modified drop-collapse technique for surfactant quantitation and screening of biosurfactant-producing microorganisms. *Journal of Microbiological Methods*, *32*(3), 273-280.

Bordoloi, N. K., & Konwar, B. K. (2008). Microbial surfactant-enhanced mineral oil recovery under laboratory conditions. *Colloids and Surfaces B: Biointerfaces*, *63*(1), 73-82.

Briffa, J., Sinagra, E., & Blundell, R. (2020). Heavy metal pollution in the environment and their toxicological effects on humans. *Heliyon*, *6*(9).

Câmara, J. M. D. D. A., Sousa, M. A. D. S. B., Barros Neto, E. L. D., & Oliveira, M. C. A. D. (2019). Application of rhamnolipid biosurfactant produced by *Pseudomonas aeruginosa* in microbial-enhanced oil recovery (MEOR). *Journal of Petroleum Exploration and Production Technology*, *9*, 2333-2341.

Cameotra, S. S., & Makkar, R. S. (1998). Synthesis of biosurfactants in extreme conditions. *Applied microbiology and Biotechnology*, *50*, 520-529.

Campos, J. M., Montenegro Stamford, T. L., Sarubbo, L. A., de Luna, J. M., Rufino, R. D., & Banat, I. M. (2013). Microbial biosurfactants as additives for food industries. *Biotechnology Progress*, 29(5), 1097-1108.

Cappuccino, J. G., & Sherman, N. (2013). *Microbiology: A laboratory manual*. Pearson Higher Ed.

Cerqueira dos Santos, S., Araújo Torquato, C., de Alexandria Santos, D., Orsato, A., Leite, K., Serpeloni, J. M., ... & Faccin-Galhardi, L. C. (2024). Production and characterization of rhamnolipids by *Pseudomonas aeruginosa* isolated in the Amazon region, and potential antiviral, antitumor, and antimicrobial activity. *Scientific Reports*, *14*(1), 4629.

Champion, J. T., Gilkey, J. C., Lamparski, H., Retterer, J., & Miller, R. M. (1995). Electron microscopy of rhamnolipid (biosurfactant) morphology: effects of pH, cadmium, and octadecane. *Journal of Colloid and Interface Science*, *170*(2), 569-574.

Chandankere, R., Yao, J., Cai, M., Masakorala, K., Jain, A. K., & Choi, M. M. (2014). Properties and characterization of biosurfactant in crude oil biodegradation by bacterium *Bacillus methylotrophicus* USTBa. *Fuel*, *122*, 140-148.

Chang, S. H., Wu, C. H., Wang, S. S., & Lin, C. W. (2017). Fabrication of novel rhamnolipid-oxygen-releasing beads for bioremediation of groundwater containing high concentrations of BTEX. *International Biodeterioration & Biodegradation*, *116*, 58-63.

Chaudhuri, D., Majumder, S., Datta, J., & Giri, K. (2024). Exploring the chemical space for potential inhibitors against cell surface binding protein of Mpox virus using molecular fingerprint based screening approach. *Journal of Biomolecular Structure and Dynamics*, *42*(14), 7160-7173.

Chen, I. C., & Lee, M. T. (2022). Rhamnolipid biosurfactants for oil recovery: Salt effects on the structural properties investigated by mesoscale simulations. *ACS Omega*, *7*(7), 6223-6237.

Chen, Q., Bao, M., Fan, X., Liang, S., & Sun, P. (2013). Rhamnolipids enhance marine oil spill bioremediation in laboratory system. *Marine Pollution Bulletin*, *71*(1-2), 269-275.

Chen, Q., Li, Y., Liu, M., Zhu, B., Mu, J., & Chen, Z. (2021). Removal of Pb and Hg from marine intertidal sediment by using rhamnolipid biosurfactant produced by a

Pseudomonas aeruginosa strain. *Environmental Technology & Innovation*, *22*, 101456.

Chen, S. Y., Lu, W. B., Wei, Y. H., Chen, W. M., & Chang, J. S. (2007). Improved production of biosurfactant with newly isolated *Pseudomonas aeruginosa* S2. *Biotechnology Progress*, *23*(3), 661-666.

Chen, W., Qu, Y., Xu, Z., He, F., Chen, Z., Huang, S., & Li, Y. (2017). Heavy metal (Cu, Cd, Pb, Cr) washing from river sediment using biosurfactant rhamnolipid. *Environmental Science and Pollution Research*, *24*, 16344-16350.

Cheng, T., Liang, J., He, J., Hu, X., Ge, Z., & Liu, J. (2017). A novel rhamnolipid-producing *Pseudomonas aeruginosa* ZS1 isolate derived from petroleum sludge suitable for bioremediation. *AMB Express*, *7*, 1-14.

Chio, C., Shrestha, S., Carr, G., Khatiwada, J. R., Zhu, Y., Li, O., ... & Qin, W. (2023). Optimization and purification of bioproducts from *Bacillus velezensis* PhCL fermentation and their potential on industrial application and bioremediation. *Science of the Total Environment*, *903*, 166428.

Chioma, O., Ogechukwu, M., Bright, O., Simon, O., & Chinyere, A. F. (2013). Isolation and characterization of biosurfactants producing bacteria from oil polluted soil. *Journal of Natural Sciences Research*, *3*(5), 119-123.

Choe, E., & Min, D. B. (2007). Chemistry of deep-fat frying oils. *Journal of Food Science*, *72*(5), R77-R86.

Christofi, N., & Ivshina, I. B. (2002). Microbial surfactants and their use in field studies of soil remediation. *Journal of Applied Microbiology*, *93*(6), 915-929.

Christova, N., Tuleva, B., Cohen, R., Ivanova, G., Stoev, G., Stoilova-Disheva, M., & Stoineva, I. (2011). Chemical characterization and physical and biological activities of rhamnolipids produced by *Pseudomonas aeruginosa* BN10. *Zeitschrift für Naturforschung C*, *66*(7-8), 394-402.

Chrzanowski, Ł., Ławniczak, Ł., & Czaczyk, K. (2012). Why do microorganisms produce rhamnolipids?. *World Journal of Microbiology and Biotechnology*, *28*, 401-419.

Chuah, L. F., Nawaz, A., Dailin, D. J., Oloruntobi, O., Habila, M. A., Tong, W. Y., & Misson, M. (2023). Investigating the crude oil biodegradation performance in bioreactor by using a consortium of symbiotic bacteria. *Chemosphere*, *337*, 139293.

Colombo Fleck, L., Correa Bicca, F., & Zachia Ayub, M. A. (2000). Physiological aspects of hydrocarbon emulsification, metal resistance and DNA profile of biodegrading bacteria isolated from oil polluted sites. *Biotechnology Letters*, *22*, 285-289.

Cooper D. G. (1986). Biosurfactants. *Microbiological sciences*, *3*(5), 145–149.

Cooper, D. G., & Goldenberg, B. G. (1987). Surface-active agents from two Bacillus species. *Applied and Environmental Microbiology*, *53*(2), 224-229.

Cosson, P., Zulianello, L., Join-Lambert, O., Faurisson, F., Gebbie, L., Benghezal, M., ... & Köhler, T. (2002). *Pseudomonas aeruginosa* virulence analyzed in a Dictyostelium discoideum host system. *Journal of Bacteriology*, *184*(11), 3027-3033.

Costa, S. G., Nitschke, M., Lépine, F., Déziel, E., & Contiero, J. (2010). Structure, properties and applications of rhamnolipids produced by *Pseudomonas aeruginosa* L2-1 from cassava wastewater. *Process Biochemistry*, *45*(9), 1511-1516.

Cserháti, T., Forgács, E., & Oros, G. (2002). Biological activity and environmental impact of anionic surfactants. *Environment International*, *28*(5), 337-348.

Cunha, C. D., Do Rosario, M., Rosado, A. S., & Leite, S. G. F. (2004). *Serratia* sp. SVGG16: a promising biosurfactant producer isolated from tropical soil during growth with ethanol-blended gasoline. *Process Biochemistry*, *39*(12), 2277-2282.

Dahrazma, B. (2005). *Removal of heavy metals from sediment using rhamnolipid* (Doctoral dissertation, Concordia University).

Das, A. J., Lal, S., Kumar, R., & Verma, C. (2017). Bacterial biosurfactants can be an ecofriendly and advanced technology for remediation of heavy metals and co-contaminated soil. *International Journal of Environmental Science and Technology*, *14*(6), 1343-1354.

Das, K., & Mukherjee, A. K. (2005). Characterization of biochemical properties and biological activities of biosurfactants produced by *Pseudomonas aeruginosa* mucoid and non-mucoid strains isolated from hydrocarbon-contaminated soil samples. *Applied Microbiology and Biotechnology*, *69*, 192-199.

Dashti, N., Al-Awadhi, H., Khanafer, M., Abdelghany, S., & Radwan, S. (2008). Potential of hexadecane-utilizing soil-microorganisms for growth on hexadecanol, hexadecanal and hexadecanoic acid as sole sources of carbon and energy. *Chemosphere*, *70*(3), 475-479.

Datta, D., Ghosh, S., Kumar, S., Gangola, S., Majumdar, B., Saha, R., ... & Kar, G. (2024). Microbial biosurfactants: Multifarious applications in sustainable agriculture. *Microbiological Research*, *279*, 127551.

Datta, P., Tiwari, P., & Pandey, L. M. (2018). Isolation and characterization of biosurfactant producing and oil degrading *Bacillus subtilis* MG495086 from formation water of Assam oil reservoir and its suitability for enhanced oil recovery. *Bioresource Technology*, *270*, 439-448.

de Araujo, J. S., Marcos Filho, A. O., Ribeiro, V. T., de Araujo, N. K., & de B Neto, E. L. (2020). Production of rhamnolipids by *Pseudomonas aeruginosa* ap029-glviia and application on bioremediation and as a fungicide. *Biosciences Biotechnology Research Asia*, *17*(3), 467.

de Jesús Cortés-Sánchez, A., Hernández-Sánchez, H., & Jaramillo-Flores, M. E. (2013). Biological activity of glycolipids produced by microorganisms: new trends and possible therapeutic alternatives. *Microbiological Research*, *168*(1), 22-32.

de Jesús Cortés-Sánchez, A., Hernández-Sánchez, H., & Jaramillo-Flores, M. E. (2013). Biological activity of glycolipids produced by microorganisms: new trends and possible therapeutic alternatives. *Microbiological Research*, *168*(1), 22-32.

De Lima, C. J. B., Ribeiro, E. J., Servulo, E. F. C., Resende, M. M., & Cardoso, V. L. (2009). Biosurfactant production by *Pseudomonas aeruginosa* grown in residual soybean oil. *Applied Biochemistry and Biotechnology*, *152*(1), 156-168.

Dermont, G., Bergeron, M., Mercier, G., & Richer-Laflèche, M. (2008). Soil washing for metal removal: a review of physical/chemical technologies and field applications. *Journal of Hazardous Materials*, *152*(1), 1-31.

Desai, J. D., & Banat, I. M. (1997). Microbial production of surfactants and their commercial potential. *Microbiology and Molecular Biology Reviews*, *61*(1), 47-64.

Déziel, É., Lépine, F., Dennie, D., Boismenu, D., Mamer, O. A., & Villemur, R. (1999). Liquid chromatography/mass spectrometry analysis of mixtures of rhamnolipids produced by *Pseudomonas aeruginosa* strain 57RP grown on mannitol or naphthalene. *Biochimica et Biophysica Acta (BBA)-Molecular and Cell Biology of Lipids*, *1440*(2-3), 244-252.

Diab, A. M., Ibrahim, S., & Abdulla, H. M. (2020). Safe application and preservation efficacy of low-toxic rhamnolipids produced from *ps. aeruginosa* for cosmetics and personal care formulation. *Egyptian Journal of Microbiology*, *55*(The 14th Conference of Applied Microbiology), 57-70.

Domdi, L., Lakra, A. K., Mohan, S. K., Tilwani, Y. M., Jha, N., & Arul, V. (2021). Microbial degradation of n-hexadecane using *Pseudomonas aeruginosa* PU1 isolated from transformer-oil contaminated soil. *Biocatalysis and Agricultural Biotechnology*, *38*, 102213.

El-Housseiny, G. S., Aboshanab, K. M., Aboulwafa, M. M., & Hassouna, N. A. (2020). Structural and physicochemical characterization of rhamnolipids produced by *Pseudomonas aeruginosa* P6. *AMB Express*, *10*(1), 201.

Esposito, R., Speciale, I., De Castro, C., D'Errico, G., & Russo Krauss, I. (2023). Rhamnolipid self-aggregation in aqueous media: A long journey toward the definition of structure–property relationships. *International Journal of Molecular Sciences*, *24*(6), 5395.

Etoumi, A., El Musrati, I., El Gammoudi, B., & El Behlil, M. (2008). The reduction of wax precipitation in waxy crude oils by *Pseudomonas* species. *Journal of Industrial Microbiology and Biotechnology*, *35*(11), 1241-1245.

Faisal, Z. G., Mahdi, M. S., & Alobaidi, K. H. (2023). Optimization and chemical characterization of biosurfactant produced from a novel *Pseudomonas guguanensis* strain Iraqi ZG. KM. *International Journal of Microbiology*, *2023*, 1571991.

Fang, D., Liu, Y., Dou, D., & Su, B. (2024). The unique immune evasion mechanisms of the mpox virus and their implication for developing new vaccines and immunotherapies. *Virologica Sinica*

Fernandes, N. D. A. T., de Souza, A. C., Simões, L. A., Dos Reis, G. M. F., Souza, K. T., Schwan, R. F., & Dias, D. R. (2020). Eco-friendly biosurfactant from *Wickerhamomyces anomalus* CCMA 0358 as larvicidal and antimicrobial. *Microbiological Research*, *241*, 126571.

Ferreira, A., Vecino, X., Ferreira, D., Cruz, J. M., Moldes, A. B., & Rodrigues, L. R. (2017). Novel cosmetic formulations containing a biosurfactant from *Lactobacillus paracasei*. *Colloids and Surfaces B: Biointerfaces*, *155*, 522-529.

Fischer, E. R., Hansen, B. T., Nair, V., Hoyt, F. H., Schwartz, C. L., & Dorward, D. W. (2024). Scanning electron microscopy. *Current Protocols*, 4, e1034.

Foo, W. H., Chia, W. Y., Tang, D. Y. Y., Koay, S. S. N., Lim, S. S., & Chew, K. W. (2021). The conundrum of waste cooking oil: Transforming hazard into energy. *Journal of Hazardous Materials*, *417*, 126129.

Gao, H., Wu, M., Liu, H., Xu, Y., & Liu, Z. (2022). Effect of petroleum hydrocarbon pollution levels on the soil microecosystem and ecological function. *Environmental Pollution*, *293*, 118511.

Gaur, S., Gupta, S., & Jain, A. (2021). Characterization and oil recovery application of biosurfactant produced during bioremediation of waste engine oil by strain *Pseudomonas aeruginosa* gi |KP 16392| isolated from Sambhar salt lake. *Bioremediation Journal*, *25*(4), 308-325.

Gdaniec, B. G., Bonini, F., Prodon, F., Braschler, T., Köhler, T., & Van Delden, C. (2022). *Pseudomonas aeruginosa* rhamnolipid micelles deliver toxic metabolites and antibiotics into *Staphylococcus aureus*. *IScience*, *25*(1).

George, S., & Jayachandran, K. (2009). Analysis of rhamnolipid biosurfactants produced through submerged fermentation using orange fruit peelings as sole carbon source. *Applied biochemistry and Biotechnology*, *158*, 694-705.

George, S., & Jayachandran, K. (2013). Production and characterization of rhamnolipid biosurfactant from waste frying coconut oil using a novel *Pseudomonas aeruginosa* D. *Journal of Applied Microbiology*, *114*(2), 373-383.

Ghasemi, A., Moosavi-Nasab, M., Setoodeh, P., Mesbahi, G., & Yousefi, G. (2019). Biosurfactant production by lactic acid bacterium *Pediococcus dextrinicus*

SHU1593 grown on different carbon sources: strain screening followed by product characterization. *Scientific Reports*, *9*(1), 5287.

Ghribi, D., Elleuch, M., Abdelkefi, L., & Ellouze-Chaabouni, S. (2012). Evaluation of larvicidal potency of *Bacillus subtilis* SPB1 biosurfactant against *Ephestia kuehniella* (Lepidoptera: Pyralidae) larvae and influence of abiotic factors on its insecticidal activity. *Journal of Stored Products Research*, *48*, 68-72.

Gidudu, B., & Chirwa, E. M. (2022). Evaluation of the toxicity of a rhamnolipid biosurfactant for its application in the optimization of the bio-electrokinetic remediation of petrochemical contaminated soil. *Cleaner Engineering and Technology*, *9*, 100521.

Gil, C. V., Rebocho, A. T., Esmail, A., Sevrin, C., Grandfils, C., Torres, C. A., ... & Freitas, F. (2022). Characterization of the thermostable biosurfactant produced by *Burkholderia thailandensis* DSM 13276. *Polymers*, *14*(10), 2088.

Gogoi, B., Acharjee, S. A., Bharali, P., Sorhie, V., Walling, B., & Alemtoshi. (2024). A critical review on the ecotoxicity of heavy metal on multispecies in global context: A bibliometric analysis. *Environmental Research*, *248*, 118280.

Gogoi, D., Bhagowati, P., Gogoi, P., Bordoloi, N. K., Rafay, A., Dolui, S. K., & Mukherjee, A. K. (2016). Structural and physico-chemical characterization of a dirhamnolipid biosurfactant purified from *Pseudomonas aeruginosa*: application of crude biosurfactant in enhanced oil recovery. *RSC Advances*, *6*(74), 70669-70681.

Gomaa, E. Z., & El-Meihy, R. M. (2019). Bacterial biosurfactant from *Citrobacter freundii* MG812314. 1 as a bioremoval tool of heavy metals from wastewater. *Bulletin of the National Research Centre*, *43*(1), 69.

Gong, Z., He, Q., Liu, J., Zhou, J., Che, C., Si, M., & Yang, G. (2022). Achieving "non-foaming" rhamnolipid production and productivity rebounds of *Pseudomonas aeruginosa* under weakly acidic fermentation. *Microorganisms*, *10*(6), 1091.

Goswami, D., Borah, S. N., Lahkar, J., Handique, P. J., & Deka, S. (2015). Antifungal properties of rhamnolipid produced by *Pseudomonas aeruginosa* DS9 against Colletotrichum falcatum. *Journal of Basic Microbiology*, *55*(11), 1265-1274.

Ground Water Information Booklet, Mokokchung District, Nagaland. https://www.cgwb.gov.in/old_website/District_Profile/Nagaland/Mokok.pdf

Gudina, E. J., Teixeira, J. A., & Rodrigues, L. R. (2010). Isolation and functional characterization of a biosurfactant produced by *Lactobacillus paracasei*. *Colloids and Surfaces B: Biointerfaces*, *76*(1), 298-304.

Haba, E., Abalos, A., Jauregui, O., Espuny, M. J., & Manresa, A. (2003b). Use of liquid chromatography-mass spectroscopy for studying the composition and properties of rhamnolipids produced by different strains of *Pseudomonas aeruginosa*. *Journal of Surfactants and Detergents*, *6*(2), 155-161.

Haba, E., Espuny, M. J., Busquets, M., & Manresa, A. (2000). Screening and production of rhamnolipids by *Pseudomonas aeruginosa* 47T2 NCIB 40044 from waste frying oils. *Journal of Applied Microbiology*, *88*(3), 379-387.

Haba, E., Pinazo, A., Jauregui, O., Espuny, M. J., Infante, M. R., & Manresa, A. (2003a). Physicochemical characterization and antimicrobial properties of rhamnolipids produced by *Pseudomonas aeruginosa* 47T2 NCBIM 40044. *Biotechnology and Bioengineering*, *81*(3), 316-322.

Hao, D. H., Lin, J. Q., Song, X., Lin, J. Q., Su, Y. J., & Qu, Y. B. (2008). Isolation, identification, and performance studies of a novel paraffin-degrading bacterium of *Gordonia amicalis* LH3. *Biotechnology and Bioprocess Engineering*, *13*, 61-68.

Hao, R., Lu, A., & Zeng, Y. (2004). Effect on crude oil by thermophilic bacterium. *Journal of Petroleum Science and Engineering*, *43*(3-4), 247-258.

Haque, E., Kayalvizhi, K., & Hassan, S. (2020). Biocompatibility, antioxidant and anti-infective effect of biosurfactant produced by *Marinobacter litoralis* MB15. *International Journal of Pharmaceutical Investigation*, *10*(2).

Harikrishnan, S., Sudarshan, S., Sivasubramani, K., Nandini, M. S., Narenkumar, J., Ramachandran, V., ... & Jayalakshmi, S. (2023). Larvicidal and anti-termite activities of microbial biosurfactant produced by *Enterobacter cloacae* SJ2 isolated from marine sponge Clathria sp. *Scientific Reports*, *13*(1), 15153.

Hassen, W., Neifar, M., Cherif, H., Najjari, A., Chouchane, H., Driouich, R. C., ... & Cherif, A. (2018). *Pseudomonas rhizophila* S211, a new plant growth-promoting

rhizobacterium with potential in pesticide-bioremediation. *Frontiers in Microbiology*, *9*, 34.

Haussler, S., Nimtz, M., Domke, T., Wray, V., & Steinmetz, I. (1998). Purification and characterization of a cytotoxic exolipid of *Burkholderia pseudomallei*. *Infection and Immunity*, *66*(4), 1588-1593

Hazra, C., Kundu, D., Ghosh, P., Joshi, S., Dandi, N., & Chaudhari, A. (2011). Screening and identification of *Pseudomonas aeruginosa* AB4 for improved production, characterization and application of a glycolipid biosurfactant using low-cost agro-based raw materials. *Journal of Chemical Technology & Biotechnology*, *86*(2), 185-198.

He, P., Shi, D., Li, Y., Xia, K., Kim, S. B., Dwivedi, R., ... & Zhang, F. (2023). SPR sensor-based analysis of the inhibition of marine sulfated glycans on interactions between Monkeypox virus proteins and glycosaminoglycans. *Marine Drugs*, *21*(5), 264.

Healy, M. G., Devine, C. M., & Murphy, R. (1996). Microbial production of biosurfactants. *Resources, Conservation and Recycling*, *18*(1-4), 41-57.

Henkel, M., Müller, M. M., Kügler, J. H., Lovaglio, R. B., Contiero, J., Syldatk, C., & Hausmann, R. (2012). Rhamnolipids as biosurfactants from renewable resources: concepts for next-generation rhamnolipid production. *Process Biochemistry*, *47*(8), 1207-1219.

Hiroki, M. (1992). Effects of heavy metal contamination on soil microbial population. *Soil Science and Plant Nutrition*, *38*(1), 141-147.

Hossain, M. F., Akter, M. A., Sohan, M. S. R., Sultana, N., Reza, M. A., & Hoque, K. M. F. (2022). Bioremediation potential of hydrocarbon degrading bacteria: isolation, characterization, and assessment. *Saudi Journal of Biological Sciences*, *29*(1), 211-216.

Hu, K., Xu, S., Gao, Y., He, Y., & Wang, X. (2023). Choline chloride and rhamnolipid combined with organic manures improve salinity tolerance, yield, and quality of tomato. *Journal of Plant Growth Regulation*, *42*(7), 4118-4130.

Hudu, S. A., Alshrari, A. S., Al Qtaitat, A., & Imran, M. (2023). VP37 protein inhibitors for Mpox treatment: highlights on recent advances, patent literature, and future directions. *Biomedicines*, *11*(4), 1106.

Hudzicki, J. (2009). Kirby-Bauer disk diffusion susceptibility test protocol. *American Society for Microbiology*, *15*(1), 1-23.

Hughes, M. F. (2002). Arsenic toxicity and potential mechanisms of action. *Toxicology Letters*, *133*(1), 1-16.

Hussey, M. A., & Zayaitz, A. (2007). Endospore stain protocol. *American Society for Microbiology*, *8*, 1-11.

Ibrahim, H. M. (2018). Characterization of biosurfactants produced by novel strains of *Ochrobactrum anthropi* HM-1 and *Citrobacter freundii* HM-2 from used engine oil-contaminated soil. *Egyptian Journal of Petroleum*, *27*(1), 21-29.

Jain, D. K., Collins-Thompson, D. L., Lee, H., & Trevors, J. T. (1991). A drop-collapsing test for screening surfactant-producing microorganisms. *Journal of Microbiological Methods*, *13*(4), 271-279.

Jaishankar, M., Tseten, T., Anbalagan, N., Mathew, B. B., & Beeregowda, K. N. (2014). Toxicity, mechanism and health effects of some heavy metals. *Interdisciplinary Toxicology*, *7*(2), 60.

Janek, T., Łukaszewicz, M., & Krasowska, A. (2013). Identification and characterization of biosurfactants produced by the Arctic bacterium *Pseudomonas putida* BD2. *Colloids and Surfaces B: Biointerfaces*, *110*, 379-386.

Jayasree, A. S., Latha, D., & Muthulaxmi, V. (2018). Production of biosurfactant from *Bacillus* sp. and its larvicidal activity. *International Journal of Pharmaceutical Sciences and Research*, *9*(11), 4865-4870.

Jomova, K., Jenisova, Z., Feszterova, M., Baros, S., Liska, J., Hudecova, D., ... & Valko, M. (2011). Arsenic: toxicity, oxidative stress and human disease. *Journal of Applied Toxicology*, *31*(2), 95-107.

Joshi, S., Bharucha, C., Jha, S., Yadav, S., Nerurkar, A., & Desai, A. J. (2008). Biosurfactant production using molasses and whey under thermophilic conditions. *Bioresource Technology*, *99*(1), 195-199.

Juwarkar, A. A., Nair, A., Dubey, K. V., Singh, S. K., & Devotta, S. (2007). Biosurfactant technology for remediation of cadmium and lead contaminated soils. *Chemosphere*, *68*(10), 1996-2002.

Karlapudi, A. P., Venkateswarulu, T. C., Tammineedi, J., Kanumuri, L., Ravuru, B. K., Ramu Dirisala, V., & Kodali, V. P. (2018). Role of biosurfactants in bioremediation of oil pollution-a review. *Petroleum*, *4*(3), 241-249.

Karnwal, A., Shrivastava, S., Al-Tawaha, A. R. M. S., Kumar, G., Singh, R., Kumar, A., ... & Malik, T. (2023). Microbial biosurfactant as an alternate to chemical surfactants for application in cosmetics industries in personal and skin care products: a critical review. *BioMed Research International*, *2023*(1), 2375223.

Kaszuba, M., Corbett, J., Watson, F. M., & Jones, A. (2010). High-concentration zeta potential measurements using light-scattering techniques. *Philosophical Transactions of the Royal Society*, *368*(1927), 4439-4451.

Khademolhosseini, R., Jafari, A., Mousavi, S. M., Hajfarajollah, H., Noghabi, K. A., & Manteghian, M. (2019). Physicochemical characterization and optimization of glycolipid biosurfactant production by a native strain of *Pseudomonas aeruginosa* HAK01 and its performance evaluation for the MEOR process. *RSC Advances*, *9*(14), 7932-7947.

Khan, M. B., & Sasmal, C. (2022). A detailed and systematic study on rheological and physicochemical properties of rhamnolipid biosurfactant solutions. *Journal of Colloid and Interface Science Open*, *8*, 100067.

Kim, S. K., Kim, Y. C., Lee, S., Kim, J. C., Yun, M. Y., & Kim, I. S. (2011). Insecticidal activity of rhamnolipid isolated from *Pseudomonas* sp. EP-3 against green peach aphid (*Myzus persicae*). *Journal of Agricultural and Food Chemistry*, *59*(3), 934-938.

Kimura, M. (1980). A simple method for estimating evolutionary rates of base substitutions through comparative studies of nucleotide sequences. *Journal of Molecular Evolution*, *16*, 111-120.

Kopalle, P., Pothana, S. A., & Maddila, S. (2022). Structural and physicochemical characterization of a rhamnolipid biosurfactant. *Chemical Data Collections*, *41*, 100905.

Kumar, A., Bhayana, S., Singh, P. K., Tripathi, A. D., Paul, V., Balodi, V., & Agarwal, A. (2025). Valorization of used cooking oil: challenges, current developments, life cycle assessment and future prospects. *Discover Sustainability*, *6*(1), 1-31.

Kumar, P. N., Swapna, T. H., Khan, M. Y., Reddy, G., & Hameeda, B. (2017). Statistical optimization of antifungal iturin A production from *Bacillus amyloliquefaciens* RHNK22 using agro-industrial wastes. *Saudi Journal of Biological Sciences*, *24*(7), 1722-1740.

Kumar, R., Das, A. J., & Juwarkar, A. A. (2015). Reclamation of petrol oil contaminated soil by rhamnolipids producing PGPR strains for growing *Withania somnifera* a medicinal shrub. *World Journal of Microbiology and Biotechnology*, *31*(2), 307-313.

Kumari, B., Singh, S. N., & Singh, D. P. (2012). Characterization of two biosurfactant producing strains in crude oil degradation. *Process Biochemistry*, *47*(12), 2463-2471.

Kumari, S., Gautam, K., Seth, M., Anbumani, S., & Manickam, N. (2023). Bioremediation of polycyclic aromatic hydrocarbons in crude oil by bacterial consortium in soil amended with *Eisenia fetida* and rhamnolipid. *Environmental Science and Pollution Research*, *30*(34), 82517-82531.

Lan, G., Fan, Q., Liu, Y., Chen, C., Li, G., Liu, Y., & Yin, X. (2015). Rhamnolipid production from waste cooking oil using *Pseudomonas* SWP-4. *Biochemical Engineering Journal*, *101*, 44-54.

Lang, S., & Wullbrandt, D. (1999). Rhamnose lipids–biosynthesis, microbial production and application potential. *Applied Microbiology and Biotechnology*, *51*, 22-32.

Lavorgna, M., Angelillo, S., Gentile, M., Nugnes, R., Orlo, E., Russo, C., & Isidori, M. (2020). Early genotoxic effects from exposure to environmental pollutants young people from South Italy. *European Journal of Public Health*, *30*(Supplement_5), ckaa166-131.

Ławniczak, Ł., Marecik, R., & Chrzanowski, Ł. (2013). Contributions of biosurfactants to natural or induced bioremediation. *Applied Microbiology and Biotechnology*, *97*, 2327-2339.

Leahy, J. G., & Colwell, R. R. (1990). Microbial degradation of hydrocarbons in the environment. *Microbiological Reviews*, *54*(3), 305-315.

Li, C., Zhou, K., Qin, W., Tian, C., Qi, M., Yan, X., & Han, W. (2019). A review on heavy metals contamination in soil: effects, sources, and remediation techniques. *Soil and Sediment Contamination: An International Journal*, *28*(4), 380-394.

Li, K., Cui, Y. C., Zhang, H., Liu, X. P., Zhang, D., Wu, A. L., ... & Tang, Y. (2015). Glutamine reduces the apoptosis of H9C2 cells treated with high-glucose and reperfusion through an oxidation-related mechanism. *PLoS One*, *10*(7), e0132402.

Lin, F. F., Besserer, G. J., & Pitts, M. J. (1987). Laboratory evaluation of crosslinked polymer and alkaline-polymer-surfactant flood. *Journal of Canadian Petroleum Technology*, *26*(06).

Liu, H., Wang, H., Chen, X., Liu, N., & Bao, S. (2014). Biosurfactant-producing strains in enhancing solubilization and biodegradation of petroleum hydrocarbons in groundwater. *Environmental Monitoring and Assessment*, *186*, 4581-4589.

Loganathan, T., Fletcher, J., Abraham, P., Kannangai, R., Chakraborty, C., El Allali, A., ... & Zayed, H. (2024). Expression analysis and mapping of Viral—Host Protein interactions of Poxviridae suggests a lead candidate molecule targeting Mpox. *BMC Infectious Diseases*, *24*(1), 483.

Loiseau, C., Portier, E., Corre, M. H., Schlusselhuber, M., Depayras, S., Berjeaud, J. M., & Verdon, J. (2018). Highlighting the potency of biosurfactants produced by pseudomonas strains as anti-legionella agents. *BioMed Research International*, *2018*(1), 8194368.

Lopes, P. R. M., Montagnolli, R. N., Dilarri, G., Mendes, C. R., Cruz, J. M., Bergamini-Lopes, M. P., ... & Bidoia, E. D. (2024). Combination of *Pseudomonas aeruginosa* and rhamnolipid for bioremediation of soil contaminated with waste lubricant oil. *Applied Biochemistry and Microbiology*, *60*(4), 627-639.

Lotfabad, T. B., Abassi, H., Ahmadkhaniha, R., Roostaazad, R., Masoomi, F., Zahiri, H. S., ... & Noghabi, K. A. (2010). Structural characterization of a rhamnolipid-type biosurfactant produced by *Pseudomonas aeruginosa* MR01: enhancement of di-

rhamnolipid proportion using gamma irradiation. *Colloids and Surfaces B: Biointerfaces*, *81*(2), 397-405.

Lotfabad, T. B., Shourian, M., Roostaazad, R., Najafabadi, A. R., Adelzadeh, M. R., & Noghabi, K. A. (2009). An efficient biosurfactant-producing bacterium *Pseudomonas aeruginosa* MR01, isolated from oil excavation areas in south of Iran. *Colloids and Surfaces B: Biointerfaces*, *69*(2), 183-193.

Lovaglio, R. B., dos Santos, F. J., Junior, M. J., & Contiero, J. (2011). Rhamnolipid emulsifying activity and emulsion stability: pH rules. *Colloids and Surfaces B: Biointerfaces*, *85*(2), 301-305.

Luna, J. M., Rufino, R. D., & Sarubbo, L. A. (2016). Biosurfactant from *Candida sphaerica* UCP0995 exhibiting heavy metal remediation properties. *Process Safety and Environmental Protection*, *102*, 558-566.

Maadurshni, G. B., Tharani, G. K., Udayakumar, I., Nagarajan, M., & Manivannan, J. (2022). Al_2O_3 nanoparticles trigger the embryonic hepatotoxic response and potentiate TNF-α-induced apoptosis—modulatory effect of p38 MAPK and JNK inhibitors. *Environmental Science and Pollution Research*, *29*(36), 54250-54263.

Maczek, J., Junne, S., & Götz, P. (2007). Examining biosurfactant producing bacteria—an example for an automated search for natural compounds. *Application Note CyBio AG*, *16*.

Maier, R. M., & Soberon-Chavez, G. (2000). *Pseudomonas aeruginosa* rhamnolipids: biosynthesis and potential applications. *Applied Microbiology and Biotechnology*, *54*, 625-633.

Maillard, A. P. F., Espeche, J. C., Maturana, P., Cutro, A. C., & Hollmann, A. (2021). Zeta potential beyond materials science: Applications to bacterial systems and to the development of novel antimicrobials. *Biochimica et Biophysica Acta (BBA)-Biomembranes*, *1863*(6), 183597.

Maity, S., Das, S., Mohapatra, S., Tripathi, A. D., Akthar, J., Pati, S., ... & Samantaray, D. P. (2020). Growth associated polyhydroxybutyrate production by the novel Zobellellae tiwanensis strain DD5 from banana peels under submerged fermentation. *International Journal of Biological Macromolecules*, *153*, 461-469.

Makkar, R., & Cameotra, S. (2002). An update on the use of unconventional substrates for biosurfactant production and their new applications. *Applied Microbiology and Biotechnology*, *58*, 428-434.

Manivasagan, P., Sivasankar, P., Venkatesan, J., Sivakumar, K., & Kim, S. K. (2014). Optimization, production and characterization of glycolipid biosurfactant from the marine actinobacterium, *Streptomyces* sp. MAB36. *Bioprocess and Biosystems Engineering*, *37*, 783-797.

Matho, M. H., de Val, N., Miller, G. M., Brown, J., Schlossman, A., Meng, X., ... & Zajonc, D. M. (2014). Murine anti-vaccinia virus D8 antibodies target different epitopes and differ in their ability to block D8 binding to CS-E. *PLoS Pathogens*, *10*(12), e1004495.

Md, F. (2012). Biosurfactant: production and application. *Journal of Petroleum & Environmental Biotechnology*, *3*(4), 124.

Mendes, A. N., Filgueiras, L. A., Pinto, J. C., & Nele, M. (2015). Physicochemical properties of rhamnolipid biosurfactant from *Pseudomonas aeruginosa* PA1 to applications in microemulsions. *Journal of Biomaterials and Nanobiotechnology*, *6*(1), 64-79.

Meng, L., Li, H., Bao, M., & Sun, P. (2017). Metabolic pathway for a new strain *Pseudomonas synxantha* LSH-7′: from chemotaxis to uptake of n-hexadecane. *Scientific Reports*, *7*(1), 39068.

Mielko, K. A., Jabłoński, S. J., Milczewska, J., Sands, D., Łukaszewicz, M., & Młynarz, P. (2019). Metabolomic studies of *Pseudomonas aeruginosa*. *World Journal of Microbiology and Biotechnology*, *35*, 1-11.

Mishra, A., & Trivedi, R. K. (2019). Synthesis and characterization of biosurfactant using waste from oil processing industry as substrate by *Pseudomonas aeruginosa* (MTCC 424). *Rasayan Journal of Chemistry*, *12*(2), 1011-1021.

Mohanty, M., Mohanty, J., Priyadarsini, S., Rodríguez-Díaz, J. M., Yadav, S., Cabral-Pinto, M. M., ... & Das, A. P. (2025). Environmental Hydrocarbon Pollutants: Sources, Transport, and Effect on Human Health. In *Environmental Hydrocarbon Pollution and Zero Waste Approach Towards a Sustainable Waste Management* (pp. 21-44). Cham: Springer Nature Switzerland.

Mohebali, G., Ball, A., Kaytash, A., & Rasekh, B. (2007). Stabilization of water/gas oil emulsions by desulfurizing cells of *Gordonia alkanivorans* RIPI90A. *Microbiology*, *153*(5), 1573-1581.

Monnier, N., Furlan, A. L., Buchoux, S., Deleu, M., Dauchez, M., Rippa, S., & Sarazin, C. (2019). Exploring the dual interaction of natural rhamnolipids with plant and fungal biomimetic plasma membranes through biophysical studies. *International Journal of Molecular Sciences*, *20*(5), 1009.

Monteiro, S. A., Sassaki, G. L., de Souza, L. M., Meira, J. A., de Araújo, J. M., Mitchell, D. A., ... & Krieger, N. (2007). Molecular and structural characterization of the biosurfactant produced by *Pseudomonas aeruginosa* DAUPE 614. *Chemistry and Physics of Lipids*, *147*(1), 1-13.

Morais, S., Costa, F. G., & Pereira, M. D. L. (2012). Heavy metals and human health. *Environmental Health–Emerging Issues and Practice*, *10*(1), 227-245.

Morikawa, M., Hirata, Y., & Imanaka, T. (2000). A study on the structure–function relationship of lipopeptide biosurfactants. *Biochimica et Biophysica Acta (BBA)-Molecular and Cell Biology of Lipids*, *1488*(3), 211-218.

Moussa, T. A. A., Mohamed, M. S., & Samak, N. (2014). Production and characterization of di-rhamnolipid produced by *Pseudomonas aeruginosa* TMN. *Brazilian Journal of Chemical Engineering*, *31*, 867-880.

Müller, F., Hönzke, S., Luthardt, W. O., Wong, E. L., Unbehauen, M., Bauer, J., ... & Rademann, J. (2017). Rhamnolipids form drug-loaded nanoparticles for dermal drug delivery. *European Journal of Pharmaceutics and Biopharmaceutics*, *116*, 31-37.

Müller, M. M., Hörmann, B., Kugel, M., Syldatk, C., & Hausmann, R. (2011). Evaluation of rhamnolipid production capacity of *Pseudomonas aeruginosa* PAO1 in comparison to the rhamnolipid over-producer strains DSM 7108 and DSM 2874. *Applied microbiology and biotechnology*, *89*(3), 585-592.

Müller, M. M., Kügler, J. H., Henkel, M., Gerlitzki, M., Hörmann, B., Pöhnlein, M., ... & Hausmann, R. (2012). Rhamnolipids—next generation surfactants. *Journal of Biotechnology*, *162*(4), 366-380.

Mulligan, C. N. (2021). Sustainable remediation of contaminated soil using biosurfactants. *Frontiers in Bioengineering and Biotechnology*, *9*, 635196.

Mulligan, C. N., Cooper, D. G., & Neufeld, R. J. (1984). Selection of microbes producing biosurfactants in media without hydrocarbons. *Journal of fermentation Technology*, *62*(4), 311-314.

Nagarajan, M., Maadurshni, G. B., & Manivannan, J. (2024). Exposure to low dose of Bisphenol A (BPA) intensifies kidney oxidative stress, inflammatory factors expression and modulates Angiotensin II signaling under hypertensive milieu. *Journal of Biochemical and Molecular Toxicology*, *38*(1), e23533.

Ndlovu, T., Rautenbach, M., Vosloo, J. A., Khan, S., & Khan, W. (2017). Characterisation and antimicrobial activity of biosurfactant extracts produced by *Bacillus amyloliquefaciens* and *Pseudomonas aeruginosa* isolated from a wastewater treatment plant. *AMB Express*, *7*(1), 108.

Nitschke, M., Costa, S. G., Haddad, R., G. Gonçalves, L. A., Eberlin, M. N., & Contiero, J. (2005). Oil wastes as unconventional substrates for rhamnolipid biosurfactant production by *Pseudomonas aeruginosa* LBI. *Biotechnology Progress*, *21*(5), 1562-1566.

Oktari, A., Supriatin, Y., Kamal, M., & Syafrullah, H. (2017). The bacterial endospore stain on Schaeffer Fulton using variation of methylene blue solution. *Journal of Physics: Conference Series,* 812, (1), 012066.

Olu-Arotiowa, O. A., Odesanmi, A. A., Adedotun, B. K., Ajibade, O. A., Olasesan, I. P., Odofin, O. I., & Abass, A. O. (2022). Review on environmental impact and valourization of waste cooking oil. *LAUTECH Journal of Engineering and Technology*, *16*(1), 144-163.

Pacwa-Płociniczak, M., Płaza, G. A., Piotrowska-Seget, Z., & Cameotra, S. S. (2011). Environmental applications of biosurfactants: recent advances. *International Journal of Molecular sciences*, *12*(1), 633-654.

Panesar, R., Panesar, P. S., Hasija, D., Bera, M. B., & Kumar, H. (2009). Fermentative potential of *Pseudomonas aeruginosa* strain for biosurfactant production. In *Biological Forum-An International Journal,* (Vol. 1, p. 109).

Parthasarathi, R., & Sivakumaar, P. K. (2011). Biosurfactant mediated remediation process evaluation on a mixture of heavy metal spiked topsoil using soil column and batch washing methods. *Soil and Sediment Contamination: An International Journal*, *20*(8), 892-907.

Parus, A., Ciesielski, T., Woźniak-Karczewska, M., Ławniczak, Ł., Janeda, M., Ślachciński, M., ... & Chrzanowski, Ł. (2024). Critical evaluation of the performance of rhamnolipids as surfactants for (phyto) extraction of Cd, Cu, Fe, Pb and Zn from copper smelter-affected soil. *Science of The Total Environment*, *912*, 168382.

Patel, K., & Patel, M. (2020). Improving bioremediation process of petroleum wastewater using biosurfactants producing *Stenotrophomonas* sp. S1VKR-26 and assessment of phytotoxicity. *Bioresource Technology*, *315*, 123861.

Patel, R. M., & Desai, A. J. (1997). Biosurfactant production by *Pseudomonas aeruginosa* GS3 from molasses. *Letters in Applied Microbiology*, *25*(2), 91-94.

Patowary, K., Das, M., Patowary, R., Kalita, M. C., & Deka, S. (2019). Recycling of bakery waste as an alternative carbon source for rhamnolipid biosurfactant production. *Journal of Surfactants and Detergents*, *22*(2), 373-384.

Patowary, R., Patowary, K., Kalita, M. C., & Deka, S. (2016). Utilization of paneer whey waste for cost-effective production of rhamnolipid biosurfactant. *Applied Biochemistry and Biotechnology*, *180*, 383-399.

Perfumo, A., Banat, I. M., Canganella, F., & Marchant, R. (2006). Rhamnolipid production by a novel thermophilic hydrocarbon-degrading *Pseudomonas aeruginosa* AP02-1. *Applied Microbiology and Biotechnology*, *72*, 132-138.

Peter, J. K., & Singh, D. P. (2014). Characterization of emulsification activity of partially purified Rhamnolipids from *Pseudomonas fluorescens*. *International Journal of Innovation and Scientific Research*, *3*(1), 88-100.

Phulpoto, I. A., Yu, Z., Li, J., Ndayisenga, F., Hu, B., Qazi, M. A., & Yang, X. (2022). Evaluation of di-rhamnolipid biosurfactants production by a novel *Pseudomonas* sp. S1WB: optimization, characterization and effect on petroleum-hydrocarbon degradation. *Ecotoxicology and Environmental Safety*, *242*, 113892.

Pi, Y., Chen, B., Bao, M., Fan, F., Cai, Q., Ze, L., & Zhang, B. (2017). Microbial degradation of four crude oil by biosurfactant producing strain *Rhodococcus* sp. *Bioresource Technology*, *232*, 263-269.

Pohl, A. (2020). Removal of heavy metal ions from water and wastewaters by sulfur-containing precipitation agents. *Water, Air, & Soil Pollution*, *231*(10), 503.

Pornsunthorntawee, O., Chavadej, S., & Rujiravanit, R. (2009). Solution properties and vesicle formation of rhamnolipid biosurfactants produced by *Pseudomonas aeruginosa* SP4. *Colloids and Surfaces B: Biointerfaces*, *72*(1), 6-15.

Pourfadakari, S., Jorfi, S., & Ghafari, S. (2020). An efficient biosurfactant by *Pseudomonas stutzeri* Z12 isolated from an extreme environment for remediation of soil contaminated with hydrocarbons. *Chemical and Biochemical Engineering Quarterly*, *34*(1), 35-48.

Primeia, S., Inoue, C., & Chien, M. F. (2020). Potential of biosurfactants' production on degrading heavy oil by bacterial consortia obtained from tsunami-induced oil-spilled beach areas in Miyagi, Japan. *Journal of Marine Science and Engineering*, *8*(8), 577.

Radzuan, M. N., Banat, I. M., & Winterburn, J. (2017). Production and characterization of rhamnolipid using palm oil agricultural refinery waste. *Bioresource Technology*, *225*, 99-105.

Rahman, K. S. M., Rahman, T. J., McClean, S., Marchant, R., & Banat, I. M. (2002b). Rhamnolipid biosurfactant production by strains of *Pseudomonas aeruginosa* using low-cost raw materials. *Biotechnology Progress*, *18*(6), 1277-1281.

Rahman, K. S. M., Rahman, T., Lakshmanaperumalsamy, P., & Banat, I. M. (2002a). Occurrence of crude oil degrading bacteria in gasoline and diesel station soils. *Journal of Basic Microbiology*, *42*(4), 284-291.

Rahman, P. K., Pasirayi, G., Auger, V., & Ali, Z. (2010). Production of rhamnolipid biosurfactants by *Pseudomonas aeruginosa* DS10-129 in a microfluidic bioreactor. *Biotechnology and Applied Biochemistry*, *55*(1), 45-52.

Ramírez, I. M., Vaz, D. A., Banat, I. M., Marchant, R., Alameda, E. J., & Román, M. G. (2016). Hydrolysis of olive mill waste to enhance rhamnolipids and surfactin production. *Bioresource Technology*, *205*, 1-6.

Raza, Z. A., Khalid, Z. M., Khan, M. S., Banat, I. M., Rehman, A., Naeem, A., & Saddique, M. T. (2010). Surface properties and sub-surface aggregate assimilation of rhamnolipid surfactants in different aqueous systems. *Biotechnology Letters*, *32*, 811-816.

Reddy, K. S., Khan, M. Y., Archana, K., Reddy, M. G., & Hameeda, B. (2016). Utilization of mango kernel oil for the rhamnolipid production by *Pseudomonas aeruginosa* DR1 towards its application as biocontrol agent. *Bioresource Technology*, *221*, 291-299.

Rehman, R., Ali, M. I., Ali, N., Badshah, M., Iqbal, M., Jamal, A., & Huang, Z. (2021). Crude oil biodegradation potential of biosurfactant-producing *Pseudomonas aeruginosa* and *Meyerozyma* sp. *Journal of Hazardous Materials*, *418*, 126276.

Rodrigues, L., Banat, I. M., Teixeira, J., & Oliveira, R. (2006). Biosurfactants: potential applications in medicine. *Journal of Antimicrobial Chemotherapy*, *57*(4), 609-618.

Rooney, A. P., Price, N. P., Ray, K. J., & Kuo, T. M. (2009). Isolation and characterization of rhamnolipid-producing bacterial strains from a biodiesel facility. *FEMS Microbiology Letters*, *295*(1), 82-87.

Rosenberg, M., Gutnick, D., & Rosenberg, E. (1980). Adherence of bacteria to hydrocarbons: a simple method for measuring cell-surface hydrophobicity. *FEMS Microbioly Letters*, *9*(1), 29-33.

Sabarinathan, D., Vanaraj, S., Sathiskumar, S., Poorna Chandrika, S., Sivarasan, G., Arumugam, S. S., ... & Chen, Q. (2021). Characterization and application of rhamnolipid from *Pseudomonas plecoglossicida* BP03. *Letters in Applied Microbiology*, *72*(3), 251-262.

Sabturani, N., Latif, J., Radiman, S., & Hamzah, A. (2016). Spectroscopic analysis of rhamnolipid produced by produced by *Pseudomonas aeruginosa* UKMP14T. *Malaysian Journal of Analytical Sciences*, *20*, 31-43.

Safari, P., Hosseini, M., Lashkarbolooki, M., Ghorbani, M., & Najafpour Darzi, G. (2023). Evaluation of surface activity of rhamnolipid biosurfactants produced from rice bran oil through dynamic surface tension. *Journal of Petroleum Exploration and Production Technology*, *13*(10), 2139-2153.

Saharan, B. S., Sahu, R. K., & Sharma, D. (2011). A review on biosurfactants: fermentation, current developments and perspectives. *Genetic Engineering and Biotechnology Journal*, *2011*(1), 1-14.

Salihu, A., Abdulkadir, I., & Almustapha, M. N. (2009). An investigation for potential development on biosurfactants. *Biotechnology and Molecular Biology Reviews*, *3*(5), 111-7.

Samet, J. M., & Wages, P. A. (2018). Oxidative stress from environmental exposures. *Current Opinion in Toxicology*, *7*, 60-66.

San Martín, Y. B., Toledo León, H. F., Rodríguez, A. Á., Marqués, A. M., & López, M. I. S. (2021). Rhamnolipids application for the removal of vanadium from contaminated sediment. *Current Microbiology*, *78*(5), 1949-1960.

Sanjivkumar, M., Deivakumari, M., & Immanuel, G. (2021). Investigation on spectral and biomedical characterization of rhamnolipid from a marine associated bacterium *Pseudomonas aeruginosa* (DKB1). *Archives of Microbiology*, *203*, 2297-2314.

Santos, D. K. F., Meira, H. M., Rufino, R. D., Luna, J. M., & Sarubbo, L. A. (2017). Biosurfactant production from *Candida lipolytica* in bioreactor and evaluation of its toxicity for application as a bioremediation agent. *Process Biochemistry*, *54*, 20-27.

Santos, D. K. F., Rufino, R. D., Luna, J. M., Santos, V. A., & Sarubbo, L. A. (2016). Biosurfactants: multifunctional biomolecules of the 21st century. *International Journal of Molecular Sciences*, *17*(3), 401.

Saravanan, V., & Vijayakumar, S. (2012). Isolation and screening of biosurfactant producing microorganisms from oil contaminated soil. *Journal of Academia and Industrial Research*, *1*(5), 264-268.

Sarubbo, L., Brasileiro, P., Silveira, G., Luna, J., & Rufino, R. (2018). Application of a low cost biosurfactant in the removal of heavy metals in soil. *Chemical Engineering Transactions*, *64*, 433-438.

Sazykina, M. A., Minkina, T. M., Konstantinova, E. Y., Khmelevtsova, L. E., Azhogina, T. N., Antonenko, E. M., ... & Sazykin, I. S. (2022). Pollution impact on microbial communities composition in natural and anthropogenically modified soils of Southern Russia. *Microbiological Research*, *254*, 126913.

Scientific, T. (2021). Sample preparation techniques for AAS, ICP-OES and ICP-MS for regulated testing laboratories. *ThermoFisher Scientific*.

Shao, B., Liu, Z., Zhong, H., Zeng, G., Liu, G., Yu, M., ... & Zhao, C. (2017). Effects of rhamnolipids on microorganism characteristics and applications in composting: a review. *Microbiological Research*, *200*, 33-44.

Sharma, D., Ansari, M. J., Al-Ghamdi, A., Adgaba, N., Khan, K. A., Pruthi, V., & Al-Waili, N. (2015). Biosurfactant production by *Pseudomonas aeruginosa* DSVP20 isolated from petroleum hydrocarbon-contaminated soil and its physicochemical characterization. *Environmental Science and Pollution Research*, *22*, 17636-17643.

Sharma, S., Tiwari, S., Hasan, A., Saxena, V., & Pandey, L. M. (2018). Recent advances in conventional and contemporary methods for remediation of heavy metal-contaminated soils. *3 Biotech*, *8*(4), 216.

Shchelkunova, G. A., & Shchelkunov, S. N. (2022). Smallpox, monkeypox and other human orthopoxvirus infections. *Viruses*, *15*(1), 103.

Shen, C., Jiang, L., Shao, H., You, C., Zhang, G., Ding, S., ... & Meng, Q. (2016). Targeted killing of myofibroblasts by biosurfactant di-rhamnolipid suggests a therapy against scar formation. *Scientific Reports*, *6*(1), 37553.

Shetty, S. S., Deepthi, D., Harshitha, S., Sonkusare, S., Naik, P. B., & Madhyastha, H. (2023). Environmental pollutants and their effects on human health. *Heliyon*, *9*(9).

Shi, L., Liu, Z., Yang, L., & Fan, W. (2022). Effects of oil pollution on soil microbial diversity in the Loess hilly areas, China. *Annals of Microbiology*, *72*(1), 26.

Siegmund, I., & Wagner, F. (1991). New method for detecting rhamnolipids excreted by *Pseudomonas* species during growth on mineral agar. *Biotechnology Techniques*, *5*(4), 265-268.

Silva, M. D. G. C., Medeiros, A. O., Converti, A., Almeida, F. C. G., & Sarubbo, L. A. (2024). Biosurfactants: promising biomolecules for agricultural applications. *Sustainability*, *16*(1), 449.

Silva, S. N. R. L., Farias, C. B. B., Rufino, R. D., Luna, J. M., & Sarubbo, L. A. (2010). Glycerol as substrate for the production of biosurfactant by *Pseudomonas aeruginosa* UCP0992. *Colloids and Surfaces B: Biointerfaces*, *79*(1), 174-183.

Silva, V. L., Lovaglio, R. B., Von Zuben, C. J., & Contiero, J. (2015). Rhamnolipids: solution against Aedes aegypti?. *Frontiers in Microbiology*, *6*, 88.

Sim, L., Ward, O. P., & Li, Z. Y. (1997). Production and characterisation of a biosurfactant isolated from *Pseudomonas aeruginosa* UW-1. *Journal of Industrial Microbiology and Biotechnology*, *19*(4), 232-238.

Singh, J., & Kalamdhad, A. S. (2011). Effects of heavy metals on soil, plants, human health and aquatic life. *International Journal of Research in Chemistry and Environment*, *1*(2), 15-21.

Singh, P., & Tiwary, B. N. (2016). Isolation and characterization of glycolipid biosurfactant produced by a *Pseudomonas otitidis* strain isolated from Chirimiri coal mines, India. *Bioresources and Bioprocessing*, *3*, 1-16.

Singh, S. P., Bharali, P., & Konwar, B. K. (2013). Optimization of nutrient requirements and culture conditions for the production of rhamnolipid from *Pseudomonas aeruginosa* (MTCC 7815) using Mesua ferrea seed oil. *Indian Journal of Microbiology*, *53*(4), 467-476.

Sobri, I. M., Halim, M., Lai, O. M., Lajis, A. F., Yusof, M. T., Halmi, M. I. E., ... & Wasoh, H. (2018). Emulsification characteristics of rhamnolipids by *Pseudomonas aeruginosa* using coconut oil as carbon source. *Journal of Environmental Microbiology and Toxicology*, *6*(1), 7-12.

Sokan-Adeaga, A. A., Sokan-Adeaga, M. A., Sokan-Adeaga, E. D., Oparaji, A. N., Edris, H., Tella, E. O., ... & Amubieya, O. E. (2023). Environmental toxicants and

health adversities: A review on interventions of phytochemicals. *Journal of Public Health Research*, *12*(2), 22799036231181226.

Song, H., Liang, W., Luo, K., Wang, G., Li, Q., Ji, X., ... & Peng, C. (2023). Simultaneous stabilization of Pb, Cd, and As in soil by rhamnolipid coated sulfidated nano zero-valent iron: Effects and mechanisms. *Journal of Hazardous Materials*, *443*, 130259.

Sorhie, V., Alemtoshi, B. G., Walling, B., Acharjee, S. A., & Bharali, P. (2022). Role of micellar nanoreactors in organic chemistry: Green and synthetic surfactant review. *Sustainable Chemistry and Pharmacy*, *30*, 100875.

Stipcevic, T., Piljac, T., & Isseroff, R. R. (2005). Di-rhamnolipid from *Pseudomonas aeruginosa* displays differential effects on human keratinocyte and fibroblast cultures. *Journal of Dermatological Science*, 40(2), 141-143.

Su, C. (2014). A review on heavy metal contamination in the soil worldwide: Situation, impact and remediation techniques. *Environmental Skeptics and Critics*, *3*(2), 24.

Das, S., Kalita, S. J., Bharali, P., Konwar, B. K., Das, B., & Thakur, A. J. (2013). Organic reactions in "green surfactant": An avenue to bisuracil derivative. *ACS Sustainable Chemistry & Engineering*, *1*(12), 1530-1536.

Suchman, E. (2011). Polymerase chain reaction protocol. *American Society for Microbiology*, 1-14.

Sultana, S., Sultana, R., Al-Mansur, M. A., Akbor, M. A., Bhuiyan, N. A., Ahmed, S., ... & Jamal, A. S. I. M. (2024). An industrially potent rhamnolipid-like biosurfactant produced from a novel oil-degrading bacterium, Bacillus velezensis S2. *RSC Advances*, *14*(34), 24516-24533.

Sun, W., Cao, W., Jiang, M., Saren, G., Liu, J., Cao, J., ... & Naz, I. (2018). Isolation and characterization of biosurfactant-producing and diesel oil degrading *Pseudomonas* sp. CQ2 from Changqing oil field, China. *RSC Advances*, *8*(69), 39710-39720.

Tamura, K., Stecher, G., & Kumar, S. (2021). MEGA11: molecular evolutionary genetics analysis version 11. *Molecular Biology and Evolution*, *38*(7), 3022-3027.

Thakur, P., Saini, N. K., Thakur, V. K., Gupta, V. K., Saini, R. V., & Saini, A. K. (2021). Rhamnolipid the Glycolipid Biosurfactant: Emerging trends and promising strategies in the field of biotechnology and biomedicine. *Microbial Cell Factories*, *20*, 1-15.

Thio, C. W., Lim, W. H., Md. Shah, U. K., & Phang, L. Y. (2022). Palm kernel fatty acid distillate as substrate for rhamnolipids production using *Pseudomonas* sp. LM19. *Green Chemistry Letters and Reviews*, *15*(1), 83-92.

Thushari, I., & Babel, S. (2022). Comparative study of the environmental impacts of used cooking oil valorization options in Thailand. *Journal of Environmental Management*, *310*, 114810.

Touabi, L., Ismail, N. S., Bakkar, M. R., McLean, G. R., & Abo-zeid, Y. (2025). Antiviral activity of rhamnolipids nano-micelles against rhinoviruses—*in silico* docking, molecular dynamic analysis and *in-vitro* studies. *Current Issues in Molecular Biology*, *47*(5), 333.

Tuleva, B. K., Ivanov, G. R., & Christova, N. E. (2002). Biosurfactant production by a new *Pseudomonas putida* strain. *Zeitschrift für Naturforschung C*, *57*(3-4), 356-360.

Urum, K., & Pekdemir, T. (2004a). Evaluation of biosurfactants for crude oil contaminated soil washing. *Chemosphere*, *57*(9), 1139-1150.

Urum, K., Pekdemir, T., & Çopur, M. (2004b). Surfactants treatment of crude oil contaminated soils. *Journal of Colloid and Interface Science*, *276*(2), 456-464.

Usman, M. M., Dadrasnia, A., Lim, K. T., Mahmud, A. F., & Ismail, S. (2016). Application of biosurfactants in environmental biotechnology; remediation of oil and heavy metal. *AIMS Bioengineering*, *3*(3), 289-304.

Varjani, S. J., & Upasani, V. N. (2016). Carbon spectrum utilization by an indigenous strain of *Pseudomonas aeruginosa* NCIM 5514: Production, characterization and surface active properties of biosurfactant. *Bioresource Technology*, 221, 510-516.

Varjani, S. J., Rana, D. P., Bateja, S., Sharma, M. C., & Upasani, V. N. (2014). Screening and identification of biosurfactant (bioemulsifier) producing bacteria

from crude oil contaminated sites of Gujarat, India. *International Journal of Innovative Research in Science, Engineering and Technology*, *3*(2).

Walling, B., Bharali, P., Ramachandran, D., Viswanathan, K., Hazarika, S., Dutta, N., ... & Acharjee, S. A. (2023). *In-situ* biofabrication of bacterial nanocellulose (BNC)/graphene oxide (GO) nano-biocomposite and study of its cationic dyes adsorption properties. *International Journal of Biological Macromolecules*, *251*, 126309.

Walter, V., Syldatk, C., & Hausmann, R. (2010). Screening concepts for the isolation of biosurfactant producing microorganisms. *Biosurfactants*, 1-13.

Wang, H., Sun, C., Chen, X., Yan, K., & He, H. (2023). Isolation of *Pseudomonas oleovorans* carrying multidrug resistance proteins MdtA and MdtB from wastewater. *Molecules*, *28*(14), 5403.

Wang, S., & Mulligan, C. N. (2009b). Arsenic mobilization from mine tailings in the presence of a biosurfactant. *Applied Geochemistry*, *24*(5), 928-935.

Wang, X., An, J., Cao, T., Guo, M., & Han, F. (2024). Application of biosurfactants in medical sciences. *Molecules*, *29*(11), 2606.

Wang, Y., Shen, Z., Feng, F., Chen, X., Song, L., Wan, Q., ... & Yu, X. (2022). Isolation, characterization and application of the epoxiconazole-degrading strain *Pseudomonas* sp. F1 in a soil-vegetable system. *Chemosphere*, *305*, 135463.

Wei, Y. H., Chou, C. L., & Chang, J. S. (2005). Rhamnolipid production by indigenous *Pseudomonas aeruginosa* J4 originating from petrochemical wastewater. *Biochemical Engineering Journal*, *27*(2), 146-154.

Wu, J. Y., Yeh, K. L., Lu, W. B., Lin, C. L., & Chang, J. S. (2008). Rhamnolipid production with indigenous *Pseudomonas aeruginosa* EM1 isolated from oil-contaminated site. *Bioresource Technology*, *99*(5), 1157-1164.

Xu, H., Jia, Y., Sun, Z., Su, J., Liu, Q. S., Zhou, Q., & Jiang, G. (2022). Environmental pollution, a hidden culprit for health issues. *Eco-Environment & Health*, *1*(1), 31-45.

Xue, S. W., Huang, C., Tian, Y. X., Li, Y. B., Li, J., & Ma, Y. L. (2020). Synergistic effect of rhamnolipids and inoculation on the bioremediation of petroleum-contaminated soils by bacterial consortia. *Current Microbiology*, *77*(6), 997-1005.

Yamasaki, R., Kawano, A., Yoshioka, Y., & Ariyoshi, W. (2020). Rhamnolipids and surfactin inhibit the growth or formation of oral bacterial biofilm. *BMC Microbiology*, *20*, 1-11.

Yang, R., Wang, H., Shi, M., Jiang, Y., Dong, Y., & Shi, L. (2020). Biosurfactant rhamnolipid affacts the desorption of sorbed As (III), As (V), Cr (VI), Cd (II) and Pb (II) on iron (oxyhydr) oxides and clay minerals. *International Biodeterioration & Biodegradation*, *153*, 105019.

Yang, T., Li, J., Mao, Y., Wu, H., Lin, M., & Chen, L. (2024). The role of rhamnolipids in the growth and defense responses of passion fruit plants. *Physiology and Molecular Biology of Plants*, 1-13.

Yateem, A., Balba, M. T., Al-Shayji, Y., & Al-Awadhi, N. (2002). Isolation and characterization of biosurfactant-producing bacteria from oil-contaminated soil. *Soil and Sediment Contamination*, *11*(1), 41-55.

Yin, H., Qiang, J., Jia, Y., Ye, J., Peng, H., Qin, H., ... & He, B. (2009). Characteristics of biosurfactant produced by *Pseudomonas aeruginosa* S6 isolated from oil-containing wastewater. *Process Biochemistry*, *44*(3), 302-308.

Yoo, J. C., Lee, C., Lee, J. S., & Baek, K. (2017). Simultaneous application of chemical oxidation and extraction processes is effective at remediating soil co-contaminated with petroleum and heavy metals. *Journal of Environmental Management*, *186*, 314-319.

Youssef, N. H., Duncan, K. E., Nagle, D. P., Savage, K. N., Knapp, R. M., & McInerney, M. J. (2004). Comparison of methods to detect biosurfactant production by diverse microorganisms. *Journal of Microbiological Methods*, *56*(3), 339-347.

Zargar, A. N., Mishra, S., Kumar, M., & Srivastava, P. (2022). Isolation and chemical characterization of the biosurfactant produced by *Gordonia* sp. IITR100. *Plos one*, *17*(4), e0264202.

Zeng, G., Fu, H., Zhong, H., Yuan, X., Fu, M., Wang, W., & Huang, G. (2007). Co-degradation with glucose of four surfactants, CTAB, Triton X-100, SDS and Rhamnolipid, in liquid culture media and compost matrix. *Biodegradation*, *18*(3), 303-310.

Zhang, D., Luo, L., Jin, M., Zhao, M., Niu, J., Deng, S., & Long, X. (2022). Efficient isolation of biosurfactant rhamnolipids from fermentation broth via aqueous two-phase extraction with 2-propanol/ammonium sulfate system. *Biochemical Engineering Journal*, *188*, 108676.

Zhang, H. Z., Long, X. W., Sha, R. Y., Zhang, G. L., & Meng, Q. (2009). Biotreatment of oily wastewater by rhamnolipids in aerated active sludge system. *Journal of Zhejiang University Science B*, 10(11), 852-859.

Zhang, X., Xu, D., Zhu, C., Lundaa, T., & Scherr, K. E. (2012). Isolation and identification of biosurfactant producing and crude oil degrading *Pseudomonas aeruginosa* strains. *Chemical Engineering Journal*, *209*, 138-146.

Zhang, X., Zhang, X., Wang, S., & Zhao, S. (2022). Improved remediation of co-contaminated soils by heavy metals and PAHs with biosurfactant-enhanced soil washing. *Scientific Reports*, *12*(1), 3801.

Zhang, Y., & Miller, R. (1992). Enhanced octadecane dispersion and biodegradation by a Pseudomonas rhamnolipid surfactant (biosurfactant). *Applied and Environmental Microbiology*, *58*(10), 3276-3282.

Zhang, Y., & Miller, R. M. (1994). Effect of a *Pseudomonas* rhamnolipid biosurfactant on cell hydrophobicity and biodegradation of octadecane. *Applied and Environmental Microbiology*, *60*(6), 2101-2106.

Zhao, F., Jiang, H., Sun, H., Liu, C., Han, S., & Zhang, Y. (2019). Production of rhamnolipids with different proportions of mono-rhamnolipids using crude glycerol and a comparison of their application potential for oil recovery from oily sludge. *RSC advances*, *9*(6), 2885-2891.

Zhao, F., Shi, R., Ma, F., Han, S., & Zhang, Y. (2018). Oxygen effects on rhamnolipids production by *Pseudomonas aeruginosa*. *Microbial Cell Factories*, *17*, 1-11.

Zhao, F., Wang, B., Yuan, M., & Ren, S. (2022). Comparative study on antimicrobial activity of mono-rhamnolipid and di-rhamnolipid and exploration of cost-effective antimicrobial agents for agricultural applications. *Microbial Cell Factories*, *21*(1), 221.

Zhao, P., Quan, C., Jin, L., Wang, L., Wang, J., & Fan, S. (2013). Effects of critical medium components on the production of antifungal lipopeptides from *Bacillus amyloliquefaciens* Q-426 exhibiting excellent biosurfactant properties. *World Journal of Microbiology and Biotechnology*, *29*, 401-409.

Zhong, H., Liu, Y., Liu, Z., Jiang, Y., Tan, F., Zeng, G., ... & Liang, Y. (2014). Degradation of pseudo-solubilized and mass hexadecane by a *Pseudomonas aeruginosa* with treatment of rhamnolipid biosurfactant. *International Biodeterioration & Biodegradation*, *94*, 152-159.

Zhong, H., Zeng, G. M., Liu, J. X., Xu, X. M., Yuan, X. Z., Fu, H. Y., ... & Ding, Y. (2008). Adsorption of monorhamnolipid and dirhamnolipid on two *Pseudomonas aeruginosa* strains and the effect on cell surface hydrophobicity. *Applied Microbiology and Biotechnology*, *79*, 671-677.

Zhou, J., Xue, R., Liu, S., Xu, N., Xin, F., Zhang, W., ... & Dong, W. (2019). High di-rhamnolipid production using *Pseudomonas aeruginosa* KT1115, separation of mono/di-rhamnolipids, and evaluation of their properties. *Frontiers in Bioengineering and Biotechnology*, *7*, 245.

Zhu, M., Zhang, H., Cui, W., Su, Y., Sun, S., Zhao, C., & Liu, Q. (2024). Performance evaluation of rhamnolipid biosurfactant produced by *Pseudomonas aeruginosa* and its effect on marine oil-spill remediation. *Archives of Microbiology*, *206*(4), 183.

Appendix -I

i. Composition of MSM

Sl. No.	Ingredients	Per litre
1.	urea	2.0 g
2.	$(NH_4)_2SO_4$	2.0 g
3.	Na_2HPO_4	3.61 g
4.	KH_2PO_4	1.75 g
5.	$MgSO_4$ $7H_2O$	0.2 g
6.	$CaCl_2$ $2H_2O$	50 mg
7.	$FeSO_4$ $7H_2O$	1.0 mg
8.	$CuSO_4$ $7H_2O$	50 µg
9.	$MnSO_4$ $5H_2O$	10 µg
10.	H_3BO_3	10 µg
11.	$ZnSO_4$ $7H_2O$	70 µg
12.	MnO_3	10 µg
13.	pH	6.8 ± 0.2

Preparation of the Medium

All the components were dissolved in distilled/deionized water, and the volume was adjusted to 1 L. The mixture was thoroughly stirred and sterilization was carried out by autoclaving at 121 °C for 15 minutes under 15 psi pressure.

ii. Composition of BH medium

Sl. No.	Ingredients	Grams per litre
1.	Magnesium sulphate	0.200
2.	Calcium chloride anhydrous	0.020
3.	Potassium dihydrogen phosphate	1.000
4.	Dipotassium hydrogen phosphate	1.000
5.	Ammonium nitrate	1.000
6.	Ferric chloride	0.050
7.	pH	7.0 ± 0.2

Preparation of the Medium

All the components were dissolved in distilled/deionized water, and the volume was adjusted to 1 L. The mixture was thoroughly stirred and gently heated until it

reached boiling. Sterilization was carried out by autoclaving at 121 °C for 15 minutes under 15 psi pressure.

iii. Composition of MHA medium

Sl. No.	Ingredients	Grams per litre
1.	Beef extract	2.0
2.	Acid hydrolysate of casein	17.5
3.	Starch	1.5
4.	Agar	16
5.	pH	7.3 ± 0.1

Preparation of the Medium

All the components were dissolved in distilled/deionized water, and the volume was adjusted to 1 L. The mixture was thoroughly stirred and gently heated until it reached boiling. Sterilization was carried out by autoclaving at 121 °C for 15 minutes under 15 psi pressure.

iv. Composition of LBA medium

Sl. No.	Ingredients	Grams per litre
1.	Tryptone	10.000
2.	Yeast extract	5.000
3.	Sodium chloride	10.000
4.	Agar	16
5.	pH	7.5 ± 0.2

Preparation of the Medium

All the components were dissolved in distilled/deionized water, and the volume was adjusted to 1 L. The mixture was thoroughly stirred and gently heated until it reached boiling. Sterilization was carried out by autoclaving at 121 °C for 15 minutes under 15 psi pressure.

v. Composition of TSB medium

Sl. No.	Ingredients	Grams per litre
1.	Tryptone	8.500
2.	Soya peptone	1.500
3.	Sodium chloride	5.100

4.	Dextrose (Glucose)	1.770
5.	Dipotassium hydrogen phosphate	1.250
6.	Tryptose	10.380
7.	Yeast extract	3.000
8.	pH	7.3 ± 0.2

Preparation of the Medium

All the components were dissolved in distilled/deionized water, and the volume was adjusted to 1 L. The mixture was thoroughly stirred and gently heated until it reached boiling. Sterilization was carried out by autoclaving at 121 °C for 15 minutes under 15 psi pressure.

vi. Composition of PBS buffer

Sl. No.	Ingredients	Grams per litre
1.	Sodium chloride	8
2.	Potassium Chloride	0.2
3.	Sodium Phosphate Dibasic	1.44
4.	Potassium Phosphate Monobasic	0.245
5.	pH	7.4 ± 0.1

Preparation of the buffer

All the components were dissolved in distilled water, and the final volume was made up to 1 L. The pH of the solution was adjusted to 7.4, after which it was sterilized by autoclaving at 121 °C for 15 minutes.

vii. Composition of Dulbecco's Modified Eagle Medium

Components	Concentration (mg/L)
Amino Acids	
Glycine	30.0
L-Arginine hydrochloride	84.0
L-Cystine 2HCl	63.0
L-Histidine hydrochloride-H_2O	42.0
L-Isoleucine	105.0
L-Leucine	105.0
L-Lysine hydrochloride	146.0
L-Methionine	30.0

L-Phenylalanine	66.0
L-Serine	42.0
L-Threonine	95.0
L-Tryptophan	16.0
L-Tyrosine	72.0
L-Valine	94.0
Vitamins	
Choline chloride	4.0
D-Calcium pantothenate	4.0
Folic Acid	4.0
Niacinamide	4.0
Pyridoxine hydrochloride	4.0
Riboflavin	0.4
Thiamine hydrochloride	4.0
i-Inositol	7.2
Inorganic Salts	
Calcium Chloride ($CaCl_2$ $2H_2O$)	264.0
Ferric Nitrate ($Fe(NO_3)_3$ $9H_2O$)	0.1
Magnesium Sulfate ($MgSO_4$ 7H2O)	200.0
Potassium Chloride (KCl)	400.0
Sodium Bicarbonate ($NaHCO_3$)	3700.0
Sodium Chloride (NaCl)	6400.0
Sodium Phosphate monobasic (NaH_2PO_4-$2H_2O$)	141.0
Other Components	
D-Glucose (Dextrose)	1000.0
Sodium Pyruvate	110.0

viii. Abbreviation of Units/symbols

Units/symbols	Abbreviation
g	Gram
ml	Millilitres
±	Plus–minus sign
rpm	Revolutions Per Minute

v/v	Volume per volume
Mg	Milligrams
N	Normal
%	Percent
°C	Celsius
mN/m	Millinewton per meter
µL	Microliter
µm	Micrometre
mg/mL	Microgram per millilitre
ng	Nanograms
g/L	Gram per litre
CuKα	copper K-alpha
Å	Angstrom
KV	kilovolt
mA	Milliampere
h	Hour
w/v	Weight per volume
nm	Nanometre
bp	Base pair
µM	Micromolar
mm	Millimetre
ppm	Parts per million
As	Arsenic
Cd	Cadmium
Cr	Chromium
µg/ml	Microgram per millilitre
R_f	Retention Factor

ix. Composition of Crude Oil after 15, 30, 45 and 60 days of degradation

15 Days	30 Days	45 Days	60 Days
▪ Pentadecane, 2,6,10-trimethyl- ▪ Heptadecane, 2,6,10,14-tetramethyl- ▪ Heptadecane, 2,6-dimethyl-	▪ Bicyclo[4.4.1]undeca-1,3,5,7,9-pentaene ▪ Naphthalene, 1-methyl- ▪ Naphthalene, 2-methyl- ▪ Heptadecane, 2,6,10,14-tetramethyl- ▪ Dodecane, 2,6,10-trimethyl-	▪ Pentadecane, 2,6,10-trimethyl- ▪ Heptadecane, 2,6,10,14-tetramethyl-	▪ Pentadecane, 2,6,10-trimethyl- ▪ Heptadecane, 2,6,10,14-tetramethyl- ▪ Pentadecane ▪ Pentadecane, 2,6,10-trimethyl-

▪ Pentadecane, 2,6,10-trimethyl- ▪ Pentadecane, 2,6,10,14-tetramethyl- ▪ Heptadecane, 2,6,10,14-tetramethyl- ▪ 1-Hexadecanol, 2-methyl- ▪ 2-Methyl-Z-4-tetradecene ▪ Hexadecane, 1,1-bis(dodecyloxy)- ▪ Tetradecane, 2,6,10-trimethyl- ▪ Heptadecane, 2,6,10,15-tetramethyl- ▪ Dodecane, 2,6,10-trimethyl- ▪ tert-Hexadecanethiol ▪ 17-Pentatriacontene ▪ 1-Hexacosene ▪ Octadecane, 3-ethyl-5-(2-ethylbutyl)- ▪ 17-Pentatriacontene ▪ Oleic acid, 3-(octadecyloxy)propyl ester ▪ Octadecane, 3-ethyl-5-(2-ethylbutyl)- ▪ Tetrapentacontane, 1,54-dibromo-	▪ Pentadecane ▪ Naphthalene, 2,6-dimethyl- ▪ Naphthalene, 1,7-dimethyl- ▪ 1,4-Dimethylazulene ▪ Naphthalene, 1,7-dimethyl- ▪ Naphthalene, 2,6-dimethyl- ▪ Naphthalene, 1,3-dimethyl- ▪ Heptadecane, 2,6,10,14-tetramethyl- ▪ 2,6,10-Trimethyltridecane ▪ Heptadecane, 2,6,10,15-tetramethyl- ▪ 3-(2-Methyl-propenyl)-1H-indene ▪ Naphthalene, 1,4,5-trimethyl- ▪ Naphthalene, 1,4,6-trimethyl- ▪ Tetradecane, 2,6,10-trimethyl- ▪ Pentadecane, 2,6,10-trimethyl- ▪ Heptadecane, 2,6,10,15-tetramethyl- ▪ Pentadecane, 2,6,10,14-tetramethyl- ▪ Heptadecane, 2,6,10,14-tetramethyl- ▪ Pentadecane, 2,6,10-trimethyl- ▪ tert-Hexadecanethiol ▪ Erucic acid ▪ cis-10-Nonadecenoic acid ▪ Tetradecane, 2,6,10-trimethyl- ▪ Dodecane, 2,6,10-trimethyl- ▪ Heptadecane, 2,6,10,15-tetramethyl- ▪ tert-Hexadecanethiol ▪ 2-Myristynoyl pantetheine ▪ 1-Hexadecanol, 2-methyl-	▪ Dodecane, 2,6,11-trimethyl- ▪ Heptadecane, 2,6,10,14-tetramethyl- ▪ Pentadecane, 2,6,10-trimethyl- ▪ Pentadecane, 2,6,10,14-tetramethyl- ▪ Heptadecane, 2,6,10,15-tetramethyl- ▪ Dodecane, 2,6,10-trimethyl- ▪ Heptadecane, 2,6,10,14-tetramethyl- ▪ tert-Hexadecanethiol ▪ Octadecane, 3-ethyl-5-(2-ethylbutyl)- ▪ Heptadecane, 9-hexyl- ▪ tert-Hexadecanethiol ▪ 2,5-Furandione, dihydro-3-tetradecyl-	▪ Heptadecane, 2,6,10,14-tetramethyl- ▪ Pentadecane, 2,6,10,14-tetramethyl- ▪ 1-Hexadecanol, 2-methyl- ▪ 2-Methyl-Z-4-tetradecene ▪ tert-Hexadecanethiol ▪ Tetradecane, 2,6,10-trimethyl- ▪ Heptadecane, 2,6,10,15-tetramethyl- ▪ Dodecane, 2,6,10-trimethyl- ▪ tert-Hexadecanethiol ▪ Octadecane, 3-ethyl-5-(2-ethylbutyl)- ▪ Heptadecane, 9-hexyl- ▪ 5,8,11,14-Eicosatetraynoic acid ▪ 5,8,11,14-Eicosatetraynoic acid, methyl ester ▪ Tricyclo[7.4.1.1(2,7)]pentadeca-2,4,6,9,11,13-hexaene-8-ol ▪ 1-Hexadecanol, 2-methyl- ▪ 9-Hexadecenoic acid

▪ Ethanol, 2-(octadecyloxy)-	▪ n-Hexadecanoic acid ▪ Estra-1,3,5(10)-trien-17ß-ol ▪ l-(+)-Ascorbic acid 2,6-dihexadecanoate ▪ 1-Hexadecanol, 2-methyl- ▪ tert-Hexadecanethiol ▪ Erucic acid ▪ 13-Hexyloxacyclotridec-10-en-2-one ▪ 17-Octadecynoic acid ▪ Z,Z-3,15-Octadecadien-1-ol acetate ▪ trans-13-Octadecenoic acid ▪ cis-Vaccenic acid ▪ cis-13-Octadecenoic acid	▪ 17-Pentatriacontene ▪ 10-Acetoxy-2-hydroxy-1,2,6a,6b,9,9,12a-heptamethyl-1,3,4,5,6, ▪ 1,3-Diphenyl-3-methylcyclopropene ▪ 2-Myristynoyl pantetheine	▪ tert-Hexadecanethiol ▪ 10-Acetoxy-2-hydroxy-1,2,6a,6b,9,9,12a-heptamethyl-1,3,4,5,6, ▪ 1,3-Diphenyl-3-methylcyclopropene ▪ Spiro[2.3]hexane-5-carboxylic acid, 1,1-diphenyl-, methyl ester ▪ 17-Pentatriacontene ▪ 9-Hexadecenoic acid ▪ 9-Hexadecenoic acid, eicosyl ester, (Z)-

x. List of database, tools and softwares used

Sl. No.	Name of Tools/Softwares
1.	NCBI blast (https://blast.ncbi.nlm.nih.gov/Blast.cgi)
2.	MEGA 11 (Version 11.0.13)
3.	Uniprot server (Uniprot ID: Q8V4Y0)
4.	Swiss-Model online tool (https://swissmodel.expasy.org/)
5.	Pubchem database (https://pubchem.ncbi.nlm.nih.gov/)
6.	Chemdraw 3D 2021
7.	Chemdraw Ultra 12.0
8.	Chemoffice 2021
9.	Molecular Mechanics 2
10.	Swiss ADME web-based services (http://www.swissadme.ch/)
11.	Molegro Virtual Docker 6.0
12.	BIOVIA Discovery Studios 2014
13.	Microsoft Excel 2019
14.	Origin 2021

xi. Extracted ion chromatogram (EIC) Scan of BS (LC-MS)

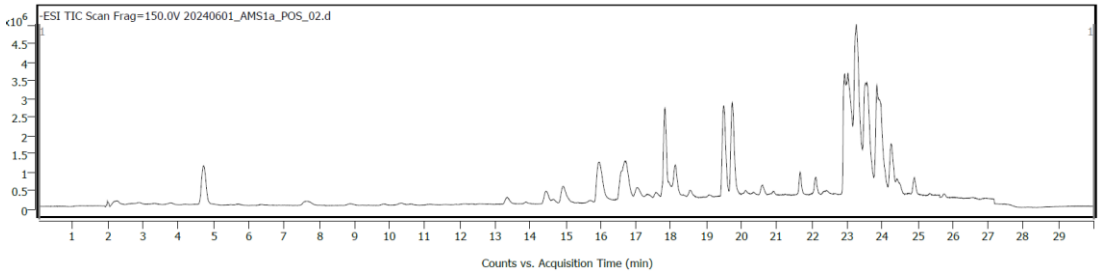

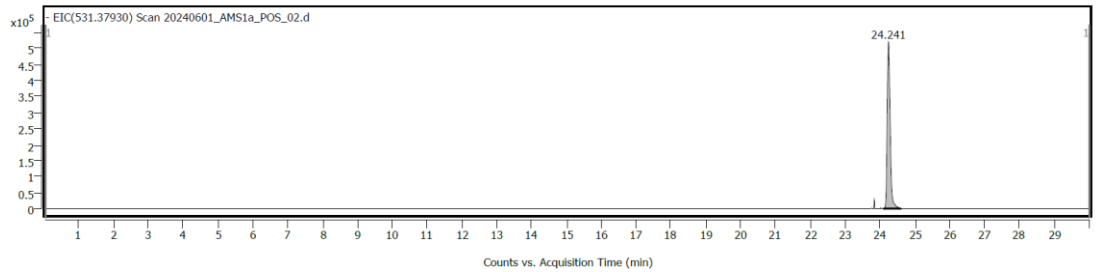

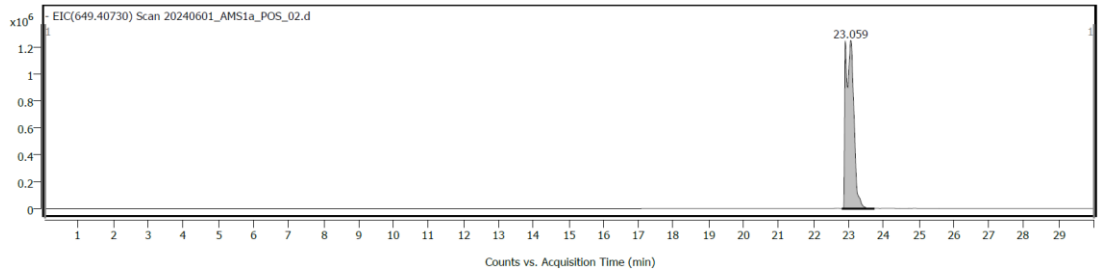

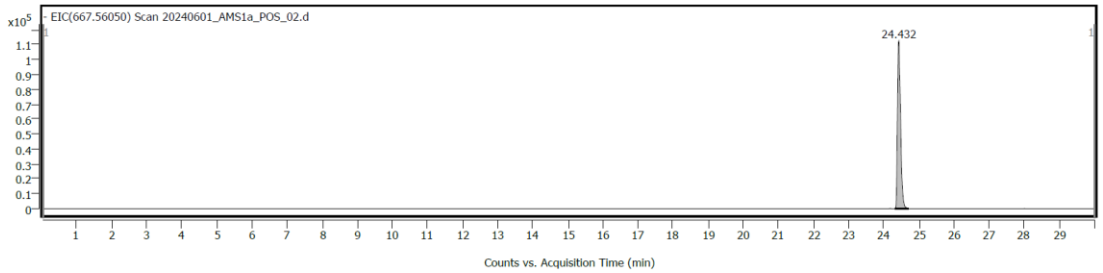

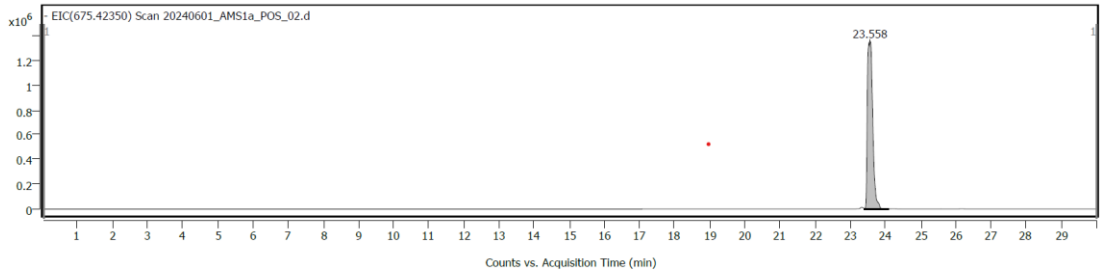

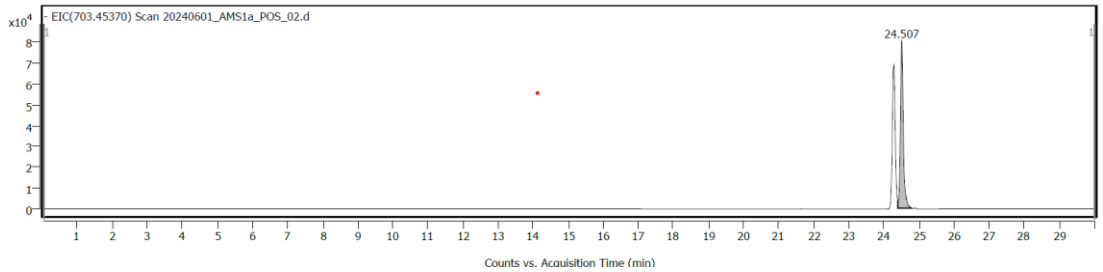

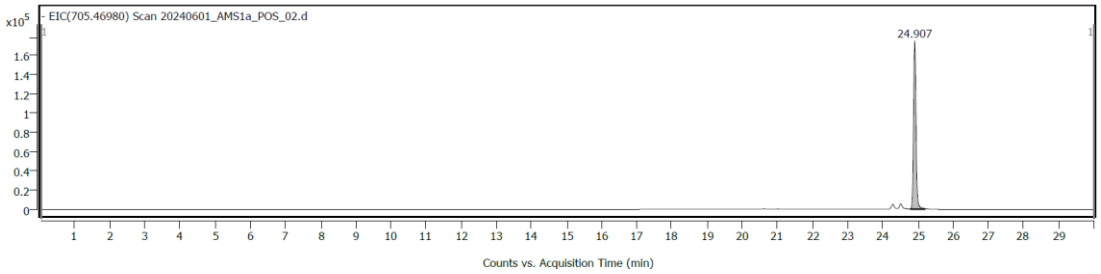

xii. Bacterial strains used in the Study

Sl. No.	Bacterial Strain	Type	Source	Reference No
1	*Bacillus subtilis*	Gram-positive	MTCC	121
2	*Listeria monocytogenes*	Gram-positive	MTCC	657
3	*Staphylococcus aureus*	Gram-positive	MTCC	3160
4	*Escherichia coli*	Gram-negative	MTCC	40
5	*Ralstonia eutropha*	Gram-negative	MTCC	8320
6	*Salmonella enterica*	Gram-negative	MTCC	1164
7	*Klebsiella pneumoniae*	Gram-negative	MTCC	618

xiii. Source and ethical approval for rat primary hepatocytes

Details	Description
Cell Type	Rat primary hepatocytes
Provided by	Dr. Manivannan's Laboratory, Bharathiar University, India
Rat Strain	Male albino Wistar rats
Age & Weight	8–10 weeks old; 180–220 g
Source of Animals	Laboratory Animal Medicine Unit, TANUVAS, Chennai, India
Housing Conditions	3 rats per cage; temperature: 25 ± 3 °C; humidity: 40–55%; light/dark cycle: 12 h/12 h
Feeding	Feed and water *ad libitum*
Ethical Approval	Animal Ethical Committee, Bharathiar University
Registration No.	722/Go/Re/S/02/CPCSEA
Proposal No.	06
Guidelines Followed	CPCSEA, New Delhi, India

xiv. Assembled FASTA Format sequence of AMS1a (16s rRNA sequencing)

>BI8615

TGGTAGTGGGGGATAACGTCCGGAAACGGGCGCTAATACCGCATA
CGTCCTGAGGGAGAAAGTGGGGGATCTTCGGACCTCACGCTATCA
GATGAGCCTAGGTCGGATTAGCTAGTTGGTGGGGTAAAGGCCTAC
CAAGGCGACGATCCGTAACTGGTCTGAGAGGATGATCAGTCACAC
TGGAACTGAGACACGGTCCAGACTCCTACGGGAGGCAGCAGTGGG
GAATATTGGACAATGGGCGAAAGCCTGATCCAGCCATGCCGCGTG
TGTGAAGAAGGTCTTCGGATTGTAAAGCACTTTAAGTTGGGAGGA
AGGGCAGTAAGTTAATACCTTGCTGTTTTGACGTTACCAACAGAAT
AAGCACCGGCTAACTTCGTGCCAGCAGCCGCGGTAATACGAAGGG
TGCAAGCGTTAATCGGAATTACTGGGCGTAAAGCGCGCGTAGGTG
GTTCAGCAAGTTGGATGTGAAATCCCCGGGCTCAACCTGGGAACT
GCATCCAAAACTACTGAGCTAGAGTACGGTAGAGGGTGGTGGAAT
TTCCTGTGTAGCGGTGAAATGCGTAGATATAGGAAGGAACACCAG
TGGCGAAGGCGACC

xv. Reagents used

Sl. No.	Reagent	Preparation
1.	Anthrone	Prepared by dissolving 0.2 grams of anthrone in 100 mL of conc. H_2SO_4
2.	Ninhydrin	Prepared by dissolving 0.35g grams of ninhydrin in 100 mL of ethanol
3.	Orcinol	Prepared by dissolving 0.19 grams of orcinol in 100 ml of 53% H_2SO_4

xvi. Interaction of viral protein with Tecovirimat

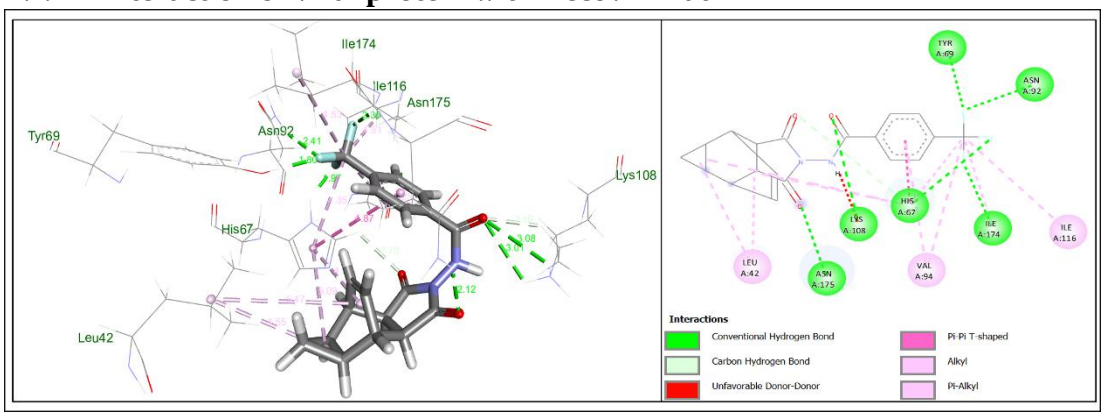

xvii. Interaction of viral protein with Aztreonam

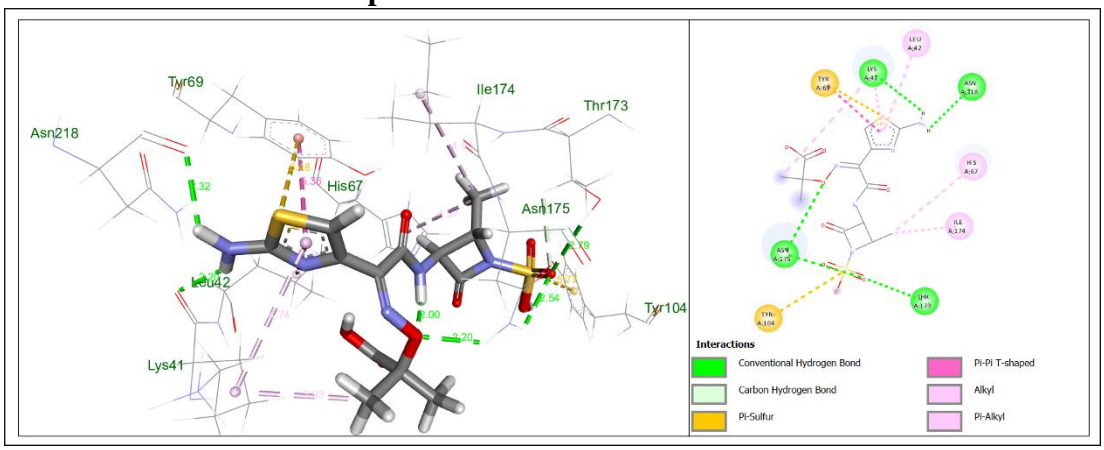

xviii. Interaction of viral protein with Lidocaine

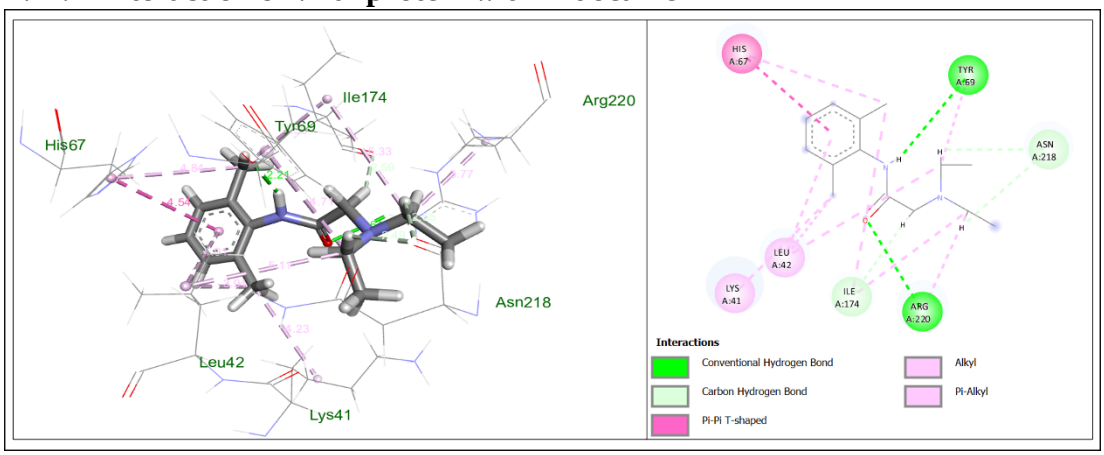

xix. Interaction of viral protein with di-RL C_8-C_{10}

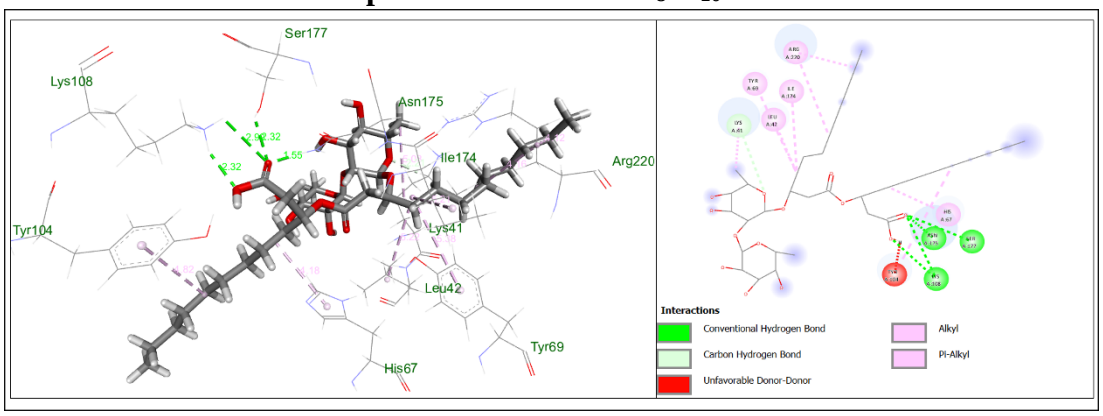

xx. Interaction of viral protein with di-RL C_{10}-C_{12}

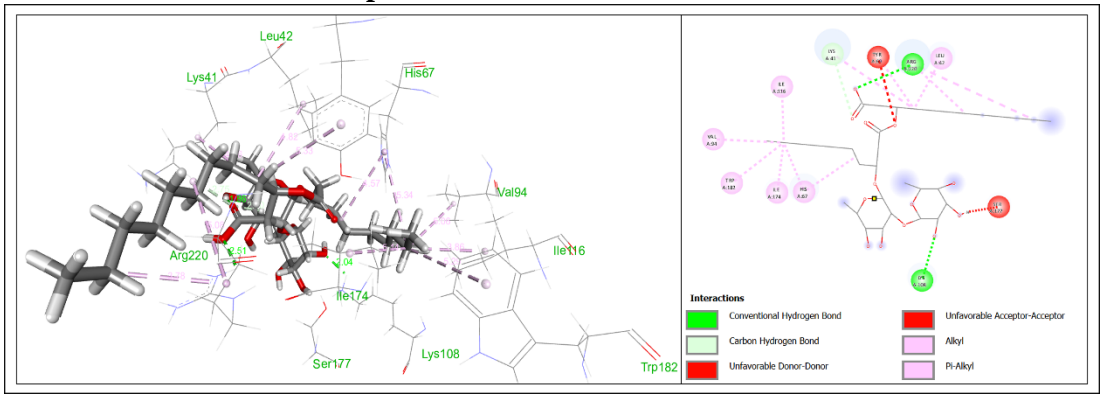

xxi. Interaction of viral protein with di-RL C_{10}-C_{14}

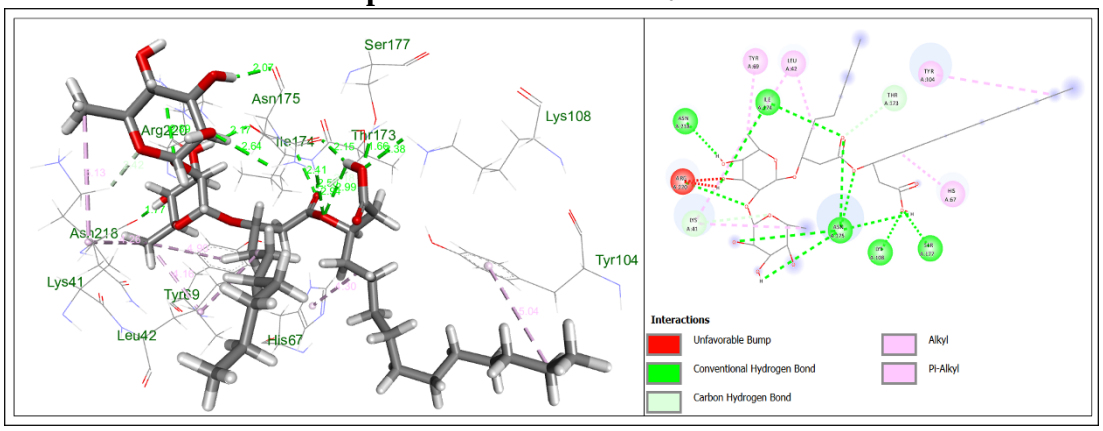

xxii. Interaction of viral protein with di-RL C_{10}-C_{14-1}

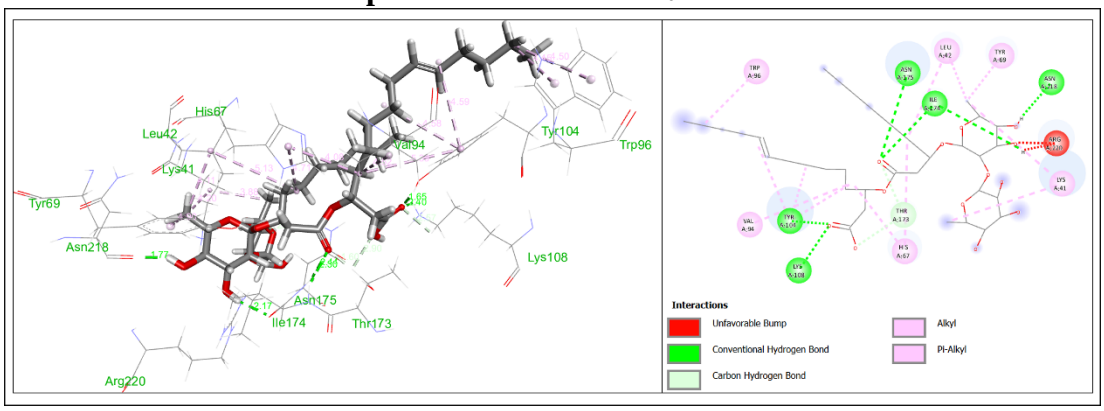

xxiii. Interaction of viral protein with di RL C_{12}-C_{12}

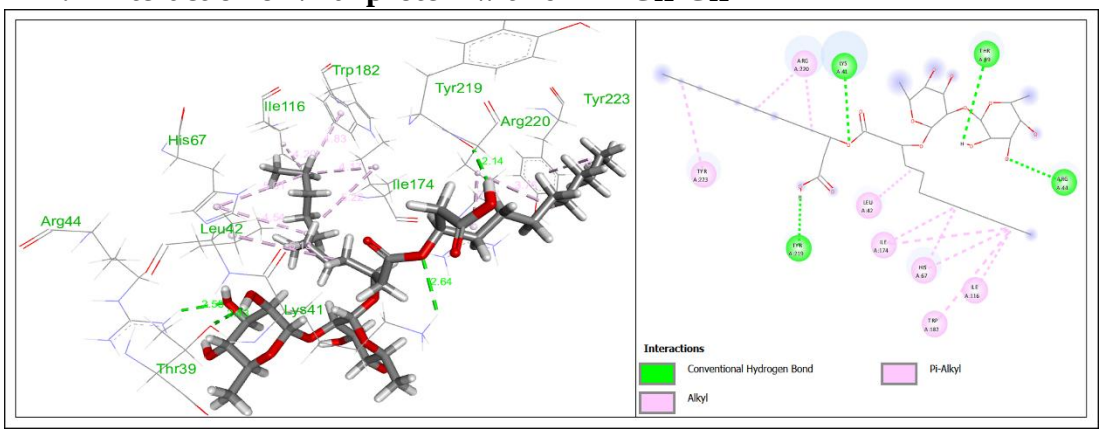

xxiv. Interaction of viral protein with di-RL C_{14}-C_{10}

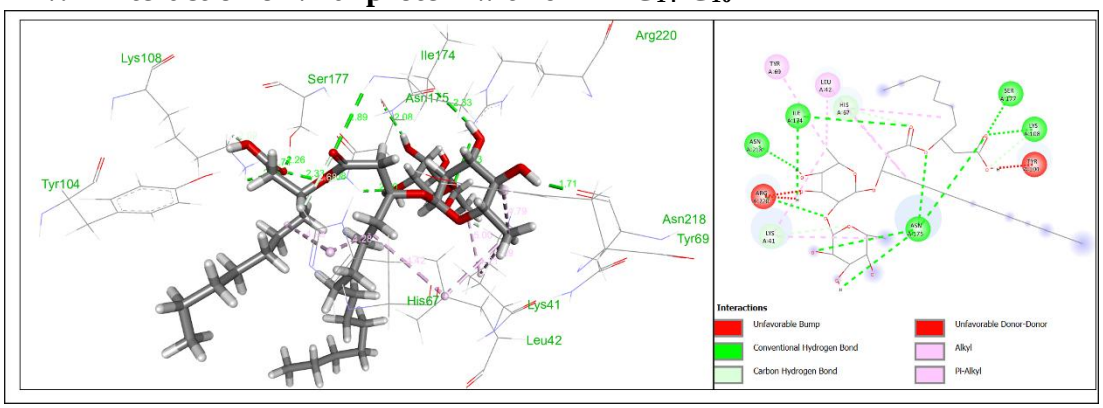

xxv. Interaction of viral protein with mono-RL C_{10}-C_{10}

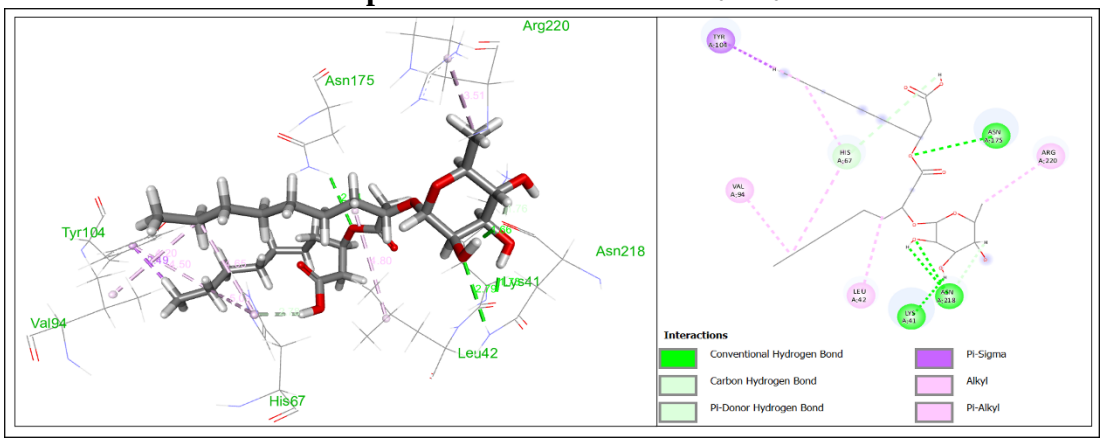

xxvi. Hydrogen bonding interactions between receptor protein and ligand and the bond distances.

Ligand	Category	Interaction	Distance (Å)
di-RL C_8-C_{10}	H Bond	LYS108:HZ1 - :[001:O13	2.99176
		LYS108:HZ2 - :[001:O12	2.32199
		ASN175:HD21 - :[001:O13	1.5511
		SER177:HG - :[001:O13	2.32096
		LYS41:HE1 - :[001:O1	2.20633
di-RL C_{10}-C_{12}	H Bond	LYS108:HZ2 - :[031:O8	2.0365
		ARG220:HH22 - :[031:O12	2.50798
		:[031:H11 - :[031:O13	1.86285
		LYS41:HE1 - :[031:O13	2.75362
		:[031:H2 - :[031:O13	2.10186
di-RL C_{10}-C_{14}	H bond	LYS108:HZ1 - :[021:O12	2.37976
		ILE174:HN - :[021:O11	2.49589
		ASN175:HN - :[021:O11	2.41014
		ASN175:HD21 - :[021:O10	2.94369
		ASN175:HD22 - :[021:O8	2.63846
		SER177:HG - :[021:O12	1.66281
		ARG220:HH21 - :[021:O3	2.89193
		:[021:H11 - ASN218:O	1.77227
		:[021:H15 - ILE174:O	2.17236
		:[021:H20 - ASN175:O	2.07285
		:[021:H32 - ASN175:OD1	2.15309

		:[021:H32 - :[021:O10	2.99302
		LYS41:HE1 - :[021:O2	2.42398
		THR173:HB - :[021:O11	2.17616
di-RL C_{10}-$C_{14:1}$	H bond	TYR104:HH - :[001:O13	1.65338
		LYS108:HZ2 - :[001:O13	2.39628
		ILE174:HN - :[001:O11	2.30079
		ASN175:HN - :[001:O11	2.44023
		:[001:H11 - ASN218:O	1.77109
		:[001:H15 - ILE174:O	2.16995
		LYS108:HE1 - :[001:O13	2.56777
		THR173:HB - :[001:O11	1.59645
		THR173:HB - :[001:O12	2.9036
		:[001:H4 - :[001:O2	2.22529
di-RL C_{12}-C_{12}	H bond	LYS41:HZ2 - :[031:O10	2.64204
		ARG44:HH11 - :[031:O7	2.54503
		:[031:H21 - THR39:OG1	2.42532
		:[031:H32 - TYR219:O	2.13506
di-RL C_{14}-C_{10}	H bond	LYS108:HZ1 - :[011:O13	2.71137
		LYS108:HZ2 - :[011:O13	2.47875
		ILE174:HN - :[011:O11	2.88865
		ASN175:HD21 - :[011:O10	3.07696
		ASN175:HD21 - :[011:O13	2.33052
		ASN175:HD22 - :[011:O8	2.49594
		SER177:HG - :[011:O13	2.26361
		ARG220:HH21 - :[011:O3	2.82693
		:[011:H11 - ASN218:O	1.71386
		:[011:H15 - ILE174:O	2.3322
		:[011:H20 - ASN175:O	2.0847
		LYS41:HE1 - :[011:O2	2.45439
		HIS67:HE1 - :[011:O11	2.68048
		LYS108:HE1 - :[011:O12	2.09324
Mono-RL C_{10}-C_{10}	H bond	ASN175:HD22 - :[031:O6	2.93736
		ASN218:HD22 - :[031:O2	2.79018

		:[031:H6 - ASN218:O	1.66047
		:[031:H11 - LYS41:O	1.73414
		:[031:H1 - ASN218:O	1.75737
		:[031:H22 - HIS67	2.77654
Chondroitin sulphate	H bond	ARG44:HH11 - :[001:O6	2.34251
		TYR69:HH - :[001:O5	1.82048
		ASN92:HD21 - :[001:O13	2.33371
		TYR104:HH - :[001:O11	1.63097
		LYS108:HZ2 - :[001:O11	2.35294
		ILE174:HN - :[001:O14	2.87169
		ASN175:HD21 - :[001:O3	2.04235
		:[001:H12 - ASN175:OD1	2.00415
		:[001:H12 - :[001:O10	2.74527
		:[001:H20 - ASN175:OD1	2.57843
		HIS67:HE1 - :[001:O1	2.3988
		HIS67:HE1 - :[001:O7	2.34985
		HIS67:HE1 - :[001:O15	2.60644
		LYS108:HE1 - :[001:O11	2.74536
		THR173:HA - :[001:O14	2.48372
		:[001:H1 - :[001:O10	4.45888
		:[001:H5 - HIS67:NE2	2.34251
	Pi-sulfur	:[001:S1 - HIS67	1.82048
Tecoverimat	H bond	HIS67:HD1 - :[001:F2	1.97477
		TYR69:HH - :[001:F1	1.79847
		ASN92:HD21 - :[001:F1	2.40981
		LYS108:HZ1 - :[001:O3	3.08382
		LYS108:HZ2 - :[001:O3	3.00882
		ILE174:HN - :[001:F3	2.3452
		ASN175:HD21 - :[001:O1	2.12339
		HIS67:HE1 - :[001:O2	2.69639
		LYS108:HE1 - :[001:O3	2.59175
Lidocaine	H bond	ARG220:HH22 - :[011:O1	2.64332
		:[011:H7 - TYR69:OH	2.20657

		:[011:H2 - ILE174:O	2.58581
		:[011:H4 - ASN218:O	2.55389
		:[011:H6 - ASN218:O	2.48991
Aztreonam	H bond	THR173:HG1 - :[001:O3	2.7895
		ASN175:HD21 - :[001:O3	2.54207
		ASN175:HD22 - :[001:O6	2.20075
		:[001:H6 - :[001:O6	2.00174
		:[001:H16 - LYS41:O	2.20241
		:[001:H17 - ASN218:O	2.32301
		THR173:HB - :[001:O3	2.97127

xxvii. Different sample collection sites in Mokokchung Town, Nagaland.

Arkong ward (AMS)

Arkong ward (SBIS)

Tongdentsuyong ward (MMS)

*Sungkomen ward (*JMS)

Kapayong sector (LLS)

Kapayong Sector (MMS)

Tsusapang sector (TSS)

Penli ward (PNS)

Majakong ward (MJS)

Sewak gate (SPS)

Appendix-II

i. Publications

- **Alemtoshi**, Sorhie, V. and Bharali, P., 2026. Leveraging the green petroleum hydrocarbon remediation potential of a biosurfactant producing indigenous Oleophilic bacterium isolated from hydrocarbon soiled environment. *Nature Environment and Pollution Technology*, *25*(1), p. B4309.
- Sorhie, V., **Alemtoshi**, Bharali, P., Ramachandran, D., Kanagasabai, V., Mahalakshmi, B., ... & Vishwakarma, V. (2025). Investigation on Physicochemical Attributes, Remediation Potential, and Therapeutic Perspective of a Bioamphiphile Produced by a Hydrocarbonoclastic Bacterium. *Chemistry Select*, *10*(28), e01173.
- Acharjee, S. A., Bharali, P., Ramachandran, D., Kanagasabai, V., Hazarika, S., Koch, P. J., ... **Alemtoshi.,**& Vishwakarma, V. (2025). Bacterial cell factories for sustainable production of green polyesters using saccharides: unlocking the potential to mitigate microplastic pollution. *Journal of Polymer Research*, *32*(7), 1-22.
- Walling, B., Bharali, P., Ramachandran, D., Kanagasabai, V., Dutta, N., Hazarika, S., ... **Alemtoshi.**, Sorhie, V & Vishwakarma, V. (2024). Bacterial valorization of agricultural-waste into a nano-sized cellulosic matrix for mitigating emerging pharmaceutical pollutants: An eco-benign approach. *International Journal of Biological Macromolecules*, *277*, 133684.
- Walling, B., Borah, A., Hazarika, S., Bharali, P., Ramachandran, D., Kanagasabai, V., ... **Alemtoshi.**, Acharjee, SA., Vishwakarma, V& Nath, P. D. (2025). Production of bacterial nanocellulose as green adsorbent matrix using distillery wastes for dye removal: a combined approach for waste management and pollution mitigation. *Biomass Conversion and Biorefinery*, *15*(5), 7265-7281.
- Acharjee, S. A., Bharali, P., Ramachandran, D., Kanagasabai, V., Gogoi, M., Hazarika, S., ... **Alemtoshi.**, Sorhie, V.,&Vishawkarma, V. (2024). Polyhydroxybutyrate (PHB)-Based sustainable bioplastic derived from Bacillus sp. KE4 isolated from kitchen waste effluent. *Sustainable Chemistry and Pharmacy*, *39*, 101507.
- Acharjee, S. A., Gogoi, B., Bharali, P., Sorhie, V., **Alemtoshi.**, &Walling, B. (2024). Recent trends in the development of Polyhydroxyalkanoates (PHAs)

based biocomposites by blending with different bio-based polymers. *Journal of Polymer Research*, *31*(4), 98.

- Gogoi, B., Acharjee, S. A., Bharali, P., Sorhie, V., Walling, B.,&**Alemtoshi**. (2024). A critical review on the ecotoxicity of heavy metal on multispecies in global context: A bibliometric analysis. *Environmental Research*, *248*, 118280.
- Boro, B., Boruah, J. S., Devi, C.,**Alemtoshi**., Gogoi, B., Bharali, P., Reddy, P. V. B., ... & Kalita, P. (2024). A novel route to fabricate ZnO nanoparticles using Xanthium indicum ethanolic leaf extract: Green nanosynthesis perspective towards photocatalytic and biological applications. *Journal of Molecular Structure*, *1300*, 137227.
- Walling, B., Bharali, P., Ramachandran, D., Viswanathan, K., Hazarika, S., Dutta, N., ... Acharjee, S. A.,&**Alemtoshi**. (2023). In-situ biofabrication of bacterial nanocellulose (BNC)/graphene oxide (GO) nano-biocomposite and study of its cationic dyes adsorption properties. *International Journal of Biological Macromolecules*, *251*, 126309.
- Bharali, P., Gogoi, B., Sorhie, V., Acharjee, S. A., Walling, B., **Alemtoshi**., Vishawkarma, V.,& Shah, M. P. (2024). Autochthonous psychrophilic hydrocarbonoclastic bacteria and its ecological function in contaminated cold environments. *Biodegradation*, *35*(1), 1-46.
- Kulnu, A. S., Acharjee, S. A., Humtsoe, R. N., Kuotsu, R., Limasenla, Walling, B., Pranjal Bharali., **Alemtoshi**., Gogoi, B., &Sorhie, V. (2024). Ethnoecological insights on wild fodder bioresources and their geospatial perspectives on sustainable piggery in Wokha and Zunheboto districts of Nagaland, India. *Genetic Resources and Crop Evolution*, *71*(2), 691-720.
- Walling, B., Bharali, P., Giridharan, B., Gogoi, B., Sorhie, V., **Alemtoshi**., & Mani, S. K. (2023). Bacterial nanocellulose: A novel nanostructured bio-adsorbent for green remediation technology. *Acta EcologicaSinica*, *43*(6), 946-967.
- Acharjee, S. A., Bharali, P., Gogoi, B., Sorhie, V., Walling, B., &**Alemtoshi**. (2023). PHA-based bioplastic: a potential alternative to address microplastic pollution. *Water, Air, & Soil Pollution*, *234*(1), 21.
- Sorhie, V., **Alemtoshi**., Gogoi, B., Walling, B., Acharjee, S. A., & Bharali, P. (2022). Role of micellar nanoreactors in organic chemistry: Green and

synthetic surfactant review. *Sustainable Chemistry and Pharmacy*, *30*, 100875.

- Sundaram, K. K., Kumar, A. V., Alphonsa, T., Rajendran, S., Rajamanickam, K., **Alemtoshi**, ... & Saravanan, K. M. (2022). COVID-19 and Tuberculosis: Two Knives in a Sheath. *Coronaviruses*, *3*(5), 33-46.
- Bharali, P., Bashir, Y., Ray, A., Dutta, N., Mudoi, P., **Alemtoshi**, ... & Konwar, B. K. (2022). Bioprospecting of indigenous biosurfactant-producing oleophilic bacteria for green remediation: an eco-sustainable approach for the management of petroleum contaminated soil. *3 Biotech*, *12*(1), 13.

Book Chapters published

- **Alemtoshi,** & Bharali, P. (2025). Greening the Grim: Biosurfactant Remediation of Heavy Metals. In *Global Perspectives of Toxic Metals in Bio Environs: Volume 2: Biotransformation, Remediation and Technological Advances* (pp. 235-254). Cham: Springer Nature Switzerland.
- Sorhie, V., Bharali, P., & **Alemtoshi.** (2022). Biosurfactant: an environmentally benign biological agent for sustainable agroecological agriculture. *Plant protection: from chemicals to biologicals. Berlin: De Gruyter*, 253-311.

ii. Patents

- Title: *Bacterial Nanocellulose Green Adsorbent Matrix using Distillery Wastes for Dye Removal and Waste Management*

  Authors:Acharjee, S. A., Bharali, P., Gogoi, B., Walling, B., **Alemtoshi**., &Sorhie, V.,

  Patent No.202431045240 A

  Publication Date: 21/06/2024
- Title: *Polyhydroxybutyrate (PHB)-based Sustainable Bioplastic derived from Bacillus sp. KE4 isolated from kitchen waste effluent*

  Authors:Acharjee, S. A., Bharali, P., Walling, B.,Gogoi, B., Sorhie, V., &**Alemtoshi**.

  Patent No.202431045242 A

  Publication Date : 21/06/2024
- Title: *Bio-fabrication of Bacterial Nano-Cellulose (BNC) /Graphene Oxide (GO) Nano-Biocomposite*

Authors:Walling, B., Bharali, P., Acharjee, S. A., Gogoi, B., **Alemtoshi**., &Sorhie, V.

Patent No.202431049557 A

Publication Date : 05/07/2024

iii. Oral presentations

- Presented a paper at an International Conference on,**'Bioresource & Bioeconomy'** (ICBB-2022) organised by Department of Botany in collaboration with Nagaland Forest Management Project, Department of Environment, Forest and Climate Change, Govt. of Nagaland, India from 19th- 21st September, 2022.
- Presented a paper at an International Conference on,**'Challenges & Prospects of Bioresource Conservation in Eastern Himalaya– with special reference to UN-Sustainable Development Goals'** held on 3-4th May, 2023 at Department of Zoology, Gauhati University, India, organised by the Department of Zoology, GU in collaboration with Pollution Control Board Assam, Assam Science Technology & Environmental Council, Aaranyak & Zoological Society of Assam.
- Presented a paper at a National Conference on, **'Recent Trends in Environmental Pollution and Health NCRTEPH 2024'** organized by the Department of Zoology, Nagaland Unversity, Lumami during 28-29 November 2024.

iv. Conferences/Seminars/Webinars/Workshops Attended

- Participated in the International webinaron "**Application ofMolecular and Bioinformatic tools in Crop Protection"** organized by theDepartment of Plant Pathology, AAU, Jorhat on 1 - 3 March, 2021.
- Participated in the International e-conference on, **"Molecules to Materials for Sustainability in XXI Century (MMS-2021)"** organized by Department of Chemistry, Institute of Science, GITAM Deemed to be University, Visakhapatnam held on 8th-9th March, 2021.
- Participated in the Indo-Canada online workshop on **"Nano-Bioengineering"** jointlyorganized by the Department of Biotechnology, Indian Institute ofTechnology (IIT) Roorkee and Centre for Biomedical Research (CBR),University of Victoria (UVic) Canada held on 13th March 2021.
- Participated in two-day seminar on "**Quality Enhancement in Research**" organized by IQAC, Nagaland University on 22nd -23rd March 2021
- Participated on a national webinar on **"World Environmental Day"** held on June 5th, 2021 organized by Department of Botany, Rajiv Gandhi University, Arunachal Pradesh, India.
- Participated in the webinar on **"COVID-19: Necessary Reflections on the Disaster Management Act, 2005"** organized by Legal Cell, Nagaland University on 17th May, 2021.
- Attended the Lecture series, **"Traditional healing system- showcasing potential journey and role of Biotechnology on mainstreaming the system- A Lecture Series"** sponsored by BIRAC, DBT, GOI, organized by

Bio-NEST, NIPER-Guwahati Incubation Center through Online mode on 26th November, 30th November & 9th December 2021.

- Participated in one-day seminar on, **"Advances in Bioscience and Technology"** organized by Department of Biotechnology, St. Joseph University on 6th May, 2022.
- Participated in one-day workshop on, **"Quality Improvement Parameters in Research Publications"** organized by Department of Chemistry and IQAC, Nagaland University on April 19th, 2023.
- Completed one-week Online Faculty Development Programme on **"Environmental Pollution and abatement"** held from 4th-9th September, 2023 organized by Nagaland University in collaboration with Mahatma Hansraj Faculty Development Centre, Hansraj College, University of Delhi.
- Participated in one-day workshop on, **"Scouting, Documentation and Dissimination of Local Grassroots Innovators from Nagaland"** organized by Department of Environmental Science & Research and Development cell (RDC), Fazl Ali College, Mokokchung, Nagaland in collaboration with National Innovation Foundation-India (NIF) on the 11th of September 2024.
- Participated in one-day seminar on "**Understanding the Importance of Altmetrics in Research**" organized by IQAC, Nagaland University on 18th September 2024
- Participated in one-day seminar on "**Role of Animals in Research**"organized by the Department of Zoology on 30th September 2024
- Participation in theInternational webinar on**"Recent Biotechnological Advancements in Agroforestry"** held on April 23rd 2025 organized by Microbiologists Society, India**.**
- Participation in awebinar on **"AI Applications in Academia"**, organized by the Department of Environmental Science, Nagaland University on the 25th of April, 2025.

Nature Environment and Pollution Technology
p-ISSN: 0972-6268 (Print copies up to 2010)
e-ISSN: 2395-3454
Vol. 25 | No. 1 | Article ID B4309 | 2026
Original Research Paper
https://doi.org/10.46488/NEPT.2026.v25i01.B4309
Open Access Journal

Leveraging the Green Petroleum Hydrocarbon Remediation Potential of a Biosurfactant Producing Indigenous Oleophilic Bacterium Isolated from Hydrocarbon Soiled Environment

Alemtoshi, Viphrezolie Sorhie and Pranjal Bharali†
Department of Environmental Science, Nagaland University, Lumami, Zunheboto-798627, Nagaland, India
†Corresponding author: Pranjal Bharali; prangenetn@gmail.com

Abbreviation: Nat. Env. & Poll. Technol.
Website: www.neptjournal.com

Received: 07-02-2025
Revised: 23-03-2025
Accepted: 28-03-2025

Key Words:

Oleophilic bacterium
Hydrocarbons
Rhamnolipid biosurfactant
Thermostability
Crude oil bioremediation

Citation for the Paper:

Alemtoshi, Sorhie, V. and Bharali, P., 2026. Leveraging the green petroleum hydrocarbon remediation potential of a biosurfactant-producing indigenous oleophilic bacterium isolated from a hydrocarbon-soiled environment. *Nature Environment and Pollution Technology*, 25(1), B4309. https://doi.org/10.46488/NEPT.2026.v25i01.B4309

Note: From 2025, the journal has adopted the use of Article IDs in citations instead of traditional consecutive page numbers. Each article is now given individual page ranges starting from page 1.

ABSTRACT

The present investigation focused on the physicochemical characterization and bioprospecting of an indigenous oleophilic bacterium (OB) and its biosurfactant (BS) for bioremediation. Within 14 days of culture at 30°C with 2% (v/v) n-hexadecane, the OB could reduce the surface tension of the culture medium by up to 34.4 mNm^{-1}. Standard screening tests verified that the isolated OB produced BS and identified it as *Pseudomonas aeruginosa*. BS production was 434.7 $mg.L^{-1}$, with a CMC of 195.6 $mg.L^{-1}$, and was purified and characterized using standard chromatographic and spectroscopic techniques. FTIR analysis confirmed the glycolipid nature of BS. TLC of the partially purified BS revealed two homologues of rhamnolipid (RL), which were subsequently confirmed by NMR. Seven distinct RL congeners were identified using LC-MS, of which di-RLs constituted a notably large proportion. The surface and emulsification activities of BS demonstrated significant stability against various pH levels, temperatures, salinities, and metal ions. Furthermore, OB was able to utilize crude oil within 60 days, as confirmed by GC-MS. In the soil washing experiment, BS separated ≥80% of the crude oil from the contaminated sand at the CMC. The results suggest that the RLs and their producer isolated from automobile workshops in Mokokchung are not only the first report from Nagaland, India, but are also promising for various applications in the bioremediation of extreme and complex environments, including addressing regional environmental issues in Nagaland.

INTRODUCTION

There is mounting global concern over the degradation of the environment by various anthropogenic chemical contaminants that are continuously released into our surroundings, causing severe environmental degradation. Petroleum hydrocarbons are one of the most common contaminants that affect different components of the environment. These pollutants are released into the environment mainly through oil spills during extraction, transportation, and refinement leaks, raising serious issues for the environment, ecological systems, and public health, leading to both short- and long-term environmental harm (Chandankere et al. 2014, Gote et al. 2023). Heavy metals such As, Cd, Cu, Zn and Pb are another group of hazardous, non-biodegradable, and persistent environmental pollutants that cause prolonged ecological and environmental damage as they tend to pass and magnify from one food chain to another, obstructing biological pathways, disrupting cellular functions, and causing diseases and damage to various organs (Das et al. 2017). In the environment, these heavy metal pollutants are found in association with sub-surface soil sediments, which often results in their release into groundwater, leading to contamination (Yang et al. 2020).

Existing conventional physical and biological technologies used for the remediation of these environmental pollutants are often associated with several

(12) PATENT APPLICATION PUBLICATION
(19) INDIA
(22) Date of filing of Application :12/06/2024

(21) Application No.202431045240 A
(43) Publication Date : 21/06/2024

(54) Title of the invention : Bacterial Nanocellulose Green Adsorbent Matrix using Distillery Wastes for Dye Removal and Waste Management

(51) International classification :C02F1/28, C12P19/04, B01J20/24, B01J20/30
(86) International Application No :NA
Filing Date :NA
(87) International Publication No : NA
(61) Patent of Addition to Application Number :NA
Filing Date :NA
(62) Divisional to Application Number :NA
Filing Date :NA

(71)**Name of Applicant :**
1)Nagaland University
Address of Applicant :Nagaland University, Lumami, Zunheboto-798627, Nagaland, India Zunheboto ---------- ----------
Name of Applicant : NA
Address of Applicant : NA
(72)**Name of Inventor :**
1)Bendangtula Walling
Address of Applicant :Applied Environmental Microbial Biotechnology Laboratory, Department of Environmental Science, Nagaland University, Lumami, Zunheboto-798627, Nagaland, India Zunheboto ---------- ----------
2)Pranjal Bharali
Address of Applicant :Applied Environmental Microbial Biotechnology Laboratory, Department of Environmental Science, Nagaland University, Lumami, Zunheboto-798627, Nagaland, India Zunheboto ---------- ----------
3)Shiva Aley Acharjee
Address of Applicant :Applied Environmental Microbial Biotechnology Laboratory, Department of Environmental Science, Nagaland University, Lumami, Zunheboto-798627, Nagaland, India Zunheboto ---------- ----------
4)Bhagyudoy Gogoi
Address of Applicant :Applied Environmental Microbial Biotechnology Laboratory, Department of Environmental Science, Nagaland University, Lumami, Zunheboto-798627, Nagaland, India Zunheboto ---------- ----------
5)Alemtoshi
Address of Applicant :Applied Environmental Microbial Biotechnology Laboratory, Department of Environmental Science, Nagaland University, Lumami, Zunheboto-798627, Nagaland, India Zunheboto ---------- ----------
6)Viphrezolie Sorhie
Address of Applicant :Applied Environmental Microbial Biotechnology Laboratory, Department of Environmental Science, Nagaland University, Lumami, Zunheboto-798627, Nagaland, India Zunheboto ---------- ----------

(57) Abstract :
The invention is usage of rice beer stillage as a carbon source to produce bacterial nanocellulose (BNC). A method of production of Bacterial Nanocellulose (BNC) comprising the steps of: preparation of carbon source from rice beer stillage; and production and purification of BNC. The BNC made using rice beer stillage has excellent thermostability (up to 380 °C), a dense nano-fibrous network with cellulose I type properties, and a high crystallinity index (86.23%). It demonstrated a high water-holding capacity (97.53 g g−1) and a robust tensile strength (68.044 MPa). BNC also demonstrated its recyclable nature by going through several cycles of sorption and desorption. According to this invention, waste distillery stillage may be efficiently used as a sustainable raw material to produce BNC that is safe for the environment and has a wide range of uses.

(12) PATENT APPLICATION PUBLICATION
(19) INDIA
(22) Date of filing of Application :12/06/2024

(21) Application No.202431045242 A
(43) Publication Date : 21/06/2024

(54) Title of the invention : Polyhydroxybutyrate (PHB)-based Sustainable Bioplastic derived from Bacillus sp. KE4 isolated from kitchen waste effluent

(51) International classification :C12P1/04, C12P7/625, C12P7/42, C12P7/52, C12N1/20
(86) International Application No :NA
Filing Date :NA
(87) International Publication No : NA
(61) Patent of Addition to Application Number :NA
Filing Date :NA
(62) Divisional to Application Number :NA
Filing Date :NA

(71)**Name of Applicant :**
1)Nagaland University
Address of Applicant :Nagaland University, Lumami, Zunheboto-798627, Nagaland, India Zunheboto ---------- ----------
Name of Applicant : NA
Address of Applicant : NA
(72)**Name of Inventor :**
1)Shiva Aley Acharjee
Address of Applicant :Applied Environmental Microbial Biotechnology Laboratory, Department of Environmental Science, Nagaland University, Lumami, Zunheboto-798627, Nagaland, India Zunheboto ---------- ----------
2)Pranjal Bharali
Address of Applicant :Applied Environmental Microbial Biotechnology Laboratory, Department of Environmental Science, Nagaland University, Lumami, Zunheboto-798627, Nagaland, India Zunheboto ---------- ----------
3)Bendangtula Walling
Address of Applicant :Applied Environmental Microbial Biotechnology Laboratory, Department of Environmental Science, Nagaland University, Lumami, Zunheboto-798627, Nagaland, India Zunheboto ---------- ----------
4)Bhagyudoy Gogoi
Address of Applicant :Applied Environmental Microbial Biotechnology Laboratory, Department of Environmental Science, Nagaland University, Lumami, Zunheboto-798627, Nagaland, India Zunheboto ---------- ----------
5)Viphrezolie Sorhie
Address of Applicant :Applied Environmental Microbial Biotechnology Laboratory, Department of Environmental Science, Nagaland University, Lumami, Zunheboto-798627, Nagaland, India Zunheboto ---------- ----------
6)Alemtoshi
Address of Applicant :Applied Environmental Microbial Biotechnology Laboratory, Department of Environmental Science, Nagaland University, Lumami, Zunheboto-798627, Nagaland, India Zunheboto ---------- ----------

(57) Abstract :
Using glucose as the carbon source, Bacillus sp. KE4 produced polyhydroxybutyrate (PHB) with a maximum dry cell weight (DCW) of 4.4 g/l and a PHB concentration of 3.1 g/l. PHB content is 70.4% of DCW, while the PHB yield is 0.15 g/g. A variety of characterization methods are employed to validate the biopolymer's structure as PHB, exhibiting superior thermal stability. It is discovered that the extracted PHB is not cytotoxic and had a partially crystalline structure. After 28 days of soil burial, biodegradation experiments showed that the biopolymer film had broken down by 61.34%. These findings point to possible uses in agriculture, medicine, and packaging.

(12) PATENT APPLICATION PUBLICATION

(19) INDIA

(22) Date of filing of Application :28/06/2024

(21) Application No.202431049557 A

(43) Publication Date : 05/07/2024

(54) Title of the invention : Bio-fabrication of Bacterial Nano-Cellulose (BNC) /Graphene Oxide (GO) Nano-Biocomposite

(51) International classification	:C02F0101300000, C12P0019040000, C02F0001280000, B01J0020280000, B01J0020260000
(86) International Application No Filing Date	:NA :NA
(87) International Publication No	: NA
(61) Patent of Addition to Application Number Filing Date	:NA :NA
(62) Divisional to Application Number Filing Date	:NA :NA

(71)**Name of Applicant :**

1)Nagaland University

Address of Applicant :Nagaland University, Lumami Headquarters, Zunheboto district, Nagaland Zunheboto ---------- ----------

Name of Applicant : NA

Address of Applicant : NA

(72)**Name of Inventor :**

1)Bendangtula Walling

Address of Applicant :Applied Environmental Microbial Biotechnology Laboratory, Department of Environmental Science, Nagaland University, Lumami, Zunheboto-798627, Nagaland, India Zunheboto ---------- ----------

2)Pranjal Bharali

Address of Applicant :Applied Environmental Microbial Biotechnology Laboratory, Department of Environmental Science, Nagaland University, Lumami, Zunheboto-798627, Nagaland, India Zunheboto ---------- ----------

3)Shiva Aley Acharjee

Address of Applicant :Applied Environmental Microbial Biotechnology Laboratory, Department of Environmental Science, Nagaland University, Lumami, Zunheboto-798627, Nagaland, India Zunheboto ---------- ----------

4)Bhagyudoy Gogoi

Address of Applicant :Applied Environmental Microbial Biotechnology Laboratory, Department of Environmental Science, Nagaland University, Lumami, Zunheboto-798627, Nagaland, India Zunheboto ---------- ----------

5)Alemtoshi

Address of Applicant :Applied Environmental Microbial Biotechnology Laboratory, Department of Environmental Science, Nagaland University, Lumami, Zunheboto-798627, Nagaland, India Zunheboto ---------- ----------

6)Viphrezolie Sorhie

Address of Applicant :Applied Environmental Microbial Biotechnology Laboratory, Department of Environmental Science, Nagaland University, Lumami, Zunheboto-798627, Nagaland, India Zunheboto ---------- ----------

(57) Abstract :

In this invention, a time-dependent technique is used to synthesize Bacterial Nanocellulose/Graphene Oxide Nano-Biocomposites (BNC-GO-NBCs) by Komagataeibacter saccharivorans NUWB1. The dried BNC-GO-NBC exhibited great tensile strength (84.72 MPa), enhanced thermostability (up to 380°C), high crystallinity (74.21%), and a porous structure with embedded GO layers, according to physicochemical examination. A mesoporous structure with a significant adsorption capacity for cationic dyes is shown by the N2 adsorption-desorption isotherm. Additionally, the substance demonstrated the ability to regenerate and shown non-cytotoxic qualities in tests for oxidative stress, cell cytotoxicity, and antibacterial activity. These results point to BNC-GO-NBC's intriguing potential for environmental applications, including dye adsorption.